



**Microenvironmental characterization of pancreatic islets
within their endogenous niche towards a bioengineered
microtissue for β -cell replacement therapy**

Nicole Kattner

Thesis submitted for the degree of Doctor of Philosophy

Newcastle University

Faculty of Medical Sciences

Institute of Cellular Medicine

September, 2019

Abstract

Type 1 diabetes is characterised by insulin deficiency leading to chronic hyperglycaemia causing microvascular and macrovascular complications. Current treatment with glucose monitoring and insulin administration can cause recurrent serious hypoglycaemia significantly impacting on quality of life. Despite considerable advances towards an artificial pancreas, only pancreatic β -cell replacement therapy can restore truly normal glucose homeostasis. Existing clinical options for this are whole pancreas and isolated islet transplantation. Pancreas transplantation requires major abdominal surgery and can lead to dangerous early complications including pancreatitis, as the organ is particularly susceptible to *post mortem* stress prior to reimplantation. When successful, pancreas transplantation usually leads to insulin independence. Islet transplantation is a minimally invasive procedure, but many islets are also lost through *post mortem* stress associated with isolation and transplantation, negatively impacting on islet microenvironment, viability, mass and function. Long term insulin independence is rarely sustained. The overall aim of the work comprising this thesis was to explore tissue engineering approaches to provide isolated islets with sufficient replacement of the lost niche to maintain integrity, mass, viability and function and therefore transplant outcomes. The research question hereby was, how the culture of islets in proximity or contact with a hydrogel impacts on islet health with the hypothesis that the replacement of lost ECM via a hydrogel will improve islet integrity, viability and function after isolation and prior to transplant.

Specific objectives were:

1. To characterise the islet niche *in situ* within human donor pancreas and analyse acute changes related to ischaemia, tissue processing and islet isolation.
2. To evaluate biocompatibility and impact on islet integrity, viability and function of extracellular matrix (ECM) replacement through a novel collagen-containing hydrogel.
3. To explore bioengineering approaches to reduce the impact of hypoxia on islets combined with a hydrogel ECM niche to form a tissue-engineered β -cell replacement product.

Islet microenvironment, integrity and morphology *in situ* was analysed in a pancreas with minimal ischaemic damage by immunohistochemistry (IHC), immunofluorescence staining (IF) and electron microscopy (EM) analysis revealing peri-islet basement membrane (BM), peri-vascular BM, rich vascularisation and endocrine cell-to-cell connections. Impact of ischaemia on donor pancreata was analysed by EM analysis leading to development of the Newcastle EM Ischaemia Score (NEMIS). Characterisation of isolated islets with IHC, IF and EM showed loss of peri-islet BM and reduced integrity through the isolation process.

Biocompatibility of a novel ECM replacement hydrogel comprising collagen I, alginate and fibrinogen (CAF) with a pseudoislet model derived from the MIN6 β -cell line and primary human islets was confirmed by propidium iodide (PI) viability staining and integrity scoring. Maintained metabolic function was confirmed by Seahorse flux analysis.

Towards islet hypoxia reduction an electrospun nanofiber membrane to provide microchannels for oxygen delivery and dynamic culture to prevent islet clumping were assessed. Expression of hypoxia-induced gene signature was reduced in dynamic culture with maintained viability (PI staining), and improved integrity scores, but decreased ATP production (Seahorse flux analysis). As a final step a perfusion system was developed to facilitate ECM replacement simultaneously with decreased hypoxia.

In conclusion, the quality of transplanted pancreatic tissue is negatively impacted through organ preservation and islet isolation. A new EM ischaemia score has been developed to inform better selection of donor organs. A novel collagen-containing hydrogel has a potential in replacement of islet ECM, but hypoxia remains an unresolved challenge to successful β -cells tissue engineering. Reducing hypoxia with dynamic culture enables maintained islet quality *in vitro* and an engineered perfusion system may enable preparation of novel β -cell microtissue for successful transplantation without the detriment of prolonged *ex vivo* hypoxia.

Declaration

I hereby declare that all work for this submitted thesis is entirely my own. All work has been performed by me unless otherwise stated and all sources of information have been acknowledged by means of reference.

Nicole Kattner

Acknowledgement

This project was funded by the EPSRC CL086 studentship 150648356 EPSRC RiHN Feasibility Studies (UK) (EP/M017559/1).

This thesis would not have been possible without the help of various people:

I want to thank my supervisors Prof Jim Shaw, Prof Kenny Dalgarno, Dr Bill Scott and Dr Marina Ferreira-Duarte for their continuous support, profound knowledge and helpful discussions throughout my whole project.

Thank you to the Translational Regenerative Medicine Laboratories for the biopsy handling, islet isolation and providing donor information and the QUOD Expand project for providing pancreas biopsies. A special thank you to Minna Honkanen-Scott for her continuous help with islet QC protocols. I also want to thank Nicola Dyson for her help with the TEM samples and the discussions about the EM scoring.

I want to thank the EM department and especially Dr Kathryn White and Tracey Davey who patiently taught me heavy metal processing, ultrathin cutting and how to use the TEM.

I further want to thank Dr Satomi Miwa and Deborah Cornell for their help with the Seahorse experiments. I want to thank Dr Dina Tiniakos and Dr Yvonne Bury for taking out time of their busy schedules and explaining the pancreas histology to me. I also want to thank Marta Bourne and Michelle Thursby for all their support and help throughout my project. I further want to thank my collaborators Dr Kathrin Arden, Dr Lena Eliasson, Lynn Tindale and Bart Wagner for their helpful discussions and profound knowledge.

I want to thank my colleges who became my friends over the last few years. Najwa, Xuefei, Rashmi, Sarah, Anneliese and Tabby. Thank you so much for all your help, encouragement, helpful discussions, kind words, positivity and establishment of the cake group! I could not have done it without you!

Last I want to thank my wonderful family and friends, especially my parents and my boyfriend for their continuous support through my journey!

Published abstracts

Kattner N, Miwa S, Cornell D, Al-Jahdhami N, Arden C, Dalgarno K, Ferreira-Duarte A, Shaw JAM, Scott III WE, *Assessment of a novel hydrogel to replace extracellular matrix lost in isolated islets prior to transplantation: impact of collagen/alginate/fibrin hydrogel on islet morphology, viability and function*, IPITA Meeting Recordings (2019).

Kattner N, Tiniakos D, Bury Y, White K, Davey T, Eliasson L, Tindale L, Wagner B, Honkanen-Scott M, Dyson N, Dalgarno K, Ferreira-Duarte A, Ploeg RJ, Shaw JAM, Scott III WE, *Transmission electron microscopy analysis of stress induced changes during pancreas preservation*, IPITA Meeting Recordings (2019).

Habart D, Matzner F, Blažek A, Bělohávek P, Berková Z, Scholz H, Friberg A, Gmyr V, Kerr-Conte J, Bosco D, Parnaud G, Lacallard V, Habartová A, Doppenberg J, Engelse MA, Wilhelm J, Abdullah M, Golab K, Witkowski P, Honkanen-Scott M, Kattner N, Shaw JAM, Leontovych I, Kosinová L, Pátíková A, Vojtíšková A, Saudek F, *IsletNet: an Online Service for Standardized Islet Counting*, IPITA Meeting Recordings (2019).

Kattner N, Marshall H, White K, Davey T, Tiniakos D, Honkanen-Scott M, Ferreira-Duarte A, Shaw JAM, Scott III WE, *Microenvironmental characterisation of islets of Langerhans in human deceased donor pancreas and isolated islets*, IPITA Meeting Recordings (2017).

Publications in preparation.

Table of Content

1	Chapter 1. Introduction	1
1.1	Human pancreas structure and acinar tissue	1
1.2	The exocrine pancreas	1
1.2.1	The endocrine pancreas.....	2
1.2.2	Human islet structure and function.....	2
1.2.3	Insulin biosynthesis and glucose homeostasis	4
1.3	Tissue structure and its role in function	6
1.3.1	Extracellular matrix.....	6
1.3.2	Islet connectivity	8
1.4	Diabetes mellitus.....	10
1.4.1	Type 1 diabetes.....	10
1.4.2	Type 2 diabetes.....	12
1.4.3	Gestational diabetes	13
1.4.4	Other forms of diabetes.....	13
1.4.5	Complications.....	14
1.4.6	Management of diabetes.....	15
1.5	Current β -cell replacement therapy.....	16
1.5.1	Pancreas transplantation.....	16
1.5.2	Islet isolation and transplantation.....	17
1.5.2.1	Impact of isolation and transplantation on islets and their ECM	19
1.5.2.2	Islet preservation	21
1.5.2.3	Transplantation site.....	21
1.5.3	Secondary sources of β -cells.....	22
1.6	Tissue Engineering.....	23
1.6.1	Tissue engineering for islet transplantation	24

1.6.1.1	Scaffolds for islet transplantation	24
1.6.1.2	Combination of material and isolated islets.....	25
1.7	Aims.....	28
2	Chapter 2. Methods.....	31
2.1	Tissue Culture	31
2.1.1	MIN6 β -cell line culture	31
2.1.1.1	MIN6 sub culture	31
2.1.1.2	Pseudoislet generation and culture	32
2.1.2	Human islet culture.....	32
2.1.2.1	Donor information.....	33
2.1.3	Mouse islets	36
2.1.3.1	Mouse islet isolation.....	36
2.1.3.2	Mouse islet culture	36
2.1.4	Propidium iodide staining.....	36
2.1.5	Islet equivalent (IEQ) estimation	37
2.2	Tissue fixation and processing for paraffin embedding.....	37
2.3	Tissue fixation and processing for Transmission electron microscopy (TEM)....	38
2.4	Immunofluorescence staining (IF).....	39
2.5	RNA extraction and processing	41
2.5.1	RNA extraction	41
2.5.2	Complementary DNA synthesis	42
2.5.3	Quantitative real time PCR	43
2.6	Protein extraction and processing	44
2.6.1	Protein extraction	44
2.6.2	Bradford assay	44
2.7	Seahorse flux analysis and normalisation	45

2.7.1	Seahorse flux analysis	45
2.7.2	DNA extraction.....	46
2.7.3	PicoGreen™ analysis.....	46
2.8	Tissue engineering.....	47
2.8.1	Electrospun nanofiber membrane.....	47
2.8.2	Collagen I/alginate/fibrinogen Hydrogel	47
2.8.2.1	Hydrogel generation.....	47
2.8.2.2	PI staining	48
2.8.2.3	RNA extraction.....	48
2.8.2.4	Freeze drying and scanning electron microscopy (SEM) analysis	49
2.8.2.5	Swelling analysis	49
2.8.3	Orbital shaker method.....	49
2.8.4	Perifusion development.....	49
2.9	Statistical analysis.....	50
3	Chapter 3. Impact of <i>post mortem</i> ischaemia, tissue processing and islet isolation on islet microenvironment, integrity, morphology and function.....	51
3.1	Introduction.....	51
3.2	Aims.....	52
3.3	Results	53
3.3.1	Islets in their endogenous niche in situ in human and mouse tissue.....	53
3.3.1.1	Human tissue with short cold ischemia time	53
3.3.1.1.1	Histological assessment with Haematoxylin & Eosin, Sirius red/Fast green and immunoperoxidase staining	53
3.3.1.1.2	Human pancreas assessment through immunofluorescence staining	56
3.3.1.2	Human pancreatic tissue with low CIT assessed at ultrastructural level	60

3.3.2	Impact of post mortem ischemia and tissue processing on the islet microenvironment, integrity and morphology.....	65
3.3.2.1	Histological assessment of human pancreata with H&E and SR/FG....	66
3.3.2.2	Ultrastructural assessment of human pancreata with TEM	68
3.3.2.3	Development of the Newcastle Electron Microscopy Ischaemia Score (NEMIS) for analysis of ultrastructural stress induced changes during pancreas preservation	70
3.3.2.4	Assessment of developmental cohort with NEMIS.....	73
3.3.3	Impact of islet isolation on islet microenvironment, integrity and morphology	77
3.3.3.1	Histological assessment of isolated islets.....	78
3.3.3.2	Immunofluorescence assessment of isolated human islets.....	79
3.3.3.3	Ultrastructural assessment of isolated human islets	82
3.4	Discussion.....	89
3.4.1	Microenvironment in normal pancreas.....	89
3.4.2	Impact of CIT	90
3.4.3	Impact of isolation	93
4	Chapter 4. Providing extracellular matrix replacement to islets through a collagen/alginate/fibrinogen hydrogel.....	95
4.1	Introduction.....	95
4.2	Aims.....	98
4.3	Results	99
4.3.1	Establishment of a MIN6 pseudoislet model and characterization of integrity and function.....	99
4.3.1.1	Viability of pseudoislet model Day 5 and Day 6 after generation.....	99
4.3.1.2	Immunofluorescence staining of MIN6 pseudoislets.....	100
4.3.1.3	TEM analysis of MIN6 pseudoislets	101

4.3.1.4	Analysis of metabolic function of MIN6 pseudoislets	102
4.3.2	Providing ECM components via coating of tissue culture wells with CAF hydrogel and impact on pseudoislet model	107
4.3.2.1	Hydrogel components dissolved in media	107
4.3.2.2	CAF analysis	109
4.3.2.3	Viability assessment in the presence of CAF	111
4.3.2.4	Protein expression of key marker in pseudoislets via IF after ECM presence	114
4.3.2.5	Metabolic activity of pseudoislets in the presence of CAF	115
4.3.2.6	Integrity index of pseudoislets after CAF presence.....	115
4.3.3	Analysis of human isolated islets.....	117
4.3.3.1	Viability of human isolated islets over time of culture	118
4.3.3.2	Metabolic function of human isolated islets after isolation	119
4.3.4	Impact of hydrogel presence on human isolated islets.....	120
4.3.4.1	Viability assessment of human isolated islets after culture on CAF-coated wells	120
4.3.4.2	Protein expression of human isolated islets after CAF presence.....	122
4.3.4.3	Metabolic analysis of human isolated islets in the presence of CAF .	123
4.4	Discussion.....	124
4.4.1	Pseudoislet model.....	124
4.4.2	Cytocompatibility of CAF with pseudoislet model	126
4.4.3	Cytocompatibility of CAF with human isolated islets	127
5	Chapter 5. Development of bioengineering approaches to reduce hypoxia in β -cell/hydrogel products.....	129
5.1	Introduction.....	129
5.2	Aims.....	130
5.3	Results	131

5.3.1	Microwells in hydrogel as ECM replacement	131
5.3.2	Coated wells in dynamic culture for reduction of hypoxia.....	133
5.3.2.1	Morphology and integrity assessment	133
5.3.2.2	Viability assessment	134
5.3.2.3	Hypoxia assessment with pimonidazole staining and gene expression 135	
5.3.2.4	Metabolic assessment of static and rotation culture in CAF-coated wells 138	
5.3.3	Electrospun nanofiber membrane for improved revascularisation of isolated islets 139	
5.3.3.1	Fibre analysis and mouse islet seeding	139
5.3.3.2	Viability assessment of mouse islets over culture time	140
5.3.3.3	Immunofluorescent staining of mouse islets after culture on membrane 141	
5.3.4	Hydrogel perfusion for reduction of hypoxia in encapsulated pseudoislets 142	
5.3.4.1	Morphology of encapsulated pseudoislets in static culture	142
5.3.4.2	Viability of encapsulated islets	144
5.3.4.3	Gene expression of encapsulated pseudoislets	145
5.3.4.4	Protein expression of encapsulated islets with and without hypoxia reduction 146	
5.3.4.5	Perifusion of CAF hydrogel	147
5.4	Discussion.....	148
5.4.1	Microwells.....	148
5.4.2	CAF-coating in combination with dynamic culture.....	150
5.4.3	Nanofiber membrane	151
5.4.4	Perifusion of encapsulated pseudoislets	151

6	Chapter 6. General discussion and future experiments.....	153
6.1	General discussion	153
6.1.1	Microenvironment of islets.....	155
6.1.2	ECM replacement	156
6.1.3	Hypoxia reduction.....	157
6.2	Future experiments.....	160
7	References	161

List of Figures

FIGURE 1.1: PANCREAS TISSUE STRUCTURE.....	1
FIGURE 1.2: ENDOCRINE CELL DISTRIBUTION IN HUMAN ISLETS.....	2
FIGURE 1.3: VASCULAR SYSTEM AROUND AND IN THE ISLET OF A RAT DEMONSTRATING THE DENSE VASCULARISATION.....	3
FIGURE 1.4: STRUCTURE OF PROINSULIN WITH THE A-CHAIN, B-CHAIN AND C-PEPTIDE.	4
FIGURE 1.5: SCHEMATIC SUMMARY OF INSULIN STIMULUS SECRETION COUPLING (LEMAIRE AND SCHUIT, 2012).	5
FIGURE 1.6: INSULIN RELEASE AFTER FOOD INTAKE WITH CHARACTERISTIC TWO PHASES IN RESPONSE TO HIGH BLOOD GLUCOSE LEVELS (HOLT ET AL., 2010).....	6
FIGURE 1.7: SCHEMATIC OF EXTRACELLULAR MATRICES AND THEIR COMPONENTS WHEN FORMING BM OR INTERSTITIAL MATRIX.....	7
FIGURE 1.8: TRANSMISSION ELECTRON MICROSCOPY OF HUMAN PANCREAS.....	8
FIGURE 1.9: CELL-TO-CELL CONNECTIONS BETWEEN SINGLE B-CELLS NAMED GAP JUNCTIONS, TIGHT JUNCTIONS AND ADHERENS JUNCTION.....	9
FIGURE 1.10: INCIDENCE FOR TYPE 1 DIABETES WORLDWIDE (KATSAROU ET AL., 2017).	11
FIGURE 1.11: PROGRESSION OF TYPE 1 DIABETES PRESENTED BY PRESYMPTOMATIC STAGES 1 AND 2 FOLLOWED BY SYMPTOMATIC STAGE 3 WITH CHANGES IN FUNCTIONAL B-CELL MASS (KATSAROU ET AL., 2017).	12
FIGURE 1.12: SCHEMATIC OF ISLET EXTRACTION AND DELIVERY PROCESS.	18
FIGURE 1.13: ARCHITECTURE OF MOUSE ISLETS.....	19
FIGURE 1.14: PRINCIPLE OF TISSUE ENGINEERING WITH THE COMBINATION OF CELLS, BIOMATERIALS AND OTHER FACTORS TO ACHIEVE A BIOENGINEERED CONSTRUCT READY FOR TRANSPLANTATION IN PATIENTS.....	23
FIGURE 1.15: ENCAPSULATION STRATEGIES FOR ISOLATED ISLETS WITH MACROENCAPSULATION (EXTRAVASCULAR), MICROENCAPSULATION, ULTRA-THIN COATINGS AND MACROENCAPSULATION (INTRAVASCULAR)(SONG AND ROY, 2015).	26
FIGURE 2.1: SCHEMATIC SET UP FOR PERIFUSION OF HYDROGEL/B-CELL CONSTRUCT.	49
FIGURE 2.2: PERIFUSION SYSTEM WITH CHAMBERS, PERISTALTIC PUMP, FISH PUMP AND MEDIA TANK. .	50
FIGURE 3.1: ANALYSIS OF HUMAN PANCREATIC TISSUE IN A DONOR WITH SHORT CIT THROUGH H&E STAINING AT LOW MAGNIFICATION.....	54
FIGURE 3.2: ANALYSIS OF HUMAN PANCREATIC TISSUE IN A DONOR WITH SHORT CIT THROUGH DIFFERENT HISTOLOGICAL STAINS AT HIGHER MAGNIFICATION.	55
FIGURE 3.3: PANCREAS TISSUE STAINED FOR PAN-CADHERIN AND E-CADHERIN.	56
FIGURE 3.4: PANCREAS TISSUE STAINED FOR CD31 AND VIMENTIN.	57
FIGURE 3.5: DISTRIBUTION OF BM IN PANCREAS TISSUE WITH LOW CIT.	58

FIGURE 3.6: ANALYSIS OF HUMAN PANCREATIC TISSUE WITH LOW CIT THROUGH IMMUNOFUORESCENCE STAINING OF LAMININ AND COLLAGEN IV AT HIGHER MAGNIFICATION.....	59
FIGURE 3.7: ULTRASTRUCTURAL ANALYSIS OF MOUSE PANCREAS TISSUE WITH TEM.	61
FIGURE 3.8: ULTRASTRUCTURAL ANALYSIS OF HUMAN ACINAR TISSUE WITH SHORT CIT.....	63
FIGURE 3.9: ULTRASTRUCTURAL ANALYSIS OF HUMAN ENDOCRINE TISSUE WITH LOW CIT.....	64
FIGURE 3.10: EXAMPLE IMAGES FOR HISTOLOGICAL ANALYSIS OF PANCREAS TISSUE.	67
FIGURE 3.11: ULTRASTRUCTURAL ACUTE DAMAGE THROUGH HYPOXIA IN EXOCRINE TISSUE.	69
FIGURE 3.12: TEM SECTION IS DIVIDED INTO FIVE AREAS TO CHOOSE FIVE CELLS IN EACH AREA WITH LOW MAGNIFICATION TO REDUCE BIAS.....	70
FIGURE 3.13: CORRELATION PLOTS BETWEEN CIT AND NEMIS SCORES.	75
FIGURE 3.14: NEMIS ANALYSIS FOR FIVE DBD AND EIGHT DCD DONORS.....	76
FIGURE 3.15: NEMIS ANALYSIS FOR ACINAR AND ENDOCRINE CELLS FROM SIX DIFFERENT DONORS.	77
FIGURE 3.16: HISTOLOGICAL ASSESSMENT OF ISOLATED ISLETS WITH H&E AND SR/FG STAINING.....	78
FIGURE 3.17: IMMUNOFUORESCENCE ASSESSMENT OF DBD-3.....	80
FIGURE 3.18: NO PRIMARY ANTIBODY CONTROL FOR IF STAINING OF DBD-3.	81
FIGURE 3.19: ULTRASTRUCTURAL ASSESSMENT OF HUMAN ISOLATED ISLETS.....	83
FIGURE 3.20: CORRELATION BETWEEN CIT AND ENDOCRINE DAMAGE SCORES.....	88
FIGURE 4.1: GLUCOSE METABOLISM WITH GLYCOLYSIS AND OXIDATIVE PHOSPHORYLATION.	96
FIGURE 4.2: MITOCHONDRIAL ELECTRON TRANSPORT CHAIN WITH COMPLEX I, II, II, IV, AND ATP SYNTHASE AND IMPACT OF OLIGOMYCIN, FCCP AND ANTIMYCIN A.	97
FIGURE 4.3: EXAMPLES FOR VIABILITY ASSESSMENT OF PSEUDOISLETS (P27) ON DAY 5 AFTER GENERATION.	99
FIGURE 4.4: VIABILITY OF MIN6 PSEUDOISLETS (P23-P27) ON DAY 5 AND DAY 6 AFTER GENERATION.	100
FIGURE 4.5: IMMUNOFUORESCENCE STAINING OF MIN6 PSEUDOISLETS FIVE DAYS AFTER GENERATION.	100
FIGURE 4.6: TEM ANALYSIS OF MIN6 PSEUDOISLETS AT DAY 5.	101
FIGURE 4.7: SEAHORSE FLUX ANALYSIS FOR METABOLIC CHARACTERISATION OF PSEUDOISLETS.....	106
FIGURE 4.8: PSEUDOISLETS (P25) AFTER 72 H CULTURE IN CONTROL WELLS (A), MEDIUM SUSPENDED WITH COLLAGEN I (B), ALGINATE (C) OR FIBRINOGEN (D).....	107
FIGURE 4.9: VIABILITY OF PSEUDOISLETS (P25+P26) AFTER CULTURE IN CONTROL MEDIA OR MEDIA WITH DISSOLVED COLLAGEN I, ALGINATE OR FIBRINOGEN.	108
FIGURE 4.10: SEM ANALYSIS OF FREEZE-DRIED CAF HYDROGEL.....	109
FIGURE 4.11: ENERGY DISPERSIVE X-RAY SPECTROSCOPY (EDS) OF CAF HYDROGEL (2:1:2).....	110
FIGURE 4.12: VIABILITY ASSESSMENT OF PSEUDOISLETS CULTURED ON CONTROL WELLS (A+C) AND CAF-COATED WELLS (B+D).....	112
FIGURE 4.13: VIABILITY OF PSEUDOISLETS ASSESSED AFTER 72 H OF CULTURE ON TISSUE CULTURE PLASTIC (CONTROL) OR CAF-COATED WELLS (CAF).....	113

FIGURE 4.14: VIABILITY OF PSEUDOISLETS CULTURED FOR 72 H ON TISSUE CULTURE PLASTIC (CONTROL) OR CAF-COATED WELLS (CAF) ASSESSED PER IEQ GROUP.....	113
FIGURE 4.15: IMMUNOFLUORESCENCE STAINING OF PSEUDOISLETS AFTER 72 H CULTURE ON TISSUE CULTURE PLASTIC (ROW A AND B) OR CAF-COATED WELLS (ROW C AND D).	114
FIGURE 4.16: ATP PRODUCTION IN PSEUDOISLETS AFTER 72 H OF CULTURE ON TISSUE CULTURE PLASTIC (CONTROL) OR CAF-COATED WELLS (CAF).....	115
FIGURE 4.17: INTEGRITY INDEX OF PSEUDOISLETS AFTER CULTURE IN CONTROL AND CAF-COATED WELLS.	116
FIGURE 4.18: DITHIZONE STAINING OF HUMAN ISOLATED ISLETS DURING ISLET QUALITY CONTROL.	118
FIGURE 4.19: VIABILITY OF HUMAN ISLETS OVER TIME IN STATIC CULTURE IN NON-ADHERENT TISSUE CULTURE PLATES UP TO FIVE DAYS.....	119
FIGURE 4.20: ATP PRODUCTION PER WELL OF HUMAN ISOLATED ISLETS.....	120
FIGURE 4.21: VIABILITY ASSESSMENT OF HUMAN ISOLATED ISLETS CULTURED ON CONTROL WELLS (A+C) AND CAF-COATED WELLS (B+D).	121
FIGURE 4.22: VIABILITY OF HUMAN ISOLATED ISLETS (HI-6 AND HI-8) AFTER 72 H CULTURE ON TISSUE CULTURE PLASTIC OR CAF-COATING.....	121
FIGURE 4.23: IF STAINING OF HUMAN ISOLATED ISLETS AFTER 72 H OF CULTURE IN CONTROL OR CAF-COATED WELLS.	122
FIGURE 4.24. NO PRIMARY ANTIBODY CONTROL OF FIGURE 4.23.	123
FIGURE 4.25: ATP PRODUCTION PER WELL OF HUMAN ISOLATED ISLETS (IL-6 AND IL-7) AFTER 72 H OF CULTURE ON CONTROL OR CAF-COATED WELLS (ON DAY 6 AFTER ISOLATION).	124
FIGURE 5.1: MICROWELLS IN 2% AGAROSE HYDROGEL.....	132
FIGURE 5.2: CAF HYDROGELS AFTER REMOVAL FROM THE STAMP IN PBS IN A 12-WELL PLATE.....	132
FIGURE 5.3: PSEUDOISLETS AFTER 72 H OF STATIC (A+B) OR ROTATION (C+D) CULTURE IN CONTROL WELLS (A+C) OR CAF-COATED WELLS (D).	133
FIGURE 5.4: INTEGRITY SCORE OF PSEUDOISLETS AFTER STATIC AND ROTATION CULTURE IN CONTROL AND CAF-COATED WELLS (N≥2).	134
FIGURE 5.5: VIABILITY ASSESSMENT OF PSEUDOISLETS (P27-P29) IN DIFFERENT CULTURE SYSTEMS INCLUDING STATIC CONTROL, STATIC CAF, ROTATION CONTROL AND ROTATION CAF.	135
FIGURE 5.6: IMMUNOFLUORESCENCE STAINING OF PSEUDOISLETS AFTER DIFFERENT CULTURE CONDITIONS WITH PIMONIDAZOLE (PIM) IN GREEN (A2, B2, C2, D2) AND DAPI IN BLUE (A3, B3, C3, D3).....	136
FIGURE 5.7: NO PRIMARY ANTIBODY CONTROL OF PSEUDOISLETS AFTER DIFFERENT CULTURE CONDITIONS WITH PIMONIDAZOLE (PIM) IN GREEN (A2, B2, C2, D2) AND DAPI IN BLUE (A3, B3, C3, D3).....	137
FIGURE 5.8: EXPRESSION OF INSULIN GENES (INS 1 AND INS 2), HYPOXIA INDUCED GENES (LDHA, MCT4, GLUT1) AND UROCORTIN 3 (U3) IN PSEUDOISLETS (P26 AND P27) AFTER 72 H OF CULTURE IN STATIC CONTROL, STATIC CAF, ROTATION CONTROL, AND ROTATION CAF CONDITIONS.	138

FIGURE 5.9: ANALYSIS OF METABOLIC ACTIVITY OF PSEUDOISLETS (P27 AND P28) CULTURED ON CAF- COATED WELLS IN STATIC (S1+S2) OR ROTATION (R1+R2) CONDITION.	139
FIGURE 5.10: ELECTROSPUN NANOFIBERS WITH MOUSE ISLETS.	140
FIGURE 5.11: VIABILITY OF DIFFERENT BATCHES OF MOUSE ISLETS AT DAY 1-4 OF CULTURE IN CONTROL WELLS.	141
FIGURE 5.12: IMMUNOFLUORESCENCE STAINING OF MOUSE ISLETS AFTER CULTURE ON ELECTROSPUN NANOFIBER MEMBRANE FOR THREE DAYS.	142
FIGURE 5.13: PSEUDOISLETS AFTER CULTURE OF 72 H IN CONTROL WELLS (A) AND ENCAPSULATED (B+C).	143
FIGURE 5.14: INTEGRITY SCORE OF PSEUDOISLETS AFTER STATIC CULTURE ENCAPSULATED IN CAF HYDROGEL COMPARED TO ISLETS IN STATIC CONTROL CONDITIONS.....	143
FIGURE 5.15: VIABILITY ASSESSMENT WITH PI STAINING WITH TWO EXAMPLES OF ENCAPSULATED PSEUDOISLETS SHOWN AFTER 72 H OF STATIC CULTURE.	144
FIGURE 5.16: VIABILITY OF PSEUDOISLETS AFTER 72 H OF STATIC CULTURE IN CONTROL WELLS AND ENCAPSULATED IN HYDROGEL.....	145
FIGURE 5.17: HYPOXIA INDUCED GENE EXPRESSION OF ENCAPSULATED PSEUDOISLETS AFTER 72 H OF STATIC VERSUS ROTATION CULTURE.	146
FIGURE 5.18: IMMUNOFLUORESCENCE STAINING OF ENCAPSULATED ISLETS AFTER STATIC (1A-AD) AND ROTATION CULTURE (2A-2D).	146
FIGURE 5.19: NO PRIMARY ANTIBODY CONTROL OF IMMUNOFLUORESCENCE STAINING OF ENCAPSULATED ISLETS AFTER STATIC (1A-AD) AND ROTATION CULTURE (2A-2D).	147
FIGURE 5.20: PHOTOGRAPHS OF THE PERFUSION SET UP WITH HYDROGEL.....	147
FIGURE 5.21: THREE MEMBRANES WITH CAF HYDROGEL BEFORE AND AFTER ~7 H OF PERFUSION.....	148
FIGURE 6.1: LOSS OF ISLET MASS THROUGH THE ISOLATION AND TRANSPLANTATION PROCESS.....	153

List of Tables

TABLE 1.1: ADVANTAGES AND DISADVANTAGES FOR SYNTHETIC AND NATURAL POLYMERS FOR SCAFFOLD MANUFACTURING (KAVIANI AND AZARPIRA, 2016, PEREZ-BASTERRECHEA ET AL., 2018).	25
TABLE 2.1: PANCREAS AND ISLET DONOR INFORMATION.	34
TABLE 2.2: DIAMETER RANGE OF ISLETS AND CONVERSION FACTOR FOR IEQ ASSESSMENT	37
TABLE 2.3: PRIMARY ANTIBODIES USED FOR STAINING WITH COMPANY AND DILUTION	40
TABLE 2.4: SECONDARY ANTIBODIES WITH COMPANY AND DILUTION	41
TABLE 2.5: CONDITIONS FOR THE THERMAL CYCLER FOR CDNA SYNTHESIS.	42
TABLE 2.6: DNA PROBES FOR QPCR WITH GENE NAME, GENE SYMBOL, SPECIES AND DETECTED TRANSCRIPT.	43
TABLE 2.7: COMPOSITION PROTEIN EXTRACTION BUFFER	44
TABLE 3.1: INFORMATION FOR PANCREAS DBD DONORS WITH ASCENDING CIT.	65
TABLE 3.2: INFORMATION FOR PANCREAS DCD DONORS WITH ASCENDING CIT.	66
TABLE 3.3: NEWCASTLE ELECTRON MICROSCOPY ISCHAEMIA SCORE (NEMIS) FOR ASSESSMENT OF PANCREATIC ACINAR CELLS	71
TABLE 3.4: NEMIS FROM 0 TILL 3 FOR NUCLEUS, MITOCHONDRIA, ER AND VACUOLISATION WITH EXAMPLE IMAGES.	72
TABLE 3.5: DEGRADATION SCORES FOR DEVELOPMENTAL COHORT.	73
TABLE 3.6: TWO-TAILED SPEARMAN CORRELATION AND SIGNIFICANCE OF CIT AND NEMIS SCORES FOR ALL DONORS AS WELL AS DBD AND DCD SEPARATE.	74
TABLE 3.7: ISOLATED ISLET BATCHES FROM DBD DONORS.	77
TABLE 3.8: ISOLATED ISLETS BATCHES FROM DCD DONORS.	78
TABLE 3.9: ELECTRON MICROSCOPY ENDOCRINE DAMAGE SCORE FOR ASSESSMENT OF ACUTE DAMAGE IN ENDOCRINE CELLS.	84
TABLE 3.10: ADDITIONAL CATEGORIES TO EXTEND NEMIS TO ELECTRON MICROSCOPY ENDOCRINE DAMAGE SCORE FOR ASSESSMENT OF ISOLATED ISLETS.	85
TABLE 3.11: SCORES FOR ENDOCRINE CELLS IN TISSUE AND ISOLATED ISLETS SAMPLES.	86
TABLE 3.12: TWO-TAILED SPEARMAN'S RHO CORRELATION OF ENDOCRINE DAMAGE SCORES AND CIT FOR ENDOCRINE CELLS IN TISSUE SAMPLES.	87
TABLE 4.1: SCORES FOR PSEUDOISLET INTEGRITY INDEX AFTER MATSUMOTO (MATSUMOTO ET AL., 2004)	116
TABLE 4.2: DONOR DATA OF HUMAN ISOLATED ISLETS WITH DONOR NUMBER, LDIS NUMBER, GENDER, BMI, DONOR TYPE, COLD ISCHAEMIA TIME, PURITY AND VIABILITY.	117
TABLE 6.1: ADVANTAGES AND DISADVANTAGES OF DIFFERENT ISLET MODELS USED IN THIS THESIS.	154

List of Abbreviations

Abbreviation	Description
ATP	Adenosine triphosphate
AGE	Advanced glycation end products
Tris	2-Amino-2-(hydroxymethyl)propane-1,3-diol
BM	Basement membrane
BMI	Body mass index
BSA	Bovine serum albumin
Ca²⁺	Calcium
CaCl₂	Calcium chloride
CaO₂	Calcium peroxide
CO₂	Carbon dioxide
FCCP	Carbonyl cyanide 4-(trifluoromethoxy) phenylhydrazone
CGA	Chromogranin A
CIT	Cold ischaemia time
CAF	Collagen I + alginate + fibrinogen
cDNA	Complementary DNA
CMRL	Connaught Medical Research Laboratories
CSII	Continuous subcutaneous insulin infusion
ddH₂O	Demineralised water
DCCT	Diabetes Control and Complications Trial
DBD	Donor after brain death
DCD	Donor after circulatory death
DMEM	Dulbecco Modified Eagle Medium
DMSO	Dimethyl sulfoxide
ETC	Electron transport chain
ER	Endoplasmic reticulum
EDS	Energy dispersive X-ray spectroscopy
EDTA	Ethylenediaminetetraacetic acid
ECAR	Extracellular acidification rate

ECM	Extracellular matrix
FBS	Foetal bovine serum
Glut1	Glucose transporter 1
H&E	Haematoxylin & Eosin
HTK	Histidine tryptophan ketoglutarate
hESCs	Human embryonic stem cells
hiPSCs	Human induced pluripotent stem cells
IF	Immunofluorescence
iPSCs	Induced pluripotent stem cells
IBMIR	Instant blood mediated inflammatory reaction
Ins 1	Insulin 1
Ins 2	Insulin 2
IEQ	Islet equivalent
LDHA	Lactate dehydrogenase
MODY	Maturity onset diabetes of youth
Mct4	Monocarboxylate transporter 4
NEMIS	Newcastle Electron Microscopy Ischaemia Score
NHSBT	NHS blood and transplant
NAD	Nicotinamide adenine dinucleotide
n/s	Not specified
OXPHOS	Oxidative phosphorylation
OCR	Oxygen consumption rate
PP	Pancreatic polypeptide
PAK	Pancreas after kidney
PTK	Pancreas transplanted alone
PBS	Phosphate buffered saline
PIM	Pimonidazole
PCL	Polycaprolactone
PLA	Polylactic acid
PLGA	Polylactic-co-glycolic acid
PGA	Polyglycolic acid

PI	Propidium iodide
QUOD	Quality in Organ Donation
qRT-PCR	Quantitative real time PCR
SEM	Scanning electron microscopy
SD	Standard deviation
SPK	Simultaneous pancreas kidney
SR/FG	Sirius red/Fast green
K⁺	Sodium
SDS	Sodium dodecyl sulphate
TEM	Transmission electron microscopy
UK	United Kingdom
UKPDS	United Kingdom Prospective Diabetes Study
UW	University of Wisconsin
U3	Urocortin 3
VEGF-A	Vascular endothelial growth factor A

Chapter 1. Introduction

1.1 Human pancreas structure and acinar tissue

The pancreas is a complex organ located behind the stomach in the upper abdomen with length in the adult male ranging from 14-18 cm and a weight of about 100 g (Longnecker, 2014, Lankisch and Banks, 1998). The organ can be divided into tail, body, head and uncinate process, whereby the head is located near the duodenum and the tail near the spleen (Wittingen and Frey, 1974, Longnecker, 2014). The pancreas primarily consists of two components, the exocrine and the endocrine compartment.

1.2 The exocrine pancreas

The exocrine tissue secretes digestive enzymes transported into the gut via the pancreatic duct into the duodenum (Figure 1.1). This makes up more than 95% of the pancreas and includes acinar cells, duct cells, vessels, nerves and extracellular matrix (ECM)(Longnecker, 2014, Lankisch and Banks, 1998). The digestive juice is produced by acinar cells which are grouped in grape like tubular networks named acini which converge into the duct system (Longnecker, 2014, Bardeesy and DePinho, 2002, Lankisch and Banks, 1998). The duct system comprises the intralobular ducts, interlobular ducts and main pancreatic duct, which transports the digestive enzymes from the pancreas to the small intestine (Longnecker, 2014).

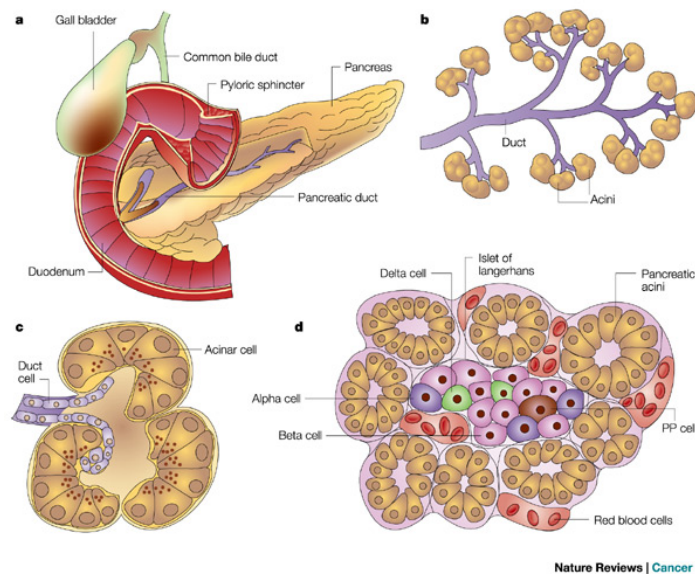


Figure 1.1: Pancreas tissue structure.

a) pancreas and duodenum connected via the duct b) exocrine pancreas macrostructure and c) exocrine pancreas microstructure d) endocrine pancreas in between exocrine pancreas (Bardeesy and DePinho, 2002).

1.2.1 The endocrine pancreas

1.2.2 Human islet structure and function

The second function of the pancreas is tight regulation of blood glucose levels through the production and release of hormones into the bloodstream - predominantly insulin and glucagon. The endocrine compartment is comprised of islets of Langerhans which are distributed throughout the whole pancreas. Islets make up just 1-2% of the pancreatic tissue with a size range of 50 μm to 400 μm diameter (Longnecker, 2014, Nam et al., 2010, Stendahl et al., 2009).

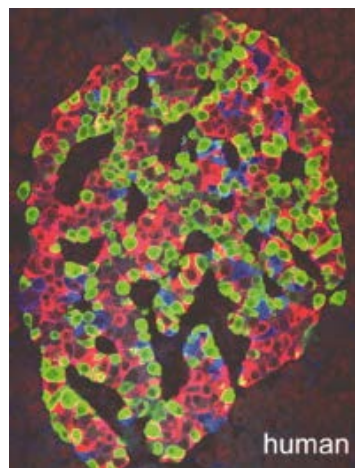


Figure 1.2: Endocrine cell distribution in human islets.

Human islet in a post mortem pancreas tissue section with immunofluorescence staining for insulin (red), glucagon (green) and somatostatin (blue). Picture from (Cabrera et al., 2006).

The distribution of islets through the pancreas is not uniform with estimates that up to 45% of all islets may be found in the tail (Wittingen and Frey, 1974). Islets contain different cell types (Figure 1.2) which synthesize, store and secrete distinct hormones: α -cells (glucagon), β -cells (insulin), δ -cells (somatostatin) and PP-cells (pancreatic polypeptide) (Bardeesy and DePinho, 2002, Cabrera et al., 2006). It is not finally clarified if the composition of different cell types in human islets follows a specific distribution or not, compared to rodent islets where β -cells are located in the core and mantled by a thinner layer of the other endocrine cells (Steiner et al., 2010, Cabrera et al., 2006, Bosco et al., 2010). In human islets it has also been reported that islets in the neck of the pancreas possess a higher proportion of α -cells (Cabrera et al., 2006). Islets are highly vascularised

(Figure 1.3), consequently every single endocrine cell is located near a blood vessel (Bonner-Weir and Orci, 1982, Cabrera et al., 2006). Despite representing a small proportion of the pancreas (2-3%), islets receive between 15% and 20% of the pancreatic blood flow with up to ten-fold higher blood flow compared to the exocrine tissue (Holt et al., 2010, Lifson et al., 1989).

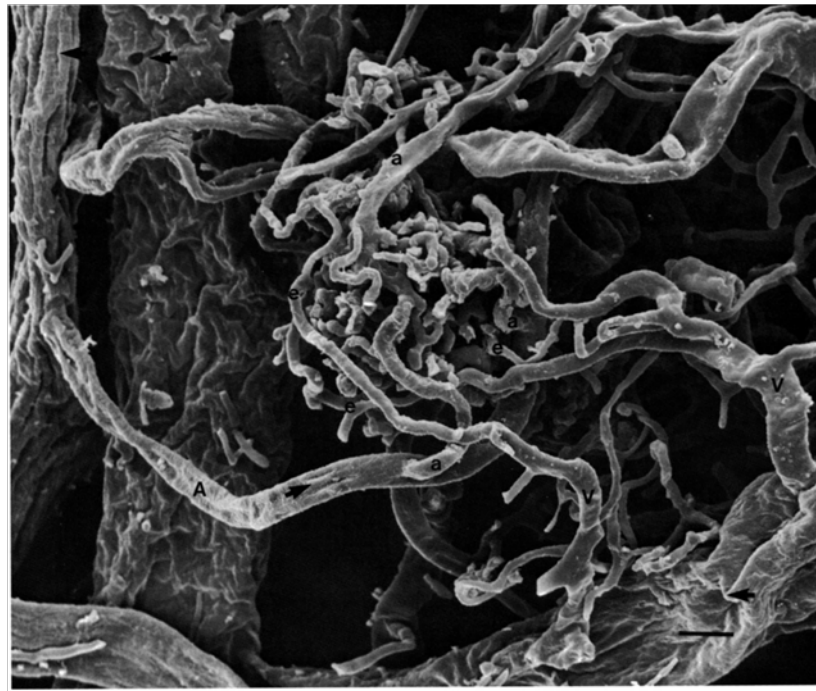


Figure 1.3: Vascular system around and in the islet of a rat demonstrating the dense vascularisation. Picture from (Bonner-Weir and Orci, 1982).

1.2.3 Insulin biosynthesis and glucose homeostasis

The different cell types in islets produce different hormones to regulate glucose homeostasis. Insulin is produced by β -cells and secreted in response to elevated blood glucose levels.

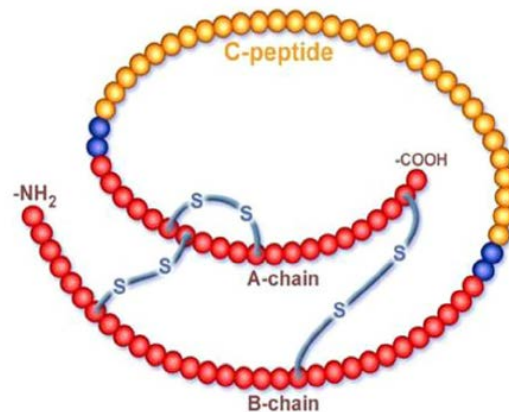


Figure 1.4: Structure of proinsulin with the A-chain, B-chain and C-peptide.
Picture from (Akinlade et al., 2014).

The β -cells have a high metabolic activity due to constant insulin synthesis and secretion and therefore also a high mitochondrial activity. Expression of the insulin gene is induced in the presence of increased blood glucose level by enhanced activity of transcription factors including Pdx-1, NeuroD1/ β 2 and MafA (Andrali et al., 2008). These transcription factors are influenced by changes in glucose concentration through several mechanisms including translocation to the nucleus, altered binding activity and interaction with other proteins (Andrali et al., 2008). Activation of the transcription factors leads to expression of the insulin gene and translation of the polypeptide, preproinsulin, comprising a signal peptide, A-chain, B-chain and C-chain (also called C-peptide) (Holt et al., 2010). With the cleavage of the signal peptide proinsulin with the A chain and the B chain of insulin and the C-peptide is transported into secretory vesicles (Holt et al., 2010, Steiner et al., 2009) (Figure 1.4). There, the C-peptide chain is cleaved and stored together with mature insulin in secretory granules until exocytosis occurs (Holt et al., 2010, Steiner et al., 2009). Through intake of carbohydrates, blood glucose levels rise leading to proportionate insulin release as shown in Figure 1.5 (Lemaire and Schuit, 2012). Glucose is transported inside

the β -cell through a glucose transporter where it is phosphorylated by glucokinase (Ashcroft and Rorsman, 2012, Holt et al., 2010). Subsequently it is metabolised inside the mitochondria via aerobic glycolysis and mitochondrial oxidation leading to an increase of adenosine triphosphate (ATP) (Lemaire and Schuit, 2012, Holt et al., 2010). High levels of ATP in the β -cell leading to closure of K^+ -channels and, in turn, depolarisation of the cell membrane which is followed by opening of Ca^{2+} channels (Lemaire and Schuit, 2012, Holt et al., 2010, Rorsman et al., 2000). Influx of Ca^{2+} ions leads to exocytosis of insulin granules (Ashcroft and Rorsman, 2012, Holt et al., 2010).

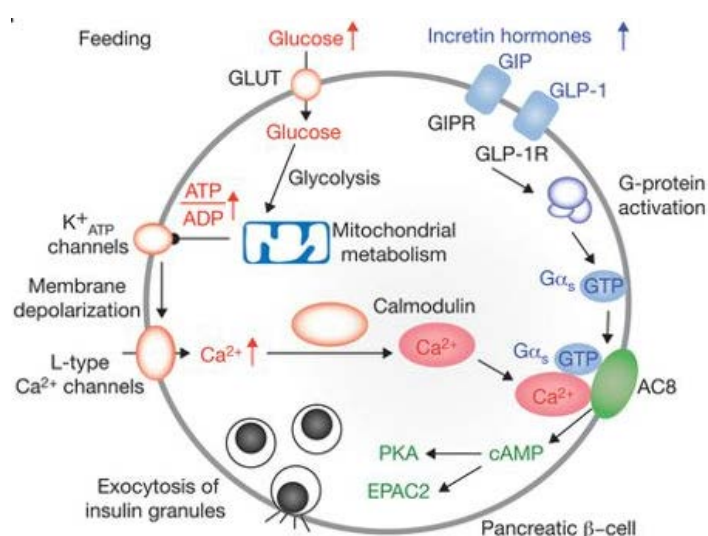


Figure 1.5: Schematic summary of insulin stimulus secretion coupling (Lemaire and Schuit, 2012).

Secretion of insulin takes place in different ways. First there is a basal secretion which controls the blood glucose levels during fasting, constituting approximately 50% of overall secretion (Polonsky et al., 1988). Second, insulin is released by the β -cell in response to carbohydrate intake in two phases (Grayson et al., 2013) (Figure 1.6). The first phase occurs fast after the increase of blood glucose levels and peaks quickly (Ashcroft and Rorsman, 2012). This is possible due to membrane bound insulin granules which can be released in a time span of a few minutes (Holt et al., 2010). Subsequently the second phase occurs which is ATP-dependent, and a more sustained and slower insulin release continuing as long as the blood glucose levels are high (Holt et al., 2010, Rorsman et al., 2000).

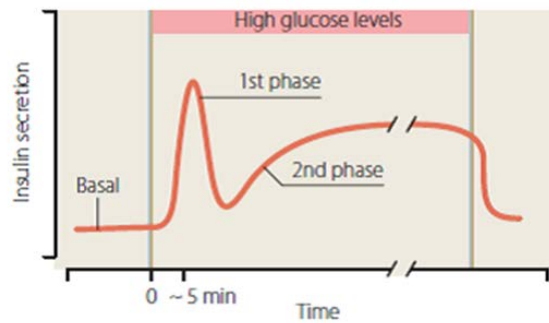


Figure 1.6: Insulin release after food intake with characteristic two phases in response to high blood glucose levels (Holt et al., 2010).

1.3 Tissue structure and its role in function

1.3.1 Extracellular matrix

ECM is present in two different forms, the basement membrane (BM) and the interstitial matrix, distinguishable through their structure (Figure 1.7).

In general ECM is present in various tissues as BM where the matrix is in close contact to cells separating different structures from one another (Theocharis et al., 2016, LeBleu et al., 2007). Main components are collagen IV and laminin forming two networks which are linked by additional ECM proteins, such as nidogen and perlecan (LeBleu et al., 2007, Jayadev and Sherwood, 2017, Pozzi et al., 2017). Furthermore, minor factors specific to individual tissue requirements including different proteins, glycoproteins, and proteoglycans, including argin, fibulin, hemicentin, collagen XV, collagen XVIII, SPARC and BM90 may form part of the network (LeBleu et al., 2007, Jayadev and Sherwood, 2017).

ECM can also be present as interstitial matrix where it provides a scaffold for cells and defines the characteristics of tissues, such as mechanical properties (Theocharis et al., 2016). Main components include fibrous proteins, polysaccharides and proteoglycans. ECM proteins are for example elastins, fibronectins, laminins and collagens, with fibrous collagen, especially collagen I, being most abundant forming a three-dimensional mesh (Frantz et al., 2010). Additionally proteoglycans, glycoproteins and polysaccharides like fibronectin or hyaluronic acid are capable of retaining water thus forming a gel like structure (Hynes and Naba, 2012). Further compounds such as growth factors can bind to components of the ECM functioning as a reservoir and can be released if required or triggered (Frantz et al., 2010).

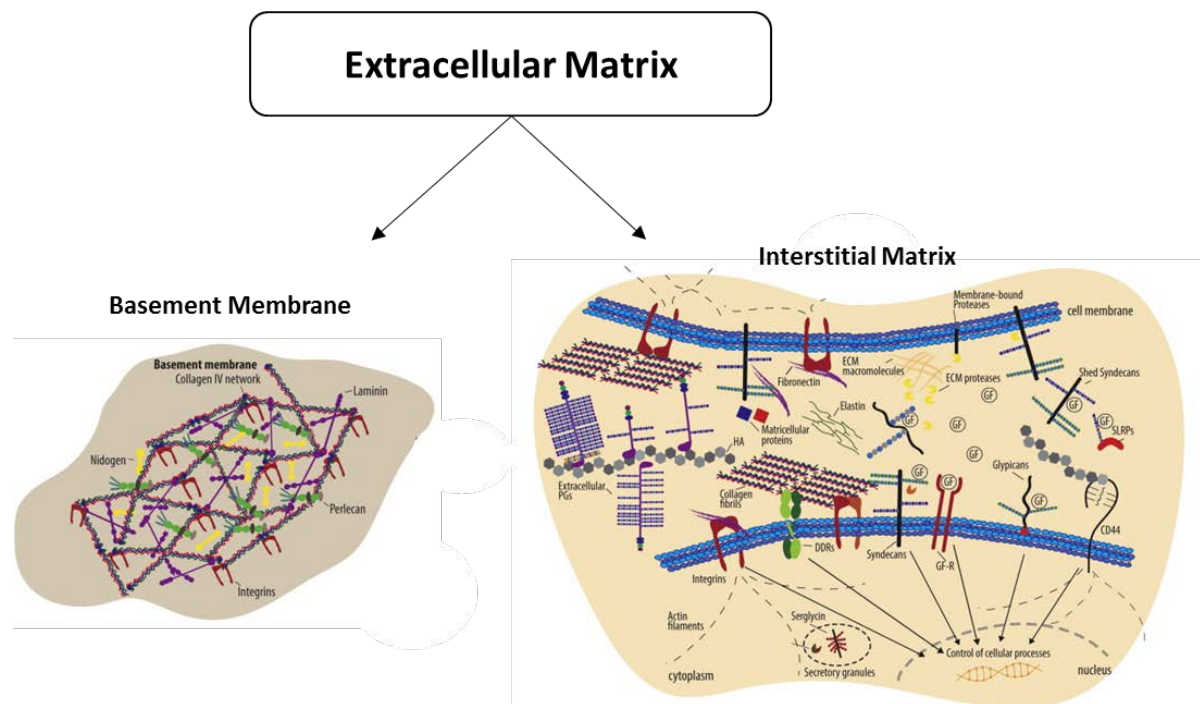


Figure 1.7: Schematic of extracellular matrices and their components when forming BM or interstitial matrix. Modified from (Theocharis et al., 2016).

Specifically in the pancreas, ECM is present as BM around the border of the islets and around acinar clusters as well as BM around the vessels inside of islets (Wang et al., 1999, van Deijnen et al., 1992, Otonkoski et al., 2008). The main components are collagen IV, laminin, perlecan and fibronectin and it functions as a three-dimensional barrier structure which provides structural support for different cell types and tissues, playing a role also in cell signalling (Salvay et al., 2008, Cross et al., 2017). The BM around the vessels in human islets has a characteristic appearance of a doubled layered structure and is secreted by endothelia cells (Otonkoski et al., 2008, Nikolova et al., 2006, Virtanen et al., 2008). Additionally the whole islet is surrounded by a discontinuous BM also called peri-islet capsule which separates the endocrine cells from the exocrine cells of the pancreas (van Deijnen et al., 1992). The capsule shown in Figure 1.8 consists of two layers of BM with ECM components including collagen fibres in between the layers (van Deijnen et al., 1992). Analysis of decellularized organs showed the matrisome of complete human pancreas matrix composed mostly of different collagens especially fibril forming collagens with collagen I the most abundant as well as collagen IV which is part of the BM (Sackett et al., 2018). Second most abundant in the ECM of human pancreas were glycoproteins like

fibrillin and laminin. It was shown that the composition of ECM in islets is impacting on their mechanical properties especially stiffness showing the importance of ECM for tissue properties (Nagy et al., 2018). Furthermore, it is suggested that mechanical stimuli impact on the insulin response in MIN6 pseudoislets (Nyitray et al., 2014). In addition, changes to the ECM may promote the activation and infiltration of immune cells in the islet microenvironment leading to β -cell destruction and therefore Type 1 diabetes (Bogdani et al., 2017).

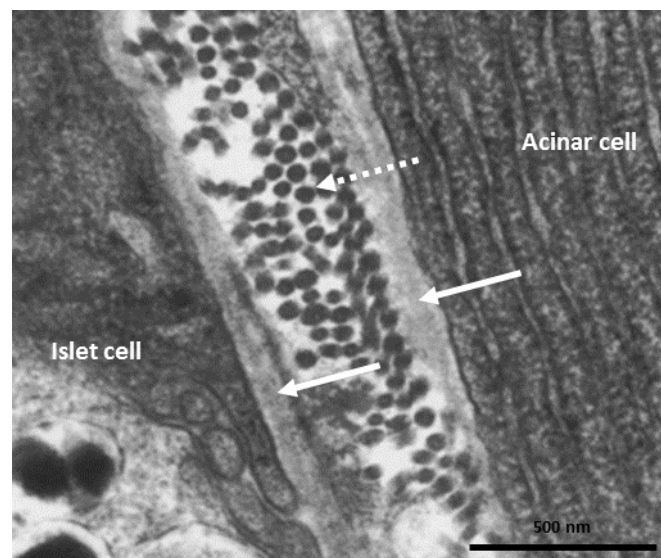


Figure 1.8: Transmission electron microscopy of human pancreas. The islet cell is separated from an acinar cell by two layers of BM (arrows) with ECM components including collagen fibres (dashed arrow) in between. Figure altered from (van Deijnen et al., 1992).

1.3.2 Islet connectivity

Signalling through cell-to-cell and cell-to-matrix connections can impact on the viability and function of islets and are important for the integrity. Connections between islet cells can be formed through adherens junctions, tight junctions or gap junctions and they are densely distributed in the islet indicating a tightly packed arrangement (Heileman et al., 2016) (Figure 1.9). Gap junctions in between β -cells are built up by connexin Cx36, which forms a channel between two cells (Peiris et al., 2014). Adherens junctions built up by E-Cadherin connect the actin cytoskeleton of two cells with each other (Fuchs and Raghavan, 2002). The last form of cell-to-cell adhesion observed in islets are tight junctions which

seal the interstitial space between two single cells (Heileman et al., 2016, Tsukita et al., 2001). Cell-to-cell connections are important to maintain the integrity of islets, as well as for the communication between single islet cells especially the regulation of electrical activity and insulin secretion in response to changing blood glucose levels (Benninger et al., 2011).

In addition, islet cells are in contact with the ECM in the peri-islet capsule and in the BM around the vessels inside the islet (Figure 1.9). This contact is built up by transmembrane receptors called integrins, which can influence β -cell function, survival, proliferation, motility, differentiation and insulin secretion (Kaido et al., 2006). Through the attachment of ECM proteins to the integrin receptor on the cell surface of the islet, intracellular signal cascades are activated. Different cascades are influenced through this binding and in turn influence the proliferation, survival and migration of the cell (Townsend and Gannon, 2019). Loss of the connection to the matrix can lead to matrix detachment-induced apoptosis called anoikis, which shows that the cell-matrix interactions are important for islet survival (Irving-Rodgers et al., 2014, Cross et al., 2017). The connection to the BM around the vasculature appears to be especially important, since the islet is highly vascularised providing cell-to-matrix contact for the majority of the islet cells (Nikolova et al., 2006).

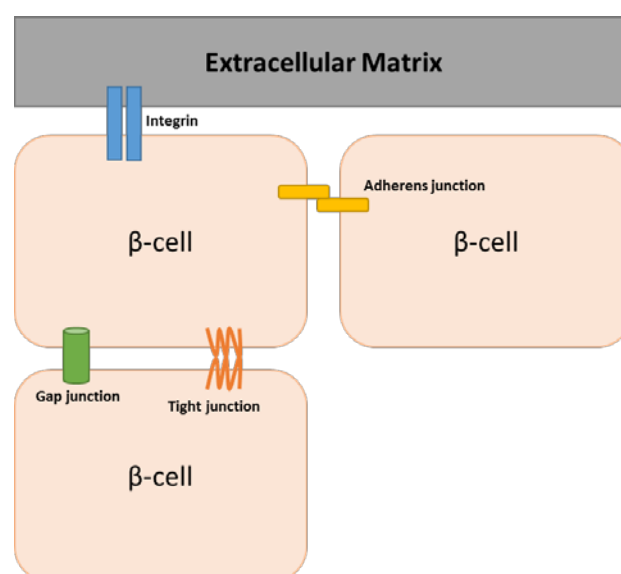


Figure 1.9: Cell-to-cell connections between single β -cells named gap junctions, tight junctions and adherens junction. Cell-to-matrix connections between β -cells and the ECM composed of integrins.

1.4 Diabetes mellitus

Diabetes mellitus encompasses metabolic diseases characterised by high blood glucose levels leading to at least relative insulin deficiency, associated with risk of long-term as well as short-term complications (American Diabetes Association, 2010, World Health Organisation, 1999).

1.4.1 Type 1 diabetes

Type 1 diabetes is characterised by insulin deficiency leading to necessity for insulin replacement for survival. It is believed to be an autoimmune disease where β -cells are attacked and killed by the immune system of the patient (Atkinson et al., 2014). The β -cells are important for regulation of blood glucose levels and through loss of normal function this regulation is lost. The trigger for this autoimmune attack is still not clear, but it is suggested that there is a genetic as well as an environmental component which can influence the development of Type 1 diabetes (Harjutsalo et al., 2008, Barrett et al., 2009). The HLA genotypes DR and DQ, where multiple susceptible gene loci have been identified, are associated with an increased risk of Type 1 diabetes (Daneman, 2006, Haller et al., 2005). However, no single gene is either necessary or sufficient for the development of Type 1 diabetes (Haller et al., 2005). Nonetheless, a higher incidence rate has been shown in certain populations (Barrett et al., 2009, Harjutsalo et al., 2008). The rapid rise in incidence over recent years suggests environmental factors rather than genetic components may be the critical factor for development of Type 1 diabetes, since the transmission of specific haplotypes would take longer to develop (Gillespie et al., 2004). Several environmental factors have been postulated including obesity, vitamin D deficiency, viral infection and early exposure to cow's milk (Harjutsalo et al., 2008, Knip et al., 2005, Vaarala et al., 2002).

Additionally, an analysis of children from Asian populations in the United Kingdom (UK) showed that they have a much higher incidence rate of Type 1 diabetes than children in Asia (Raymond et al., 2001). Next to factors associated with geographic locations such as viruses, environmental toxins or foods are suspected as triggers for Type 1 diabetes (Daneman, 2006). Diagnosis occurs most commonly in children with increased diagnosis in particular geographic locations and ethnic groups (Figure 1.10) (Haller et al., 2005, Holt et al., 2010).

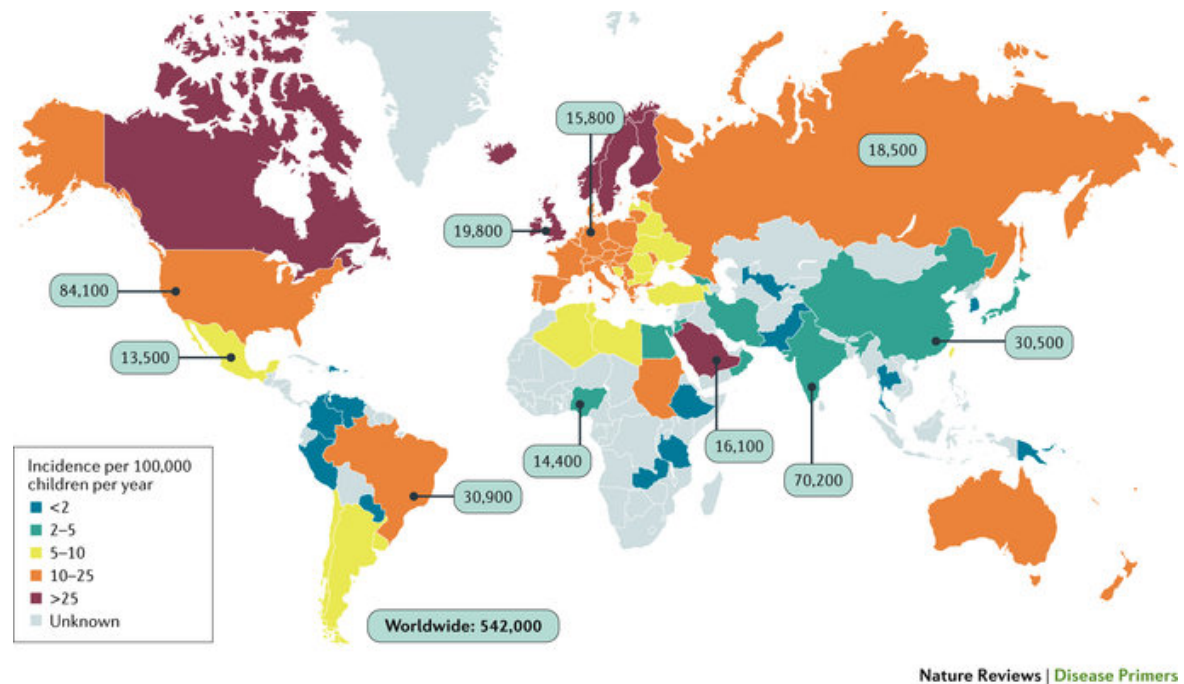


Figure 1.10: Incidence for Type 1 diabetes worldwide (Katsarou et al., 2017).

Type 1 diabetes is increasingly diagnosed in adults across the full age range (Harjutsalo et al., 2008, Haller et al., 2005, Thunander et al., 2008). For the diagnosis of diabetes a fasting blood glucose level of more than 7.0 mmol/l is required, although there is no need to obtain a fasting test if random unfasted glucose is significantly elevated (>11.1 mmol/l) (Atkinson et al., 2014). Additionally HbA1c level is measured, providing an indication of the average blood glucose concentration over several months with a level higher than 6.5% being diagnostic for diabetes (Nathan, 2009). Additionally characteristic autoantibodies to islet cells, insulin or glutamic acid decarboxylase can usually be detected (Atkinson et al., 2014). At the point of diagnosis approximately 10-20% of functioning β -cell mass is left (Knip et al., 2005) (Figure 1.11). Shortly after diagnosis a transient restoration of function with decreased injected insulin requirement can take place (Abdul-Rasoul et al., 2006). This so called 'honeymoon phase' can last from several weeks to months and the insulin requirement can be completely redundant (Abdul-Rasoul et al., 2006).

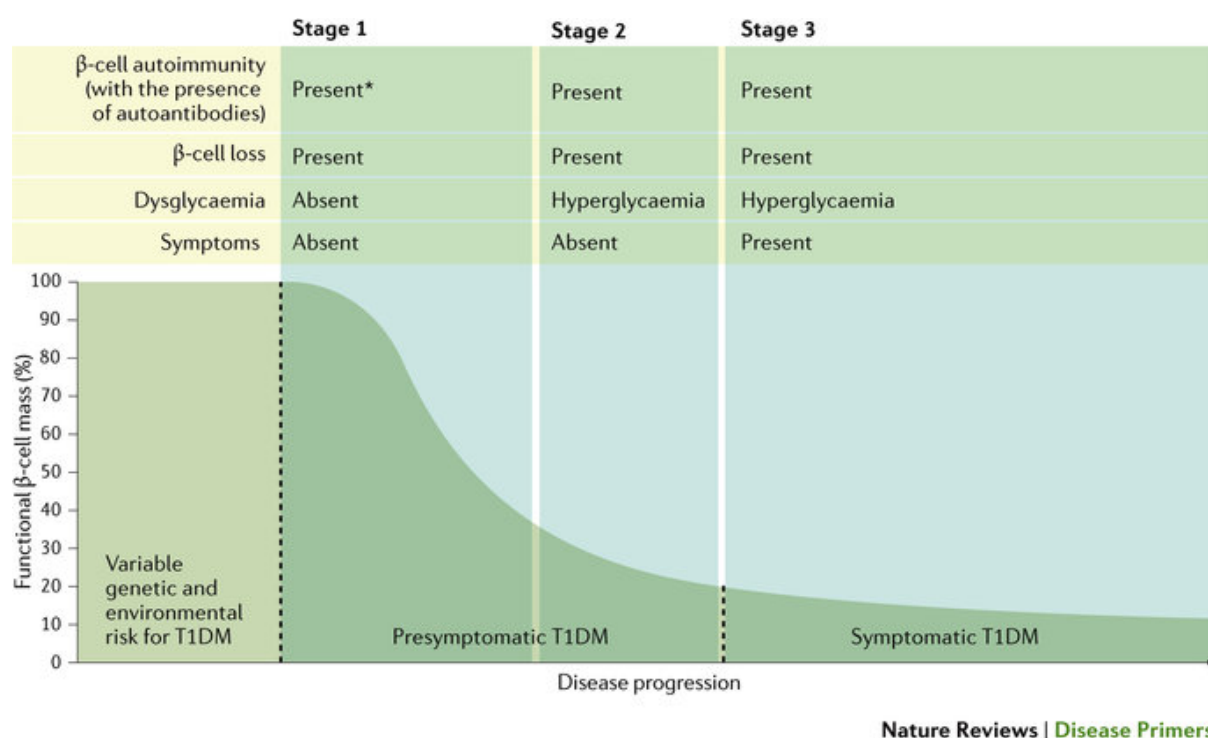


Figure 1.11: Progression of Type 1 diabetes presented by presymptomatic stages 1 and 2 followed by symptomatic stage 3 with changes in functional β -cell mass (Katsarou et al., 2017).

1.4.2 Type 2 diabetes

The commonest form of diabetes mellitus is Type 2 diabetes, making up around 90-95% of all diabetes patients and is characterised by insulin resistance within the target tissues (American Diabetes Association, 2010). It is often linked with obesity (associated with insulin resistance) which, together with other environmental and genetic factors, increases the risk of development of Type 2 diabetes (Kahn et al., 2006, Temneanu et al., 2016). It is normal that sensitivity to insulin changes during life, but in patients with Type 2 diabetes the pancreatic β -cell cannot compensate for these changes which leads to constantly high blood glucose levels (Kahn et al., 2006). Genetic predisposition can increase insulin resistance of the tissue which leads to more stress for the β -cells. Patients with Type 2 diabetes also have relative insulin deficiency (American Diabetes Association, 2010). It can be asymptomatic, or symptoms can develop over several months and years, similar to those in Type 1 diabetes including thirst and excessive urine production (Temneanu et al., 2016).

1.4.3 Gestational diabetes

Another form of diabetes is gestational diabetes where women develop glucose intolerance during the pregnancy (Bottalico, 2007). Through placental hormones, insulin resistance is increased, and greater β -cell function is required to maintain normal blood glucose (Plows et al., 2018). With a genetic predisposition the cells may not be able to cope with this amount of stress and the mother will develop diabetes. Onset can occur at any stage of pregnancy, but it is more common during the last third, and for women with a family history of diabetes, obesity, advanced maternal age or related to certain ethnicities (Bottalico, 2007). The high blood glucose resolves after the birth of the child, however, the mother is at high risk of developing Type 2 diabetes later in life (American Diabetes Association, 2004).

1.4.4 Other forms of diabetes

There are a number of rarer forms of diabetes. One category is maturity onset diabetes of youth (MODY). It usually presents in children and teenager and is thought to be caused by single gene mutations leading to dysfunction of β -cells (Holt et al., 2010). Identified mutations affect either the enzyme glucokinase or transcription factors which are important for β -cell development and function (Holt et al., 2010, McDonald and Ellard, 2013).

Another category of diabetes is neonatal diabetes. It is diagnosed in children with an age of under six months and can be permanent or transient (Holt et al., 2010). It can also be associated with neurological abnormalities including mental and physical developmental delay (Lemelman et al., 2018). Like MODY it is caused by gene mutations which influence β -cell function and development (Lemelman et al., 2018, Støy et al., 2007). The majority have mutation affecting the K^+ -channel and therefore the exocytosis of insulin vesicles (Holt et al., 2010).

Additionally, diabetes can develop through pharmaceutical interactions or secondary to pancreatic diseases including pancreatitis. Pharmaceutical interactions may reduce synthesis or secretion of insulin or they can reduce insulin sensitivity (Holt et al., 2010, American Diabetes Association, 2010). Diseases of the exocrine pancreas including pancreatic cancer, pancreatitis or cystic fibrosis are categorised as Type 3c diabetes with different mechanisms leading to hyperglycaemia (Hart et al., 2016). Whereas it is believed

that in cases of pancreatic cancer hyperglycaemia is caused through paraneoplastic effects, it is believed that in the case of pancreatitis inflammatory destruction of the pancreas may lead to impaired glucose homeostasis (Sah et al., 2013, Hart et al., 2016).

1.4.5 Complications

Diabetes can cause specific microvascular complications including retinopathy, nephropathy and neuropathy (Forbes and Cooper, 2013). These are caused by chronic high blood glucose levels which can occur with all forms of diabetes (Holt et al., 2010). High blood glucose levels influence different mechanisms in the cells, which induce complications (Forbes and Cooper, 2013). For example, high blood glucose can lead to an increased flux of the polyol pathway creating a redox imbalance of oxidized and reduced nicotamine adenine dinucleotide (NADH/NAD⁺) increasing oxidative stress and therefore complications of diabetes (Yan, 2018). Another consequence of high blood glucose levels is the increased formation of advanced glycation end products (AGE) which can alter tissue properties and causing microvascular complications (Singh et al., 2001). Through the glycation of proteins their structure and function is disrupted and for example for ECM proteins like collagen and fibrinogen this can impact on organ function or lead to vascular dysfunction increasing complications of diabetes (Singh et al., 2014, Strieder-Barboza et al., 2019). Different studies showed increased AGE formation in tissues of diabetic patients with the possibility of suppression of AGE production through pharmacological intervention leading to inhibition of deterioration of diabetic complications including neuropathy (Kawai et al., 2010, Strieder-Barboza et al., 2019).

The Diabetes Control and Complications Trial (DCCT) showed that intensive insulin therapy in patients with Type 1 diabetes could reduce complications of high blood glucose (The Diabetes Control and Complications Trial Research Group, 1993, Nathan, 2014). The UK Prospective Diabetes Study (UKPDS) showed that the intensive treatment with insulin or sulphonylureas reduced microvascular complications in Type 2 diabetes (UK Prospective Diabetes Study Group, 1998).

Diabetes is also a risk factor for macrovascular disease in parallel with obesity, high fat levels, high blood pressure and smoking (Forbes and Cooper, 2013). Associated complications include increased risk of a heart attack (myocardial infarction) or a stroke, atheroma and a reduction in life expectancy and may be addressed with a healthy lifestyle

including weight control and physical activity, avoidance of smoking, reducing of blood pressure and lipid control (Daneman, 2006).

1.4.6 Management of diabetes

Currently there is no cure for Type 1 diabetes, however with the discovery of insulin in 1922 inevitable early mortality was prevented (Banting et al., 1922, Holt et al., 2010). The primary treatments for Type 1 diabetes combine careful glucose monitoring with exogenous insulin treatment (Atkinson et al., 2014). It is thought that the long-term life expectancy of newly diagnosed people with Type 1 diabetes could be increased due to improvements in glucose monitoring and insulin administration (Miller et al., 2012), but this does not diminish the uninterrupted burden of self-management. Additionally, self-administration of exogenous insulin by injection or continuous subcutaneous insulin infusion (CSII) pumps can lead to dangerously low glucose levels (The Diabetes Control and Complications Trial Research Group, 1993). Some patients may lose their hypoglycaemia awareness resulting in an increased risk of hypoglycaemic events requiring assistance from another person and occasionally death (Martín-Timón and Del Cañizo-Gómez, 2015). These attacks are one of the greatest fears of people with Type 1 diabetes. It was shown that the intensive treatment in the DCCT led to an increased rate of hypoglycaemic events (Nathan, 2014). This shows that hypoglycaemia is a major limiting factor towards achieving blood glucose control (Daneman, 2006). Reasons for hypoglycaemic attacks can vary, but typically result from the administration of an insulin dose too high for the requirements affected by food intake and physical activity (Daneman, 2006). These events can lead to fear and anxiety in patients resulting in an impaired glycaemic control (Katsarou et al., 2017). In cases of severely impaired blood glucose control β -cell replacement therapy in the form of pancreas or islet transplantation can be an option.

For the treatment of Type 2 diabetes insulin resistance has to be addressed. This can be achieved with drugs such as metformin or thiazolidinediones (Bailey, 2005). Insulin or sulphonylureas administration may be used for intensive blood glucose control to decrease the risk of microvascular complications (UK Prospective Diabetes Study Group, 1998). The potential for recovery of β -cell function following a marked reduction in insulin resistance with, in some cases, diabetes remission has been demonstrated through

bariatric surgery or very low calorie diet (Knop and Taylor, 2013, Taylor, 2013). Pancreas transplantation in combination with a kidney transplant can be an option in selected cases of people with insulin-treated Type 2 diabetes in renal failure (Hudson et al., 2015). With avoidance of immunosuppression and engraftment of sufficient β -cell mass through improved encapsulation strategies or alternative cell sources such as induced pluripotent stem cells (iPSCs), β -cell replacement therapy may become a treatment option for more patients with Type 2 diabetes (Sneddon et al., 2018).

1.5 Current β -cell replacement therapy

1.5.1 *Pancreas transplantation*

Transplantation of a whole pancreas typically leads to insulin independence and can be a treatment option for Type 1 diabetes patients with severe recurrent hypoglycaemia and complete unawareness as well as patients in need of another donor organ for example kidney. The pancreas can either be transplanted alone (PTA), after a kidney transplantation (PAK) or simultaneous with a kidney (SPK) with a 1-year pancreas graft survival of 87% for SPK compared to 78% for PTA (Flatt et al., 2019)

In the UK patients are considered for transplantation if they experience severe hypoglycaemic events and/or chronic renal failure if they have a body mass index (BMI) from under 30 kg/m² and are fit enough to survive the transplantation (Mittal and Gough, 2014, White et al., 2009). However, the operation is a major abdominal surgery with various complications including thrombosis, bleeding, graft pancreatitis or infection leading to a relaparotomy rate of 31% and graft loss of 9% in a single centre study (Kopp et al., 2018). Despite constant improvements the mortality rate for pancreas recipients are still up to 4% at one year post transplantation and up to 20% five years' post transplantation evidencing the severity of the procedure (Gruessner and Gruessner, 2013). For transplantation a deceased organ is required which can be obtained from a donor after brain death (DBD) or a carefully selected donor after circulatory death (DCD) with both demonstrating comparable short term results (Muthusamy et al., 2012). For DCD donors limited cold ischaemia time (CIT) is preferable due to a significant impact of CIT on graft survival and may be achieved by prioritising local transplant centres (Hudson et al., 2015). In the UK pancreas donors with an age of <60 years and a BMI of <30 kg/m² are accepted for transplantation and pancreata are allocated on a national basis according to

an allocation scheme considering CIT, HLA sensitization, dialysis status, waiting time, age matching, donor BMI and HLA mismatch (Hudson et al., 2015, Flatt et al., 2019).

An additional advantage of transplantation of the whole organ is that islets remain in their natural environment and experience less damage compared to an islet transplantation, where they are separated from acinar tissue and transplanted into the portal vein of the patient.

1.5.2 Islet isolation and transplantation

Another possible treatment of Type 1 diabetes is islet transplantation. It is used for some Type 1 diabetes patients who suffer from severe blood glucose lability and is now the standard of care treatment for individuals with severe recurrent hypoglycaemia in the UK with the goal to eliminate hypoglycaemia (Espes et al., 2016, Brooks et al., 2013). Compared to whole pancreas transplantation, islet transplantation is a minimally invasive alternative to treat severe hypoglycaemia but does not routinely deliver sustained insulin independence (Okere et al., 2016, Shapiro et al., 2000). Islets are isolated from a deceased pancreas with nationwide allocation in the UK according to the same allocation scheme as whole pancreas transplantation (Hudson et al., 2015). Donors with higher BMI are 'weighted' higher for islet transplantation due to better isolation outcomes with increased BMI (Hudson et al., 2015, Johnson et al., 2014). During the isolation procedure endocrine tissue is enzymatically and mechanically separated from exocrine tissue using manual or automated methods (Ricordi et al., 1988). Briefly, the pancreas is perfused with a collagenase solution before being cut and transferred into a Ricordi chamber for digestion at 37°C combined with gentle shakes (Qi et al., 2009a). Islets are then purified from exocrine tissue with a cell separator (COBE) using density gradients leading to fractions with different purities (Qi et al., 2009b). Quality control with assessment of viability, purity and islet yield with IEQ counting follows (Brooks et al., 2013). Prediction of function after transplant can be achieved with glucose induced insulin secretion analysis, oxygen consumption rate (OCR)/DNA measurements, transplantation in a mouse model or analysis of gene expression profiles (Papas et al., 2007, Hanson et al., 2010, Kurian et al., 2017). For islet transplantation as part of the UK integrated islet transplant program, islet mass >3000 IEQ/kg, viability of >70% and purity >30% are required for the use of an islet preparation for transplantation (Brooks et al., 2013).

If islets pass quality control and a suitable recipient is available, they are injected into the portal vein in a minimally invasive procedure for the patient (Shapiro et al., 2000) (Figure 1.12).

The required immunosuppression for both pancreas and islets transplants is associated with increased risk of infections and malignancy in addition to having side effects which may impact on quality of life (Hsu and Katelaris, 2009). Additionally, the types of immunosuppressive agents must be carefully considered as corticosteroids are toxic for the islet cells (McCall and Shapiro, 2012). This finding among other changes led to the landmark development of the Edmonton protocol in 2000. Not only was the immunosuppression protocol adapted to better suit islet transplantation, but also several sequential transplants were undertaken in each recipient until insulin independence was achieved (Shapiro et al., 2000). However, major limitations subsequent to transplantation including the instant blood mediated inflammatory reaction (IBMIR), hypoxia, inflammatory infiltration or mechanical injury followed by islet cell loss of up to 60% still need to be addressed (McCall and Shapiro, 2012, Biarnes et al., 2002, Bennet et al., 2011). IBMIR takes place, when platelets bind to the surface of the islets and leukocytes infiltrate them leading to inflammatory and thrombotic reactions (McCall and Shapiro, 2012). These negative effects impair the outcome of islet transplantation, despite administration of heparin or insulin.

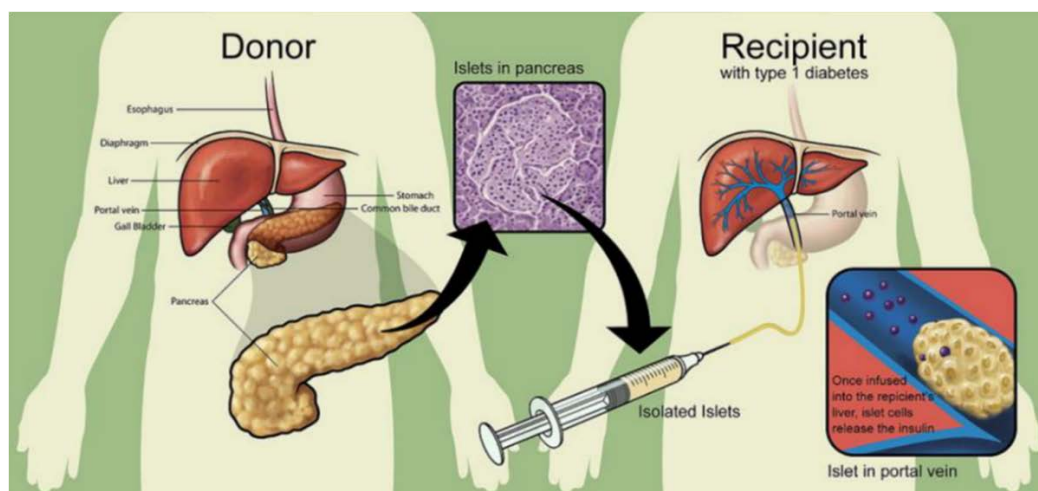


Figure 1.12: Schematic of islet extraction and delivery process.

Islets are enzymatically isolated from a donor pancreas and injected into the portal vein of the recipient. Image from (Naftanel and Harlan, 2005).

1.5.2.1 Impact of isolation and transplantation on islets and their ECM

For research purposes islet transplantation in rodents is often performed as a readily accessible model. It is, however, important to note the differences in islet cytoarchitecture. Mouse islets (Figure 1.13) have a core of β -cells mantled by a belt of α -cells, δ -cells and PP-cells (Bosco et al., 2010). They also contain proportionally more β -cells and fewer α -cells compared to human islets (Cabrera et al., 2006).

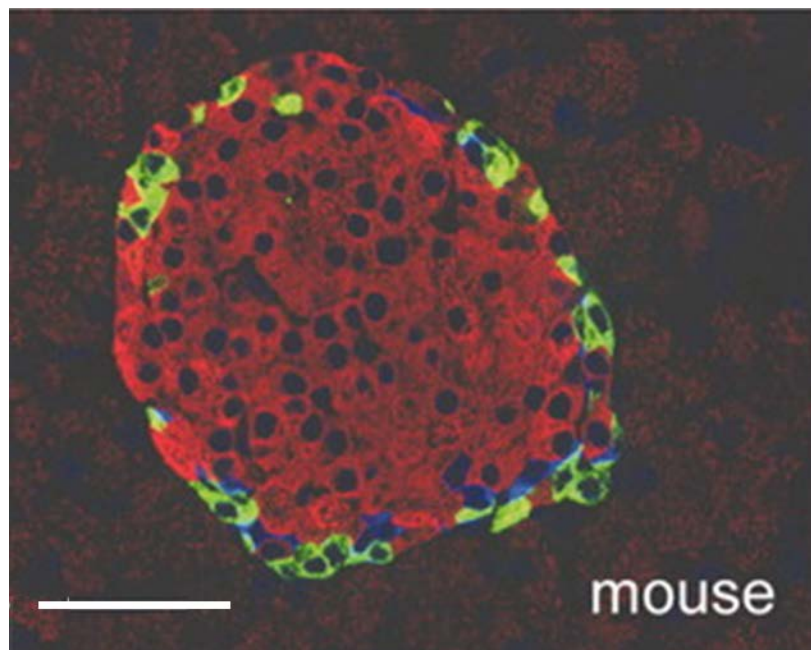


Figure 1.13: Architecture of mouse islets.

In the core of the islet β -cells (red) are located surrounded by α -cells (green) and δ -cells (blue). Scale bar 50 μ m. Image adapted from (Cabrera et al., 2006).

ECM is a complex network including a variety of proteins and glycoproteins as described in 1.3. During the isolation process, ECM components are digested with an enzyme cocktail consisting mostly of collagenase (Qi et al., 2009a, Ricordi et al., 1988). Collagen, especially from the BM, is the main target and every component of the ECM is influenced differently during the digestion process (Cross et al., 2017, Irving-Rodgers et al., 2014). The composition and integrity of ECM seems to be influenced by a range of factors including CIT and BMI leading to differences during digestion and therefore different isolation outcomes (Hanley et al., 2008, Kin et al., 2008). For example, organs with higher CIT showed increased amount of pan-laminin after isolation compared to organs with

shorter CIT, but further studies need to clarify the cause (Cross et al., 2017). After isolation the BM around islets is lost, but BM around vasculature inside of islets is still visible with declining staining intensity over four days in culture (Cross et al., 2017, Irving-Rodgers et al., 2014, Wang et al., 1999). Loss of cell-matrix connection leads to an integrin-mediated programmed cell death process called anoikis (Thomas et al., 1999).

In addition to that, the vascular system is impacted as well with loss of endothelial cells over culture time and destruction of some vascular BM proteins negatively impacting on survival and function of the islets. It was shown that components of the vascular BM including laminin-411 and laminin-511 upregulate insulin expression and proliferation in MIN6 β -cells revealing their importance for islet function and survival (Nikolova et al., 2006).

Additionally, the whole isolation and transplantation process is stressful for islets and leads to increased cytotoxicity after isolation and during subsequent culture (Daoud et al., 2010a, Cross et al., 2017). Loss of contact with the ECM also changes integrin expression on the cell membrane of islet cells influencing cell survival (Wang et al., 1999). In culture following isolation recovery of BM was observed by Wang et al. after five days of culture, but not by Irving-Rodgers et al. after four or seven days of culture (Wang et al., 1999, Irving-Rodgers et al., 2014).

Through the isolation process islets are also cut off from their blood supply leading to hypoxia in the core especially in large islets leading to necrotic cell death (Giuliani et al., 2005). This can lead to further stress and decrease function and viability of islets during culture and in the early stages after transplantation (Dionne et al., 1993, MacGregor et al., 2006).

Once transplanted, revascularisation can provide islets with sufficient oxygen and nutrient supply, but it can take up to ten days till the glomerular microvascular network is rebuilt (Menger et al., 1989). Transplanted islets show revascularisation mainly in the periphery of the islets and in the stroma around islets (Mattsson et al., 2002). BM is rebuilt and may be secreted by endothelial cells, but not islet cells themselves (Irving-Rodgers et al., 2014).

1.5.2.2 Islet preservation

Before transplantation islets are preserved for at least 24 h in the UK (British Transplantation Society, 2019). Typical protocols in other centres internationally include islet culture of up to 72 h with some centres extending up to one week (Kin et al., 2008, Scharp et al., 1990). The Edmonton protocol of 2000 tried to avoid culture of islets and transplanted them immediately (Shapiro et al., 2000). There is still a controversy regarding whether a preservation period improves or decreases outcomes of islet transplantation (Shapiro et al., 2006). Nevertheless, there are other advantages of a culture period before transplantation. For example it provides more time for the centre to prepare the transplantation which also includes more time for the recipient to travel to the transplant centre (Shapiro, 2011, Shapiro et al., 2006). Additionally, there is more time to start immunosuppressive protocols and for additional quality controls of donor islets (British Transplantation Society, 2019, Kin et al., 2008). Culture of islets can also increase purity and therefore potentially lower the immune response towards the donor tissue triggered by dying acinar tissue (Chun et al., 2008). However, the survival rate of islets in culture is decreasing with time and remaining islets are often fragmented with smaller cell clusters in comparison to intact islets which complicates proper analysis (Matsushima et al., 2016, Lim et al., 2011). Additionally, the lack of oxygen leads to necrotic cores with decreasing viability after seven days (or less) in culture (Irving-Rodgers et al., 2014). For future culture systems it is important to increase viability and function for a better transplantation outcome (Chow et al., 2010).

1.5.2.3 Transplantation site

The commonly used transplant site for islet transplantation is the portal vein (Shapiro, 2012). However, there are several disadvantages including IBMIR, liver inflammation, bleeding and thrombosis or toxicity, which can be increased by the intake of immunosuppressive drugs (McCall and Shapiro, 2012, Shapiro, 2012). Additionally, monitoring of the graft within the liver is difficult (McCall and Shapiro, 2012). Other potential transplant sites are subcutaneous, omental, kidney capsule or testis (Matsushima et al., 2016). The kidney capsule is used as a transplant model in rodents, but due to anatomical differences cannot be used in humans (Blomeier et al., 2006). The omentum was chosen recently due to its easy access in animal models and initial human

transplants have commenced (Espes et al., 2016, Berman et al., 2016). It was shown that adipose tissue leads to an increase in vascular endothelial growth factor A (VEGF-A) and therefore a better revascularisation (Espes et al., 2016). Other possible sites for islet transplantation can be immune privileged sites including testis or the anterior chamber of the eye where it is hoped to decrease the requirement for immunosuppressive drugs (McCall and Shapiro, 2012).

1.5.3 Secondary sources of β -cells

One of the remaining challenges in β -cell replacement therapy is the source of a sufficient supply of islets or β -cells, particularly given the current limitations of immunoreaction against transplanted material and damage to the donor organ though warm/cold ischaemic time. Alternative cell sources may overcome these challenges, improve transplantation outcomes and extend the application of β -cell replacement to more patients. Potential sources include porcine islets and differentiated β -cells from human embryonic stem cells (hESCs) or human induced pluripotent stem cells (hiPSCs) (Kieffer et al., 2017, Sneddon et al., 2018).

Several studies of xenotransplantation into non-human primates and human patients with Type 1 diabetes showed restoration of normoglycaemia but regulatory and ethical challenges remain (van der Windt et al., 2012). Furthermore, rejection of porcine material has to be prevented through additional immunosuppression or encapsulation techniques (Park et al., 2015).

Differentiated β -cells from hESCs or hiPSCs may represent an alternative cell source for β -cells without ischaemic damage and, in the case of hiPSCs, without alloimmune reaction. Stem cells possess the ability to renew tissues and to differentiate into the required cell types (Moore et al., 2015). It is possible to mature hESCs into cells expressing certain key markers of β -cells which not only produce insulin through glucose stimulation, but reverse diabetes in a mouse model (Rezania et al., 2014). However, the application of hESCs raises potential ethical concerns and concerns regarding teratoma formation (Moore et al., 2015). Another disadvantage is the alloimmune reaction towards the foreign cells which may be overcome using hiPSCs. It was shown that hiPSCs from non-diabetic donors and donors with Type 1 diabetes can be matured *in vitro* into cells expressing β -cell markers, respond to a glucose challenge *in vitro* and in a mouse model (Millman et al., 2016).

Further research needs to improve the yields of matured cells with successful scale-up and improve maturation protocols, since mature cells generated to date express some distinct β -cell markers, but remain different from β -cells in islets (Rezania et al., 2014, Millman et al., 2016).

1.6 Tissue Engineering

Tissue engineering combines regenerative medicine and material sciences to develop tissues or organs to restore function in damaged organs or tissues (Vacanti and Langer, 1999, Perez-Basterrechea et al., 2018). Tissue engineering approaches can provide three-dimensional constructs for regeneration of tissues and organs made out of a combination of cells, biomaterials and specific factors such as VEGF-A as shown in Figure 1.14 (O'Brien, 2011). Different materials can be combined to achieve optimal mechanical properties including stiffness, and with the addition of ECM components and factors the specific niche for cells can be created, playing a vital role in tissue organisation and function. Various tissues have been developed for *in vitro* and *in vivo* applications including skin, cartilage and bone constructs (O'Brien, 2011).

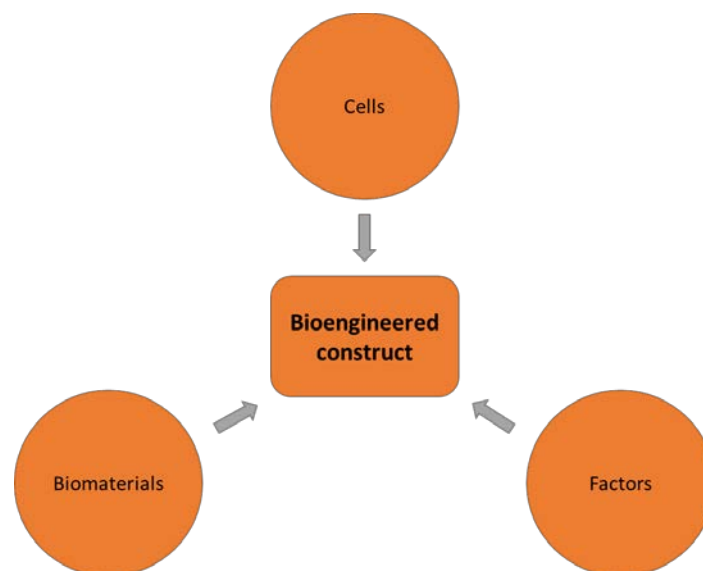


Figure 1.14: Principle of tissue engineering with the combination of cells, biomaterials and other factors to achieve a bioengineered construct ready for transplantation in patients.

1.6.1 Tissue engineering for islet transplantation

The isolation process separates the endocrine from the exocrine parts of the pancreas in preparation for islet transplantation. However, through this process islets lose contact to their surrounding BM, which is negatively impacting on their viability and function and therefore transplant outcomes (Cross et al., 2017, Irving-Rodgers et al., 2014). Additionally, the blood supply is discontinued decreasing nutrient and oxygen transfer (Komatsu et al., 2017). Tissue engineering approaches including application of matrices and scaffolds aim to replace the lost BM to provide cell-matrix-connections, improve islet viability and function and therefore quality after isolation and prior transplantation.

1.6.1.1 Scaffolds for islet transplantation

Culture of islets on scaffolds could be an option to provide mechanical support after the isolation process (Perez-Basterrechea et al., 2018). Requirements for the scaffold materials include: Ability to mimic natural pancreas, providing a three-dimensional environment, biocompatibility, degradability, ability to support and protect isolated islets as well as implementing sufficient mechanical integrity (Perez-Basterrechea et al., 2018, Xu et al., 2019, Kaviani and Azarpira, 2016, Blomeier et al., 2006).

Scaffolds can be composed of synthetic or natural materials with advantages and disadvantages of them both (Table 1.1). Synthetic materials like polyglycolic acid (PGA), polylactic acid (PLA), polycaprolactone (PCL) or polylactic-co-glycolic acid (PLGA) can provide controllable physical and mechanical properties, but demonstrate limited biocompatibility as well as producing acidic by-products during degradation (Chan and Leong, 2008, Perez-Basterrechea et al., 2018, Kumar et al., 2018). In contrast, natural materials show an enhanced biocompatibility along with improved functionality and are either polysaccharides including alginate, chitosan and agarose or polypeptides including collagen, fibrin and silk (Perez-Basterrechea et al., 2018, Kumar et al., 2018). Alginate is widely used for encapsulation of islets due to its biocompatibility and low cost although it can attract immune cells leading to formation of fibrotic capsules (Xu et al., 2019). Scaffolds in the form of hydrogels have the advantage of a high surface area to volume ratio which is beneficial for an effective oxygen and mass transfer (Daoud et al., 2011, Salvay et al., 2008).

Table 1.1: Advantages and disadvantages for synthetic and natural polymers for scaffold manufacturing (Kaviani and Azarpira, 2016, Perez-Basterrechea et al., 2018).

	Advantages	Disadvantages
Synthetic polymers	<ul style="list-style-type: none"> • Availability • Specific degradation rate/biodegradable • Non-immunogenicity • Good mechanical strength • Controllable characteristics • Synthesized on large scale 	<ul style="list-style-type: none"> • Lack of biological activity • Hydrophobic nature → reduces biocompatibility • Release acidic by-products during degradation
Natural polymers	<ul style="list-style-type: none"> • Higher biocompatibility • No inflammatory response • Biological activity (cell adhesion/growth/differentiation) 	<ul style="list-style-type: none"> • Biochemical properties can limit certain approaches • Variation in degradation rate • Poor mechanical strength

Combination of more than one material with complementary mechanical and biological features may provide an optimal construct for improved viability and function of isolated islets (Xu et al., 2019, Perez-Basterrechea et al., 2018). Combination of polymers with natural ECM components is crucial for cell adhesion and growth inside the construct (Daoud et al., 2011, Stendahl et al., 2009). These are also important to promote the neovascularisation of islets (Daoud et al., 2011).

1.6.1.2 Combination of material and isolated islets

ECM lost through isolation may be replaced through combining isolated islets with biomaterials. Ideally biomaterials should provide the surrounding microenvironment with cell-to-matrix contacts, mechanical stimulation as well as improving revascularisation in addition to delivering immune protection (Stendahl et al., 2009, Daoud et al., 2011). Various techniques have been proposed to combine isolated islets with ECM materials.

Isolated islets can be either seeded onto a construct or incorporated during its manufacture (Daoud et al., 2010b, Marchioli et al., 2015). Constructs for seeding can be

scaffolds, hydrogels or electrospun nanofiber membranes (Daoud et al., 2010b). Incorporation of islets within materials is termed encapsulation and can be divided into macroencapsulation, microencapsulation or nanoencapsulation according to islet number and volume of material (Figure 1.15) (Song and Roy, 2015).

For macroencapsulation a number of islets are encapsulated in a gel or device which allows a greater control over gel parameters but limits oxygen and nutrient transfer (Song and Roy, 2015, Desai and Shea, 2017). Macroencapsulation can either be extravascular or intravascular which allows the perfusion of the construct (Song and Roy, 2015). During microencapsulation single islets are encapsulated in a gel and a number of these microencapsulated islets are transplanted, which increases the surface area to volume ratio and improves nutrient exchange (Song and Roy, 2015, Desai and Shea, 2017). Limitations are the need for a suitably large transplantation site as well as the need for prevascularisation of the site. For nanoencapsulation, islets are coated in a conformal way or with a layer-by-layer technique to enhance oxygen and nutrient supply, but protect against the immune cells (Vaithilingam et al., 2017).

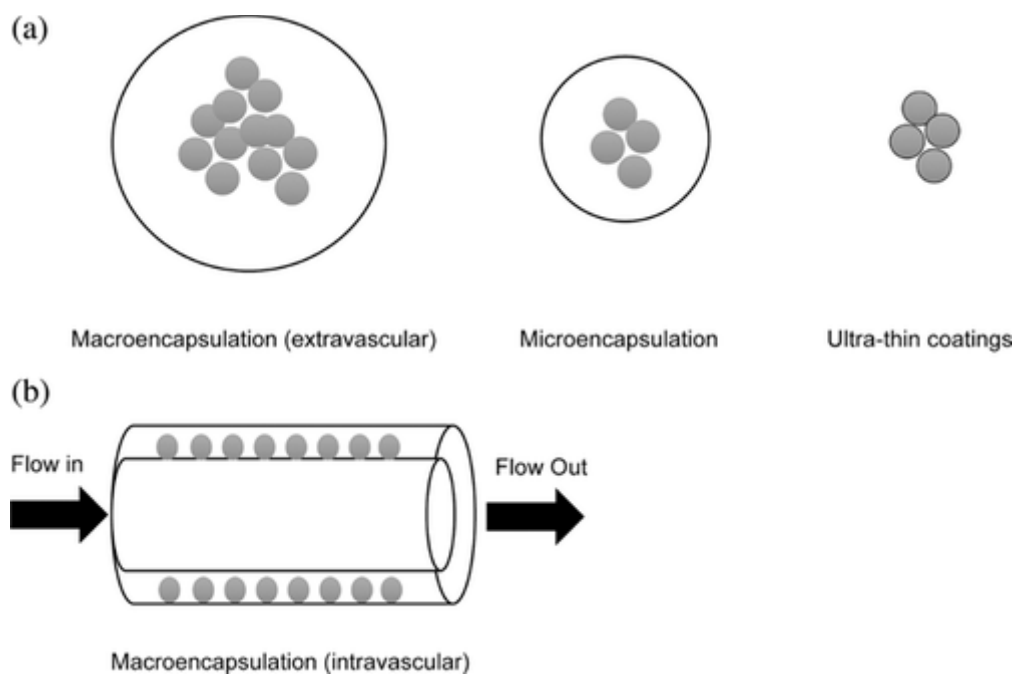


Figure 1.15: Encapsulation strategies for isolated islets with macroencapsulation (extravascular), microencapsulation, ultra-thin coatings and macroencapsulation (intravascular)(Song and Roy, 2015).

Culture of islets seeded on three-dimensional PGA scaffolds prolonged the survival and increased the function of rat islets over a culture period of up to 14 days (Chun et al., 2008). The PGA scaffold was modified with poly-L-lysine to provide a better adherence for the islet cells (Chun et al., 2008). Transplantation of islets seeded on a scaffold into the peritoneal cavity of mice showed improved islet function, functional vessels and maintenance of islet morphology (Blomeier et al., 2006). Additionally the amount of required islets could be decreased with the use of the scaffold compared to the conventional method of islets transplantation under the kidney capsule in this rodent model (Blomeier et al., 2006). Addition of the ECM proteins collagen IV, fibronectin or laminin to the scaffold improved function of transplanted islets as well as the size of the islets at 297 days after transplantation compared to non-coated scaffolds (Salvay et al., 2008). A higher vascular density was found in islets transplanted on coated scaffolds compared to the non-coated control (Salvay et al., 2008). Especially the inclusion of collagen IV caused rapid euglycemia and a better performance in a glucose tolerance test in mice (Salvay et al., 2008). Summed up, this study showed a significant positive influence of ECM proteins on transplantation in mice (Salvay et al., 2008). Combination of a scaffold and a hydrogel was even more beneficial, which leads to the conclusion firstly that the 3D culture with ECM components is beneficial for function and secondly that the increased mechanical and diffusivity features of a scaffold further increase function (Daoud et al., 2011).

Encapsulation of islets in a gel composed of collagen I, collagen IV and fibronectin improved the insulin release compared to islets in suspension or in a collagen I gel (Daoud et al., 2011). Advantage of encapsulation of islets in a hydrogel or scaffold is that the islets cannot migrate through the tissue, but stay in the desired site (Blomeier et al., 2006).

One emerging technique for encapsulation would leverage 3D bioprinting to provide three-dimensional organization of cells in a printed scaffold (Marchioli et al., 2015). Many different approaches can be conceived of, like printing of isolated islets for a transplant, printing different primary cells into an islet-like structure or printing stem cell derived endocrine cells which can form islets during printing or culture (Murphy and Atala, 2014).

1.7 Aims

Islets are complex micro-organs surrounded by a specific microenvironment impacting on endocrine function. A better understanding of how acute stress such as organ preservation and the isolation process impacts on the islet niche is required to improve islet viability and function. There is also a need to characterise the impact of ECM replacement strategies on the health of isolated islets in order to determine optimal strategies for improving transplant outcomes. This thesis set out to answer how the microenvironment of islets changes through acute stress or the isolation procedure and how the impact of stress on the tissue can be quantified with the hypothesis that these changes influence islet health and a better quantification method will help towards a better understanding of the status of whole pancreata and single islets. This thesis also wanted to answer the question how the provision of a three-component hydrogel impacts on islet health with the hypothesis that the culture of islets in proximity or contact with the hydrogel improves islet integrity, viability and function. Further this thesis set out to answer how a nanofiber membrane, different hydrogel designs or dynamic culture systems impact on islet health through reduction of hypoxia in combination of ECM presence with the hypothesis, that the reduction of hypoxic stress improves islet integrity, viability and function.

This thesis had the following aims and objectives:

Aim 1: To characterise the islet niche *in situ* and analyse acute changes related to ischaemia, tissue processing and islet isolation.

Objective 1.1: To characterise islet microenvironment, integrity and morphology *in situ* in a pancreas with minimal ischaemic exposure.

Objective 1.2: To characterise the impact of ischaemia and tissue processing on islet microenvironment, integrity and morphology.

Objective 1.3: To characterise the impact of islet isolation on islet microenvironment, viability, integrity.

Aim 2: To assess ECM replacement through a novel collagen, alginate, fibrinogen (CAF) hydrogel and characterise impact of hydrogel on pseudoislets and human isolated islets.

Objective 2.1: To establish a reproducible model for human islets from the MIN6 β -cell line and characterise integrity and function.

Objective 2.2: To assess biocompatibility of CAF hydrogel with pseudoislet model through assessment of viability, morphology and function.

Objective 2.3: To assess biocompatibility of CAF hydrogel with human isolated islets through assessment of viability, morphology and function.

Aim 3: To develop bioengineering approaches to reduce hypoxic impact on β -cells and restore lost ECM in the islet microenvironment.

Objective 3.1: To develop a bioengineered construct with CAF hydrogel.

Objective 3.2: To characterise impact of dynamic culture on pseudoislet viability and gene expression with and without the presence of CAF hydrogel.

Objective 3.3: To characterise the impact of an electrospun nanofiber membrane on viability and morphology in mouse islets.

Objective 3.4: To develop a proof of concept system for hydrogel perfusion.

Objective 3.5: To characterise CAF hydrogel in a perfusion system.

Chapter 2. Methods

All chemicals and general reagents were purchased from Sigma Aldrich (Dorset, UK), Thermo Fisher Scientific (Waltham, USA) or Melford (Suffolk, UK) if not otherwise declared.

2.1 Tissue Culture

2.1.1 MIN6 β -cell line culture

MIN6 cells are a mouse insulinoma cell line generated by an *in vivo* mutation of the SV40 T antigen leading to β -cell tumours (Miyazaki et al., 1990). MIN6 cells behave similar to primary islets with a 6-7 fold increase of insulin secretion through glucose stimulation of 25 mmol/l as well as characteristic glucose metabolism including phosphorylation via glucokinase (Ishihara et al., 1993).

MIN6 cells used in this thesis were kindly provided by Dr Catherine Arden at Newcastle University and used between passages p24 and p29. Cells were cultured in high glucose Dulbecco Modified Eagle Medium (DMEM) (D6429 Sigma-Aldrich) containing 4.5 g/l glucose, L-glutamine and sodium bicarbonate and supplemented with 1% 100x penicillin/streptomycin, 0.0005% β -mercaptoethanol, 15% foetal bovine serum (FBS) and 2.5% 1M HEPES solution. Cells were cultured at 37°C and 5% CO₂ in 75 cm² tissue culture flasks with the culture medium changed every two till three days.

2.1.1.1 MIN6 sub culture

MIN6 cells were split when they reached ~80% confluence. After the cells were washed with 5-8 ml of phosphate buffered saline (PBS), they were incubated with 2 ml of 1x trypsin for 5 min at 37°C. The flask was gently tapped against the hand to observe, if cells detach from the surface and completely washed off with 10 ml culture media. Subsequently the cell suspension was centrifuged for 3 min at 549 g and the supernatant discarded. The pellet was then resuspended in 10 ml growth media and split in convenient dilutions (1:5 or 1:10 in a 75 cm² flask).

For storage MIN6 cells were split as described before. The cell pellet was resuspended in 1 ml of 10% dimethyl sulfoxide (DMSO) and 90% FBS and transferred into a cryovial. The vial was then incubated in a Nalgene® Mr Frosty at -80°C for ~24 h. Subsequently cells were transferred into liquid nitrogen for long-term storage.

For recovery, MIN6 cells were thawed in a 37°C water bath and the 1 ml cell suspension was added to 9 ml growth media. This was followed by centrifugation for 3 min at 549 g and the supernatant discarded. The pellet was resuspended in 12 ml culture media and transferred into a 75 cm² culture flask. Subsequently the cells were incubated at 37°C and 5% CO₂ until they reached 80% confluence.

2.1.1.2 Pseudoislet generation and culture

‘Pseudoislets’ describe a three-dimensional cell cluster generated from single cells which allows the study of β -cell microtissue without the need for primary islets. It has been shown that MIN6 pseudoislets function similar to mouse islets and they are a valid model for islet research (Hauge-Evans et al., 1999, Persaud et al., 2010).

Pseudoislets were generated by culturing MIN6 cells in suspension culture after splitting as described above. After resuspending the pellet, 1.5 ml MIN6 cell suspension was transferred into a non-adherent culture dish with 6.5 ml culture medium. After 2-3 days, the forming cell aggregates were transferred from the dish into a 15 ml falcon and spun down for 1 min at 44 g. The supernatant was discarded, and the pellet was gently resuspended in 8 ml fresh growth medium. The forming cell clusters were then transferred back into the cell culture dish. Pseudoislets were used after five days of non-adherent culture.

2.1.2 Human islet culture

Isolated islets were provided from the Transplant Regenerative Medicine Laboratory at Newcastle University or isolation centres in Canada (Edmonton) and the United Kingdom (Edinburgh, London, Oxford). Deceased donor pancreata were accessed under appropriate ethical approval (05/MRE09/48 or 16/NE/0230) and adhering to the Human Tissue Act at Newcastle University following informed donor family consent. Isolated islets were given an internal number for identification (LDIS).

Human islets were cultured in Connaught Medical Research Laboratories (CMRL) 1066 medium (Mediatech Inc., Manassas, USA) supplemented with 1.2% 100x penicillin/streptomycin, 1.2% 1M HEPES solution and 2% human serum albumin (Gemini Bio-Products, USA) in T175 suspension flasks with a density of 200IEQ/cm². Culture conditions were at 37°C and 5% CO₂ with a medium change every 2-3 days. For that, islets were

transferred in a tube, centrifuged at 44 g for 1 min and the supernatant discarded. The pellet was then resuspended in fresh medium and the islet suspension was carefully transferred back into the culture flask.

2.1.2.1 Donor information

Key information regarding the status of donor pancreata included in these studies, prior to islet isolation or biopsy removal, is included in Table 2.1.

Table 2.1: Pancreas and islet donor information.

17 pancreata were used with 10 (47%) being from female donors and 7 (41%) from DBD, with average (range) in age of 50 (25-73) years, BMI of 27 (18-33) kg/m², CIT of 18.1 (4.0-55.4) h and WIT of 27.2 (17-37) min.

21 islet preparations were used with 10 (48%) being from female donors and 13 (62%) from DBD, with average (range) in age of 48 (24-66) years, BMI of 28 (17-37) kg/m², CIT of 10.5 (2.8-26.2) h and WIT of 18.5 (12-25) min.

Abbreviations: Body mass index (BMI), donor after circulatory death (DCD), donor after brain death (DBD), cold ischaemia time (CIT) – defined from cross clamp till fixation, warm ischaemia time (WIT) – defined as functional ischaemia, blood glucose at admission (BG ADM), blood glucose at retrieval (BG RET), diabetes history (DH), islet volume fraction (IVF), not specified (n/s).

LDIS NUMBER	TISSUE TYPE	GENDER	AGE	BMI [KG/M ²]	DONOR TYPE	CIT [H]	WIT [MIN]	HBA1C [MMOL/MOL]	BG ADM [MMOL/L]	BG RET [MMOL/L]	DH	PURITY [IVF]	VIABILITY [DITHIZONE NEGATIVE]
169	pancreas	female	64	26	DCD	16.5	32	n/s	n/s	9.1	No	-	-
172	pancreas	male	25	23	DCD	8.0	18	n/s	n/s	n/s	No	-	-
173	pancreas	male	43	27	DBD	5.1	-	n/s	n/s	n/s	No	-	-
192	islets	male	51	33	DBD	4.0	-	n/s	n/s	9.4	No	90%	50%
193	pancreas	male	71	31	DCD	n/s	31	n/s	n/s	n/s	No	-	-
194	islets	male	59	27	DCD	7.0	105	n/s	n/s	6.6	No	90%	91%
195	islets	male	45	28	DBD	n/s	-	n/s	n/s	n/s	No	-	-
196	islets	male	51	24	DBD	12.5	-	n/s	n/s	n/s	n/s	76%	40%
204	islets	female	56	27	DBD	13.0	-	n/s	8.7	9	No	70%	48%
206	islets	female	49	31	DBD	26.2	-	n/s	10	6.4	No	85%	58%
209	islets	female	38	36	DBD	26.0	-	n/s	n/s	7.4	No	65%	70%
210	islets	male	24	31	DBD	12.5	-	n/s	n/s	n/s	n/s	5%	70%
211	islets	male	45	31	DCD	n/s	13	n/s	5.2	n/s	No	95%	70%
214	pancreas	male	49	32	DBD	27.0	-	40	n/s	n/s	No	-	-
215	islets	male	28	24	DCD	9.9	25	n/s	n/s	n/s	No	50%	73%
218	pancreas	male	53	23	DCD	8.8	17	n/s	n/s	6.4	No	-	-
219	pancreas	male	39	28	DCD	29.8	29	n/s	n/s	n/s	No	-	-
221	pancreas	female	57	23	DBD	38.1	-	36	n/s	8.3	No	-	-
225	islets	male	39	25	DCD	6.9	20	n/s	n/s	7.9	No	45%	78%
226	pancreas	female	39	24	DBD	18.0	-	36	8.6	n/s	No	-	-
229	islets	Female	51	16.5	DBD	2.8	-	n/s	n/s	n/s	n/s	30%	99%
231	pancreas	female	65	18	DCD	6.4	34	32	n/s	n/s	No	-	-

LDIS NUMBER	Tissue Type	Gender	Age	BMI [kg/m²]	Donor type	CIT [h]	WIT [min]	HbA1c [mmol/mol]	BG adM [mmol/L]	BG retl [mmol/L]	DH	purity	viability
236	islets	female	53	37	DBD	11.3	-	n/s	n/s	n/s	n/s	43%	97%
237	pancreas	male	69	29	DBD	6.3	-	n/s	n/s	n/s	No	-	-
239	islets	female	66	30	DCD	11.8	n/s	n/s	n/s	n/s	n/s	n/s	n/s
244	both	female	49	27	DCD	13.2	12	31	n/s	n/s	No	50%	78%
245	islets	female	65	29	DCD	12.3	n/s	n/s	n/s	n/s	n/s	30%	82%
247	islets	female	48	33	DBD	7.7	-	n/s	n/s	9.2	No	60%	77%
248	islets	male	44	30	DBD	n/s	-	37	22.7	n/s	No	95%	71%
256	islets	male	53	26	DBD	n/s	-	36	9.3	5.8	No	80%	78%
266	islets	female	65	28	DCD	n/s	16	46	n/s	n/s	No	90%	69%
274	islets	n/s	n/s	n/s	n/s	n/s	n/s	n/s	n/s	n/s	n/s	55%	75%

2.1.3 Mouse islets

2.1.3.1 Mouse islet isolation

Rodent islets are established as well studied model for islet isolation and transplantation. C57DL/6 mice (between ten and twelve weeks of age) were used for rodent islet isolation in these studies. Mice were sacrificed by cervical dislocation and the pancreas and bile duct were exposed. Collagenase P solution (Roche, Basel, Switzerland) was injected into the ductal system. If the ductal system was difficult to access, the enzyme solution was injected directly into the pancreatic tissue and repeated local injections were performed. Afterwards the pancreas was dissected out of the abdomen and cut into small pieces. For digestion the pancreas was incubated in the enzyme solution for 10 min at 37°C. Following that, the tissue was manually swirled for 30 sec to break down as much acinar tissue as possible. The enzyme reaction was stopped by adding ME199 media (Corning®, New York, USA) containing 0.3% bovine serum albumin (BSA) and the suspension was centrifuged at 500 g for 2 min at 4°C. The pellet was then resuspended in medium containing BSA and transferred through a metal mesh to separate undigested tissue. The filtered solution was centrifuged at 500 g for 2 min at 4°C and the resulting pellet was resuspended in Histopaque®-1077 and overlaid with medium without BSA. The two-layered suspension was centrifuged for 20 min at 2,800 rpm at 4°C in a MSE Sanyo Harrier refrigerated centrifuge (MSE Ltd, London, UK). Islets are located in the supernatant and are collected in a 100 µm nylon cell strainer followed by transfer into a culture dish with medium containing BSA.

2.1.3.2 Mouse islet culture

Mouse islets were cultured in RPMI 1640 media containing 2 g/l glucose (Corning, New York, USA) supplemented with 10% FBS and 1% 100x penicillin/streptomycin overnight in a not adherent culture dish at 37°C and 5% CO₂. The following day mouse islets were handpicked for experiments under a dissecting microscope (Leica, Wetzlar, Germany).

2.1.4 Propidium iodide staining

Islets or pseudoislets were transferred into a 2 ml Eppendorf tube and allowed to settle down for 3 min. Medium was removed carefully from above and human/mouse islets were resuspended in 890 µl PBS, 100 µl dithizone and 10 µl propidium iodide (PI) solution whereas pseudoislets were resuspended in 990 µl PBS and 10 µl PI solution. The tube was

inverted to mix islets with the solution and incubated for 5 min which also allowed the islets to settle at the bottom of the Eppendorf tube. As much solution as possible was removed and 1 ml PBS was added. Islets were transferred into a 12-well plate and if possible 50 islets were assessed by estimation on how much percent of the whole islets were viable in 5% intervals. The average value and standard deviation were calculated with Microsoft Excel.

2.1.5 Islet equivalent (IEQ) estimation

For the estimation of IEQ a sample (50-100 μ l) was taken from the islet culture and transferred into a 35 mm diameter culture dish. Under the inverted microscope, the 10x objective was used to count islets according to the diameter from 50-100 μ m, 101-150 μ m, 151-200 μ m, 201-250 μ m, 251-300 or 301-350 μ m. Islet counts were then converted into IEQ by multiplication of a factor according to Table 2.2 to normalise them to the standard of 1 IEQ which equals 150 μ m diameter (Ricordi et al., 1990). With these islet equivalents and the dilution factor, the total IEQ count per sample can be calculated.

Table 2.2: Diameter range of islets and conversion factor for IEQ assessment

Diameter range for a circular islet	Multiplier for IE volume conversion
50-100 μm	0.167
101-150 μm	0.667
151-200 μm	1.685
201-250 μm	3.5
251-300 μm	6.315
301-350 μm	10.352
>400 μm	22.75

2.2 Tissue fixation and processing for paraffin embedding

Pancreas biopsies were taken by the islet isolation team and fixed in 10% formalin overnight, before exchanging the solution to 70% ethanol. Some donors were part of the Quality in Organ Donation (QUOD) Expand project, which is a part of a nationwide biobank project in the UK to collect samples of pancreas/islets, heart and lungs. QUOD was

established by NHS Blood and Transplant (NHSBT) to focus research on improving quality for organ donation and transplantation.

Isolated islet or pseudoislet samples were transferred to a 15 ml tube and allowed to settle for 3 min. The culture plate was washed with medium to detach the remaining islets from the culture plate. After a centrifugation step at 44 g for 1 min, the medium was discarded, and the pellet was resuspended in 4% formalin followed by an incubation overnight at 4°C. The next day the tube was centrifuged for 1 min at 44 g, the formalin solution discarded, and the pellet resuspended in PBS. For the embedding islets were transferred to a conical shaped plastic container and as much of the PBS as possible was removed before they were resuspended in 1% liquid agarose (Helena Biosciences Europe, Gateshead, UK) which was allowed to cool to ~37°C which is a suitable temperature for cell embedding. The agarose was allowed to harden and after transferred to an embedding cassette, there followed another incubation in 10% formalin solution.

Both tissue samples and embedded islet samples were processed for embedding and cutting of sections by the Cellular Pathology service in the Royal Victoria Infirmary Newcastle.

2.3 Tissue fixation and processing for Transmission electron microscopy (TEM)

The tissue or islet samples were fixed in glutaraldehyde solution for at least 24 h. Processing started with rinsing of the samples five times in 0.1 M cacodylate buffer (Agar Scientific Ltd, Stansted, UK) for approximately 3 min followed by 1 h incubation in 3% potassium ferrocyanide in 2% osmium tetroxide (TAAB, Aldermaston, UK) in buffer at 4°C. Subsequently washing steps followed where the samples were first rinsed twice with demineralised water (ddH₂O) which was added to the samples and removed immediately and secondly incubated five times for 3 min in ddH₂O. Biopsies were then incubated in filtered thiocarbohydroxide for 20 min at room temperature followed by washing steps as previously described. After thiocarbohydroxide was washed out the samples were treated with 2% osmium tetroxide in ddH₂O for 30 min at room temperature. Again, washing steps followed and finally biopsies were incubated in 1% uranyl acetate (TAAB, Aldermaston, UK) in the refrigerator overnight. The following day the samples were washed to remove the uranyl acetate and dehydrated with increasing concentrations of acetone. Biopsies were incubated for respectively 30 min in 25%, 50% and 70% acetone

in deionised water followed by twice in 100% acetone for 1 h. After dehydration the samples were impregnated with resin. TAAB⁴ epoxy medium resin kit (TAAB, Aldermaston, UK) was used and mixed to the specifications of the manufacturer. It was mixed well and diluted in acetone. Samples were incubated for 1 h respectively in the 25%, 50% and 75% resin followed by 100% resin overnight. The following day biopsies were incubated twice for 1 h in 100% resin and another time for at least 3 h before they were embedded in fresh 100% resin for 24-36 h at 60°C.

The processed biopsies in the resin blocks were trimmed to a trapezium shape and 1 µm or 0.5 µm sections were made with an ultramicrotome (Reichert, Vienna, Austria). These sections were stained with toluidine blue (TAAB, Aldermaston, UK) to stain acidic tissue components and is used for processed tissue sections to highlight the morphology (Sridharan and Shankar, 2012). The distinct morphology helps to characterize the semithin section under light microscopy to find a suitable area for ultrathin cuts. Eventually the block was trimmed further to reduce the surface area for cutting and as soon as the right size and the right area were reached, ultrathin sections of approximately 70 nm were made. Ultrathin sections were stretched with chloroform (VWR International, Radnor, USA) aerosol and placed carefully on suitable grids (Gilder Grids, Grantham, UK). These samples could then be analysed with the TEM.

2.4 Immunofluorescence staining (IF)

4 µm sections were cut onto slides and placed in Histo-ClearTM II solution (National Diagnostics, Atlanta, USA) for 10 min to remove the paraffin from the sections. For rehydration the slides were placed for 3 min in 100% ethanol and 3 min in 90% ethanol followed by deionised water. Afterwards the water was replaced with PBS, where the slides could be retained until antigen retrieval. 2-Amino-2-(hydroxymethyl)propane-1,3-diol/Ethylenediaminetetraacetic acid (TRIS/EDTA) pH 9 buffer or citrate pH 6 buffer was transferred into a pressure pod with the slides and heated up in the microwave for 20 min. Afterwards the solution was cooled down to 40°C, the sections were circled using a hydrophobic pen and incubated with blocking solution consisting of 20% FBS in PBS for 1 h to block non-specific binding. After two washing steps with PBS the primary antibodies were pipetted onto the tissue samples and incubated at 4°C overnight. Antibodies were diluted in 5% FBS in PBS according to Table 2.4 and, as a negative control, dilution buffer

alone without primary antibody was added to the section. The next day, excess antibody was washed off with two wash steps in PBS and subsequently all sections were incubated with the secondary antibodies for 1 h at room temperature. Antibodies were diluted according to Table 2.4 in 5% FBS in PBS solution. Again, the samples were washed twice with PBS and sections were incubated with 0.1 µg/ml DAPI solution for 5 min. Finally, slides were mounted using mounting medium containing DAPI (Vector Laboratories, Burlingame, USA). Nail polish was applied as a seal around the glass plates to prevent dehydration of the stained sections. The samples were stored at 4°C in a light-proof box to prevent quenching of the fluorescence signal. For image analysis a Leica SP8 STED confocal microscope (Leica, Wetzlar, Germany) was used. The control sections with no primary antibodies were used to adjust suitable exposure times for the different filters and then staining was analysed on the sections containing primary antibodies.

Table 2.3: Primary antibodies used for staining with company and dilution

Antibody	Host species	Company	Dilution
Rabbit polyclonal to CD31 (ab28364) (Lot: GR150486-14)	Rabbit	Abcam, Cambridge, UK	1:100
Rabbit polyclonal to Collagen IV (ab6586) (Lot: GR 248055-3/CR 292187-6)	Rabbit	Abcam, Cambridge, UK	1:500
Human E-Cadherin Antibody (Monoclonal Mouse IgG2B Clone #180215) (Ref: MAB1838) (Lot: JAT0111031)	Mouse	R&D Systems, Minneapolis, USA	1:1000
Monoclonal Anti-Glucagon antibody produced in mouse [K79bB10] (G2654-2ML) (Lot: 084M4793)	Mouse	Sigma Aldrich, St. Louis, USA	1:100
Polyclonal Guinea Pig Anti-Insulin (Ref: A0564) (Lot: 10119708)	Guinea pig	Dako, Agilent Technologies, Santa Clara, USA	1:200
Rabbit polyclonal to Laminin (ab11575) (Lot: GR3180809-1)	Rabbit	Abcam, Cambridge, UK	1:100
Rabbit monoclonal to pan Cadherin [EPR1792Y] (ab51034) (Lot: GR73907-3)	Rabbit	Abcam, Cambridge, UK	1:100
Rabbit monoclonal to Vimentin [EPR3776] (ab92547) (Lot: GR3186827-10)	Rabbit	Abcam, Cambridge, UK	1:100

Table 2.4: Secondary antibodies with company and dilution

Antibody	Host species	Company	Dilution
Goat anti-Guinea Pig IgG (H+L) Highly Cross-Adsorbed Secondary Antibody, Alexa Fluor 488 (Ref: A11073) (Lot: 458631/1637243)	Goat	Thermo Fisher, Waltham, USA	1:500
Donkey anti-Rabbit IgG (H+L) Highly Cross-Adsorbed Secondary Antibody, Alexa Fluor 568 (Ref: A10042) (Lot: 1668655)	Donkey	Thermo Fisher, Waltham, USA	1:500
Donkey anti-Mouse IgG (H+L) Highly Cross-Adsorbed Secondary Antibody, Alexa Fluor 568 (Ref: A10037) (Lot: 1752099)	Donkey	Thermo Fisher, Waltham, USA	1:500
Donkey anti-Rabbit IgG (H+L) Highly Cross-Adsorbed Secondary Antibody, Alexa Fluor 647 (Ref: A31573) (Lot: 1826679)	Donkey	Thermo Fisher, Waltham, USA	1:500
Donkey anti-Mouse IgG (H+L) Highly Cross-Adsorbed Secondary Antibody, Alexa Fluor 647 (Ref: A31571) (Lot: 1069838)	Donkey	Thermo Fisher, Waltham, USA	1:500

2.5 RNA extraction and processing

2.5.1 RNA extraction

Samples from human isolated islets or pseudoislets were transferred into a 15 ml falcon tube and islets were allowed to settle to the bottom of the tube for 3 min. As much of the medium which the islet has been cultured in as possible was used to wash the culture plates/dishes to increase islet numbers. Islets were then centrifuged for 1 min at 44 g, the culture media was discarded, and the pellet resuspended in 1 ml PBS to wash off residues of medium. This washing step was performed an additional time before the pellet was resuspended in 250 µl of lysis buffer containing 2.5 µl 2-mercaptoethanol and snap frozen in liquid nitrogen. The samples were stored at -80°C until RNA extraction was performed with the GenElute™ total RNA purification kit according to the provided protocol (Sigma-Aldrich, St. Louis, USA).

Samples were thawed and the lysate was transferred to a filtration column followed by centrifugation for 1 min. All centrifugation steps were run at maximum speed (20,238 g

on the centrifuge used). The filtration column was discarded, and 70% ethanol was mixed with the flow-through. This was then transferred onto a binding column and centrifuged for 30 sec at maximum speed. The flow through was discarded and 250 µl of Wash Solution 1 was added. After centrifugation of 30 sec at maximum speed the membrane was incubated for 15 min with a mixture of 10 µl DNaseI and 30 µl DNase digestion buffer. Subsequently, the DNaseI was washed off with 250 µl of Wash Solution 1 followed by centrifugation for 15 sec at maximum speed. The membrane then was washed with 500 µl of Wash Solution 2 which was centrifuged for 15 sec over the membrane followed by an additional step of 500 µl Wash Solution 2 centrifuged for 2 min at maximum speed. The column was then transferred to a new collection tube and the RNA was eluted with 50 µl elution solution and centrifugation for 1 min at maximum speed. Extracted RNA was stored at -80°C until further experiments were carried out.

2.5.2 Complementary DNA synthesis

1 µl of the RNA samples were quantified with a NanoDrop™ 2000 (Thermo Fisher, Waltham, USA) and all samples were normalised to the lowest measured value. Purity of RNA samples with an A260/280 ratio ranged from ~1.2-3.7 and majority of preparations had an A260/280 ratio ~2.0. A high capacity complementary DNA (cDNA) reverse transcription kit (Applied Biosystems, Foster City, USA) was used to convert the extracted RNA into cDNA. A master mix was pipetted consisting of 2 µl 10x RT buffer, 0.8 µl 25x dNTP mix, 2 µl 10x RT random primers, 1 µl MultiScribe™ reverse transcriptase and 4.2 µl nuclease-free H₂O (Roche, Basel, Switzerland) per reaction. 10 µl of normalised RNA and 10 µl of master mix were combined. For each run, a blank sample without enzyme was added to test for contaminations. The cDNA was generated with the TC-512 gradient thermal cycler (Techne Inc., Burlington, UK) with the optimised cycling conditions for the transcriptase shown in Table 2.5.

Table 2.5: Conditions for the thermal cycler for cDNA synthesis.

Settings	Step 1	Step 2	Step 3	Step 4
Temperature	25°C	37°C	85°C	4°C
Time	10 min	120 min	5 min	∞

2.5.3 Quantitative real time PCR

The cDNA was generated from extracted RNA as described in 2.5.1 and 2.5.2 to allow assessment of RNA transcripts using quantitative real time PCR (qRT-PCR). For each DNA probe a master mix was created with a volume of 18 µl per reaction consisting of 0.5 µl DNA probe (Table 2.6), 0.5 µl TE buffer pH 8.0 (Ambion™, Thermo Fisher, Waltham, USA), 10 µl LightCycler® 480 Probes Master (Roche, Basel, Switzerland) and 7 µl H₂O. The master mix was pipetted into each well of a LightCycler® Multiwell Plate 96 (Starlab, Hamburg, Germany) and 2 µl of cDNA sample was added. The plate then was sealed with polyolefin film (Starlab, Hamburg, Germany) and spun down for 16 sec. The qPCR was carried out with a LightCycler® 480 (Roche, Basel, Switzerland) starting with a pre-incubation cycle at 95°C for 10 min followed by 50 cycles with a target of 95°C for 15 sec, 60°C for 1 min and 40°C for 10 sec. The generated gene expression data were normalised with RPLP0 as housekeeping gene and the delta-delta Ct method was used to calculate the fold change of the gene expression in different culture conditions compared to static culture on normal tissue culture plastic.

Table 2.6: DNA probes for qPCR with gene name, gene symbol, species and detected transcript.

Gene	Gene Symbol	Species	Transcript detected
Ribosomal protein, large, R0	RPLP0	Mouse	Mm00725448_s1
Insulin 1	Ins 1	Mouse	Mm01950294_s1
Insulin 2	Ins 2	Mouse	Mm00731595_gH
Glucose transporter protein type 1 (Glut 1)	Slc2a1	Mouse	Mm00441480_m1
Monocarboxylic acid transporter 4 (Mct4)	Slc16a3	Mouse	Mm00446102_m1
Lactate Dehydrogenase A	LDHA	Mouse	Mm01612132_g1
Urocortin 3	Ucn3	Mouse	Mm00453206_s1

2.6 Protein extraction and processing

2.6.1 Protein extraction

Human isolated islets or pseudoislets were transferred into a 15 ml Falcon tube and allowed to settle at the bottom under gravity for 3 min. The medium above was gently taken off and used to wash the culture plates/dishes to increase the number of islets. Islets were then spun down for 1 min at 44 g and washed with 1 ml of PBS. After an additional centrifugation of 1 min at 44 g, PBS was discarded, and islets were resuspended in 200 μ l protein extraction buffer (Table 2.7) or PBS. The islet suspension was then transferred into an Eppendorf tube and sonicated at 14 Hz for 15 s, before the samples were snap frozen in liquid nitrogen and stored at -80°C.

Table 2.7: Composition protein extraction buffer

100 mM Tris pH 7.4
100 mM KCl
1 mM EDTA
25 mM KF
0.1% Triton X-100
0.5 mM sodium orthovanadate
1% protease inhibitor

2.6.2 Bradford assay

A standard curve with BSA was generated in a clear 96 well plate for protein concentrations of 20-400 μ g/ml in a volume of 10 μ l. Therefore, an albumin standard with 2 mg/ml was diluted in protein extraction buffer or PBS with two wells for each concentration. Protein samples were centrifuged for 5 min at maximum speed and 10 μ l of the supernatant was pipetted into each of two wells. 200 μ l of 1x Bio-Rad protein assay dye reagent concentrate (Bio-Rad, Hercules, USA) was added and the plate was incubated for 5 min at room temperature before absorption was measured with a SpectraMax® 190 plate reader (Molecular Devices, San Jose, USA) at 595 nm. If absorption of undiluted

protein samples was higher than the absorption of 400 µg/ml standard, the samples were diluted, and absorption was measured after incubation with Bradford solution for 5 min. Unknown protein concentrations were calculated from the standard curve.

2.7 Seahorse flux analysis and normalisation

2.7.1 Seahorse flux analysis

The day prior to the experiment the sensor cartridge was hydrated with Seahorse XF calibration buffer (Agilent Technologies, Santa Clara, USA) and incubated at 37°C or room temperature until the experiment. Human isolated islets or pseudoislets were assessed with the IEQ method as previously described (2.1.5) and 200-300 IEQ of islets were pipetted per well into an islet capture microplate (Agilent Technologies, Santa Clara, USA) in a volume of 25 µl. After an islet capture screen was installed with the help of forceps, the well was topped up with 225 µl of culture media. The plate was incubated overnight to allow the islets to recover from transfer stress.

The next day, Seahorse assay media was prepared: 33.2 ml of basic DMEM were mixed with 17.5 µl of 1 M glucose, 350 µl of 200 mM solution of L-Glutamate, 1.05 ml of FBS and 350 µl of 100 mM Pyruvate (Gibco, Thermo Fisher, Waltham, USA). The pH of the media was checked and if necessary, adjusted to pH 7.4.

On the islet capture plate, the islet culture media was washed away from the plate with ~400 µl of assay medium twice and the wells were finally topped up with 450 µl medium. The plate was then incubated at 37°C without CO₂ for ~1 h.

During this time the injection ports of the sensor cartridge (Agilent Technologies, Santa Clara, USA) were loaded with the desired solutions. Port A was filled with 50 µl of assay medium or 25 µM glucose solution. In port B 55 µl of an oligomycin from *Streptomyces diastatochro-mogenes* solution with a concentration of 50 nM was pipetted. In port C 60 µl of 3.5 µM of carbonyl cyanide 4-(trifluoromethoxy) phenylhydrazone (FCCP) was added and in port D 65 µl of 2.5 µM antimycin A from *Streptomyces sp.* The cartridge was loaded into the XF24 Analyser (Agilent Technologies, Santa Clara, USA) for calibration, followed by the cell plate where OCR and extracellular acidification rate (ECAR) were analysed over time. The results were normalised to the amount of protein or DNA per well and ATP production could be calculated according to Mookerjee (Mookerjee et al., 2017).

2.7.2 DNA extraction

DNA extraction was performed with the DNeasy® Blood & Tissue Kit (Qiagen, Hilden, Germany). Human isolated islets or pseudoislets were washed with PBS and resuspended in 180 µl buffer ATL (Qiagen, Hilden, Germany) with 20 µl proteinase K (Qiagen, Hilden, Germany). The suspension was mixed by vortexing for ~15 sec and incubated at 56°C for 15 min. In a next step lysis buffer (buffer AL) (Qiagen, Hilden, Germany) was added, samples were mixed by vortexing and incubated for further 10 min at 56°C. Subsequently 200 µl 100% ethanol was added, samples were mixed and pipetted onto the binding column. The column was centrifuged for 1 min at 6010 g and the flow-through was discarded. 500 µl of Wash Solution 1 (buffer AW1) (Qiagen, Hilden, Germany) was pipetted onto the column and centrifuged for 1 min at 6010 g. Then 500 µl Wash Solution 2 was added (buffer AW2) (Qiagen, Hilden, Germany) and the column was centrifuged for 3 min at 18,407 g. In a last step 100 µl of elution buffer (buffer AE) (Qiagen, Hilden, Germany) was pipetted onto the membrane, incubated at room temperature for 1 min and centrifuged for 1 min at 6,010 g. DNA was stored for short term at 4°C and for long term at -20°C.

2.7.3 PicoGreen™ analysis

Quantification of DNA was performed with Quant-iT™ PicoGreen™ dsDNA Assay Kit (Invitrogen™, Thermo Fisher, Waltham, USA). With the dilution of a 2 µg/ml DNA stock solution in 1x TE buffer DNA concentrations of 1 ng/ml to 1 µg/ml were generated in duplicate wells of an opaque 96 well plate with a final volume of 100 µl/well. DNA samples were diluted in 1xTE buffer and 100 µl aliquots were pipetted into the plate. For each reaction 100 µl of PicoGreen™ working solution was added and incubated for 3 min at room temperature protected from light. Fluorescence was measured with an excitation of ~480 nm and an emission of ~520 nm. Unknown concentrations of DNA were calculated from the DNA standards.

2.8 Tissue engineering

2.8.1 *Electrospun nanofiber membrane*

Mouse islets were seeded on a PCL electrospun nanofiber membrane kindly provided from Dr Piergiorgio Gentile (Newcastle University) and cultured for 3-4 days. After that culture period islets and the membrane were washed twice with PBS and fixed in 4% formalin overnight at 4°C. The next day formalin was exchanged with PBS with storage at 4°C until the staining protocol was started. For staining the islets were incubated with 0.2% Triton-X100 for 1 h at room temperature on a shaker at low speed to permeabilise the cell membranes, followed by blocking in 20% FBS for 1 h. Primary antibodies (Table 2.3) were then incubated overnight at 4°C on a shaker at low speed. The next day islets were washed twice in PBS and incubated with the secondary antibodies (Table 2.4) for 1 h at low shaking speed followed by PBS washes. Membrane and islets were then mounted onto a glass slide and covered with a coverslip with mounting medium containing DAPI (Vector Laboratories, Burlingame, USA). Nail polish was applied as a seal around the glass plates to prevent dehydration of the stained sections. Samples were stored at 4°C in a light-proof box to prevent quenching of the fluorescence signal.

2.8.2 *Collagen I/alginate/fibrinogen Hydrogel*

2.8.2.1 Hydrogel generation

A hydrogel consisting of collagen I, alginate and fibrinogen (CAF) was produced according to an adjusted protocol after Montalbano et al. (2018). As preparation alginic acid sodium salt from brown algae (low viscosity) (Sigma Aldrich, Dorset, UK) was dissolved in PBS to reach a concentration of 5% w/v and fibrinogen from bovine plasma type I-S (Sigma Aldrich, Dorset, UK) was dissolved in PBS to obtain a concentration of 10% w/v. 6 mg/ml collagen solution pepsin soluble in 0.01 M hydrogen chloride (Collagen Solutions, Glasgow, United Kingdom) was used in the existing concentration. In a first step fibrinogen solution was mixed with alginate solution in a volume to volume ratio of 1:2 (alginate:fibrinogen). Then collagen was added with the same volume as fibrinogen leading to a volume to volume ratio of 2:1:2 (collagen:alginate:fibrinogen). For the crosslinking of alginate, a solution of CaCl₂ in a concentration of 2% was prepared by dissolving CaCl₂ in H₂O. Thrombin from bovine plasma was dissolved in DMEM basic media to achieve a

concentration of 400 U/ml for the crosslinking of fibrinogen. Both solutions were mixed in a 1:1 ratio leading to an end concentration of 1% CaCl₂ and 200 U/ml thrombin.

For the coating of wells of cell culture plates with CAF, 200 µl of precursor solution was pipetted into the well and spread as even as possible with the pipette tip. ~100 µl of crosslinking solution was added in drops on top and the gel and incubated for 30-60 min at room temperature followed by 6-24 h at 37°C. In a following step the crosslinking solution was washed off with either PBS or culture medium and islets were incubated for 72 h in the coated wells before they were analysed. Samples were taken for PI staining, embedding and staining as well as Seahorse analysis.

For the encapsulation of islets into the gel, 100 µl of CAF precursor solution was mixed with 500 IEQ of islets and pipetted onto a cell culture plate. The crosslinking solution was pipetted on top of the gel and incubated at room temperature for 30 min followed by ~2h at 37°C. Subsequently the crosslinking solution was washed off the gel with culture medium and the well was topped up with the appropriate amount of culture medium. Islets were assessed after 72 h encapsulated in the CAF hydrogel. Samples were taken for PI staining, RNA extraction and IF staining.

2.8.2.2 PI staining

Media was aspirated and gel was washed with PBS. Gel and islets were incubated in 990 µl PBS and 10 µl PI solution for 7 min in the dark. Subsequently the PI solution was removed, 1 ml PBS was added and if possible 50 islets were assessed for percentage of live cells. The average value and standard deviation were calculated with Microsoft Excel.

2.8.2.3 RNA extraction

Medium was removed from the well and the hydrogel was washed twice with PBS. Then the gels were scraped off the tissue culture well and transferred into a 1.5 ml Eppendorf tube. 250 µl of RNA lysis buffer was added and a sterile homogenizer was used to completely dissolve the gel. Samples were snap frozen in liquid nitrogen and stored at -80°C. Extraction of RNA was performed according to 2.5.1.

2.8.2.4 Freeze drying and scanning electron microscopy (SEM) analysis

Hydrogel samples were freeze dried for 48 h at 0.06 mPa and -50°C with a Christ Alpha1-2 LD plus freeze dryer (Martin Christ Gefriertrocknungsanlagen GmbH, Osterode am Harz, Germany) and analysed with a TM3030 SEM (Hitachi Ltd., Chiyoda, Japan).

2.8.2.5 Swelling analysis

Hydrogel samples were freeze dried as described before and incubated for 24 h in water. Hydrogels were weight before (W_d) and after (W_h) and swelling was calculated according to:

$$\text{Swelling (\%)} = [(W_h - W_d)/W_d] \times 100.$$

2.8.3 Orbital shaker method

To reduce hypoxia in islets, dynamic culture through a rotation platform was added to the gel system. 6 well plates were coated with CAF as described in 2.8.2. Islets were then seeded on top of the hydrogel with 1,000-2,000 IEQ/well and incubated on the orbital shaker adjusted to 60 rpm. Islets without presence of CAF and islets with and without CAF in static culture were used as comparison. Samples were taken for PI staining and RNA analysis.

2.8.4 Perifusion development

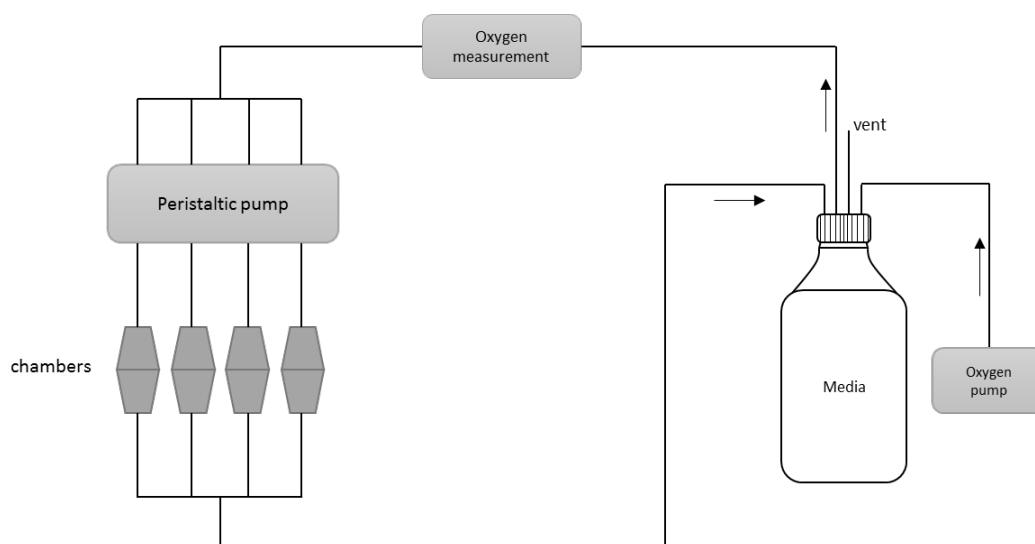


Figure 2.1: Schematic set up for perifusion of hydrogel/ β -cell construct.

A perifusion system was developed to provide oxygenated medium flow through a hydrogel/cell construct to decrease hypoxia (Figure 2.1). Perifusion chambers were

connected via tubing to a tank containing medium. Two sets of tubing was used for the set up: Fisherbrand™ Silicon Platinum-cured Tubing with an outer diameter of 4.5 mm (product code: 11552563, Fisher Scientific, Loughborough, United Kingdom) and Masterflex L/S® Precision Pump Tubing Peroxide-Cured Silicone L/S 16 (product code: WZ-96400-16, Cole-Parmer®, Eaton Socon, United Kingdom). An off-the-shelf fish tank pump provided oxygenation of the medium in the tank. A 302S peristaltic pump (Watson Marlow, Falmouth, UK) with a 314 four roller five channel micro pump head (Watson Marlow, Falmouth, UK) was used to provide movement of medium through the system. Oxygen content of the medium was measured with a Fibox 4 oxygen sensor (PreSens Precision Sensing GmbH, Regensburg, Germany). The final system without the oxygen sensors is pictured in Figure 2.2. For the development phase sterile PBS (Sigma-Aldrich, Dorset, United Kingdom).



Figure 2.2: Perfusion system with chambers, peristaltic pump, fish pump and media tank.

2.9 Statistical analysis

Mean values and standard deviations were calculated in Excel. Unpaired Student's t-tests and multiple Student's t-test were carried out with GraphPad Prism 8 (GraphPad Software Inc., California, USA). Spearman's rho correlation (two-tailed) was performed with SPSS Statistics (IBM, New York, USA).

Chapter 3. Impact of *post mortem* ischaemia, tissue processing and islet isolation on islet microenvironment, integrity, morphology and function

3.1 Introduction

In pancreas tissue, islet cells are surrounded by a specific microenvironment composed of ECM, vasculature and exocrine cells providing a defined niche (Longnecker, 2014). The microenvironment can be altered through disease exposure including pancreatitis and cystic fibrosis leading to pancreatic pathologies identifiable with traditional histopathology and at an ultrastructural level by TEM analysis (Pickartz et al., 2007). Pathological changes can progress over time impacting pancreas morphology (Sheppard and Nicholson, 2002). In the case of pancreatitis, histology typically shows development of fibrotic tissue especially around ducts accompanied by infiltration of lymphocytes, plasma cells and eosinophilic cells (Pickartz et al., 2007). In addition to established disease/gross pathology, other factors including donor age and donor BMI have been shown to impact on organ morphology. At an ultrastructural level it was observed that the amount of lipid droplets in endocrine cells correlated with donor BMI and the amount of lipofuscin correlated with age (Cnop et al., 2010, Rosengren et al., 2012).

During organ retrieval, blood supply to the organ is stopped and the organ is flushed with specialised cold-preservation solution for transport (NHSBT, 2018b). During this period termed 'cold ischaemia', the organ typically has no access to oxygen and increasing hypoxic exposure can impact on tissue structure and single cell status (Zhang et al., 2018, Nevalainen and Anttinen, 1977). Specialised retrieval and transport protocols have been developed in an effort to decrease impact of hypoxia on tissue primarily by cooling the organ to approximately 4°C (NHSBT, 2018b). Specialised cold-preservation solutions such as University of Wisconsin (UW) solution or histidine-tryptophan-ketoglutarate (HTK) solution have been developed to maintain the intracellular milieu during cold storage as ion channels stop functioning at low temperatures (Iwanaga et al., 2008). In the UK usually UW solution is used for in situ perfusion and organ transport (NHSBT, 2018b). However, stress through absence of sufficient oxygen supply can impact on organ function and cell status and therefore outcomes of transplantation (Rudolph et al., 2017).

Once the organ is connected to the vascular system of the transplant recipient in a whole organ transplant, blood flow is re-established to the pancreas and specifically to the islets. However, complications after pancreas transplantation can include reperfusion injury or graft thrombosis and these can decrease organ function and transplantation outcomes (Gruessner and Gruessner, 2016, Humar et al., 2004).

For isolated islet transplantation, endocrine and exocrine tissue is separated by enzymatic and mechanical procedures (Qi et al., 2009a, Qi et al., 2009b). The isolation process especially impacts on islet microenvironment with loss of the peri-islet capsule and loss of connection to the vasculature system of the organ (Wang et al., 1999, Irving-Rodgers et al., 2014, Cross et al., 2017). The loss of BM is not only a loss of the specific microenvironment, but also loss of key cell-matrix connections which may lead to anoikis, thereby impacting on viability and function of islets (Irving-Rodgers et al., 2014). Loss of blood supply means that islets rely on passive diffusion alone from the moment of isolation until they revascularize which may take between ten days and one month (Menger et al., 1989, Carlsson et al., 2001). This leads to formations of hypoxic gradients inside the islets and may lead to core necrosis, particularly in larger islets, which can impact on function (Komatsu et al., 2017). Following transplantation, complications including IBMIR further impact on viability and function of islets, negatively impacting transplantation outcomes (McCall and Shapiro, 2012, Biarnes et al., 2002, Bennet et al., 2011).

3.2 Aims

Achieving optimal and sustained engrafted endocrine cell function is the priority for any β -cell replacement therapy. Therefore, it is crucial to understand the impact of acute stress on viability and function of endocrine cells to enable future improvements in pancreas and islet transplantation procedures and possible interventions for improved endocrine function after transplantation.

Overall aim: To characterise the islet niche *in situ* and analyse acute changes related to ischaemia, tissue processing and islet isolation.

Objective 1: To characterise islet microenvironment, integrity and morphology *in situ* in a pancreas with minimal ischaemic exposure.

Objective 2: To characterise the impact of ischaemia and tissue processing on islet microenvironment, integrity and morphology.

Objective 3: To characterise the impact of islet isolation on islet microenvironment, viability, integrity.

3.3 Results

3.3.1 *Islets in their endogenous niche in situ in human and mouse tissue*

3.3.1.1 Human tissue with short cold ischemia time

A pancreas from a donor with short CIT off 5 h 3 min allowed analysis of general pancreatic features with assessment through histology and at an ultrastructural level. The pancreas was obtained from a 43-year-old non-diabetic male DBD donor with a BMI of 26.8 kg/m² and no known pancreatic disease before death pathology.

3.3.1.1.1 Histological assessment with Haematoxylin & Eosin, Sirius red/Fast green and immunoperoxidase staining

A pancreas biopsy stained for Haematoxylin & Eosin (H&E) analysed in lower magnification illustrated general features of the organ (Figure 3.1). The majority of the section was comprised of acinar tissue appearing darker compared to islets. Islets of Langerhans appeared more eosinophilic usually with a round or oval shape and are distributed throughout the whole section with some examples indicated by a white arrow. Other visible features include ducts (D) and blood vessels (BV). Additionally, pancreatic fat visualised as round holes was visible dispersed through the section.

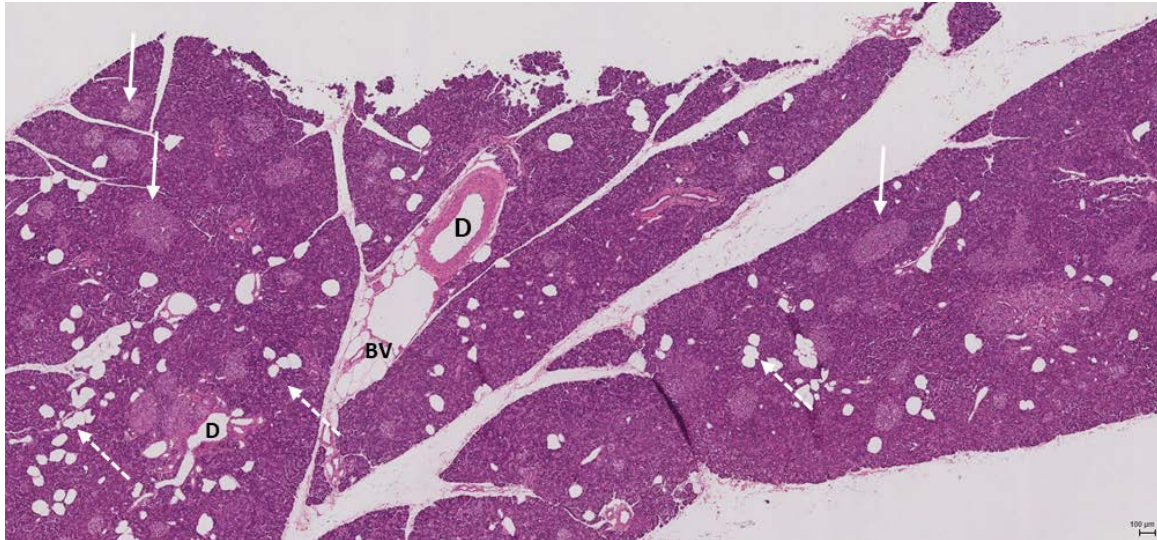


Figure 3.1: Analysis of human pancreatic tissue in a donor with short CIT through H&E staining at low magnification. Pancreas section from a male donor, DBD, 43 years, CIT 5 h 3 min. Islets appeared more eosinophilic (examples indicated with arrows) and were distributed through the whole section. Some ducts (D) and a blood vessel (BV) could be identified in addition to pancreatic fat (examples indicated with dashed arrows). Scale bar 100 μ m.

Figure 3.2A shows a pancreas section after H&E staining with two islets indicated by white dotted lines, appearing more eosinophilic containing larger nuclei compared to acinar tissue. Throughout the acinar tissue, some areas stained pinker indicating higher content of acinar vesicles whereas other areas appeared bluer indicating higher content of RNA and the presence of nuclei (Longnecker, 2014). The general morphology showed how acinar cells are grouped together as acini. In panel B the same area was assessed after a Sirius red/Fast green (SR/FG) stain with SR binding to all types of collagens, FG binding to all non-collagen proteins and a counter stain with haematoxylin staining nuclei blue. Again, islets appeared brighter compared to acinar tissue and were surrounded by a BM consisting of collagen. Collagen was also present inside islets and throughout the acinar tissue. Figure 3.2C shows, in a similar area, staining of the endocrine granule marker, chromogranin A, in red indicating the location of islets. Blood vessels were identified through staining of CD31 with DAB (brown) and were dispersed throughout the pancreas tissue as well as around and inside islets. Nuclei are stained blue through haematoxylin staining.

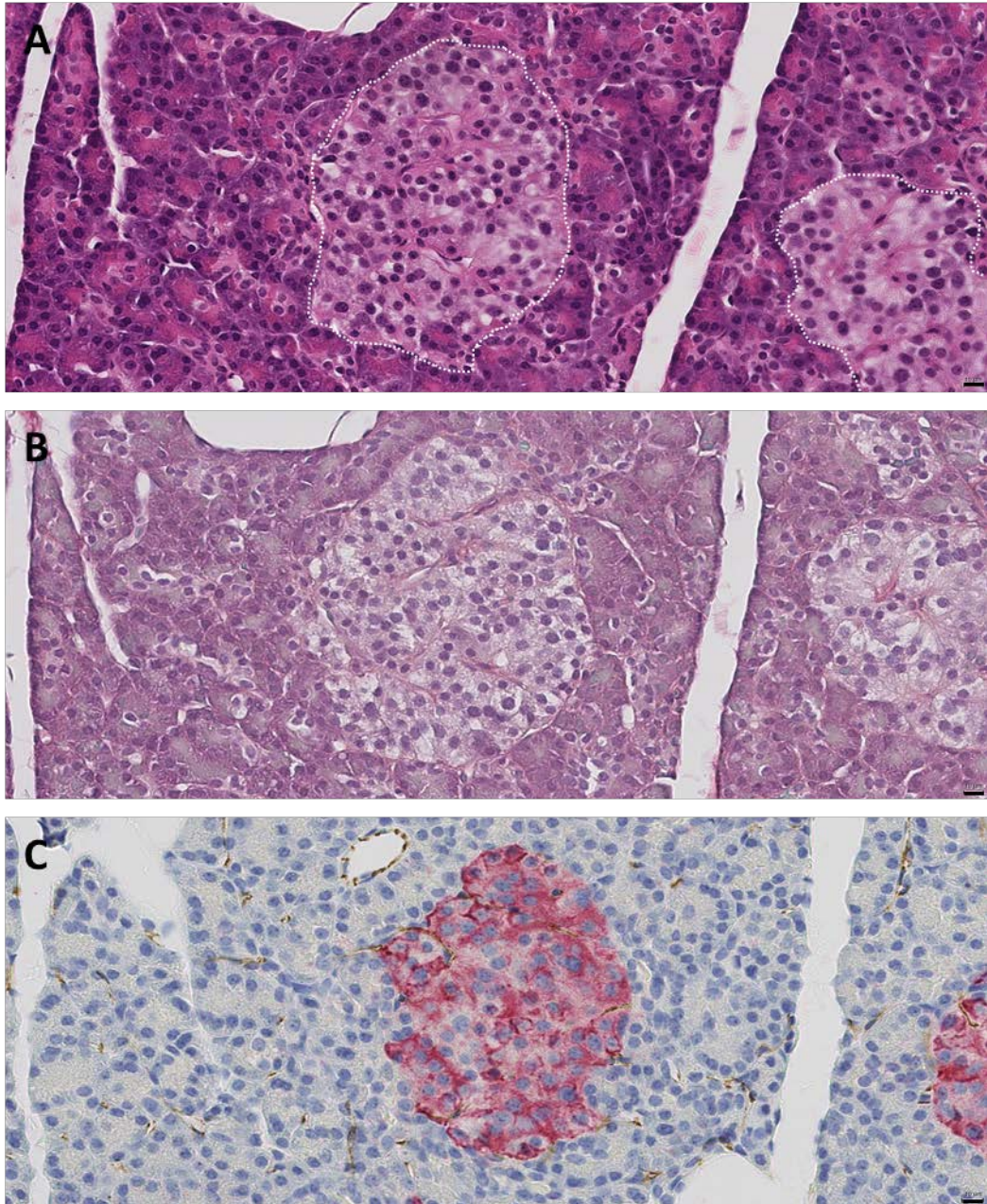


Figure 3.2: Analysis of human pancreatic tissue in a donor with short CIT through different histological stains at higher magnification. H&E showed a brighter eosin stain in islets, which are indicated by a white dotted line, compared to acinar tissue appearing darker (A). Sirius red and Fast green staining (B) stained collagen in red surrounding the islets and vasculature inside islets as well as BM throughout acinar tissue. Staining for CD31 in brown and chromogranin A in red (C) indicated the location of islets and endothelial cells within the tissue. Scale bars: 10 μ m.

3.3.1.1.2 Human pancreas assessment through immunofluorescence staining

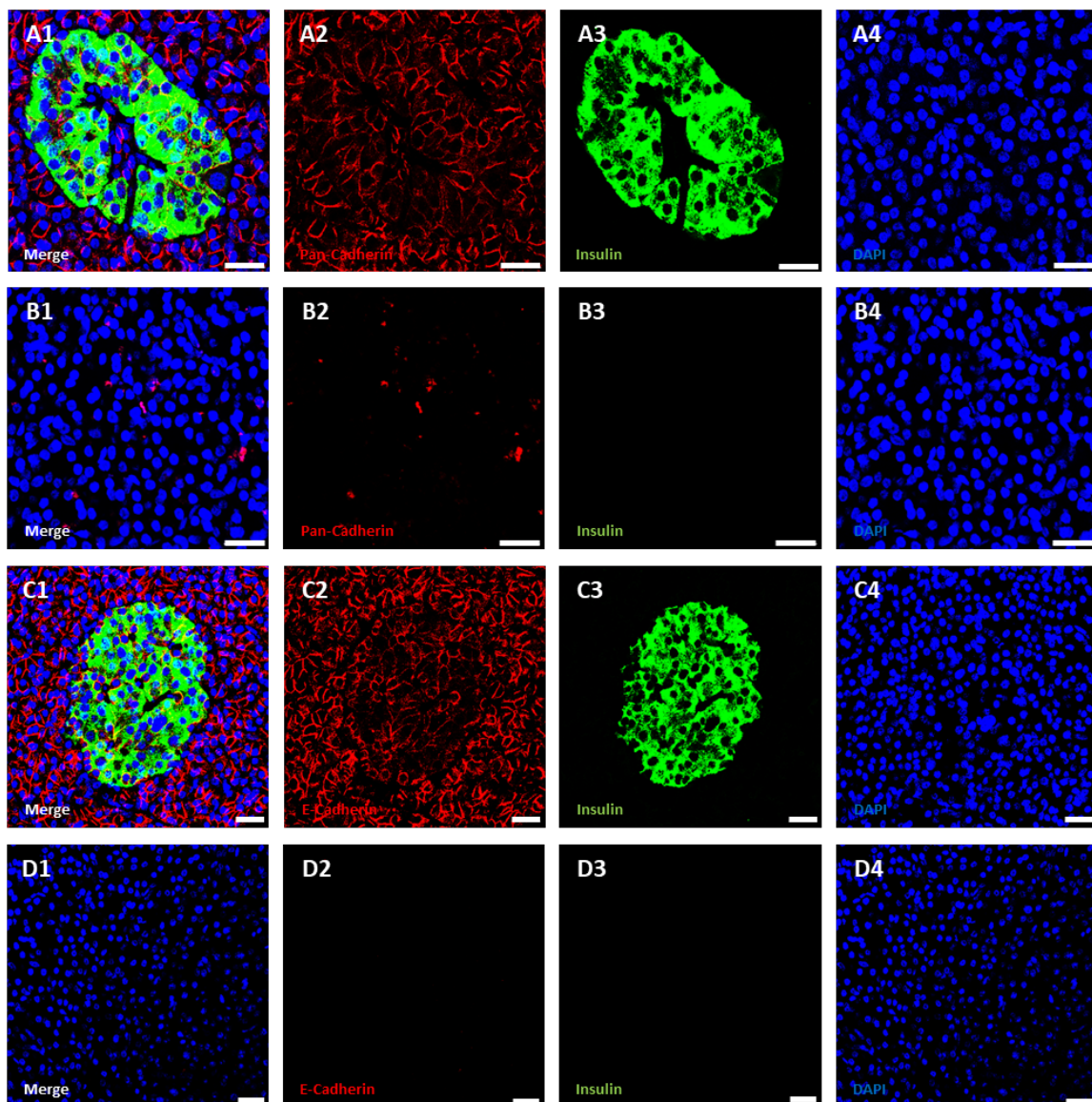


Figure 3.3: Pancreas tissue stained for pan-cadherin and E-cadherin. (A1-A4) Staining for pan-cadherin in red, insulin in green and DAPI in blue. (B1-B4) No primary antibody control for pan-cadherin staining. (C1-C4) Staining for E-cadherin in red, insulin in green and DAPI in blue. (D1-D4) No primary antibody control for E-cadherin staining. Scale bars 25 μ m.

Staining for CD31 in red (Figure 3.4 A1-A4) indicated the distribution of blood vessels in pancreatic tissue and specifically within islets (using insulin co-staining). Blood vessels could be observed in acinar tissue with potentially higher density in the proximity of and inside the islet. Staining for vimentin (Figure 3.4 C1-C4) indicated the distribution of cells of mesenchymal origin including endothelial cells which confirmed the presence of blood vessels in and around islets.

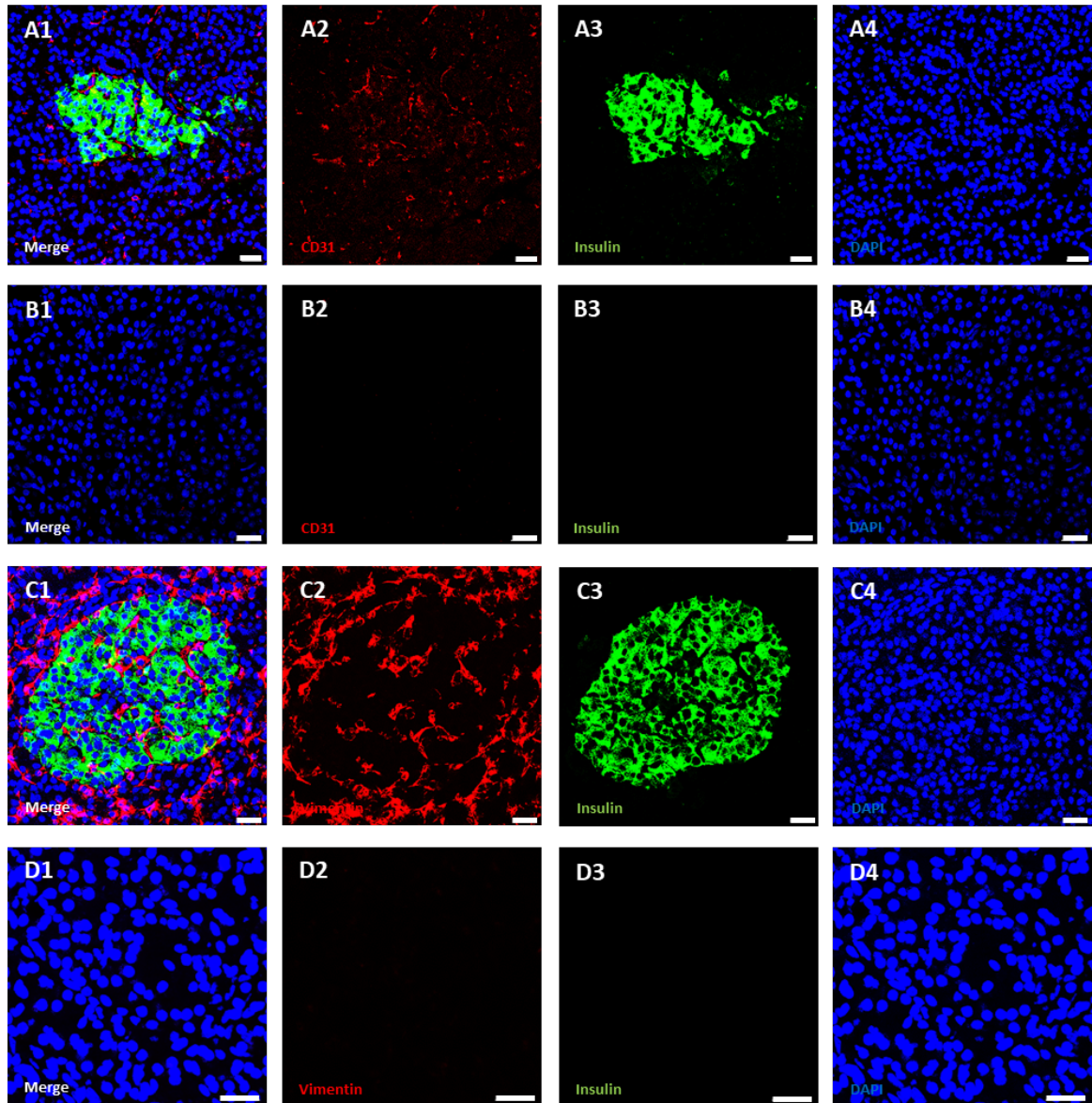


Figure 3.4: Pancreas tissue stained for CD31 and vimentin. (A1-A4) Staining for CD31 in red, insulin in green and DAPI in blue. (B1-B4)) No primary antibody control for CD31 staining. (C1-C4) Staining for vimentin in red, insulin in green and DAPI in blue. (D1-D4) No primary antibody control for vimentin staining. Scale bars 25 μm.

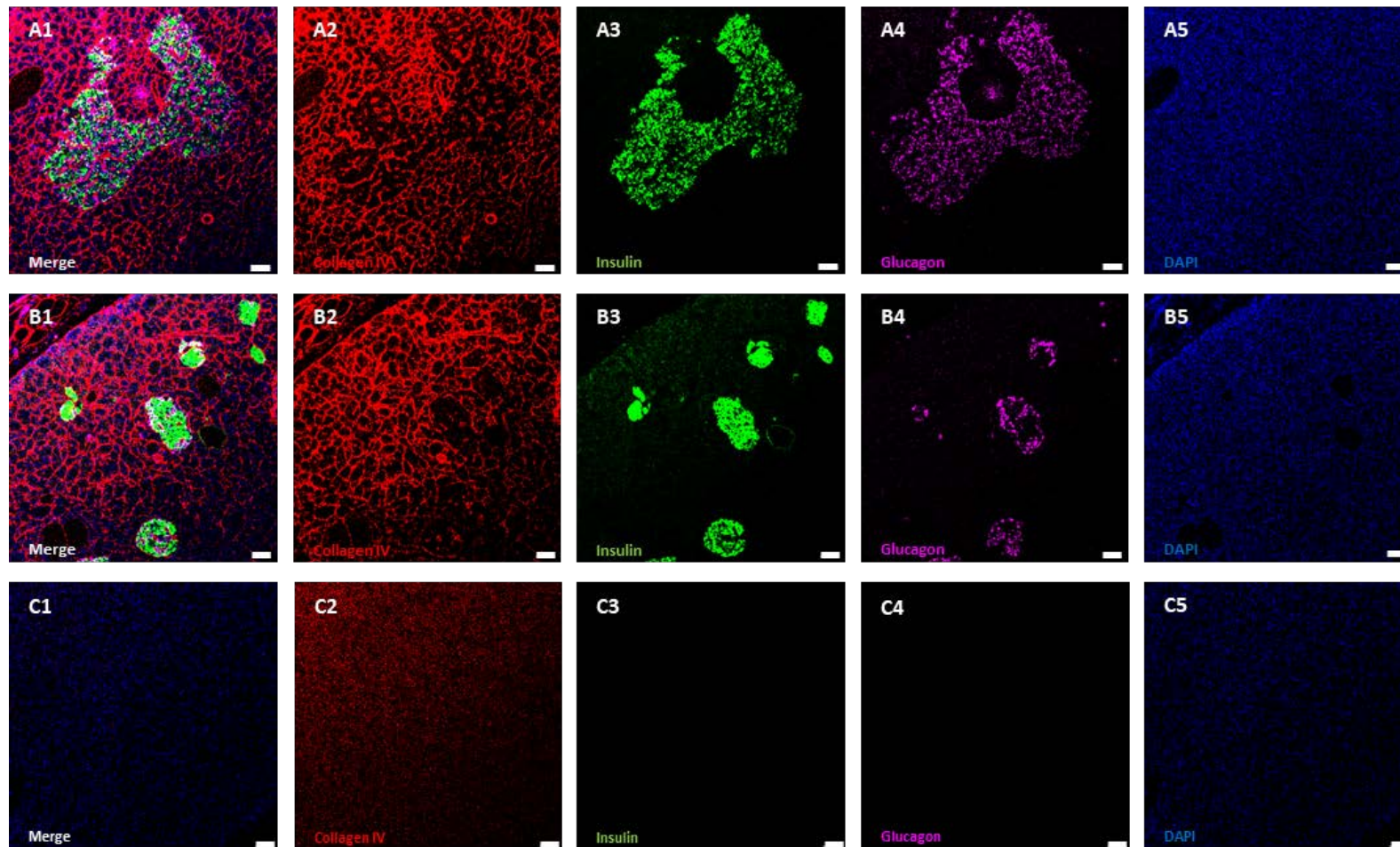


Figure 3.5: Distribution of BM in pancreas tissue with low CIT.

Analysis of human pancreatic tissue through immunofluorescence staining of collagen IV at low magnification. Sections are shown from two different locations (row A and row B). Staining for collagen IV in red indicating BM around islets, vasculature and acini (column 2), insulin in green indicating the position of islets (column 3), glucagon in pink indicating the position of islets (column 4) and DAPI in blue showing nuclei (column 5). Column 1 shows a merge of all staining for each location indicating the presence of glucagon and insulin in different islets as well as presence of BM in and around islets and in acinar tissue. Row C: no primary control. Scale bar: 50 μm .

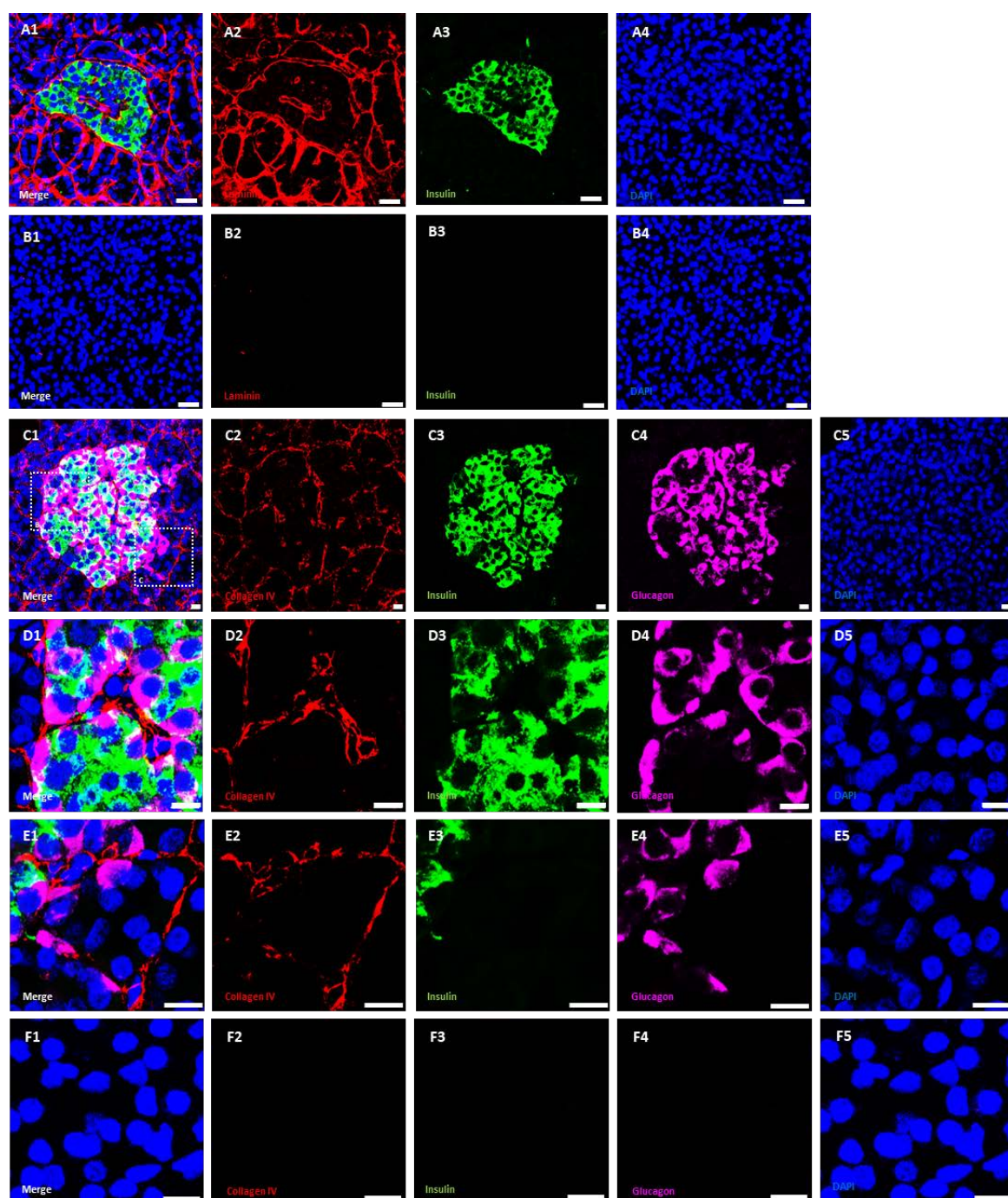


Figure 3.6: Analysis of human pancreatic tissue with low CIT through immunofluorescence staining of laminin and collagen IV at higher magnification. (A1-A4) Staining for laminin in red, insulin in green and DAPI in blue. (B1-B4) No primary control for laminin staining. (C1-C5) Staining for collagen IV in red, insulin in green, glucagon in pink and DAPI in blue. Higher magnification of collagen IV distribution in D1-D5 and E1-E5 indicated with the boxes in C1. (F1-F5) No primary control for collagen IV staining. Scale bar for A1-B4: 25 μ m. Scale bar for C1-F5: 10 μ m.

Distribution of BM in pancreas tissue was investigated with staining for collagen IV at low magnification (Figure 3.5). BM was present in acinar tissue around acini, ducts and blood vessels as well as around islets and inside of islets in a vascular distribution (Figure 3.5 A2 + B2). At higher magnification, staining for laminin (Figure 3.6 A2) and collagen IV (Figure 3.6 C2) demonstrated the double layered BM in the peri-islet capsule and the presence of BM around the vasculature inside islets. Figure 3.6 D2 and E2 showed the collagen network building the scaffold of the BM. Glucagon staining in Figure 3.6 D4 and E4 shows the distribution of α -cells adjacent to the BM of the vasculature or the peri-islet capsule.

3.3.1.2 Human pancreatic tissue with low CIT assessed at ultrastructural level

To analyse pancreas tissue with CIT as low as possible, a mouse pancreas was removed from a recently deceased animal and biopsies were immediately taken for TEM fixation and processing. This work was done in compliance with UK law under Schedule 1 protocols. Analysis revealed characteristic morphology of exocrine and endocrine parts. Acinar cells could be identified by acinar vesicles (AV) and the presence of a high amount of endoplasmic reticulum (ER) (Figure 3.7 A) whereas islet cells could be identified through the presence of numerous endocrine vesicles (Figure 3.7 A-D). Endocrine vesicles of different islet cells possessed distinct characteristics on TEM. Vesicles from δ -cells were filled with uniform brighter electron density and in mouse islets could be found at the core of the islet in line with prior descriptions from the literature (Figure 3.7 C) (Stendahl et al., 2009). The α -cell and β -cell vesicles contained a core with higher electron density surrounded by a halo in mature vesicles and with decreasing halo in immature vesicles (Figure 3.7 C+D). Furthermore, pre-existing pathology in form of lipofuscin (LF) and lipid droplets (LD) was present in the tissue (Figure 3.7 A-D).

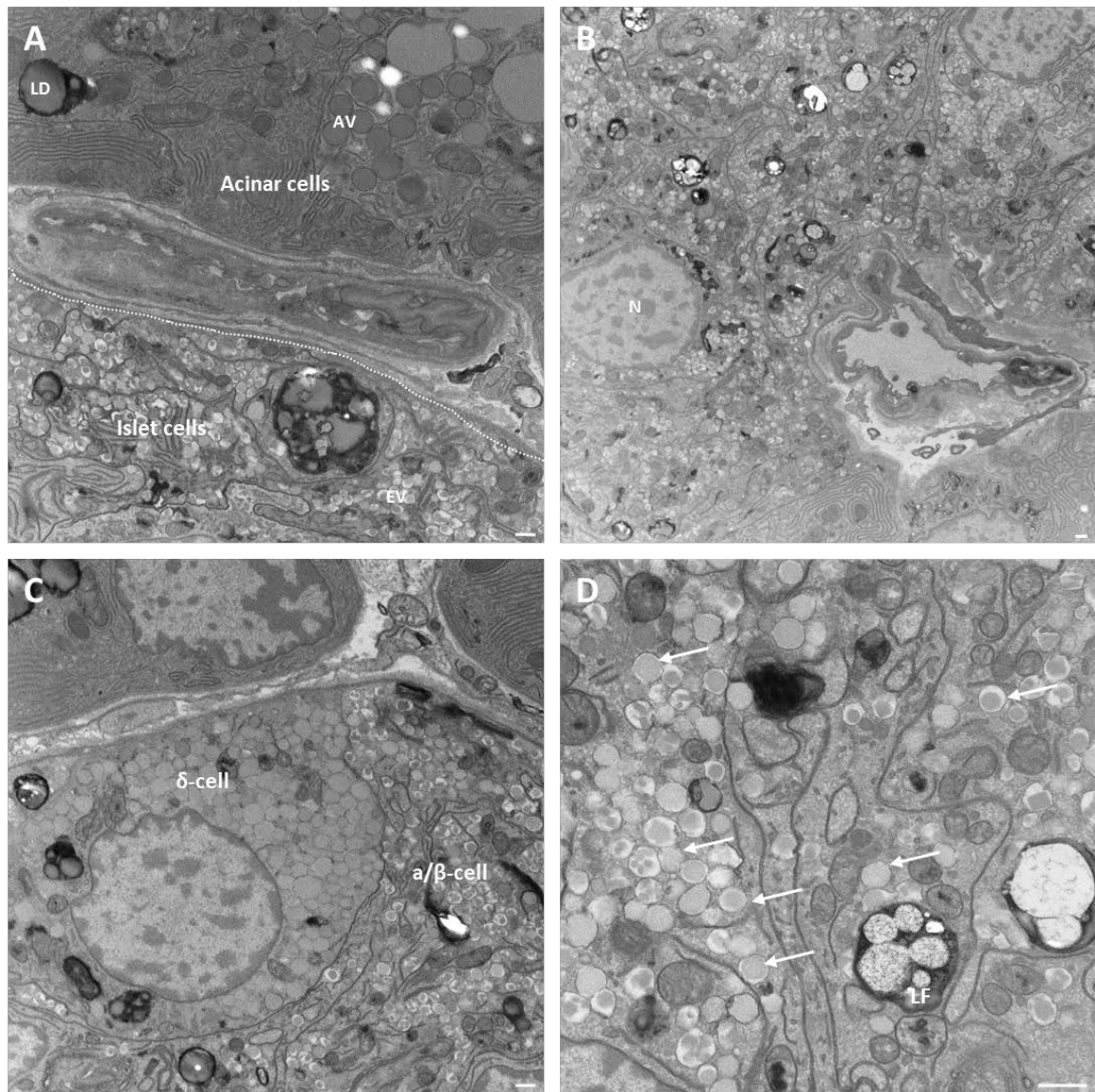


Figure 3.7: Ultrastructural analysis of mouse pancreas tissue with TEM.

(A) Interface between exocrine and endocrine tissue (marked by white line). Islets possessed characteristic endocrine vesicles (EV) with electron dense core surrounded by light halo whereas acinar vesicles (AV) appear fully filled. (B) Endocrine cells inside an islet with one nucleus (N) visible. (C) Two different islets cells could be differentiated by their distinct vesicles. (D) Characteristic hormone vesicles (arrows) with electron dense core mantled by light area inside the granule. Lipofuscin (LF) visible inside islet cells. Scale bars: 500 nm.

The ultrastructural level examination of short CIT human pancreas tissue displayed the same features as mouse pancreas tissue. Acinar cells were grouped together as acini (Figure 3.8 A) or around an acinar lumen (Figure 3.8 C+D) and comprised characteristic acinar vesicles (AV) as well as a high amount of visible ER (Figure 3.8 A,B,D). Islets could be identified through the presence of endocrine vesicles (EV) showing different appearance for different islet cell types filling most of the cell (Figure 3.9 A-C). In β -cells, vesicles possessed a halo surrounding an electron dense core, sometimes even square-shaped (Figure 3.9 A-C). Some vesicles possessed a smaller to no halo together with a less dense core depending on the maturation status of insulin. Endocrine vesicles of α -cells appeared similar to β -cells, which made it difficult to distinguish between them without immunogold labelling. Cells solely with filled vesicles possessing light electron density were believed to represent δ -cells (Figure 3.9 C). Additionally, ultrastructure analysis confirmed presence of BM around islets, indicated by a less electron dense area next to the cell membrane followed by an electron dense line revealing the interface of endocrine and exocrine tissue (Figure 3.9 D). In some cases, this interface was filled with additional ECM components including collagen fibres (Figure 3.9 D+E). Pre-existing pathology in form of lipofuscin and lipid droplets could be observed in human tissue as well as mouse tissue (Figure 3.9 A+C).

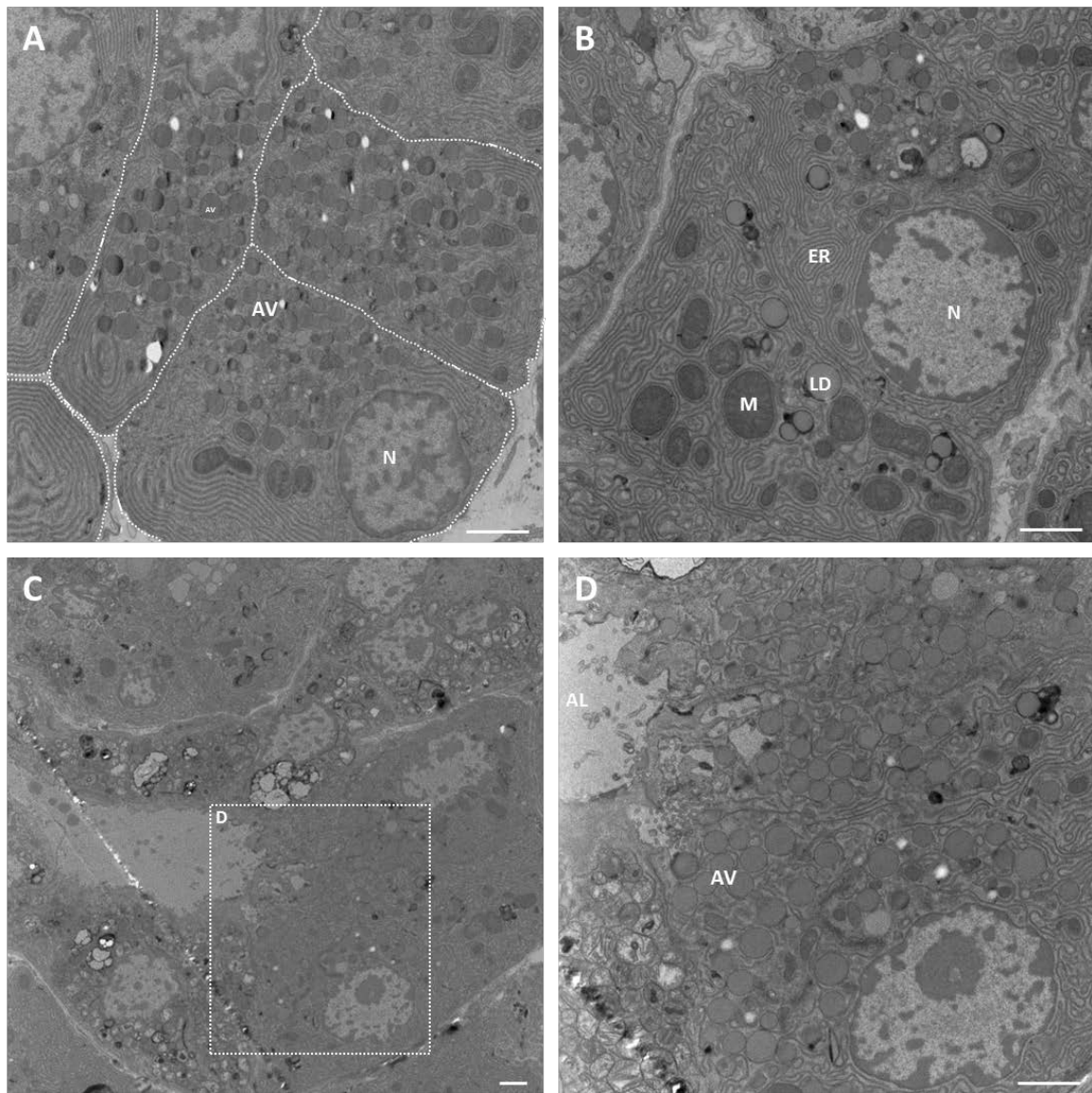


Figure 3.8: Ultrastructural analysis of human acinar tissue with short CIT. (A) Acinar cells characterised by acinar vesicles (AV) with visible nucleus (N), endoplasmic reticulum (ER), mitochondria (M) and lipid droplets (LD). (B) Acinar cells grouped together to form acini. (C) Acinar cells forming acinar lumen (AL) with white box indicating image part D. (D) Higher magnification of AL with microvilli and adjacent acinar cells. Scale bars: 2 μ m.

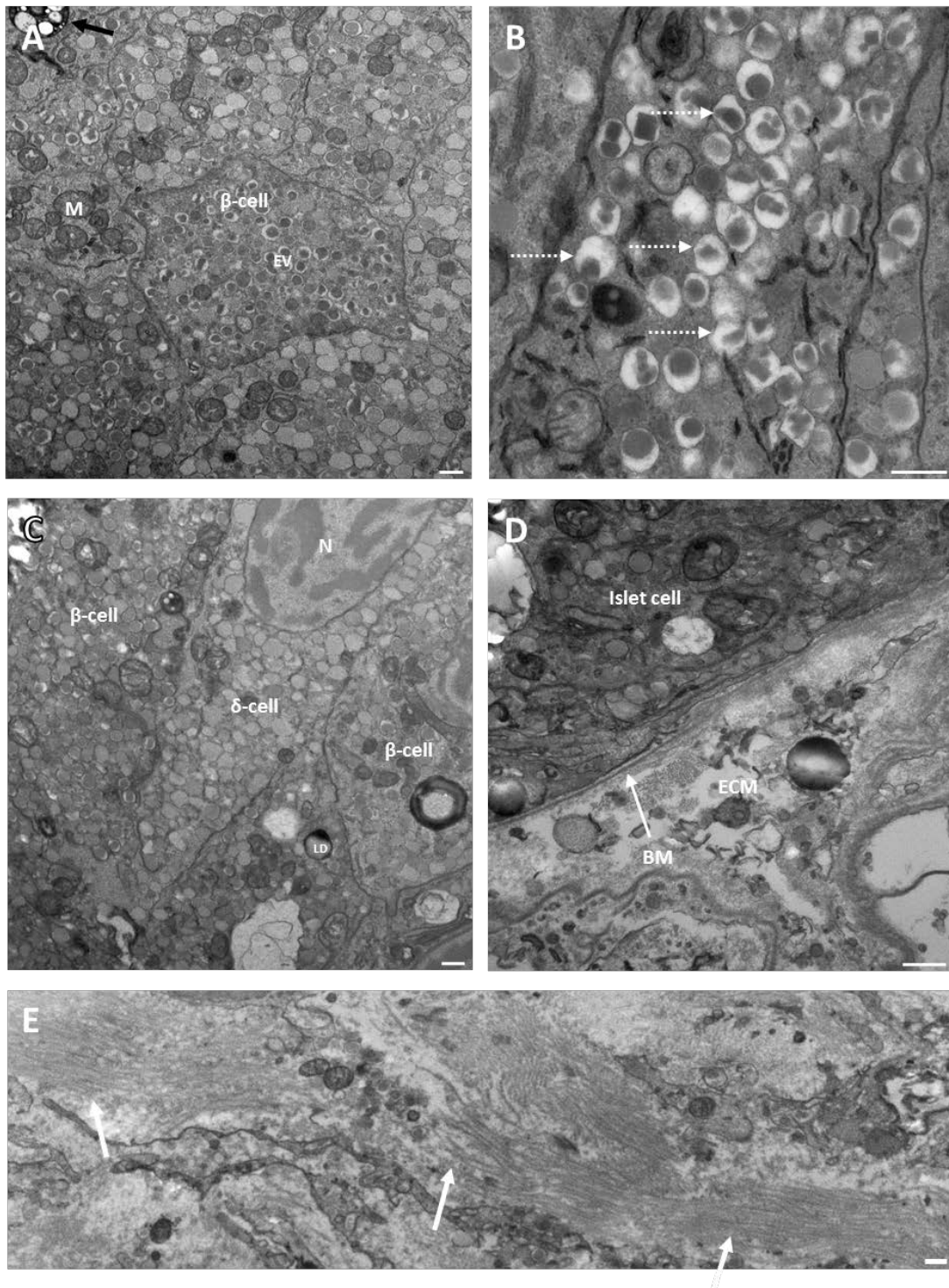


Figure 3.9: Ultrastructural analysis of human endocrine tissue with low CIT.

(A) Group of endocrine cells inside an islet with high amount of characteristic endocrine vesicles (EV) which were designated β -cells. No other cell organelles visible except mitochondria (M). Lipofuscin (black arrow) visible in endocrine cell. (B) EV (dashed arrows) which were believed to be from β -cells with characteristic halo around an electron dense core. (C) Different islets cells could be characterised through their distinct vesicles. The β -cells possessed vesicles with a bright mantle around an electron dense core whereas vesicles in δ -cells were completely filled with a medium electron density. Intracellular lipid droplet (LD) visible in endocrine cell. (D) Outside of an islet with characteristic basement membrane (BM) consisting of a lighter electron density right next to the cell membrane followed by a darker electron dense line (arrow). Outside of the islets, ECM components including collagen fibres were visible. (E) ECM components of pancreas tissue. Collagen fibres (arrows) displayed as dark electron dense lines (longitudinal section) or circles (cross section) depending on the angle of fixation and micro-sectioning. Scale bars: 500 nm.

3.3.2 Impact of post mortem ischemia and tissue processing on the islet microenvironment, integrity and morphology

With the retrieval of an organ, the blood supply stops and there is a rapid onset of hypoxia/anoxia in cells. Prolonged exposure to these conditions leads to a number of changes in cell organelles ultimately substantial damage to whole cell morphology. To investigate impact of post mortem ischemia on cell integrity and morphology, four DBD (Table 3.1) and eight DCD donors (Table 3.2) were assessed with histological samples including H&E and SR/FG and with TEM at an ultrastructural level. CIT of studied donors ranged from 6 h 20 min till 38 h 8 min in DBD donors (Table 3.1) and 6 h 26 min till 29 h 48 min in DCD donors (Table 3.2).

*Table 3.1: Information for pancreas DBD donors with ascending CIT.
With two donors (50%) female, age of (average (\pm SD)) 53.5 (\pm 12.7) [years] and BMI of 26.9 (\pm 4.1) [kg/m²]. LDIS number for internal reference.*

Pancreas number	LDIS number	Donor Type	CIT [h]	WIT [min]	Gender	Age [years]	BMI [kg/m ²]
1	237	DBD	6.3	-	male	69	29.1
2	226	DBD	18.0	-	female	39	24.0
3	214	DBD	27.0	-	male	49	31.5
4	221	DBD	38.1	-	female	57	23.0

Table 3.2: Information for pancreas DCD donors with ascending CIT. With four donors (50%) female, age of (average (\pm SD)) 49.5 (\pm 17.7) [years] and BMI of 24.2 (\pm 3.2) [kg/m²]. LDIS number for internal reference.

Pancreas number	LDIS number	Donor Type	CIT [h]	WIT [min]	Gender	Age [years]	BMI [kg/m ²]
1	231	DCD	6.4	34	female	65	17.7
2	172	DCD	8.0	18	male	25	22.8
3	218	DCD	8.8	17	male	53	22.9
4	232	DCD	8.9	33	female	73	24.8
5	215	DCD	9.9	25	male	28	24.0
6	244	DCD	13.2	12	female	49	26.6
7	169	DCD	16.5	32	female	64	26.4
8	219	DCD	29.8	29	male	39	28.3

3.3.2.1 Histological assessment of human pancreata with H&E and SR/FG

H&E and SR/FG staining revealed different pathological characteristics of pre-existing pathology as well as acute changes to tissue morphology with examples shown in Figure 3.10. Pathology in the pancreas which developed over a period over several weeks till years included fibrosis (Figure 3.10 A), microadenoma (Figure 3.10 B), PanIN-1 (Figure 3.10 C), hyperplasia of islets (Figure 3.10 D) and pancreatitis (Figure 3.10 E). Acute changes included inflammation (Figure 3.10 E), oedema (Figure 3.10 D+F), fat necrosis (Figure 3.10 G), tissue necrosis (Figure 3.10 H) and haemorrhage (Figure 3.10 E,G,H). Acute changes may develop during prolonged ischaemia and manifest as changes to cell morphology and cell organelles including the nucleus. For a more detailed analysis of ischaemia impact on pancreata at a cellular level, biopsies were analysed with TEM analysis.

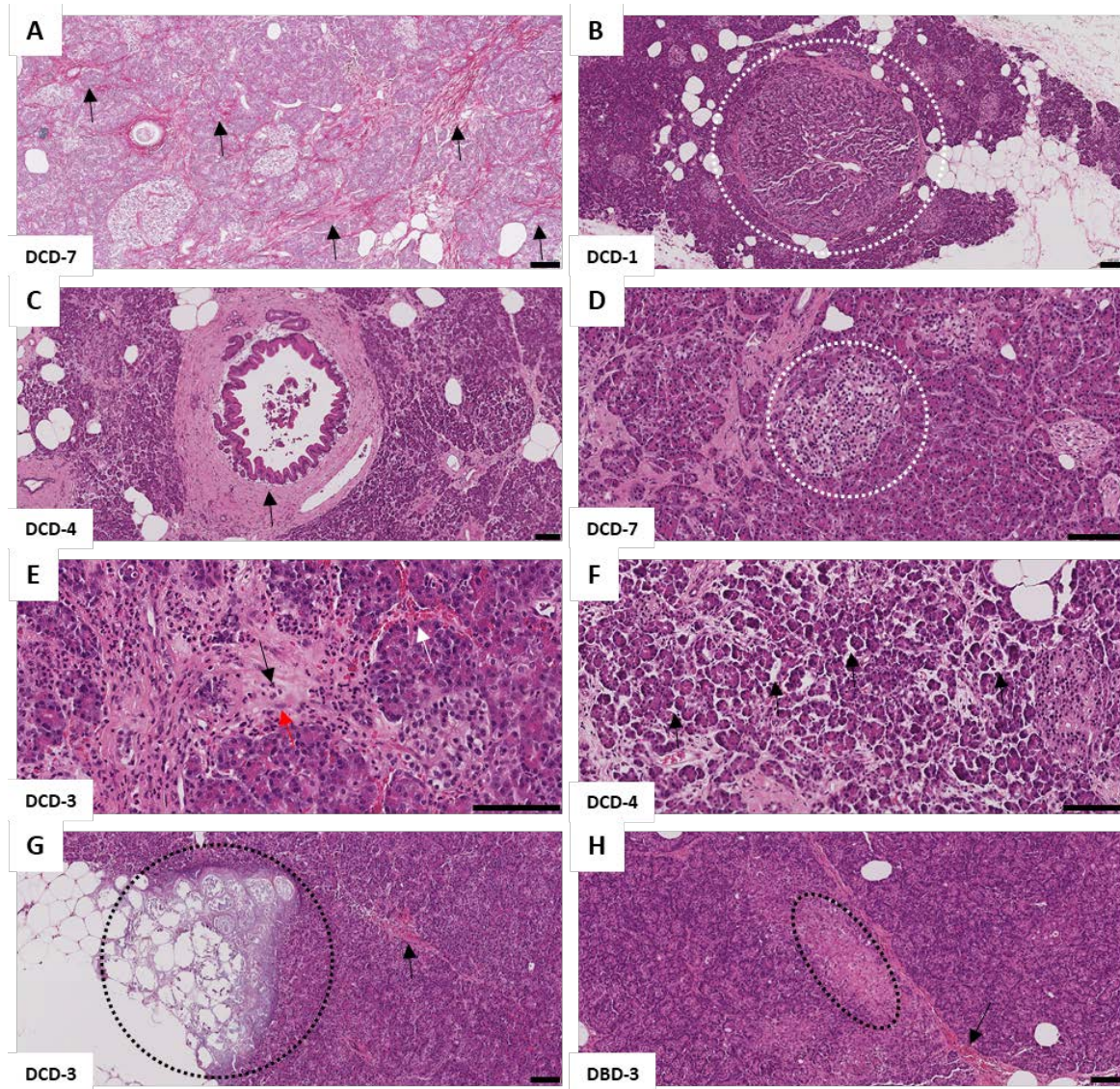


Figure 3.10: Example images for histological analysis of pancreas tissue.

A: SR/FG staining indicating distribution of fibrosis in the tissue in red (some areas indicated with black arrows). B: Islet (white dotted line) with a diameter of ~1 mm indicating microadenoma. C: Pancreatic intraepithelial neoplasia 1 (PanIN 1). D: Islet (white dotted line) with a diameter above 250 μm (hyperplasia) with oedema visible inside the islet. E: Pancreas tissue with infiltration of mast cells (example indicated with red arrow) and neutrophils (example indicated with black arrow) as well as visible red blood cells (indicated with white arrow) showing possible haemorrhage. F: Atrophic area of acinar tissue with space in between tissue (black arrows) and little amount of cytoplasm. G: Area of fat necrosis indicated with black dotted line as well as possible haemorrhage (black arrow). H: Necrotic area indicated with black dotted line with dissolving cells visible. In addition red blood cells (black arrow) indicate possible haemorrhage. Scale bars: 100 μm .

3.3.2.2 *Ultrastructural assessment of human pancreata with TEM*

The TEM enabled assessment of tissue at an ultrastructural level. By investigating different donors, recurring features of acute damage through hypoxia could be identified (Figure 3.11). Normal nuclei appeared with a dark nuclear membrane and dark chromatin inside distributed evenly throughout the nucleus as well as in contact with the nuclear membrane (Figure 3.11 A1). Larger chromatin clumps in a fairly round shape located inside the nucleus could be identified as a nucleoli. Through prolonged hypoxic exposure, chromatin inside the nucleus could clump together and, in some cases, detach from the nuclear membrane (Figure 3.11 A2). Normal mitochondria appeared as darker cell organelles with oblong shape (Figure 3.11 B1) and in higher magnification single cristae inside the mitochondria as well as the doubled layered membrane were visible. Acute damage could be identified by a swelling of the mitochondria leading to a brighter electron density inside as well as a rounder shape (Figure 3.11 B2). In some cases, the cristae could be damaged and/or the shape of the mitochondria was destroyed. Furthermore, ER could start to dilate through hypoxic stress impacting on cell morphology and integrity leading to difficulties identifying individual cells and even between organelles compared to cells with normal appearing ER (Figure 3.11 C1+C2). Another sign of damage included development of vacuoles inside of the cell impacting on the overall cell morphology and integrity as well as increasing difficulty to identify single cells or cell organelles compared to normal morphology (Figure 3.11 D1+D2).

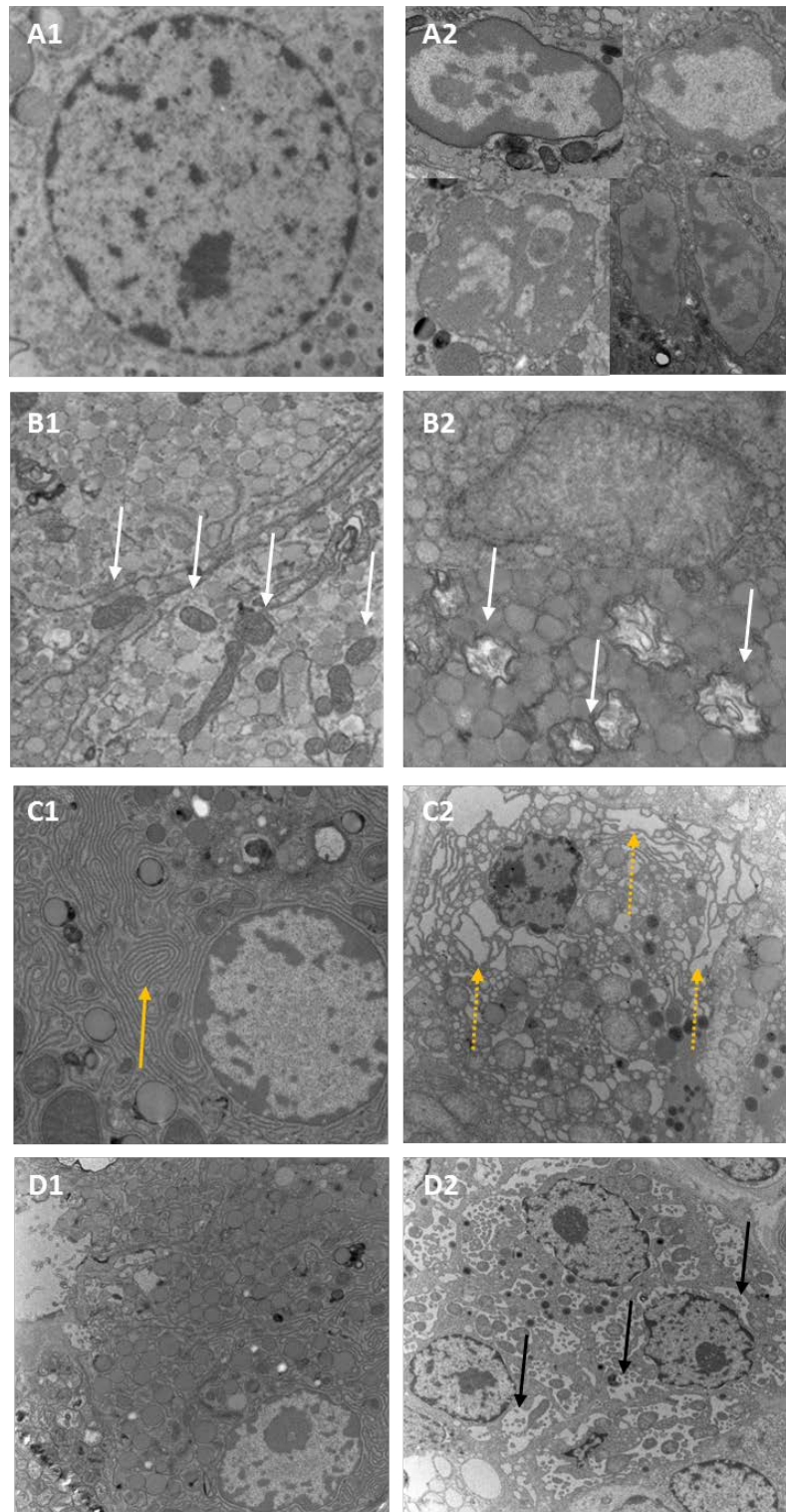


Figure 3.11: Ultrastructural acute damage through hypoxia in exocrine tissue. Normal (A1) and changed nuclei (A2), normal (B1) and changed mitochondria (B2) (white arrows), normal ER (C1) (yellow arrow) and dilated ER (C2) (dashed yellow arrows) as well as normal cell morphology (D1) and changed morphology through vacuolisation (D2) (black arrows) are visible.

3.3.2.3 Development of the Newcastle Electron Microscopy Ischaemia Score (NEMIS) for analysis of ultrastructural stress induced changes during pancreas preservation

With these recurrent characteristics the Newcastle Electron Microscopy Ischaemia Score (NEMIS) was developed in collaboration with Nicola Dyson from the Transplant Regenerative Medicine Laboratory at Newcastle University and helpful feedback from the QUOD expand TEM project group. The scoring system was created to investigate if the observed damage correlated with increasing CIT in donor pancreata. However, one TEM section just represents $<1 \text{ mm}^2$ of the whole organ and therefore is solely giving an indication of the organ status.

The protocol for imaging was therefore optimized to assess sections from two different areas of the pancreas. It was decided to assess 25 cells per section from five different areas (Figure 3.12). The first cells in each area were marked with low magnification to avoid bias and the four additional cells should all be in contact with each other. Excluded were cells which did not possess typical features of acinar cells including ductal cells or endothelial cells. Magnification for imaging should exceed 4,000x and if possible, images for mitochondria assessment should be taken with a magnification of 6,000x or higher.

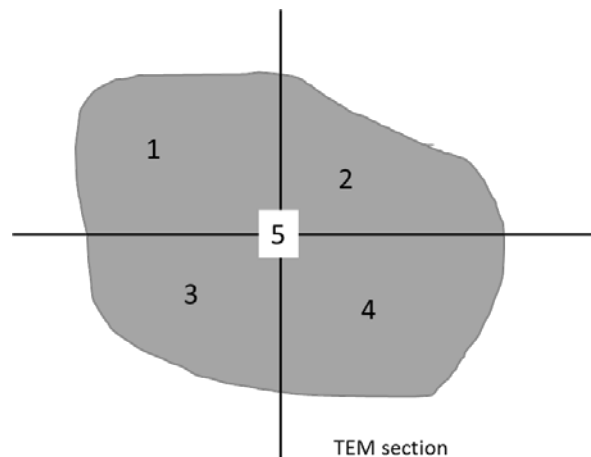


Figure 3.12: TEM section is divided into five areas to choose five cells in each area with low magnification to reduce bias.

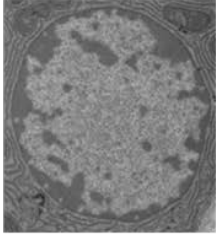
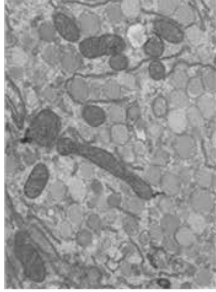
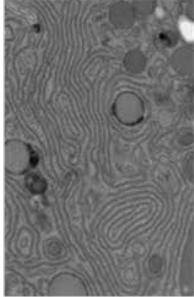
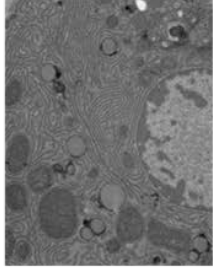
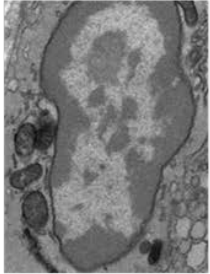
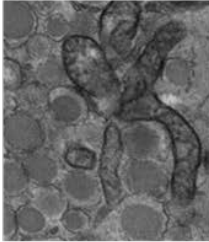
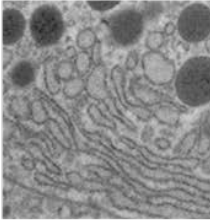
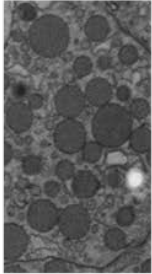
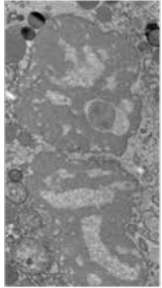
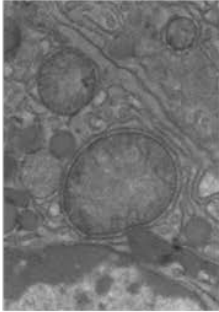
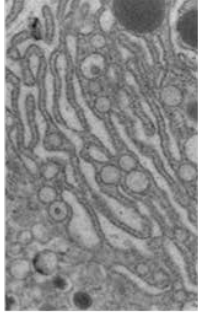
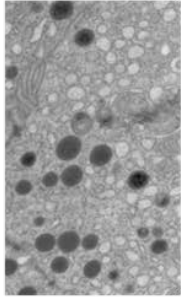
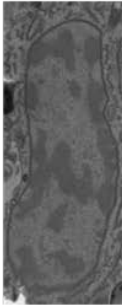
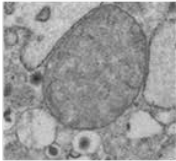
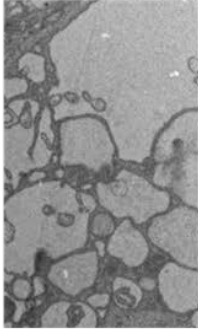
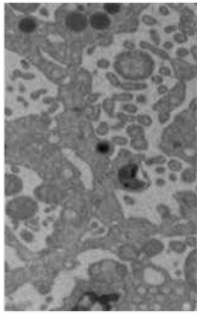
A 'degradation' score was developed combining the assessment of nuclei, mitochondria, ER and vacuolisation from scores 0 for normal appearance and increasing degradation with score 1 to 3 (Table 3.3 and Table 3.4) (Wahba et al., 2016). In more detail a nucleus

with normal appearance was scored as 0. Condensation of chromatin from a mild through to moderate state was scored as 1 and from a moderate to severe state was scored as 2. Severe condensation of chromatin as well as detachment of chromatin from the nuclear membrane was scored as 3. Normal appearing sausage shaped condense packed mitochondria were scored as 0 and if they had a less condense and more open appearance they were scored as 1. If they appeared swollen with a rounder shape and lighter electron dense areas in the core the score 2 was given. A score of 3 was chosen if mitochondria were swollen and cristae were disrupted or not visible anymore or if mitochondria were difficult to identify due to loss of characteristic shape and morphology. If ER in the whole cell appeared as electron dense lines representing normality a score of 0 was given. ER with mild dilation was scored as 1, with moderate dilation as 2 and with severe dilation as 3. For the category of vacuolisation, the morphology of the whole cell was assessed. If no vacuoles were observed a score of 0 was given. If vacuoles took up to 25% of the whole cell it was categorised as mild vacuolisation and scored as 1. Moderate vacuolisation was scored as 2 and indicated vacuoles in 25% till 50% of the cell. If vacuoles were taking up over 50% of the cell it was categorised as severe vacuolisation and a score of 3 was given.

Table 3.3: Newcastle Electron Microscopy Ischaemia Score (NEMIS) for assessment of pancreatic acinar cells

Degradation score	Nucleus	Mitochondria	ER	Vacuolisation
0	Normal appearance	Normal appearance	Normal appearance	Absent
1	Chromatin condensation (mild-moderate)	Open appearance	Mild dilation	Mild vacuolisation (0-25% of cell)
2	Chromatin condensation (moderate-severe)	Swollen appearance	Moderate dilation	Moderate vacuolisation (25-50% of cell)
3	Chromatin condensation and detachment from nuclear membrane	Swollen appearance and disrupted cristae	Severe dilation	Severe vacuolisation (>50% of cell)

Table 3.4: NEMIS from 0 till 3 for Nucleus, Mitochondria, ER and vacuolisation with example images.

Degradation score	Nucleus	Mitochondria	ER	Vacuolisation
0				
1				
2				
3				

3.3.2.4 Assessment of developmental cohort with NEMIS

Pre-existing images of the developmental cohort including five DBD and eight DCD donors were assessed with the degradation score. Analysis included tissue from male DBD donor with very short CIT labelled as DBD-0. Table 3.5 displays DBD donors with increasing CIT, followed by DCD donors with increasing CIT. It is important to note that initial sampling was done prior to establishment of QUOD protocols and before imaging was optimized. 3-24 cells were scored for each donor according to availability of images and displayed are the averages of all cells scored for the according category.

*Table 3.5: Degradation scores for developmental cohort.
With LDIS identification number, CIT [h], number of cells scored, average nucleus score, average mitochondria score, average ER score, average vacuolisation score and average total cell score of each donor.*

Donor number	LDIS number	CIT [h]	Cells scored	Nucleus score	Mitochondria score	ER score	Vacuolisation score	Total donor score
DBD-0	173	5.1	12	0.83	1.33	0.33	0.92	3.41
DBD-1	237	6.3	6	0.00	1.61	2.50	2.67	6.51
DBD-2	226	18.0	5	0.80	2.37	3.00	3.00	9.17
DBD-3	214	27.0	11	1.00	2.34	0.55	1.36	5.25
DBD-4	221	38.1	3	0.33	2.00	2.67	3.00	8.00
DCD-1	231	6.4	6	0.50	1.43	0.50	1.00	3.43
DCD-2	172	8.0	24	1.04	1.93	0.57	1.83	5.30
DCD-3	218	8.8	19	0.26	1.77	2.53	2.26	6.82
DCD-4	232	8.9	5	0.00	2.10	0.60	0.60	3.30
DCD-5	215	9.9	18	0.22	1.74	0.67	1.61	4.24
DCD-6	244	13.2	5	0.00	1.54	1.20	1.00	3.74
DCD-7	169	16.5	11	1.08	0.88	0.10	0.90	2.59
DCD-8	219	29.8	19	0.50	2.33	1.29	1.57	5.69

The quantified scores were correlated with the available donor data. Results for Spearman correlation of NEMIS with CIT are shown in Table 3.6. The scores for nuclei had the lowest correlation with the CIT of all donors as well as separated analysis for DBD and DCD. NEMIS for mitochondria significantly correlated with CIT of all donors, but did not show significance in separate analysis of DBD and DCD. NEMIS for ER, vacuolisation and the total score did not show a significant correlation and lower correlation coefficients after the analysis with CIT from DCD. The correlation graphs in Figure 3.13 show distribution of the single scores, indicating that some outliers may impact on the correlation.

Table 3.6: Two-tailed Spearman Correlation and significance of CIT and NEMIS scores for all donors as well as DBD and DCD separate.

Statistics were calculated with SPSS.

		Nucleus- score	Mitochondria- score	ER- score	Vacuolisation- score	Total- score
CIT_{ALL}	<i>Correlation Coefficient</i>	0.136	0.577*	0.357	0.226	0.324
	<i>Sig. (2-tailed)</i>	0.659	0.039	0.231	0.458	0.280
CIT_{DBD}	<i>Correlation Coefficient</i>	0.000	0.600	0.500	0.616	0.500
	<i>Sig. (2-tailed)</i>	1.000	0.285	0.391	0.269	0.391
CIT_{DCD}	<i>Correlation Coefficient</i>	-0.012	0.095	0.238	-0.275	-0.071
	<i>Sig. (2-tailed)</i>	0.977	0.823	0.570	0.509	0.867

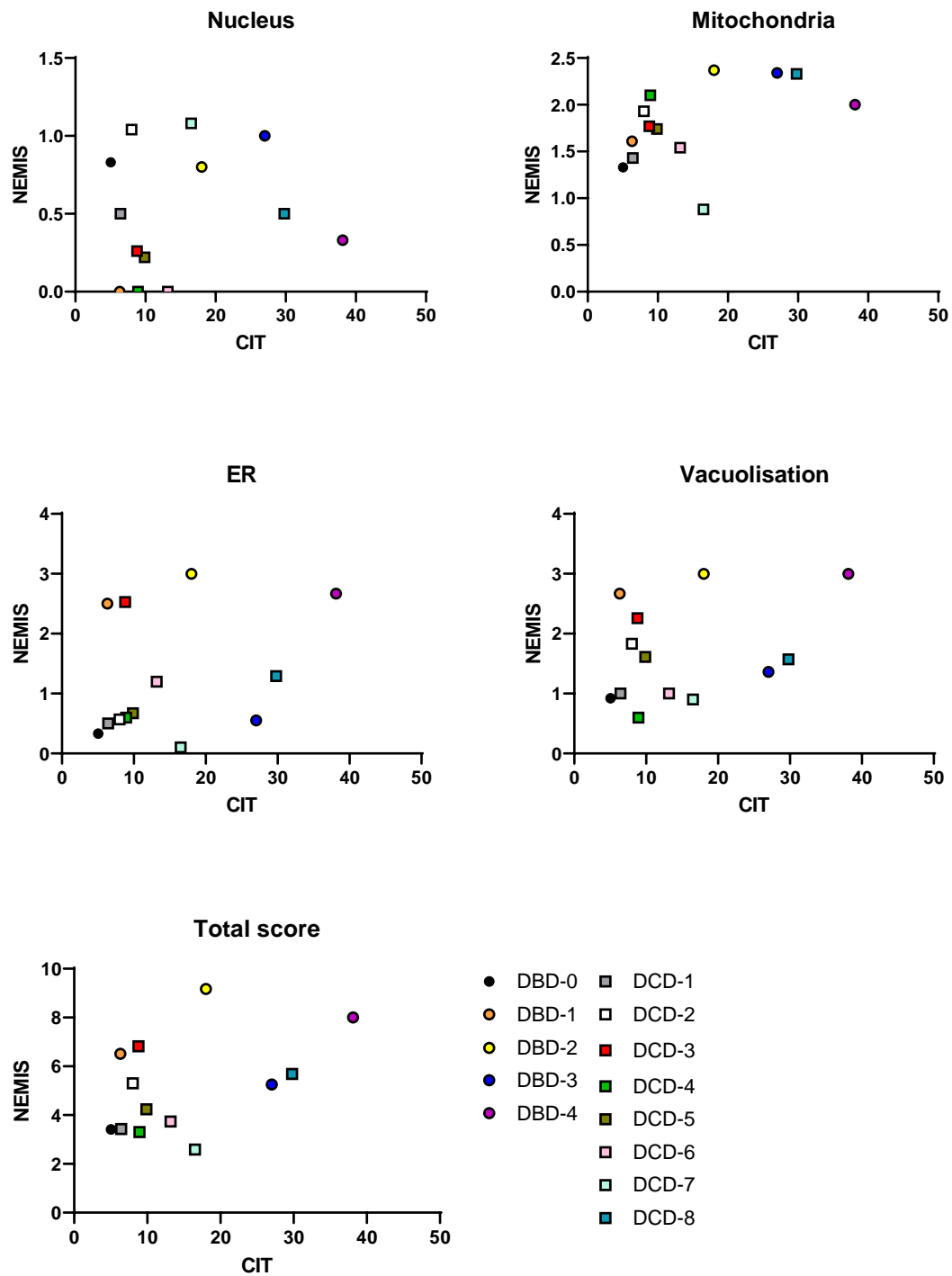


Figure 3.13: Correlation plots between CIT and NEMIS scores. For nuclei (A), mitochondria (B), ER (C), vacuolisation (D) and total scores (E). Values for pancreata from DBD donors displayed with circles and from DCD donors with squares.

No significant difference could be observed of the assessed NEMIS between the five DBD or eight DCD donors, although the average values for DCD organs seemed to be lower indicating less ischaemic damage (Figure 3.14) whereby the average CIT for DBD organs was 18.9 (± 14.0) h and for DCD organs was 12.7 (± 7.6) h.

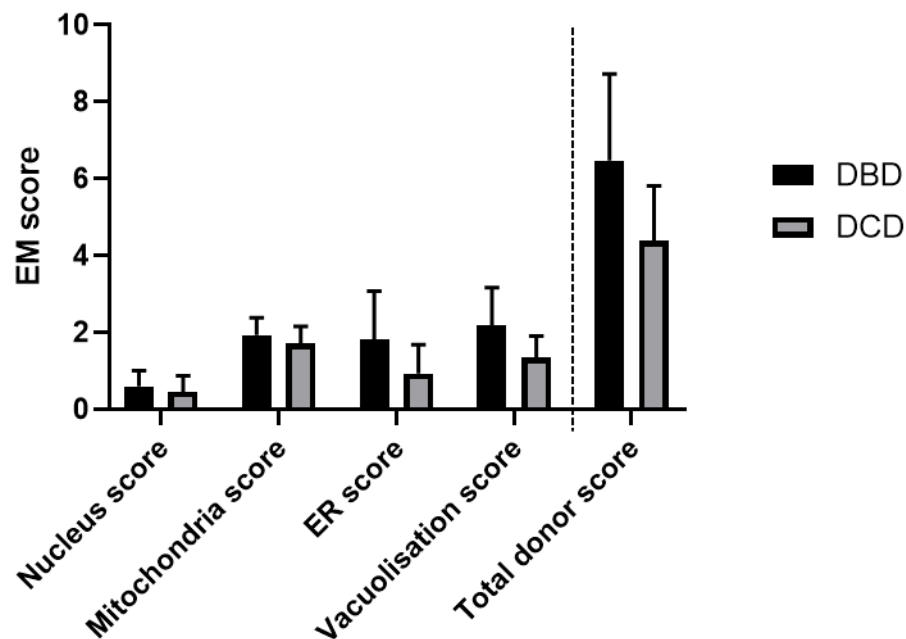


Figure 3.14: NEMIS analysis for five DBD and eight DCD donors. Average for donors displayed with standard deviation (SD).

Average scores for acinar and endocrine cells from six different donors showed differences in degradation (Figure 3.15). NEMIS for nuclei, mitochondria and ER were potentially higher in endocrine cells but with no significant difference. On the other hand, scores for vacuolisation were significantly lower in endocrine cells compared to acinar cells ($p < 0.001$).

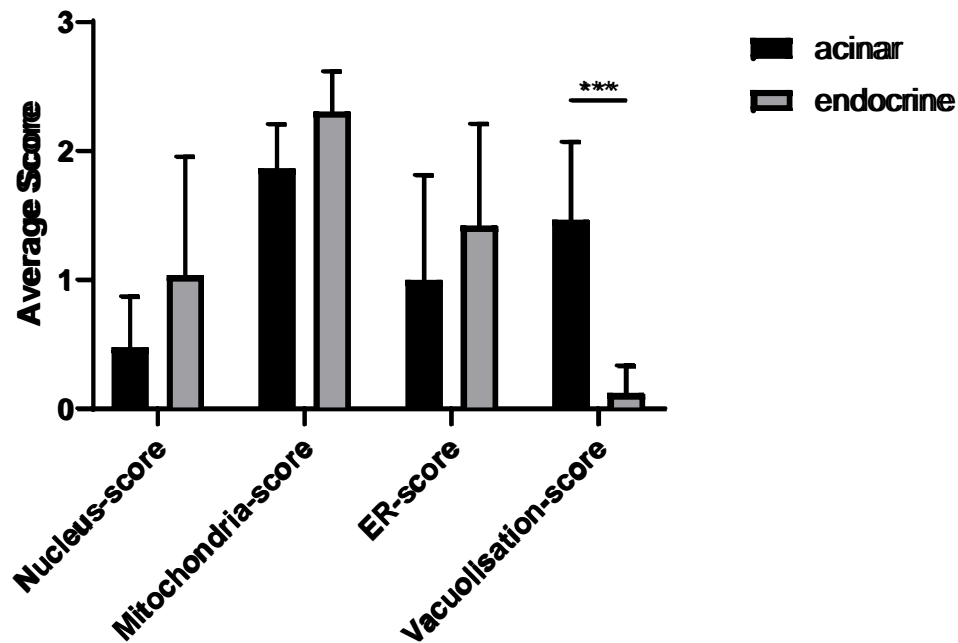


Figure 3.15: NEMIS analysis for acinar and endocrine cells from six different donors.

Average displayed with SD. Multiple Student's t-test revealed significant difference of acinar and endocrine score for vacuolisation ($p < 0.001$).

3.3.3 Impact of islet isolation on islet microenvironment, integrity and morphology

During the isolation process, islets can be separated from exocrine tissue through enzymatically and mechanic breaking of pancreas tissue impacting on islet viability, morphology and function. A variety of isolated islets from DBD and DCD donors were analysed with histology, immunofluorescence or TEM (Table 3.7 + Table 3.8).

Table 3.7: Isolated islet batches from DBD donors.

Islet number	LDIS number	Donor Type	CIT [h]	WIT [min]	Gender	Age [years]	BMI [kg/m ²]	Purity	Viability
1	229	DBD	2.8	-	female	51	16.5	30%	99%
2	237	DBD	6.3	-	male	69	29.1	79%	80%
3	247	DBD	7.7	-	female	48	32.5	60%	77%
4	236	DBD	11.3	-	female	53	37.0	42.5%	96.5%
5	196	DBD	12.5	-	male	51	24.4	76%	40%

Table 3.8: Isolated islets batches from DCD donors.

Islet number	LDIS number	Donor Type	CIT [h]	WIT [min]	Gender	Age [years]	BMI [kg/m ²]	Purity	Viability
1	225	DCD	6.9	20	male	39	24.8	45%	78%
2	194	DCD	7.0	105	male	59	26.8	90%	91%
3	215	DCD	9.9	25	male	28	24.0	50%	73%
4	245	DCD	12.3	n/s	female	65	28.8	30%	82%
5	244	DCD	13.2	12	female	49	26.6	50%	78%

3.3.3.1 Histological assessment of isolated islets

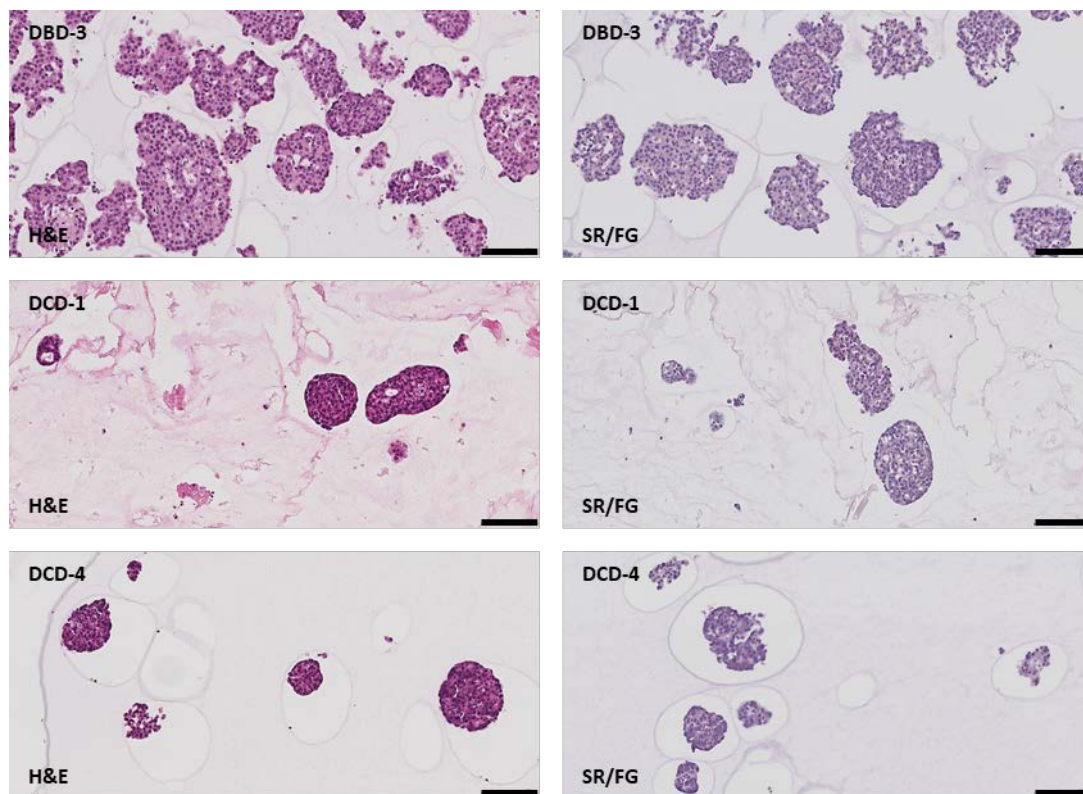


Figure 3.16: Histological assessment of isolated islets with H&E and SR/FG staining. Isolated islets from one DBD and two DCD donors (DBD-3, DCD-1 and DCD-4). Scale bars 100 μ m.

H&E staining of isolated islets (Figure 3.16 left column) highlighted the successful removal of exocrine tissue as well as impact of isolation on the integrity of islets. Some islets possessed a regular circular shape (DCD1 and DCD4) whereas others displayed a higher fragmentation with uneven shape (DBD-3). SRFG staining (Figure 3.16 right column) confirmed successful purification of endocrine tissue but also revealed absence of perivascular capsule in all islets assessed (DBD-3, DCD-1, DCD-4). In some islets a faint red collagen signal inside of islets was visible (DBD-3).

3.3.3.2 Immunofluorescence assessment of isolated human islets

IF staining showed localization of specific proteins in human isolated islets. Figure 3.17 showed an example for islets from donor DBD-3. After isolation islets still stained positive for insulin and glucagon (Figure 3.17 A2+A3), with a higher positivity of glucagon compared to islets assessed in tissue with short CIT (Figure 3.6 C4, D4, E4). Collagen IV and laminin staining confirmed loss of peri-islet capsule and showed presence of BM around vasculature inside islets (Figure 3.17 B2, C2, E2). Cell-to-cell contacts were present between all insulin positive cells (Figure 3.17 D2). No primary antibody controls confirmed specificity of antibody stains (Figure 3.19).

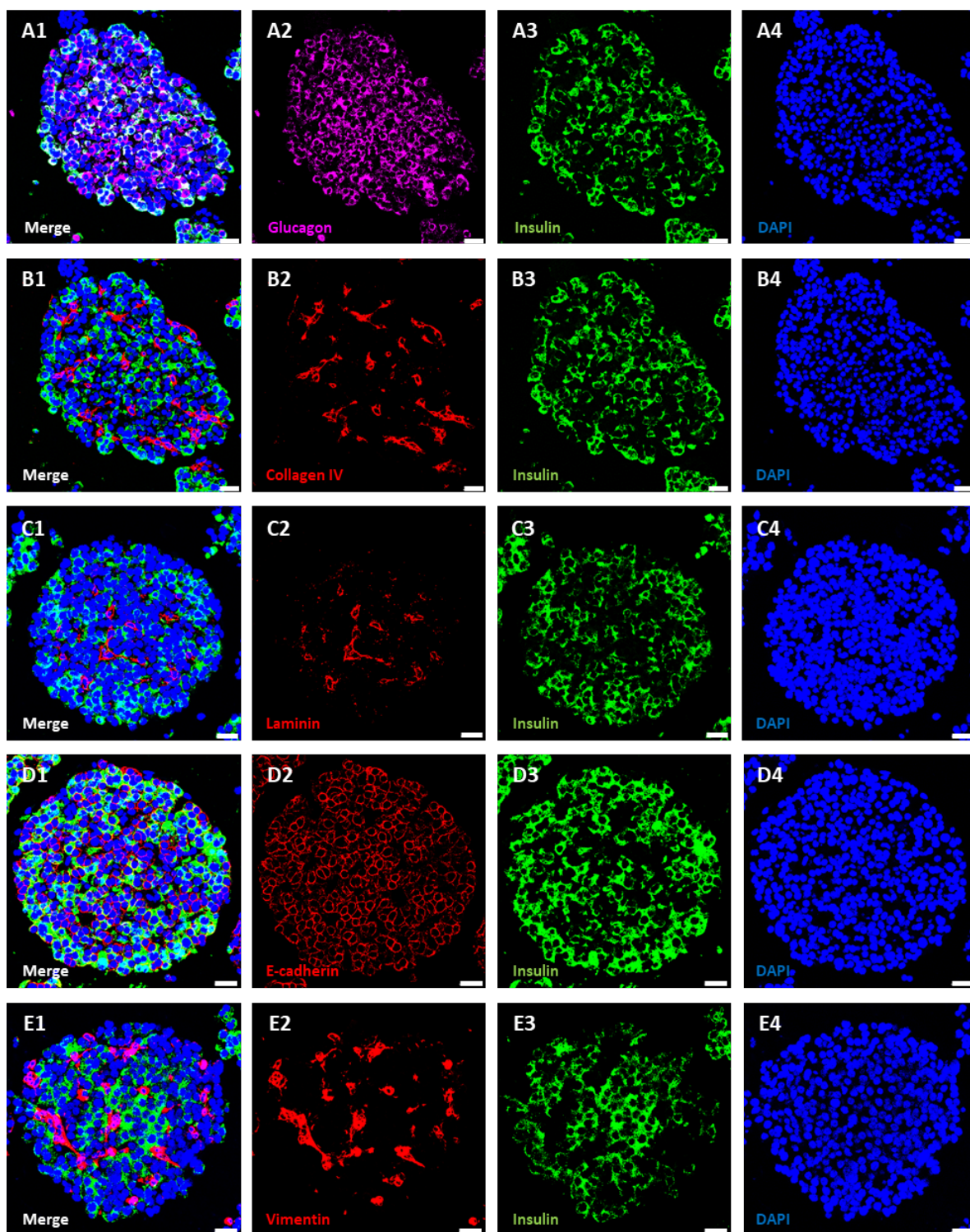


Figure 3.17: Immunofluorescence assessment of DBD-3.
For insulin (column 3), DAPI (column 4), glucagon (A2), collagen IV (B2), laminin (C2), E-cadherin (D2) and vimentin (E2).
Merge of all channels is shown in column 1. Scale bars 25 μ m.

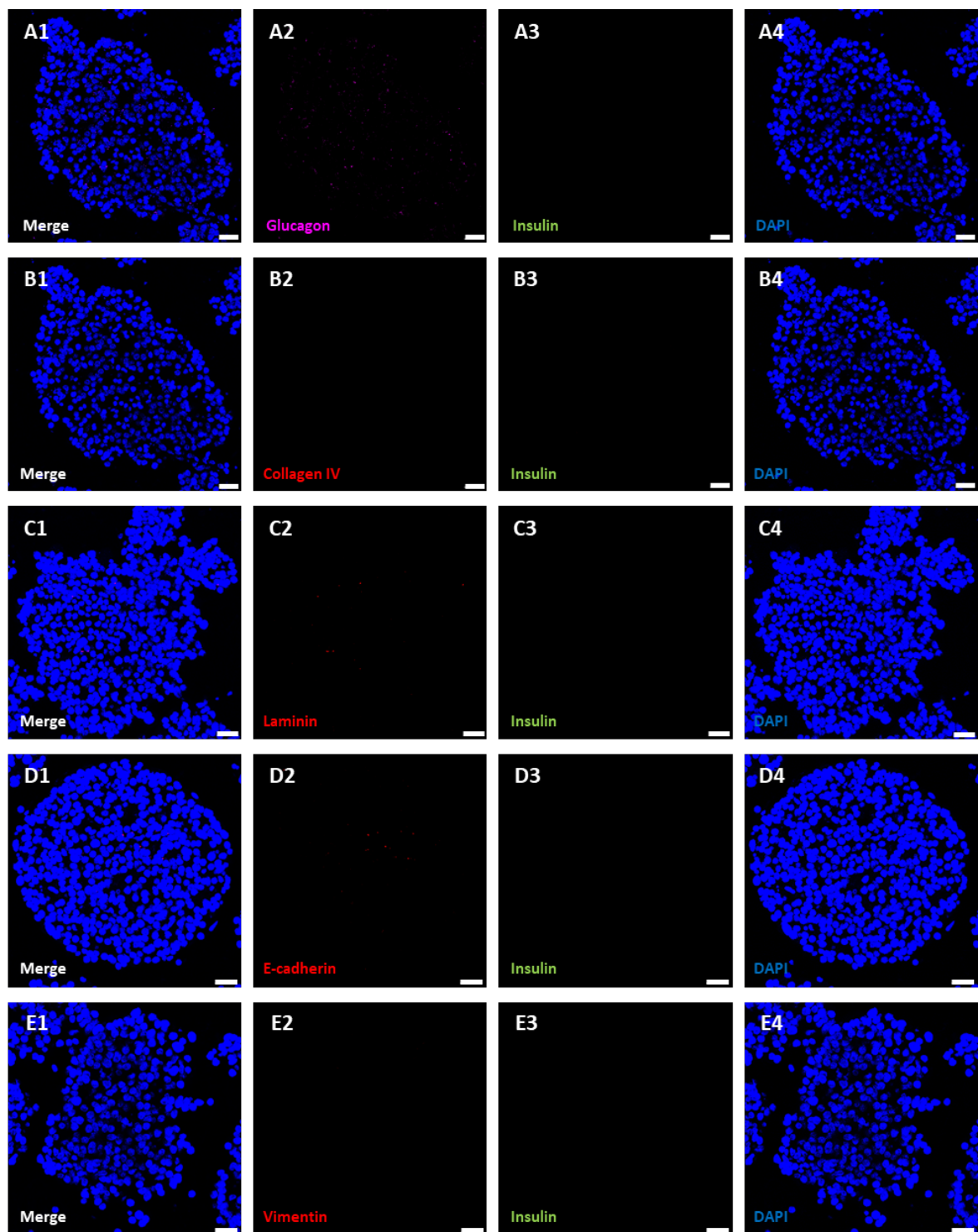


Figure 3.18: No primary antibody control for IF staining of DBD-3.
Scale bars 25 μm .

3.3.3.3 Ultrastructural assessment of isolated human islets

At an ultrastructural level, individual isolated islets from two different donors were assessed (Figure 3.19). Loss of integrity and increase in fragmentation were observed in whole islets (Figure 3.19 A+F) as well as apoptotic/necrotic cells in between normal looking islet cells (Figure 3.19 C). Images with the TEM confirmed loss of basement membrane shown with the lack of an electron light area followed by an electron dense line outside the cell membrane Figure 3.19 B,D,E,G,H). Additionally, damage to the islet cell membrane of endocrine cells at the exterior of the islet was characterised as discontinuity of the cell membrane (white arrows) (Figure 3.19 B+H). Furthermore, some islet cells possessed areas without vesicles indicated with black arrows (Figure 3.19 B,E,G). Nevertheless, nearly all observed islet cells still contained vesicles in the majority of the cell (Figure 3.19 D).

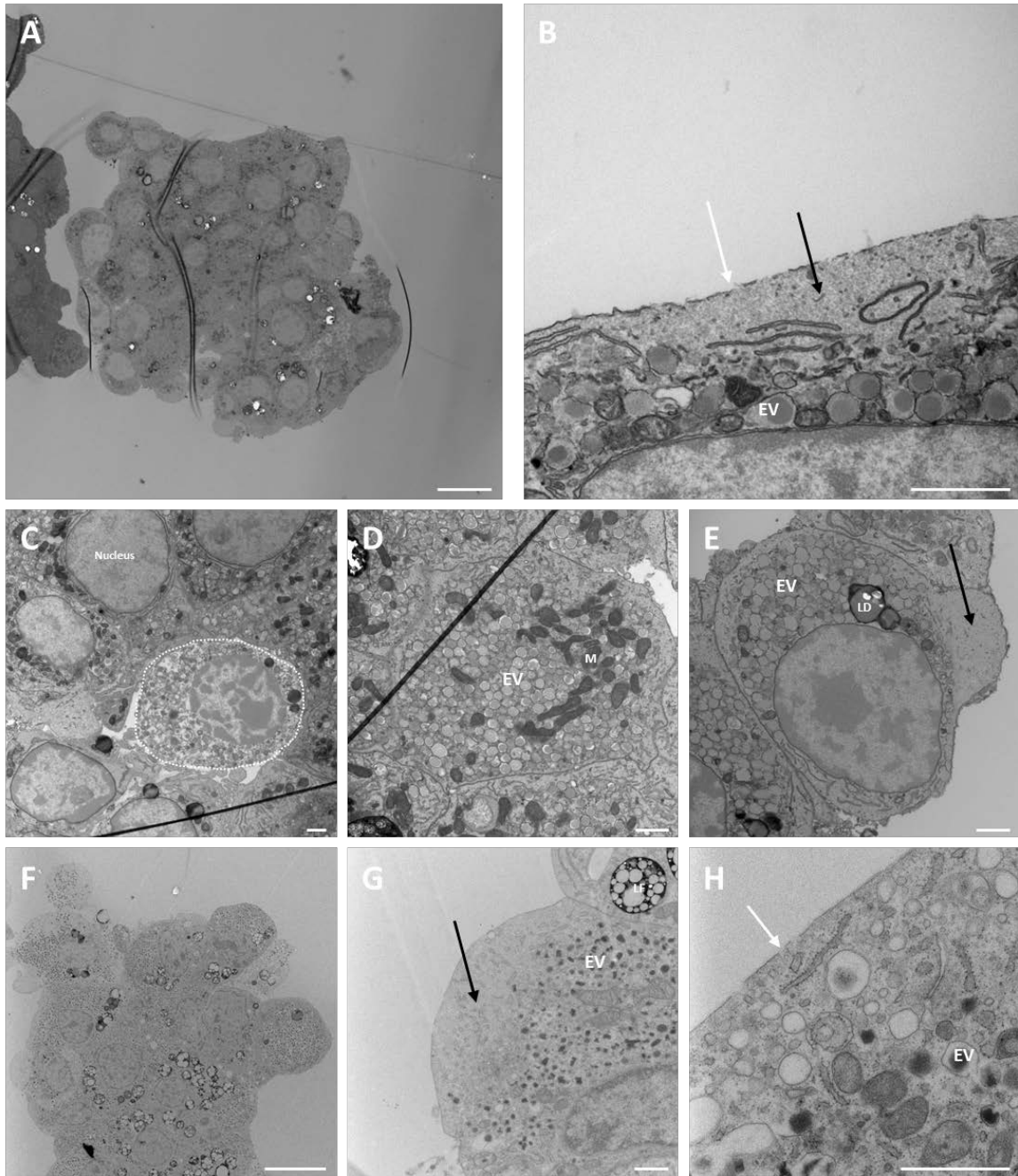


Figure 3.19: Ultrastructural assessment of human isolated islets.

(A) Whole isolated islet. (B) Islet cell identified through endocrine vesicles (EV) with discontinuous membrane (white arrow) and area without vesicles in proximity (black arrow). (C) Islet cells next to each other with necrotic cell in the middle (dashed line). (D) Islet cell containing mitochondria (M) and high number of endocrine vesicles (EV). (E) Islet cell containing lipid droplets (LD) and endocrine vesicles (EV) but area visible with no vesicles (black arrow). (F) Whole isolated islet. (G) Islet cell containing lipofuscin (LF) and endocrine vesicles (EV) but area without EV visible (black arrow). (H) Islet cell identified by EV showing disruptions in cell membrane (white arrow). Scale bars: A/F: 10 µm; B-E, G+H: 1 µm.

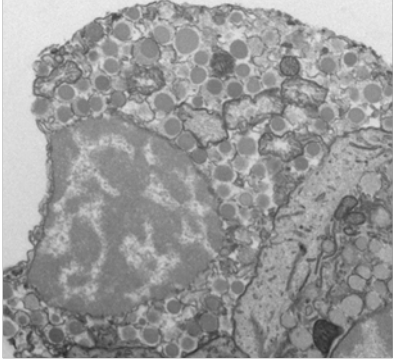
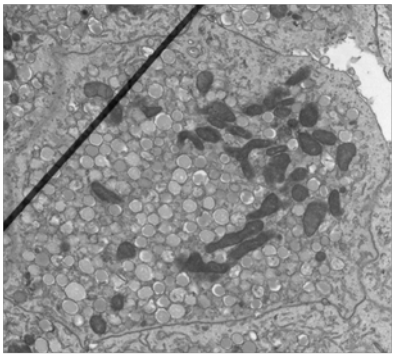
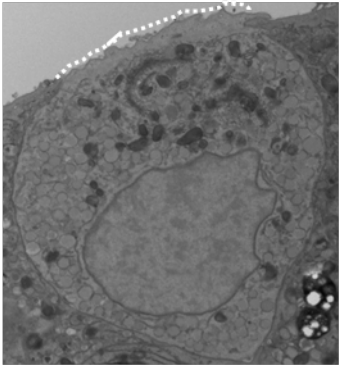
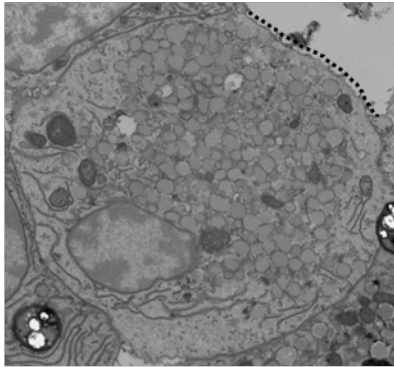
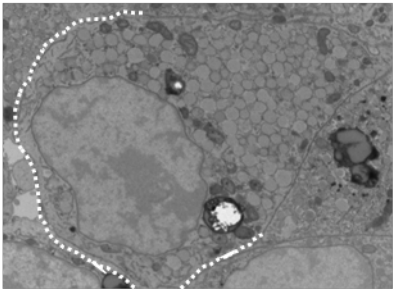
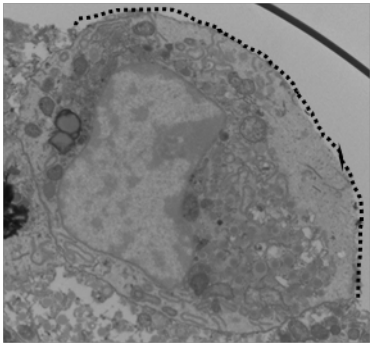
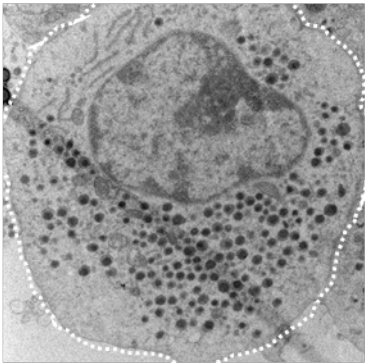
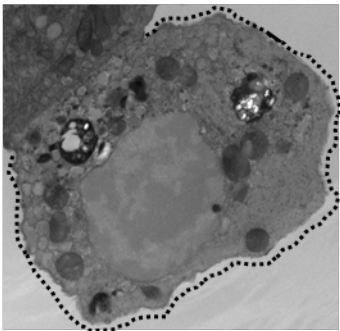
To investigate the impact of islet isolation at a cellular level, the NEMIS for assessment of acute changes in acinar tissue (see 3.3.2.3) was extended to include changes to presence of islet vesicles and damage to islet cell membrane (Table 3.9 + Table 3.10). Regarding endocrine vesicles, a score of 0 was given if vesicles were present throughout the whole of the cell cytoplasm. Areas without vesicles next to the islet cell membrane with at least a diameter of a typical endocrine vesicle were assumed as loss of vesicles. This loss next to 25% of the whole length of the islet cell membrane was scored with 1, loss of vesicles at 25%-50% of the whole length was scored with 2 and loss of vesicles at >50% of the whole length was scored with 3. An intact islet cell membrane was scored 0. Presence of <25% discontinuous cell membrane was scored with 1, 25%-50% was scored with 2 and >50% was scored with 3.

Table 3.9: Electron Microscopy Endocrine Damage Score for assessment of acute damage in endocrine cells. Assessment includes nuclei, mitochondria, ER, vacuolisation, vesicles and cell membrane. Scores value from 0 indicating normal appearance over 1 and 2 till 3 considering increasing damage.

Score	Nucleus	Mitochondria	ER	Vacuolisation	Vesicles	Cell membrane
0	Normal appearance	Normal appearance	Normal appearance	Absent	Present	Intact
1	Chromatin condensation (mild-moderate)	Open appearance	Mild dilation	Mild vacuolisation (0-25% of cell)	Mild vesicle loss (<25% of cell membrane)	<25% discontinuous cell membrane
2	Chromatin condensation (moderate-severe)	Swollen appearance	Moderate dilation	Moderate vacuolisation (25-50% of cell)	Moderate vesicle loss (25% -50% of cell membrane)	25% -50% discontinuous cell membrane
3	Chromatin condensation and detachment from nuclear membrane	Swollen appearance and disrupted cristae	Severe dilation	Severe vacuolisation (>50% of cell)	Severe vesicle loss (>50% of cell membrane)	>50% discontinuous cell membrane

Table 3.10: Additional categories to extend NEMIS to Electron Microscopy Endocrine Damage Score for assessment of isolated islets.

White dotted line indicates area next to islet cell membrane without vesicles. Black dotted line indicates length of disrupted islet cell membrane.

Score	Vesicles	Cell membrane
0		
1		
2		
3		

The developed additional scores were applied in combination with the NEMIS to existing TEM images of endocrine cells in six tissue samples and two batches of isolated islets (Table 3.11). Islets were fixed in the first 24 h after the isolation process and all available cells containing endocrine vesicles and displaying viable morphology including intact nuclear membrane were assessed. Although only two isolated islet preparations were studied, scores for nuclei, mitochondria, ER and vacuolisation appeared higher in endocrine cells in pancreatic tissue compared to endocrine cells in isolated islets. Especially the degradation in mitochondria seemed to be higher in endocrine cells *in situ* compared to isolated islets. Loss of endocrine vesicles as well as damage to islet cell membrane appeared to be higher in isolated islets.

Table 3.11: Scores for endocrine cells in tissue and isolated islets samples.

LDIS number	Type	CIT [h]	Nucleus-score	Mitochondria-score	ER-score	Vacuolisation-score	Vesicle-score	Membrane-score
173	tissue	5.05	0.47	2.02	0.52	0.05	0.80	0.00
172	tissue	8	2.50	2.22	1.00	0.00	0.86	0.00
218	tissue	8.78	0.17	2.33	1.71	0.13	2.30	0.10
232	tissue	8.93	1.75	2.85	2.70	0.00	1.45	0.00
215	tissue	9.87	1.00	2.00	0.86	0.00	1.35	0.00
219	tissue	29.8	0.33	2.42	1.73	0.55	2.11	0.08
215	isolated	9.87	0.20	1.05	0.68	0.08	2.48	1.00
244	isolated	13.17	0.22	1.16	1.00	0.40	2.90	1.00

Analysis of endocrine damage scores of endocrine cells in pancreas tissue with CIT revealed no significant Spearman's rho correlation in any case (Table 3.12). However, together with analysis of scatter plots (Figure 3.20, circles) a trend for a positive correlation of CIT with ER-, vesicle- and total score could be observed. No trend could have been observed for the nucleus score, whereas mitochondria scores seemed high and impact of CIT on cell membrane seemed low in all assessed pancreata. Vacuolisation of endocrine cells was challenging to assess due to the high amount of endocrine vesicles, which may explain some of the low numbers. Two preparations of isolated islets allowed

analysis of the ultrastructural level with the endocrine damage score (Figure 3.20, triangles). Impact of CIT on nuclei as well as mitochondria seemed lower compared to tissue scoring (although numbers are clearly too low for definitive conclusions), whereas no trend was observed for scoring of ER and vacuolisation. Impact on loss of endocrine vesicles as well as cell membranes was higher, which may be the results of the isolation process.

Table 3.12: Two-tailed Spearman's rho correlation of Endocrine damage scores and CIT for endocrine cells in tissue samples.

		Nucleus-score	Mitochondria-score	ER-score	Vacuolisation-score	Vesicle-score	Membrane-score	Total-score
CIT	<i>Correlation Coefficient</i>	-0.200	0.314	0.543	0.213	0.600	0.304	0.543
	<i>Sig. (2-tailed)</i>	0.704	0.544	0.266	0.686	0.208	0.558	0.266

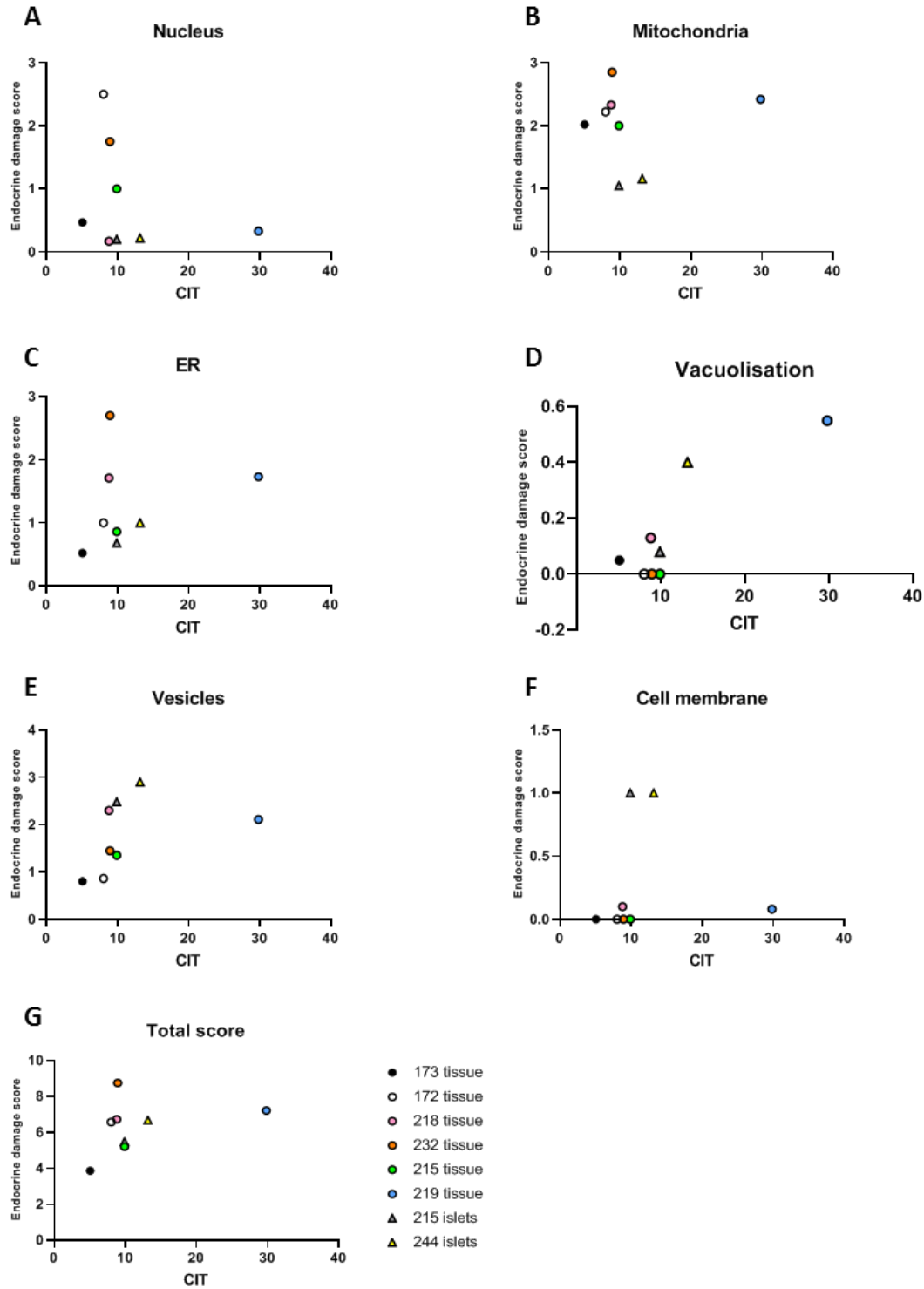


Figure 3.20: Correlation between CIT and endocrine damage scores. For nuclei (A), mitochondria (B), ER (C), vacuolisation (D), vesicles (E), cell membrane (F) and total score (G). Degradation was analysed for endocrine cells in tissue (circles) as well as in isolated islets (triangles).

3.4 Discussion

This chapter set out to answer how the microenvironment of islets changes through acute stress or the isolation process and how this impact can be quantified. It was hypothesised that these changes influence islet health and that a better quantification method will enable a better understanding of the organ status of the whole pancreas or isolated islets.

3.4.1 *Microenvironment in normal pancreas*

In a first step the analysis of islets and their specific microenvironment was undertaken to receive a status of normality through analysis of human tissue with short CIT of 5h.

Microenvironment was analysed with histology, immunofluorescence and at an ultrastructural level and presence of cell-to-cell connections, vasculature, collagen IV and laminin could be observed (Figure 3.2-Figure 3.6). This confirmed previous findings about islet architecture, microenvironment and vascularisation (Bosco et al., 2010, Cabrera et al., 2006, Cross et al., 2017). Staining for CGA, insulin and glucagon revealed islet size and distribution (Figure 3.2+Figure 3.6). Interestingly in the male DBD donor with short CIT, α -cells were predominantly present next to BM (Figure 3.6), mantling β -cells inside and increasing α - β -cell contact which may impact on islet physiology (Bosco et al., 2010). Contact to α -cells and proximity of glucagon signalling can improve insulin secretion significantly (Wojtusciszyn et al., 2008).

In addition to cell-to-cell contacts, cell-to-matrix contacts seem to be important for endocrine function with loss of matrix contact leading to anoikis (Irving-Rodgers et al., 2014). Staining for pan-cadherin and E-cadherin revealed presence of cell-to-cell connections throughout the islet microenvironment (Figure 3.3). Previous studies showed that the contact to ECM components impacts on β -cell function via integrin activation in mouse islets (Nikolova et al., 2006, Gan et al., 2018). With the observed cytoarchitecture it can be hypothesised that contact to ECM components and integrin signalling are important for normal α -cell function. In total the specific niche with proximity of α -cells as well as ECM components seems to be important for β -cell function (Bosco et al., 2010, Cabrera et al., 2006).

It must be taken into consideration that there are structural and cytoarchitectural differences in islets and their microenvironment in different species (Cabrera et al., 2006,

van Deijnen et al., 1992, Kim et al., 2009). Additionally, in human pancreata, variability has been reported in the islet size, cytoarchitecture and cell composition in each organ (Bonner-Weir et al., 2015, Kim et al., 2009). However, it was concluded that all islets exhibit a similar pattern of subunits with mantle-core distribution of endocrine cells, also seen in Figure 3.6 (Bonner-Weir et al., 2015).

These differences between different human pancreata could manifest through different physiology or development of diseases. Age is one of these factors impacting on islet isolation outcomes, with the proposal that differences in ECM may influence islet size and composition (Spiers et al., 2018). Islets showed a changed composition through disease-associated stress with decrease in β -cells proportions through Type 2 diabetes or cystic fibrosis (Bogdani et al., 2017, Deng et al., 2004).

The ultrastructural analysis with TEM provided a more detailed insight into islet microenvironment. Analysis of mouse tissue with short CIT and human tissue with short CIT showed no differences in appearance of acinar or endocrine cells (Figure 3.7-Figure 3.9). This confirms that the human tissue sample was adequate to investigate pancreas tissue near normality with a low CIT of 5 h.

3.4.2 Impact of CIT

Changes to pancreas morphology and structure can impact on function and therefore transplant outcomes. Analysis of different pancreata with a range of CIT was performed to quantify impact of acute cellular stress towards acinar and islet cells through TEM analysis.

Changes to pancreatic morphology and structure can be related to different donor factors such as donor age, BMI or preservation time (Spiers et al., 2018). Studies in different centres showed impact of donor BMI, donor age, donor type and CIT on long-term outcomes of pancreas transplantation (Gruessner and Gruessner, 2016, Humar et al., 2004, Rudolph et al., 2017). Organ availability remains a crucial part of pancreas transplantation especially in regards to decrease of ideal donors with young age and short CIT (Gruessner and Gruessner, 2016). The NHSBT reported 218 patients on the transplant list for pancreas transplantation in 2018 with 189 pancreata transplanted (NHSBT, 2018a). Eurotransplant reported 276 patients on the waiting list and 207 transplanted pancreata

in 2018 (Eurotransplant International Foundation, 2018). Although transplant rates range over 50%, this still leaves 13.3% and 25% on the waiting list, increasing diabetes related complications and potentially mortality. Utilisation of 'marginal' donors may provide the needed pancreata to increase transplantation rates, especially keeping in mind increasing number of diabetic patients. A single centre study showed that transplantation of extended criteria donors is possible, but a slightly higher risk with pancreata from donors of age over 45 years and weight over ~90 kg (Krieger et al., 2003). However, it is not fully understood why specific donor factors impact on outcomes of transplantation.

Therefore, a better understanding of organ status is important, especially regarding impact of CIT on organs and specifically the pancreas. Impact of acute stress could not be detected by histological assessment, but visible changes at an ultrastructural level with TEM analysis could be seen (Figure 3.10+Figure 3.11). Changes to cell organelles and cell morphology was observed in previous studies investigating hypoxia or induced apoptosis. Most observed was clumping of chromatin seen in nuclei of rat cardiomyocytes, human placenta, murine macrophage-like cell line, human pancreatic cancer cells, rat pancreas and human isolated islets (Dai et al., 2012, Hung et al., 2002, Kang et al., 2000, Liu et al., 2016, Marselli et al., 2004, Nevalainen and Anttinen, 1977, Wilhelmi et al., 2013, Zhang et al., 2018). The second most observed changes through acute stress was development of vacuoles in human placenta, human pancreatic cancer cells and rat pancreas (Dai et al., 2012, Hung et al., 2002, Nevalainen and Anttinen, 1977). Additionally, changes to mitochondria morphology and dilation of ER were visible in rat endocrine cells, human pancreatic cancer cells or rat pancreas (Dai et al., 2012, Nevalainen and Anttinen, 1977, Zhang et al., 2018). These changes were also visible in investigated TEM sections leading to development of the NEMIS (Table 3.3+Table 3.4).

Scores for mitochondria, ER and vacuolisation seem higher compared to the nucleus score (Table 3.5) indicating that chromatin clumping may be a better indication for apoptotic cells than stress induced damage through hypoxia (Kang et al., 2000). No significant correlation with the scores and CIT time of the donors could be observed (Table 3.6). However, mitochondria, ER and vacuolisation show a trend to increase with increasing CIT, leading to the assumption that these features are impacted by hypoxia. According to the presented data, mitochondria show the biggest trend with higher mitochondrial damage

with increasing CIT (Figure 3.13); perhaps related to build up of succinate associated with prolonged ischaemia and ischaemia reperfusion injury (Chouchani et al., 2014). This may indicate that mitochondria are very sensitive cell organelles towards hypoxia showing changes even with short CIT (Nevalainen and Anttinen, 1977). Furthermore, scores for DBD donors were higher with no significant difference compared to the scores of DCD donors (Figure 3.14). This may be due to a slightly higher average in CIT in the used DBD donors (18.9 h) versus DCD (12.7 h) which may confirm the trends of higher damage scores with increasing CIT.

Another possibility may be impact of inflammatory reaction induced through brain death where cytokines get released similar to observations during sepsis (Schwarz et al., 2018). It was shown previously that pancreas samples of brain dead donors had increased concentrations of tumour necrosis factor which may impact status of donor pancreata in the days following brain death, but before organ procurement (Rech et al., 2014). The NEMIS may provide a tool to better understand the factors critical to pancreas wellbeing in the peri-transplant period and may lead to development of target therapeutic interventions or further refine transplant acceptance criteria without exposing patients to unnecessary risk.

Additionally, presence of endocrine cells in some of the assessed donors enabled comparison of acinar and endocrine cells with NEMIS revealing different impact of CIT on these cells. Scores for nuclei, mitochondria and ER appeared to be possibly higher in islet cells, whereas scores for vacuolisation were significantly lower. Islet cells seem to have a very high oxygen demand with a high vascularisation and receipt of 15% and 20% of the pancreatic blood flow (Bonner-Weir and Orci, 1982, Holt et al., 2010, Lifson et al., 1989). Through the insufficient oxygen supply during organ preservation impact on endocrine cells may be higher compared to acinar cells (Olsson and Carlsson, 2011). Significantly lower vacuolisation score in islet cells may be due to the fact that endocrine cells usually possess a high amount of vesicles making it harder to assess the status of the cytoplasm.

The NEMIS in this thesis showed that CIT can impact on some cell organelles, but no significant correlation was observed. Throughout the development of NEMIS the imaging process was optimised to guarantee unbiased, high quality and standardised scoring. In addition to that biopsy sampling follows standardized procedures through QUOD

protocols, minimizing differences of tissue handling. Images of additional donors with the standardized sampling and imaging are being analysed for future investigation of impact of CIT on tissue quality. Hereby the EM analysis can provide a helpful tool for a better understanding of acute stress towards organs during the retrieval and transportation period with the limitation that it will not be suitable for pre-transplant assessment.

3.4.3 Impact of isolation

Islet isolation adds further stress onto the endocrine cells, especially through their loss of the BM and the connection to the vasculature (Cross et al., 2017, Irving-Rodgers et al., 2014, Giuliani et al., 2005). The impact of the isolation process onto islets was analysed via histopathological staining, IF staining as well as TEM analysis. It could be demonstrated that islet isolation successfully removes acinar tissue and leaves a majority of islets for transplantation (Figure 3.16). IF staining after isolation showed remaining endocrine cells positive for insulin and glucagon (Figure 3.17 A1-A4). No particular pattern according to their cytoarchitecture was observed and in some islets the signal for glucagon seemed higher compared to staining in tissue. It was shown that culture of isolated islets influences the organization of endocrine cells (Bosco et al., 2010). This study revealed that the peri-islet capsule is lost through isolation, but that the peri-vascular BM is present inside of some islets shown with presence of collagen IV and laminin inside of islets (Figure 3.17 B1-C4) in keeping with previous findings (Wang et al., 1999, Irving-Rodgers et al., 2014, Cross et al., 2017). Cell-to-cell connections were present in the whole islet (Figure 3.17 D1-D4) indicating cohesion of the endocrine cell cluster. Vimentin was used to indicate vascular distribution inside of islets because CD31 displayed weak staining increasing the difficulty to assess. This may be due to lower expression of CD31 due to fenestration of capillaries inside of islets (Bonner-Weir et al., 2015). Vascular distribution was still present in some islets after the isolation process (Figure 3.17 E1-E4) which could contribute to revascularisation after transplantation (Nykqvist et al., 2011).

At an ultrastructural level further impact of the isolation process on endocrine cells was revealed. Loss of endocrine vesicles and damage to the cell membrane of islet cells at the border of the islet was observed (Figure 3.19 A-H). Loss of membrane integrity as well as loss of insulin through the isolation process was observed previously (do Amaral et al., 2013, Brandhorst et al., 1998). These observations at TEM level were added as additional

categories to the NEMIS (Table 3.10). Two preparations of isolated islets could be compared to endocrine cell assessment in pancreatic tissue of six different donors (Table 3.11). A Spearman's rho correlation revealed a trend of impact of the isolation process on endocrine vesicle loss and membrane damage (Table 3.12). Interestingly mitochondria seemed less damaged in isolated islets, which could be due to the small sample size and further islet preparations may clarify. In the endocrine cells the correlation from the vacuolisation score with CIT was observed as relatively low compared to vacuolisation observed in acinar tissue. This again could be due to the fact that the cytoplasm is harder to assess because of the high amount of endocrine vesicles. Another possibility may be that endocrine cells are less susceptible towards vacuolisation. Assessment of increasing number of donors with the improved imaging protocol will clarify the observed results.

In summary, the microenvironment of islets is impacted through various factors. NEMIS provides a potential tool for a better understanding of the impact of organ preservation and limited oxygen supply on pancreata especially endocrine cells, but it will be unpractical for pre-transplantation analysis. Further impact on islets was observed through the isolation procedure, where islets lose their specific niche. Overall remaining challenges were the low number of investigated tissues in addition the lack of a thorough understanding of the impact of stress at a molecular level of the cells, leaving room for further investigations. In the following part of this project the focus lies on the replacement of ECM after isolation to improve islet health and function towards improved transplant outcomes.

Chapter 4. Providing extracellular matrix replacement to islets through a collagen/alginate/fibrinogen hydrogel

4.1 Introduction

During the isolation process, islets may lose their specific microenvironment (Cross et al., 2017, Irving-Rodgers et al., 2014). Replacement of this niche and especially the ECM is hypothesised to improve islet health prior to transplantation (Daoud et al., 2011). Various projects have set out to investigate possibilities for ECM replacement and improvement of islets during preservation and transplantation (Daoud et al., 2011, Marchioli et al., 2015, Najjar et al., 2015). Various techniques have been used to assess islet mass, viability and function. Function is most usually assessed by glucose induced insulin secretion, but Seahorse flux analysis is gaining increasing popularity due to insight into mechanistic understanding of underlying metabolic pathways (Daoud et al., 2011, Marchioli et al., 2015, Skrzypek et al., 2017, Wikstrom et al., 2012). During a Seahorse experiment, OCR and ECAR are measured and specific drugs are injected which affect different parts of the electron transport chain and therefore influence OCR and ECAR (Mookerjee et al., 2015, Wikstrom et al., 2012). With this information, cellular ATP production can be calculated indicating metabolic function which is tightly linked with insulin release (Wiederkehr and Wollheim, 2006, Mookerjee et al., 2017, Mookerjee et al., 2015). OCR measurements have been investigated as an indicator of islet quality and transplantation outcomes in rodent models and more recently and in auto- and allo-transplantation (Papas et al., 2007, Sweet et al., 2008, Papas et al., 2015, Kitzmann et al., 2014). Additionally, mitochondria play a vital role in the insulin secretion pathway via a complex network of metabolic reactions demonstrating the function of β -cells (Mookerjee et al., 2017). In short (Figure 4.1): Glucose is transported into β -cells where it is passed through glycolysis, producing ATP and converted to pyruvate (Kaufman et al., 2015). Pyruvate can either be reduced to lactate or oxidized by mitochondria (Mookerjee et al., 2017). If pyruvate is reduced to lactate, protons are produced influencing the extracellular acidification (Mookerjee et al., 2015). However, low levels of lactate dehydrogenase in β -cells increase pyruvate utilisation in mitochondria (Kaufman et al., 2015). If pyruvate is oxidized, it is transported into mitochondria where it enters the Krebs cycle to be completely oxidized into CO_2 and H_2O ; loading electron carriers needed for the electron transport chain (Mookerjee et al.,

2017). The electron transport chain is composed of mitochondrial complexes I-IV, which are pumping protons over the mitochondrial membrane to create a gradient for ATP synthase, which converts ADP into ATP (Wiederkehr and Wollheim, 2006).

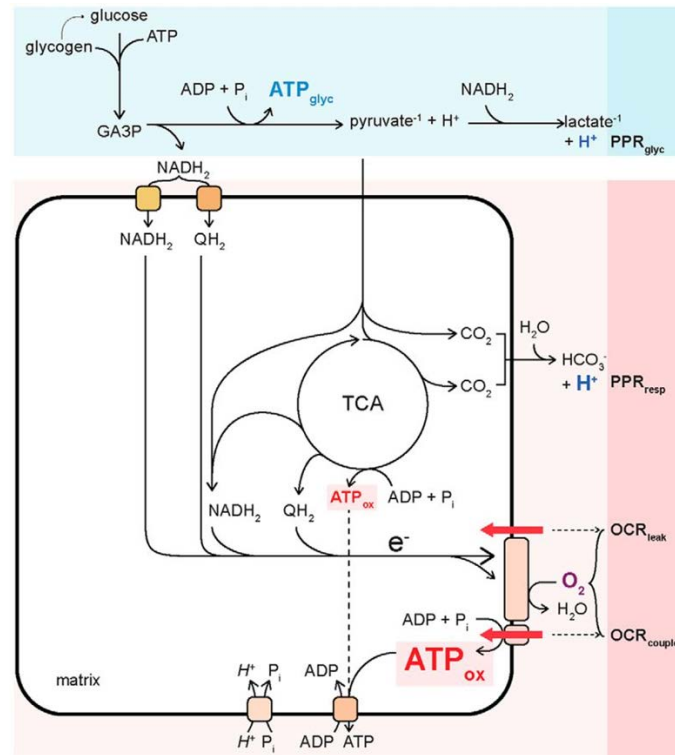


Figure 4.1: Glucose metabolism with glycolysis and oxidative phosphorylation. Picture adapted from (Mookerjee et al., 2017).

The molecules used during the Seahorse experiment impact on function of these complexes (Figure 4.2), and allow calculation of ATP production (Mookerjee et al., 2017, Mookerjee et al., 2015). Oligomycin inhibits mitochondrial ATP synthase leading to a decrease in OCR due to inhibition of oxidative phosphorylation and increase of ECAR because of an increased requirement of glycolytic ATP (Mookerjee et al., 2017, Rose et al., 2014). FCCP acts as uncoupling agent causing the inner membrane to become permeable to protons leading to increase in electron transport chain (ETC) and therefore maximal OCR (Mookerjee et al., 2015, Mookerjee et al., 2017). Antimycin A blocks complex III in the ETC and therefore fully inhibits mitochondrial respiration, leaving non-mitochondrial OCR (Rose et al., 2014). This method delivers a fast investigation of β -cell function and may predict outcomes of islet transplantation, but also help analyse strategies for improvement of viability, mass and function of β -cells.

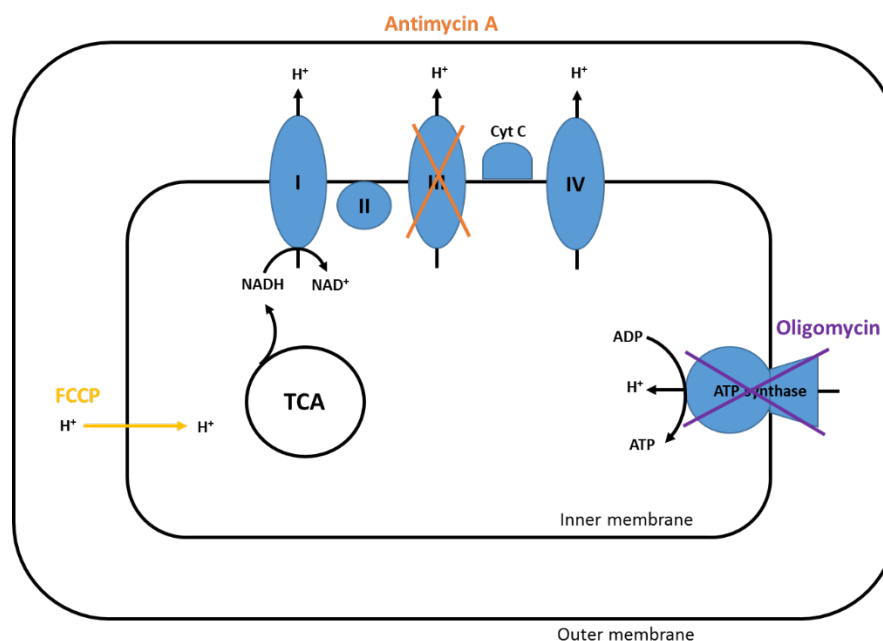


Figure 4.2: Mitochondrial electron transport chain with complex I, II, III, IV, and ATP synthase and impact of oligomycin, FCCP and antimycin A. Oligomycin inhibits ATP synthase, FCCP uncouples H⁺ transport from ATP synthase, antimycin A inhibits complex III and therefore non-mitochondrial OCR.

In this chapter, improvement of isolated islets via ECM replacement is investigated with utilization of a novel hydrogel composing of collagen I, alginate and fibrinogen (CAF) (Montalbano et al., 2018). Each of these components have been used as replacement for ECM for islets before. As first CAF component with collagen, a structural protein forming fibrillose structures, was chosen because it is the most abundant protein in pancreata (Sackett et al., 2018). Additionally, collagen provides RGD sequences required for triggering integrin mediated cell pathways involved into cell proliferation, viability and function (Kaido et al., 2006). Collagen I as ECM replacement of islets was shown to improve islet viability, adhesion, insulin expression, and insulin release (Daoud et al., 2010a, Daoud et al., 2011, Stephens et al., 2018). Secondly, alginate, a structural polysaccharide, was chosen due to its nontoxic properties and low immunogenic profile after purification (Lim and Sun, 1980, Mallett and Korbitt, 2008). Furthermore, alginate hydrogels are able to absorb a large amounts of fluid, improving nutrient supply of encapsulated cells (Montalbano et al., 2018). It has been shown that alginate encapsulated islets remain viable and maintain their function over culture *in vitro* or *in vivo* (Lim and Sun, 1980, Mallett and Korbitt, 2008, Dufrane et al., 2006). The last

component chosen for the CAF was fibrinogen, which is a glycoprotein important during blood coagulation where it gets converted to fibrin by thrombin (Chernysh et al., 2012). Fibrin gels possess viscoelastic properties, can stimulate wound healing responses and are used widely in clinical application as glue making it an ideal candidate for a transplantable hydrogel (Janmey Paul et al., 2009). Combinations of fibrin gels and islets showed improved revascularisation and long-term function as well as protection against apoptotic stimuli (Najjar et al., 2015, Kuehn et al., 2013).

Combination of stated ECM components may unite several advantages of single components which is why a combination of collagen I, alginate and fibrinogen was investigated. Encapsulation of islets in a collagen-alginate gels showed improved viability over culture, reduced hypoxia, improved function and protection from immune attack (Lee et al., 2012). Combination of fibrinogen with alginate or collagen has been investigated for cartilage and bone tissue engineering, but not previously for islets (Ma et al., 2012, Linsley et al., 2016, Montalbano et al., 2018). Furthermore, the combination of all three components showed biocompatibility, proliferation and metabolic activity of MIN6 cells, but was not analysed with pseudoislets or human isolated islets (Montalbano et al., 2018).

4.2 Aims

Loss of the specific islet niche through the isolation process is associated with decreased islet viability, mass and function impacting on transplant outcomes. Various strategies for ECM replacement therapy have shown some improvements but demonstrated limited success. A combination of three hydrogel components and its impact on a pseudoislet model as well as human isolated islets was investigated during this project with the following aim and specific objectives:

Overall aim: To assess ECM replacement through a novel (CAF) hydrogel and characterise impact of hydrogel on pseudoislets and human isolated islets.

Objective 1: To establish a reproducible model for human islets from the MIN6 β -cell line and characterise integrity and function.

Objective 2: To assess biocompatibility of CAF hydrogel with pseudoislet model through assessment of viability, morphology and function.

Objective 3: To assess biocompatibility of CAF hydrogel with human isolated islets through assessment of viability, morphology and function.

4.3 Results

4.3.1 Establishment of a MIN6 pseudoislet model and characterization of integrity and function

4.3.1.1 Viability of pseudoislet model Day 5 and Day 6 after generation

Viability of pseudoislets was assessed on Day 5 and Day 6 after generation. A range of different sized cell clusters had formed and examples for a smaller and a larger pseudoislet on Day 5 are shown in Figure 4.3 A+C. PI staining for smaller pseudoislets usually showed a few single dead cells (Figure 4.3 B) whereas core necrosis was observed in larger islets (Figure 4.3 D). The average viability of pseudoislets on Day 5 was $75\pm 11\%$ (n=4) with a decline to $64\pm 3\%$ (n=3) on Day 6. On Day 5 >90% of pseudoislets displayed a diameter between 50-100 μm . Pseudoislets assessed were generated from MIN6 at passages p23, p24, p25, and p27.

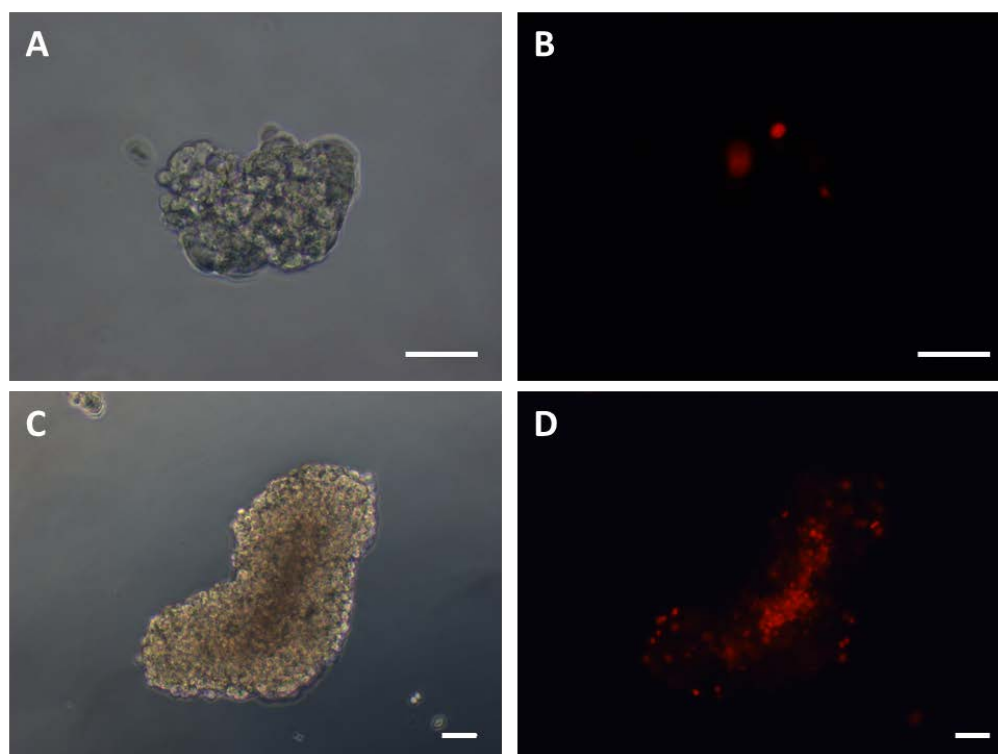


Figure 4.3: Examples for viability assessment of pseudoislets (p27) on Day 5 after generation. Bright field (A+C) and PI staining (B+D) of a smaller (A+B) and a larger (C+D) islet. Scale bar 50 μm .

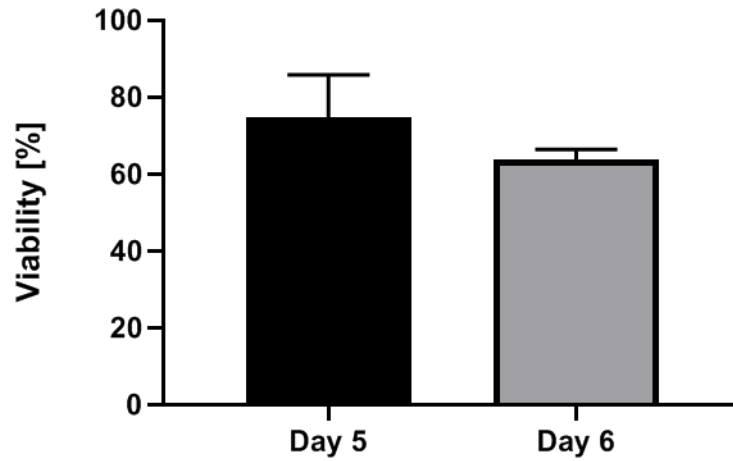


Figure 4.4: Viability of MIN6 pseudoislets (p23-p27) on Day 5 and Day 6 after generation. Average of $n=4$ (Day 5) and $n=3$ (Day 6) repeated studies displayed with SD.

4.3.1.2 Immunofluorescence staining of MIN6 pseudoislets

A pseudoislet model was generated by culture of MIN6 cells in non-adherent dishes for five days. IF staining (Figure 4.5) revealed presence of insulin (A2) in majority of cells in addition to strong cell-to-cell connections via E-cadherin especially in the middle of the pseudoislet (A3).

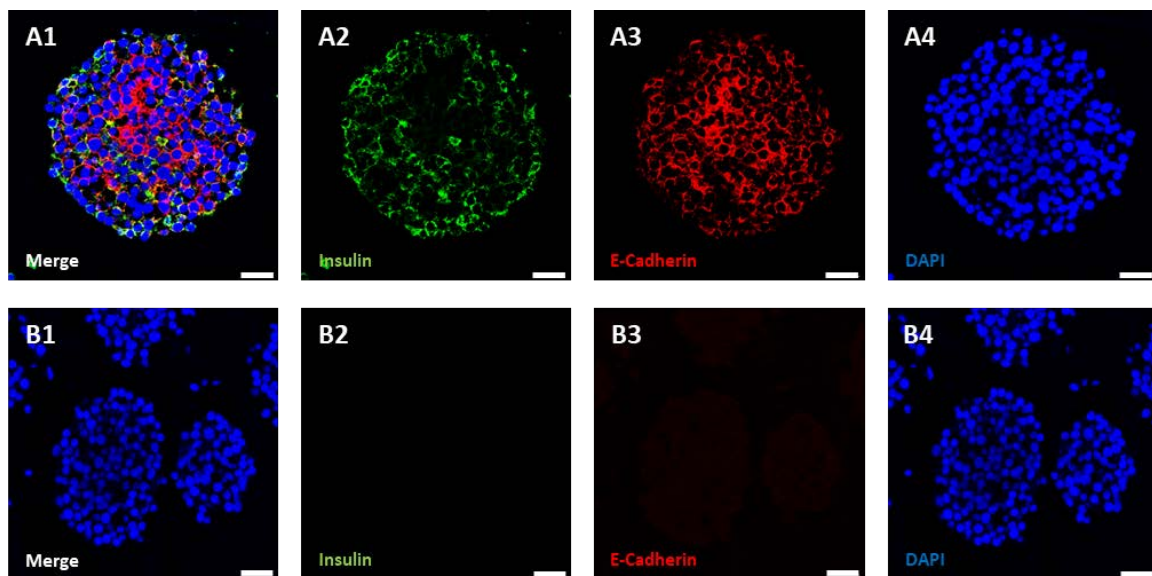


Figure 4.5: Immunofluorescence staining of MIN6 pseudoislets five days after generation. A1-A4: MIN6 pseudoislet ($\varnothing \sim 170 \mu\text{m}$) stained for insulin (green), E-cadherin (red) and DAPI (blue). B1-B4: No primary control. Scale bars: $25 \mu\text{m}$.

4.3.1.3 TEM analysis of MIN6 pseudoislets

TEM allowed analysis of pseudoislets at an ultrastructural level (Figure 4.6). An overview in lower magnification (Figure 4.6 A) showed disruption of cell-to-cell connections between some cell areas. A higher magnification allowed more detailed analysis of MIN6 cells inside the pseudoislet (Figure 4.6 B-D) revealing nuclei (N), ER (white arrow), mitochondria (M) and insulin vesicles (IV). ER and mitochondria are visible throughout the cells comparable to endocrine cells in mouse and human biopsies. Insulin vesicles are present, but in a lower quantity compared to (human) tissue samples.

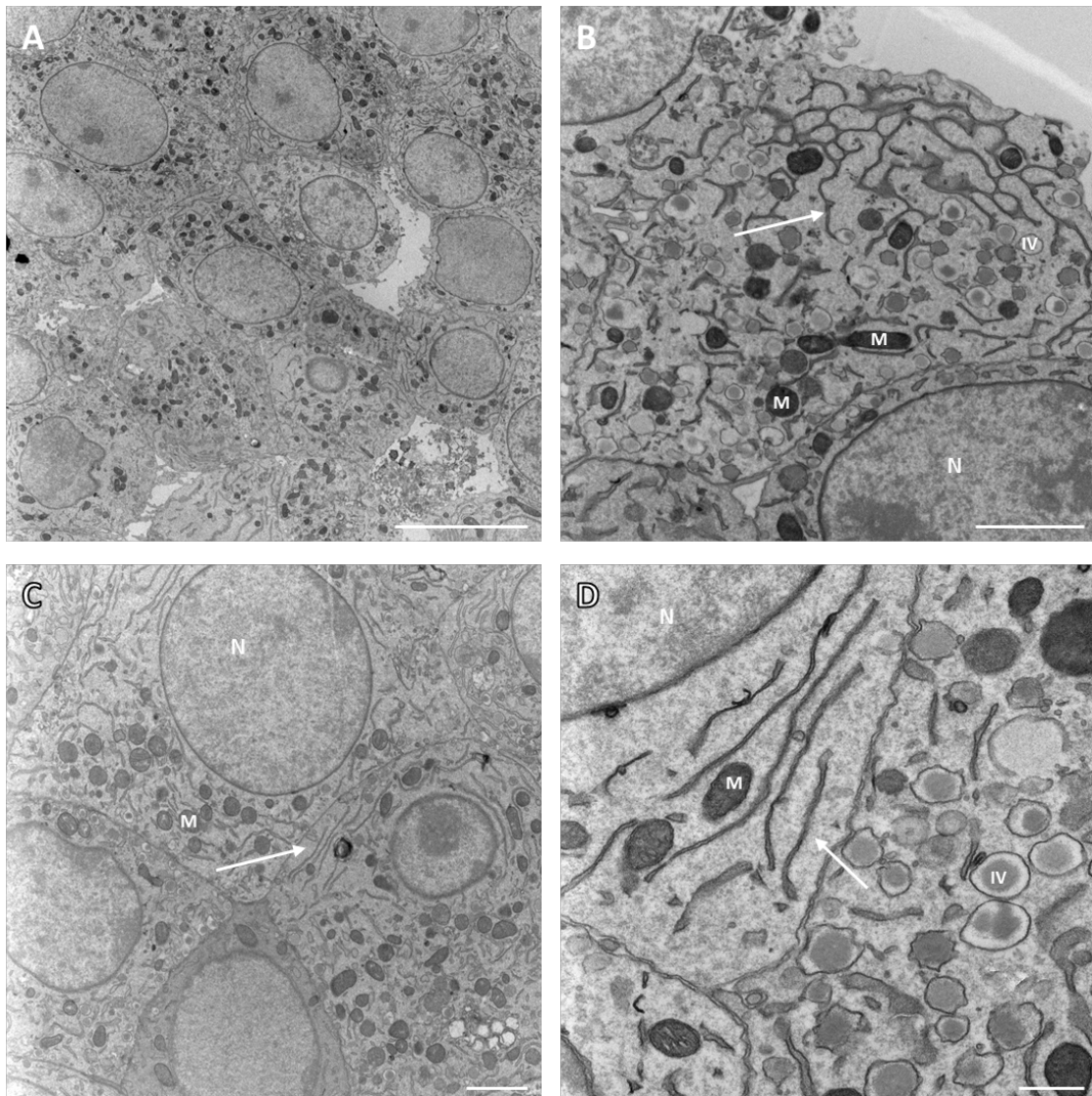


Figure 4.6: TEM analysis of MIN6 pseudoislets at Day 5.

A: Overview of an area within the pseudoislet with single MIN6 cells visible. Scale bar 10 μ m. B+C: Higher magnification showing MIN6 cells with nuclei (N), ER (arrows), mitochondria (M) and insulin vesicles (IV). Scale bars 2 μ m. D: Highest magnification revealing membranes of cells and organelles. Scale bar 500 nm.

4.3.1.4 Analysis of metabolic function of MIN6 pseudoislets

Seahorse flux analysis was used to investigate metabolic function of MIN6 pseudoislets. To achieve this, pseudoislets were transferred into islet capture microplates and islet capture screens were placed on top of the islets to prevent them from moving during injection and mixing events. Capture screens and pseudoislets were visible before and after the experiment (Figure 4.7 A+B) showing that neither islet transfer into the capture plate nor the Seahorse experiment was significantly disrupting pseudoislet integrity indicating measurements originated from pseudoislets and not from MIN6 single cells.

OCR and ECAR were measured over the duration of the Seahorse experiment with examples of two wells shown in Figure 4.7 C+D. Both rates are influenced by the injections of glucose, oligomycin, FCCP and antimycin. The first injection was either Seahorse medium (low glucose, red curve) or 25 μ M glucose (high glucose, green curve). Injection of medium did not change OCR or ECAR, but injection of glucose led to an increase in both measurements. The second injection was oligomycin leading to a decrease of OCR in both conditions and decrease of ECAR in high glucose conditions. The injection of FCCP (3) caused an increase in OCR in both conditions whereas ECAR was only slightly increased in high glucose conditions. The last injection (4) with antimycin A further decreased OCR and did not impact on ECAR in both conditions. Based on the changes in OCR and ECAR, ATP production could be calculated. To achieve this, values were obtained for: OCR_{basal} (OCR values corresponding to time points of highest ECAR values before oligomycin injection), OCR_{AA} (lowest OCR value after antimycin injection), OCR_{oligo} (lowest OCR value after oligomycin injection), and $ECAR_{basal}$ (highest ECAR value before oligomycin injection). With these values OCR_{mito} and OCR_{OXPHOS} could be calculated according to Equation (1) and (2).

$$(1) \quad OCR_{mito} = OCR_{basal} - OCR_{AA}$$

$$(2) \quad OCR_{OXPHOS} = OCR_{basal} - OCR_{oligo}$$

In the case of the example measurements for low and high glucose conditions this was:

$$\text{Low glucose: } OCR_{mito} = 45.330 - 4.360 = 40.971 \text{ (pmol OCR/min/}\mu\text{g protein)}$$

$$OCR_{OXPHOS} = 45.330 - 19.272 = 26.058 \text{ (pmol OCR/min/}\mu\text{g protein)}$$

$$\text{High glucose: } OCR_{mito} = 44.429 - 8.042 = 36.387 \text{ (pmol OCR/min/}\mu\text{g protein)}$$

$$OCR_{OXPHOS} = 44.429 - 18.492 = 25.937 \text{ (pmol OCR/min/}\mu\text{g protein)}$$

Basal ECAR for low glucose conditions was 0.220 pmol OCR/min/ μ g protein and for high glucose conditions it was 8.664 pmol OCR/min/ μ g protein (Figure 4.7 E).

Produced ATP via glycolysis could be estimated with produced PPR via glycolysis calculated with Equation (1)-(3).

$$(3) \ PPR_{total} = \frac{ECAR_{total}}{BP}$$

$$(4) \ PPR_{resp} = (10^{(pH-pK1)} / 1 + 10^{(pH-pK1)}) (\max H^+ / O_2) (OCR_{mito})$$

$$(5) \ PPR_{glyc} = PPR_{total} - PPR_{resp}$$

The buffer capacity (BP) of Seahorse medium is 0.049 mpH/pmol H⁺, pk1 (equilibrium constant of CO₂ hydration and H₂CO₃ dissociation) at 37°C of 6.093 and maximal H⁺/O₂ of 1.00, ATP production rate could be determined (Mookerjee et al., 2015).

For the two example wells ATP produced via glycolysis could be calculated as follows:

Low glucose:

$$\begin{aligned}
 ATP_{glyc} &= PPR_{glyc} \\
 &= (0.220/0.049) - \\
 &\quad ((10^{(7-6.093)}/1 + 10^{(7-6.093)})(1)(40.971)) \\
 &= -31.98 \text{ (pmol ATP/min/}\mu\text{g protein)}
 \end{aligned}$$

Negative ATP production via glycolysis means no detectable ATP production.

High glucose:

$$\begin{aligned}
 ATP_{glyc} &= PPR_{glyc} \\
 &= (8.664/0.049) - \\
 &\quad ((10^{(7-6.093)}/1 + 10^{(7-6.093)})(1)(36.387)) \\
 &= 143.37 \text{ (pmol ATP/min/}\mu\text{g protein)}
 \end{aligned}$$

ATP produced via oxidative phosphorylation could be estimated with OCR of oxidative phosphorylation times 2*2.63. For the example wells ATP produced via oxidative phosphorylation was calculated as follows:

Low glucose:

$$\begin{aligned}
 ATP_{OXPHOS} &= OCR_{OXPHOS} * 2 * 2.63 \\
 &= 26.058 * 2 * 2.63 \\
 &= 137.07 \text{ (pmol ATP/min/}\mu\text{g protein)}
 \end{aligned}$$

High glucose:

$$\begin{aligned}
 ATP_{OXPHOS} &= OCR_{OXPHOS} * 2 * 2.63 \\
 &= 25.937 * 2 * 2.63 \\
 &= 136.43 \text{ (pmol ATP/min/}\mu\text{g protein)}
 \end{aligned}$$

The total ATP production was estimated by summarizing ATP_{Glyc} and ATP_{OXPHOS} and was calculated for the two example wells as follows:

Low glucose:

$$\begin{aligned} ATP_{total} &= ATP_{Glyc} + ATP_{OXPHOS} \\ &= -31.98 + 137.07 \\ &= 105.08 \text{ (pmol ATP/min/}\mu\text{g protein)} \end{aligned}$$

High glucose:

$$\begin{aligned} ATP_{total} &= ATP_{Glyc} + ATP_{OXPHOS} \\ &= 143.37 + 136.43 \\ &= 279.80 \text{ (pmol ATP/min/}\mu\text{g protein)} \end{aligned}$$

These examples showed the impact of glucose injection on increase of ATP production via ATP_{Glyc} and similar rates of ATP_{OXPHOS} in both conditions (Figure 4.7 F+G).

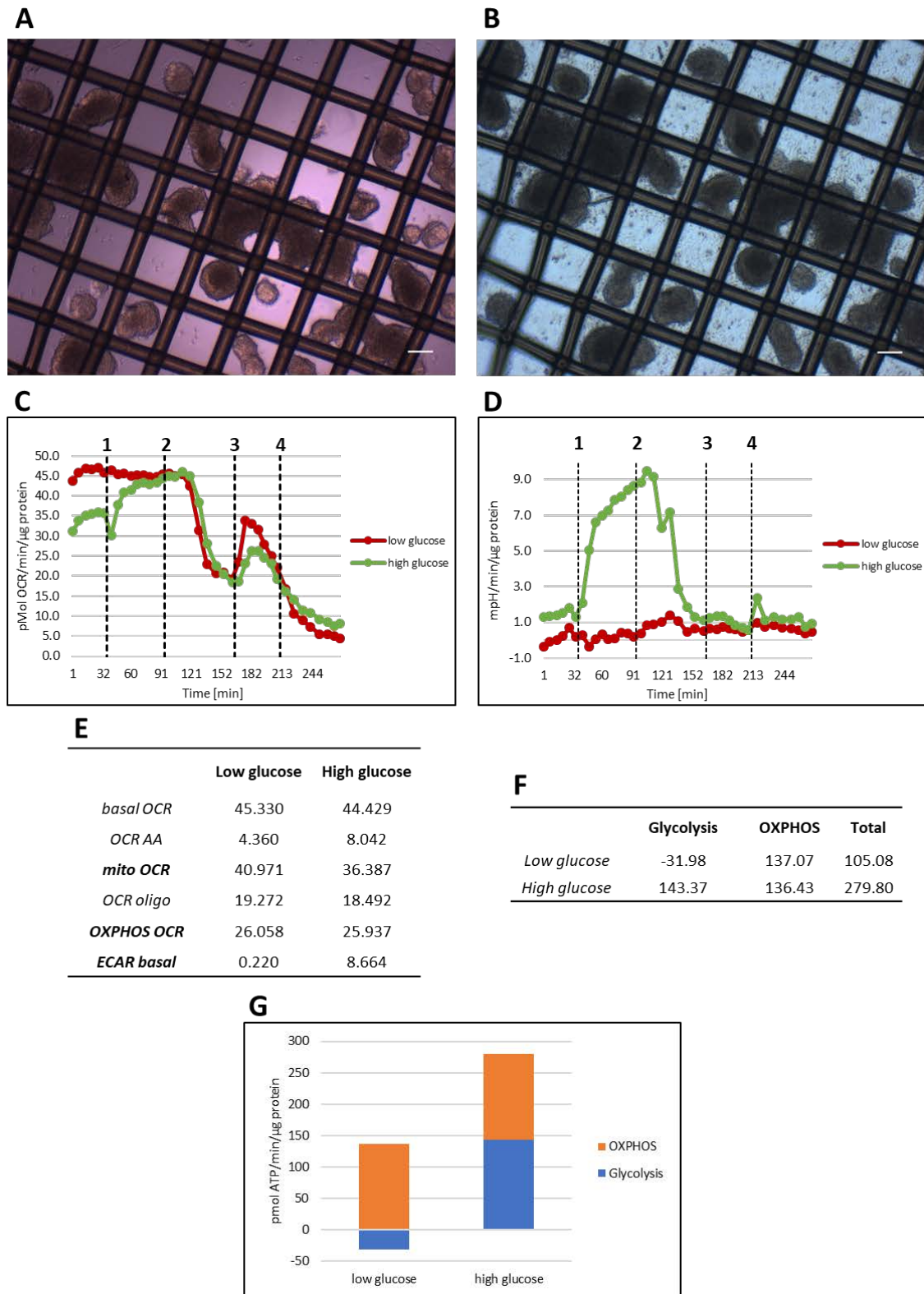


Figure 4.7: Seahorse flux analysis for metabolic characterisation of pseudoislets. Pseudoislets in islet capture plate before (A) and after (B) Seahorse flux analysis (Scale bars 100 μ m). Example of one well of OCR (C) and ECAR (D) measurements for pseudoislets with low and high glucose conditions during one experiment. Injections: (1) Seahorse medium or 25 μ M glucose, (2) 50 μ M oligomycin, (3) 3.5 μ M FCCP and (4) 2.5 μ M antimycin A. (E) Measurements of OCR and ECAR for shown example wells needed for ATP calculation. (F) ATP production via glycolysis and oxidative phosphorylation for shown example wells with low glucose and high glucose injection. (G) Graph illustrating ATP production via glycolysis and oxidative phosphorylation for calculated examples.

4.3.2 Providing ECM components via coating of tissue culture wells with CAF hydrogel and impact on pseudoislet model

To assess the impact of presence of ECM components, tissue culture wells were coated with CAF hydrogel and pseudoislets or human isolated islets were incubated in suspension culture for 72 h on top of the hydrogel. Following culture, islets were analysed for viability, protein expression and metabolic function.

4.3.2.1 Hydrogel components dissolved in media

The different hydrogel components collagen I, alginate and fibrinogen were dissolved in culture media and pseudoislets were cultured in respective media or control medium for 72 h. Bright field images showed pseudoislets after culture in control media (Figure 4.8 A), in media with supplemented collagen I (Figure 4.8 B), in medium with supplemented alginate (Figure 4.8 C), and in medium with supplemented fibrinogen (Figure 4.8 D). Over culture time pseudoislets adhered to non-adherent tissue culture plastic if cultured in control medium or medium supplemented with collagen I or fibrinogen, leading to loss of integrity and pseudocapsule with single cells growing out from the islet. Culture in medium with dissolved alginate prevented strong attachment and therefore preserved pseudocapsule and integrity of islets.

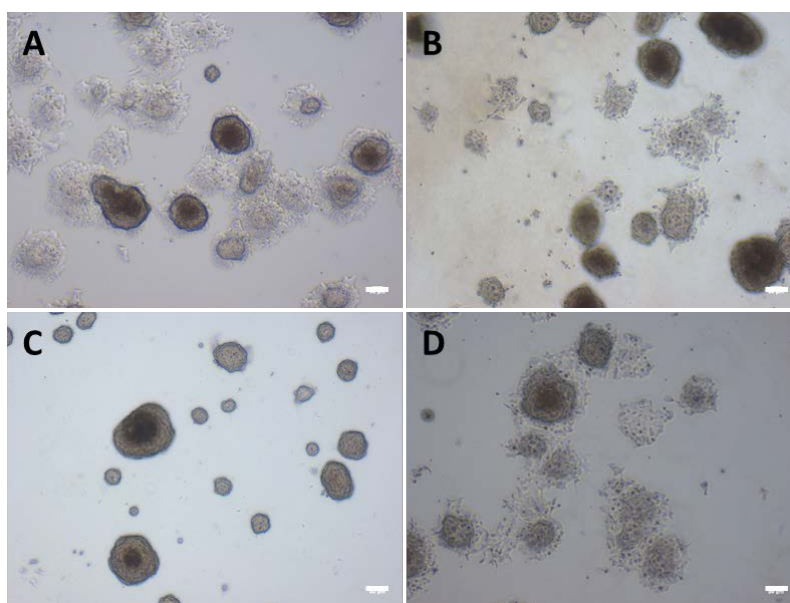


Figure 4.8: Pseudoislets (p25) after 72 h culture in control wells (A), medium supplemented with collagen I (B), alginate (C) or fibrinogen (D). Scale bars 100 μ m.

Viability was assessed in two different experiments showing average viability of $72\pm5\%$ after culture in control medium, $70\pm1\%$ after culture in medium with collagen I, $75\pm2\%$ after culture in medium with alginate and $74\pm5\%$ after culture in medium with fibrinogen (Figure 4.9). This showed none of the CAF components is toxic for MIN6 cells, but the components impact on the adherence of pseudoislets to the plastic surface. In addition, loss of integrity is not impacting on islet cell viability.

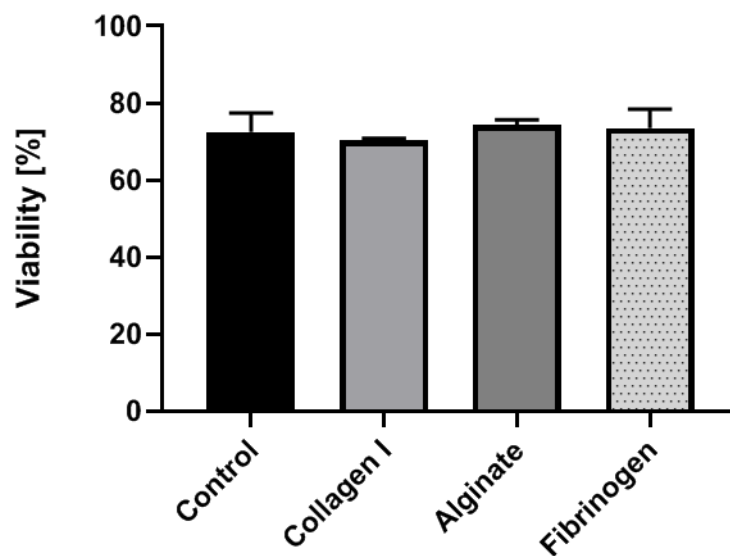


Figure 4.9: Viability of pseudoislets (p25+p26) after culture in control media or media with dissolved collagen I, alginate or fibrinogen.
Average of two independent experiments displayed with range.

4.3.2.2 CAF analysis

Analysis of freeze-dried hydrogels reveals porous structure of the gel indicating the possibility for media and nutrient transfer through the gel (Figure 4.10). A measurement with ImageJ revealed an average pore size of $\sim 11\ \mu\text{m}$ with a range of $2\text{--}36\ \mu\text{m}$ with an evenly distribution throughout the whole assessed gel surfaces. Energy dispersive X-ray spectroscopy (EDS) revealed distribution of nitrogen, carbon, calcium, sodium and chlorine throughout the gel (Figure 4.11). After carbon (64%), sodium (12%), chlorine (12%) and nitrogen (11%) were the most abundant elements. Chlorine was with 2% the least abundant from the elements measured. The high salt content can be explained with the preparation of the gel components. 5% alginate solution as well as 10% fibrinogen solution are prepared with PBS which is containing a high salt content. Further experiments of freeze-dried CAF hydrogels revealed swelling of 686% after 24 h in water.

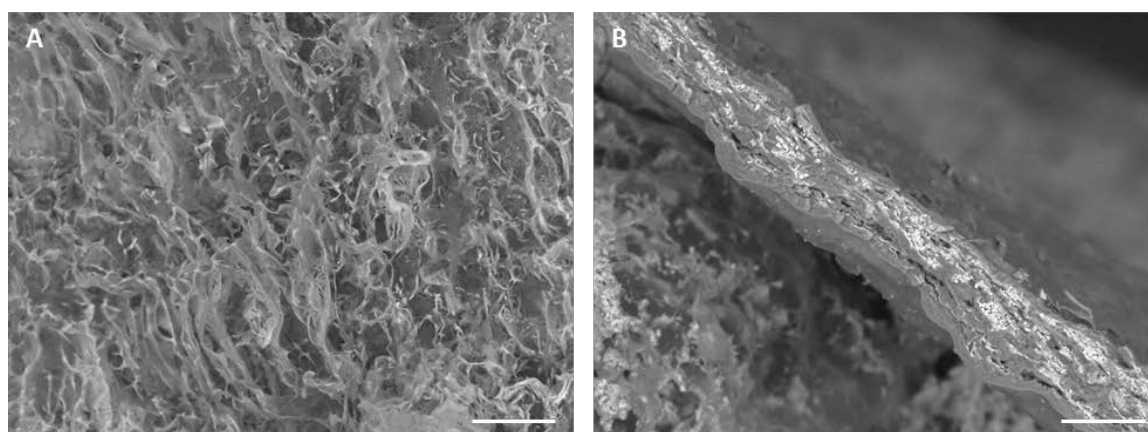


Figure 4.10: SEM analysis of freeze-dried CAF hydrogel.

A: A view from the surface showed various pores in the gel. B: View from the side showed thin thickness of the freeze-dried hydrogel but reveals porous structure inside the gel. Scale bars: $50\ \mu\text{m}$. Freeze drying and SEM analysis with support from Dr Marina Ferreira-Duarte.

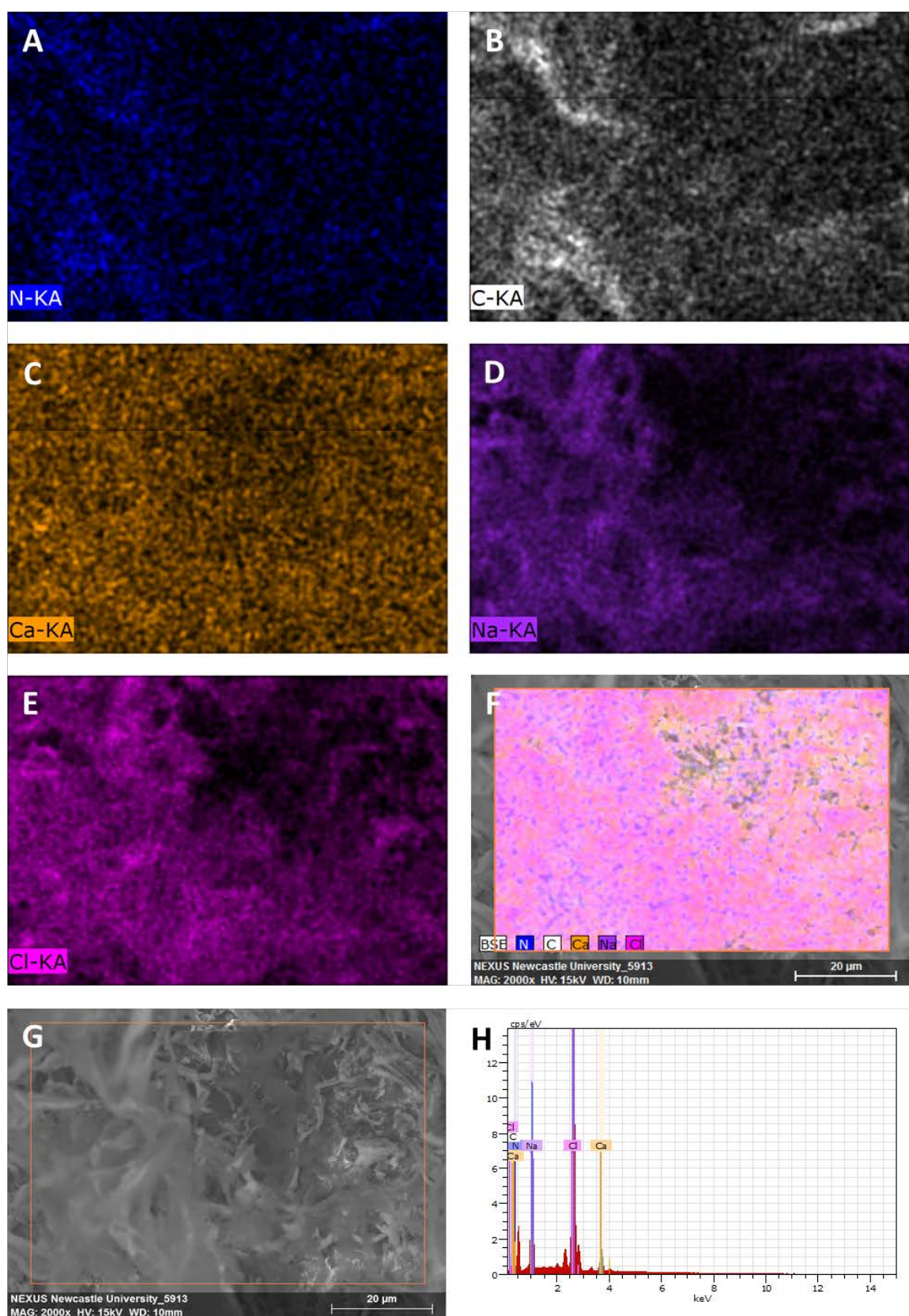


Figure 4.11: Energy dispersive X-ray spectroscopy (EDS) of CAF hydrogel (2:1:2). EDS reveals location of elements of nitrogen in blue (A), carbon in white (B), calcium in orange (C), sodium in purple (D) and chlorine in pink (E). A combination of all elements combined is shown in (F) and the original image in (G). (H) Shows the EDS analysis. EDS analysis with support from Dr Marina Ferreira-Duarte.

4.3.2.3 Viability assessment in the presence of CAF

Pseudoislets were generated over five days followed by incubation for 72 h on CAF-coated wells. Viability of up to 50 pseudoislets was assessed with PI staining. Representative pseudoislets are shown in Figure 4.12. The bright field images showed fragmentation of pseudoislets cultured on control plates (Figure 4.12 A) visible through roughened irregular appearing borders, whereas pseudoislets cultured on CAF-coating maintained their integrity with pseudocapsule evident through smooth borders (Figure 4.12 B). PI staining showed dead cells and core necrosis present in islets after both culture conditions (Figure 4.12 C+D). Assessment of size distribution with IEQ estimation was performed for four different experiments. Majority of pseudoislets had a diameter of 50-100 μm after culture in control wells ($43\pm 18\%$) and after culture in CAF coated wells ($54\pm 17\%$). A decreasing number of islets showed increasing diameter after both culture conditions with $28\pm 11\%$ with 101-150 μm , $19\pm 7\%$ with 151-200 μm , $8\pm 7\%$ with 201-250 μm , $3\pm 3\%$ with 251-300 μm and 0% with 301-350 μm for control and $29\pm 11\%$ with 101-150 μm , $11\pm 10\%$ with 151-200 μm , $2\pm 3\%$ with 201-250 μm , $3\pm 5\%$ with 251-300 μm and $1\pm 2\%$ with 301-350 μm for CAF culture.

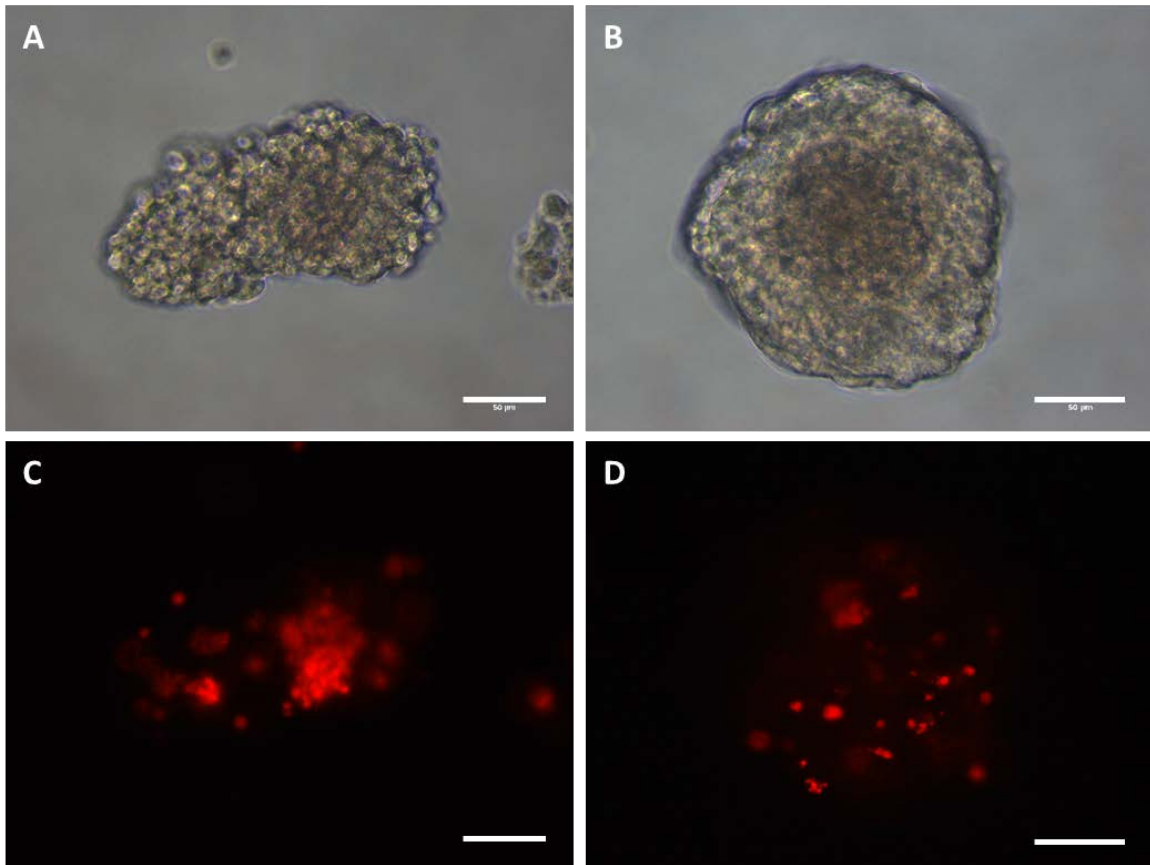


Figure 4.12: Viability assessment of pseudoislets cultured on control wells (A+C) and CAF-coated wells (B+D). Bright field images (A+B) showed size and integrity of pseudoislet. Red immunofluorescent PI staining (C+D) showed number of dead cells. Scale bars 50 μ m.

Viability of 50 islets was assessed in seven different experiments for control conditions and six for CAF conditions which were summarised in Figure 4.13. Viability of $76 \pm 6\%$ after control and $78 \pm 6\%$ after CAF culture conditions was established. An unpaired, two-tailed Student's t-test showed no significant difference between the two culture conditions ($P > 0.05$).

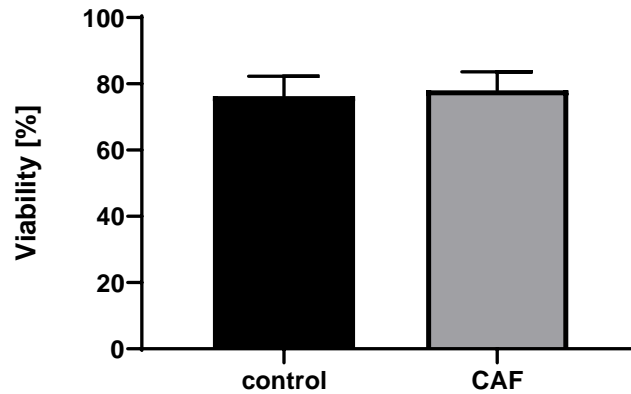


Figure 4.13: Viability of pseudoislets assessed after 72 h of culture on tissue culture plastic (control) or CAF-coated wells (CAF).

N=7 (control) and n=6 (CAF) with standard deviation with 50 islets assessed per experiment and culture condition. No significant difference of culture conditions on viability ($P > 0.05$).

A more detailed viability assessment was performed for two experiments (pseudoislets at p27 and p29) where viability was assessed of pseudoislets cultured in control wells (dark green/red) or in CAF-coated wells (bright green/red) per size group (Figure 4.14). In both experiments and conditions viability was the highest in the smallest islets (50-100 μm) with 88-94% and decreased with increasing islet size to 53-69%. No significant difference between culture conditions could be observed.

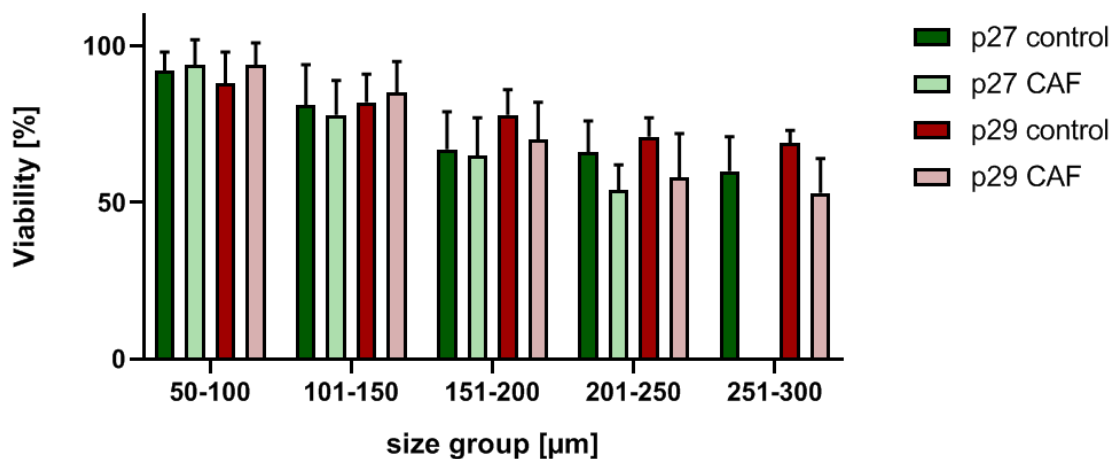


Figure 4.14: Viability of pseudoislets cultured for 72 h on tissue culture plastic (control) or CAF-coated wells (CAF) assessed per IEQ group.

Average with standard deviation displayed for each size group with 2-50 single islets assessed. Control conditions shown in dark green (p27) and dark red (p29). CAF conditions displayed in light green (p27) and light red (p29).

4.3.2.4 Protein expression of key marker in pseudoislets via IF after ECM presence

Protein expression in pseudoislets after 72 h culture in control and CAF-coated wells was assessed by IF staining with example islets shown in Figure 4.15. Insulin in green (Figure 4.15 A2+C2) which could be observed in all cells and was maintained through both culture conditions. Additionally, expression of pan-cadherin was maintained (red, Figure 4.15 A3+C3) as observed between all cells showing strong cell-to-cell connections. The pictured pseudoislet after control culture displayed a diameter of $<50\ \mu\text{m}$ whereas the pseudoislet after CAF culture displayed a diameter of $>100\ \mu\text{m}$ impacting on the brightness of the different staining.

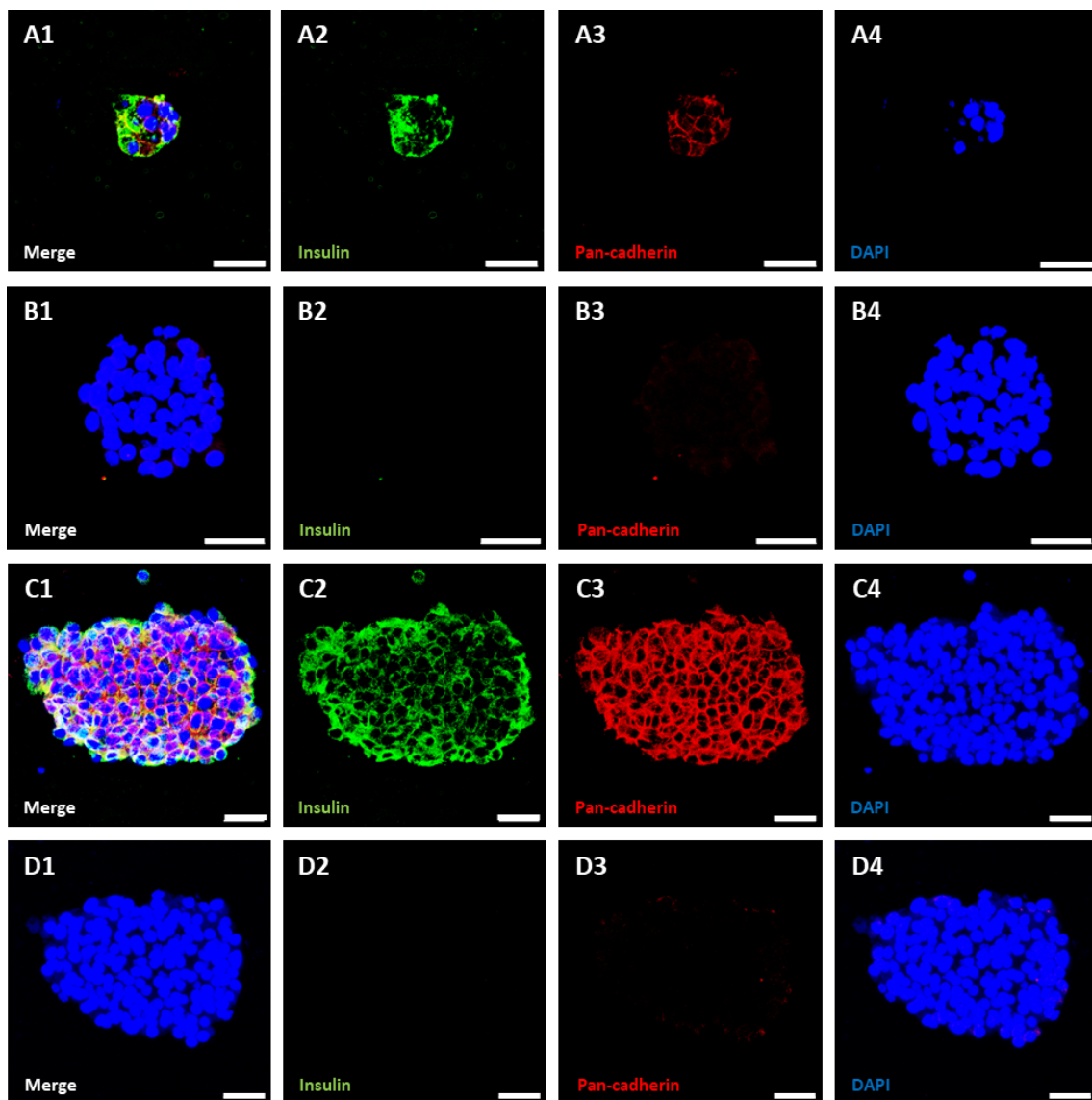


Figure 4.15: Immunofluorescence staining of pseudoislets after 72 h culture on tissue culture plastic (row A and B) or CAF-coated wells (row C and D). Pseudoislets are stained for insulin (green), pan-cadherin (red) and DAPI (blue). Row B and row D show no primary antibody control stains. Scale bars $25\ \mu\text{m}$.

4.3.2.5 Metabolic activity of pseudoislets in the presence of CAF

ATP production could be estimated through OCR and ECAR measurements during the Seahorse flux analysis. Three experiments are illustrated in Figure 4.16 with a high variability in and in between experiments. ATP production via glycolysis seemed to be higher after culture in control conditions compared to CAF-coated wells for experiment 1, whereas ATP production via oxidative phosphorylation (OXPHOS) showed a higher spread after control than CAF conditions. ATP production in experiment two and three seemed to be similar after both culture conditions.

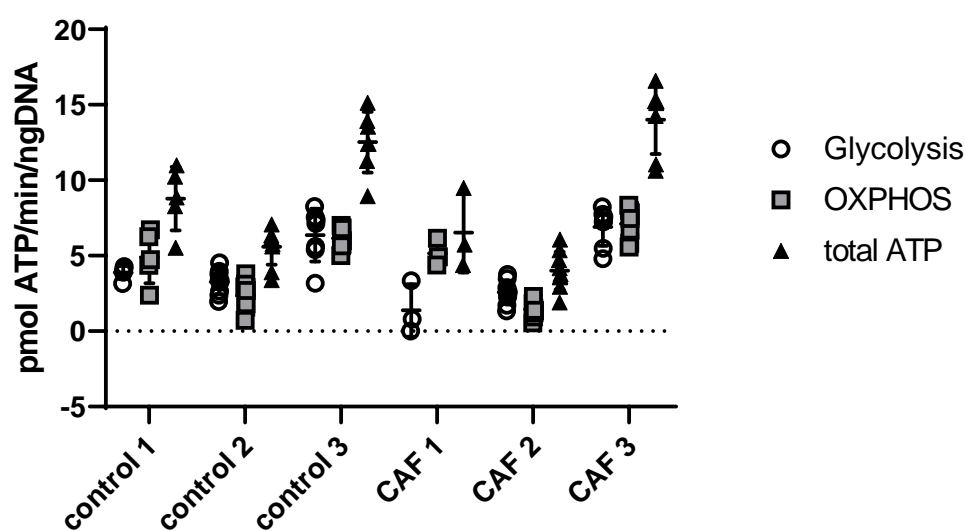


Figure 4.16: ATP production in pseudoislets after 72 h of culture on tissue culture plastic (control) or CAF-coated wells (CAF). Single values for ATP production via glycolysis, oxidative phosphorylation and total ATP production for three independent experiments are displayed.

4.3.2.6 Integrity index of pseudoislets after CAF presence

Pseudoislets were assessed for islet shape, border, integrity and diameter based on the 12-point scoring system previously described by Matsumoto (Matsumoto et al., 2004). Scores ranged from 0 till 2 with 0 showing islets with flat shape, irregular border, fragmented integrity and a diameter less than 100 μm (Table 4.1). A score of 2 was given for pseudoislets with a spherical shape, well-rounded border, compact integrity and a diameter of over 200 μm .

Table 4.1: Scores for pseudoislet integrity index after Matsumoto (Matsumoto et al., 2004)

Score	Shape	Border	Integrity	Diameter
0	Flat	Irregular	Fragmented	<100 μm
1	Characteristics of score 0 and 2			100-200 μm
2	Spherical	Well-rounded	Compact	>200 μm

Images of pseudoislets were assessed and scores given for each pseudoislet pictured. Diameter was measured with ImageJ software and transferred manually into the scores. Scores of all categories were combined to an average of different experiments per culture condition (n=4 for control and n=3 for CAF-coated wells) which described impact of CAF presence on integrity of pseudoislets (Figure 4.17). Average integrity score after culture in control wells was 2.5 ± 0.6 and after culture in CAF-coated wells 5.6 ± 0.6 showing a significant improvement ($p < 0.001$).

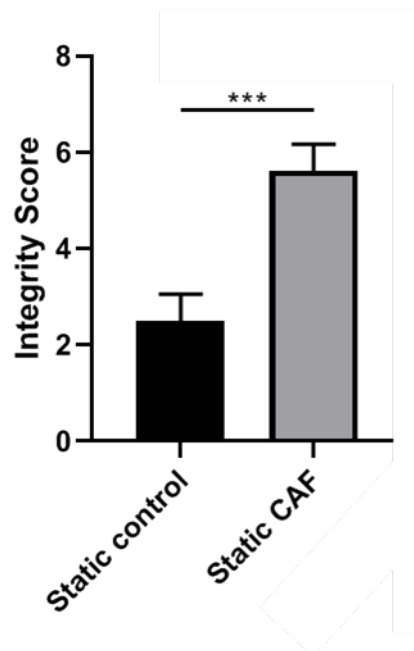


Figure 4.17: Integrity index of pseudoislets after culture in control and CAF-coated wells. Scores from 0 till 2 were given for pseudoislet shape, border, integrity and diameter (Table 4.1). Pictured were combined scores from all assessed islets from n=4 experiments for control conditions and n=3 experiments of CAF-coated wells (data shows mean \pm SD, $P < 0.001$).

4.3.3 Analysis of human isolated islets

Impact of prolonged culture as well as presence of CAF hydrogel was assessed in primary human isolated islets. Available donor data of the eight studied islet preparations is summarised in Table 4.2 and quality as well as purity during islet quality control was determined from dithizone-stained images in Figure 4.18. Of the total eight preparations used for experiments, three were from female donors and four from male donors with five organs originating from DBD and two from DCD donors. Age ranged from 24-65 [years], BMI from 25-36 [kg/m²] and CIT from ~3.5 h to ~26 h. Islet preparations had a purity between 5% and 95% and a viability between 58% and 81%.

Table 4.2: Donor data of human isolated islets with donor number, LDIS number, gender, BMI, donor type, cold ischaemia time, purity and viability.

Donor number	LDIS number	Gender	Age [years]	BMI [kg/m ²]	Donor Type	CIT [h]	Purity	Viability
HI-1	206	female	49	36.1	DBD	26.2	85%	58%
HI-2	210	male	24	30.5	DBD	12.5	5%	70%
HI-3	211	male	45	31.1	DCD	n/s	95%	81%
HI-4	247	female	48	32.5	DBD	7.7	60%	77%
HI-5	248	male	44	29.5	DBD	3.6	95%	71%
HI-6	256	male	53	25.0	DBD	6.6	80%	78%
HI-7	266	female	65	28.2	DCD	6.1	90%	69%
HI-8	274	n/s	n/s	n/s	n/s	n/s	55%	75%

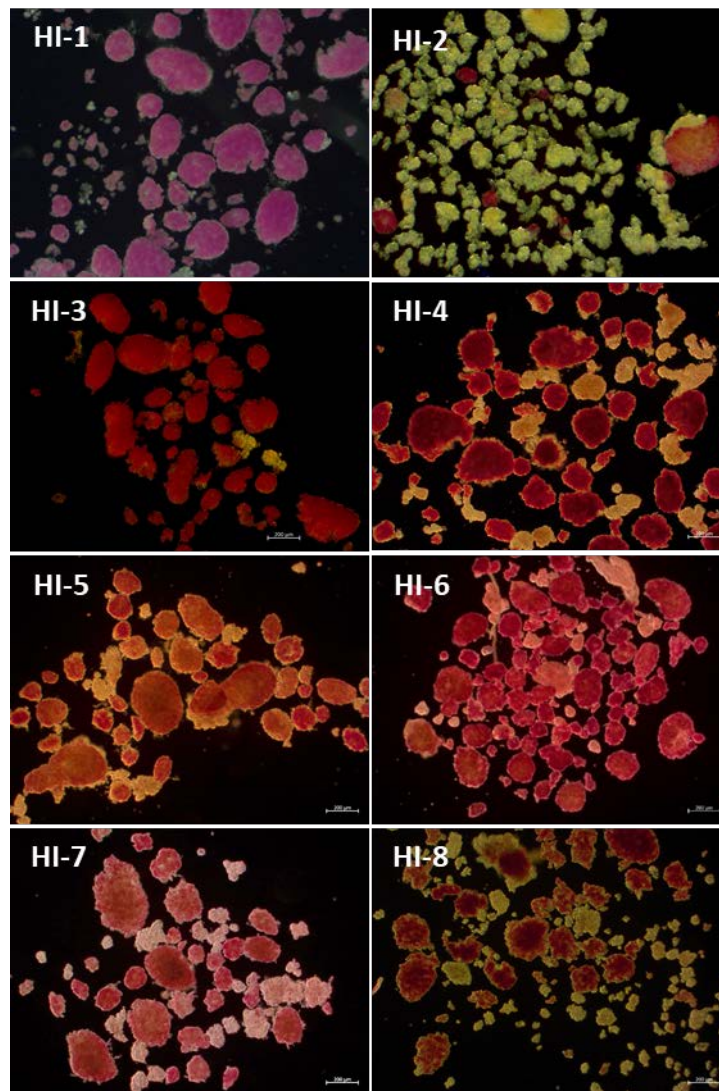


Figure 4.18: Dithizone staining of human isolated islets during islet quality control. Number of red cell clusters versus unstained clusters indicates purity. Islets were analysed after a culture period up to 24 h. Pictures were provided by Minna Honkanen-Scott. Scale bars: 200 μ m.

4.3.3.1 Viability of human isolated islets over time of culture

Viability of human isolated islets was assessed at the start ($t = 0$ h) and at time points up to five days of static culture in non-adherent tissue culture plates with $n=2-3$ islet preparations per time point (Figure 4.19). Average viability of all assessments per time point was $76.7 \pm 6\%$ at the beginning of the culture period, $78 \pm 5\%$ after 24 h, $74 \pm 5\%$ after 48 h of culture, $74 \pm 6\%$ after 72 h of culture, and $60 \pm 7\%$ after five days of culture. This indicated a stable viability up to 72 h of culture followed by a decline on Day 5 of culture.

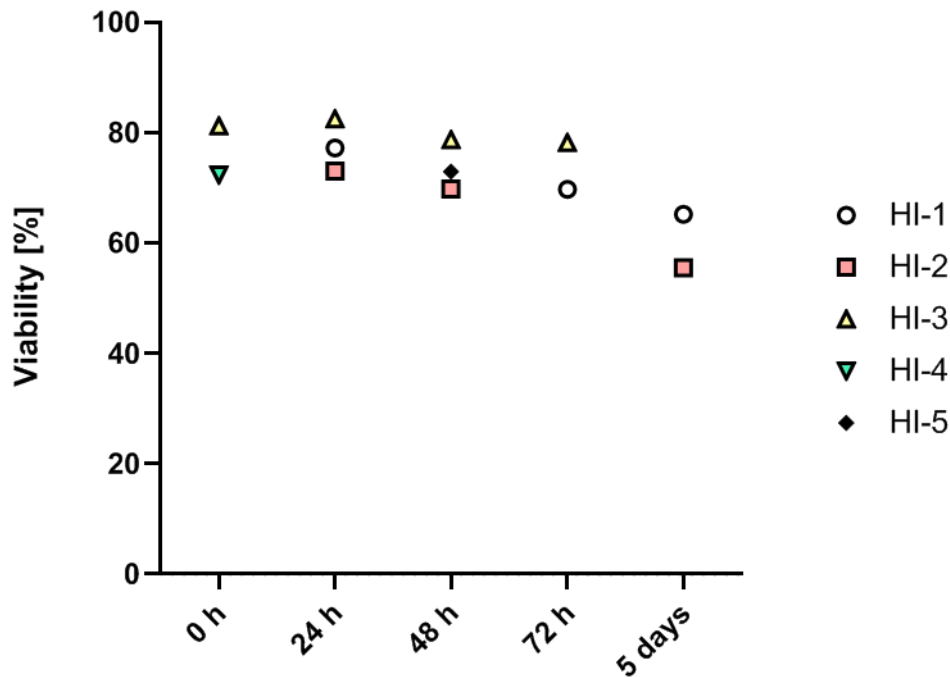


Figure 4.19: Viability of human islets over time in static culture in non-adherent tissue culture plates up to five days. Islets from five different donors (HI-1-HI-5) were assessed at different culture time points. Pictured is the average of all assessed islets at each time point for each islet preparation.

4.3.3.2 Metabolic function of human isolated islets after isolation

For metabolic assessment of human isolated islets Seahorse flux analysis was performed at Day 1 (HI-6), Day 2 (HI-7) and Day 3 (HI-5) after isolation to gain OCR and ECAR for calculation of ATP production (Paragraph 4.3.1.4). Figure 4.20 A+B showed increase in total ATP production through glucose stimulation was due to increase in ATP production via glycolysis in all three performed experiments with different variabilities of measurements in high and low glucose conditions. ATP production via OXPHOS did not seem to be influenced by glucose stimulation in observed results.

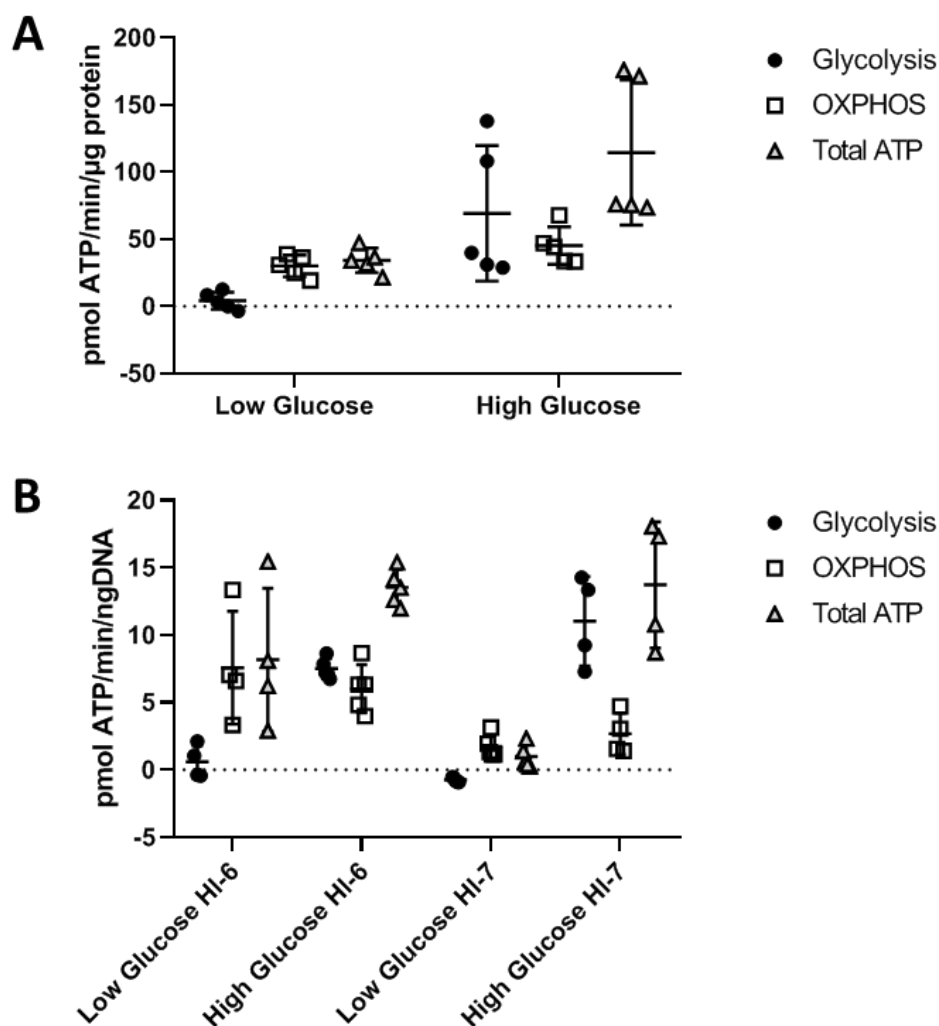


Figure 4.20: ATP production per well of human isolated islets.

ATP production via glycolysis displayed with black dots, ATP production via OXPHOS displayed with white squares and total ATP production displayed with grey triangles. A: Islets of HI-5 on the third day after isolation. ATP production was displayed per μ g protein. B: Islets of HI-6 and HI-7 on Day 1 and two after isolation with ATP displayed per ng DNA.

4.3.4 Impact of hydrogel presence on human isolated islets

4.3.4.1 Viability assessment of human isolated islets after culture on CAF-coated wells

Dithizone staining in combination with PI staining was used to assess viability of human isolated islets. Under bright field illumination, red stained cell clusters could be identified as islets with similar appearance after culture in control conditions (Figure 4.21 A) and CAF-coated wells (Figure 4.21 B). PI staining with IF analysis showed dead cells in red fluorescent staining are present in human isolated islets after both culture conditions (Figure 4.21 C+D).

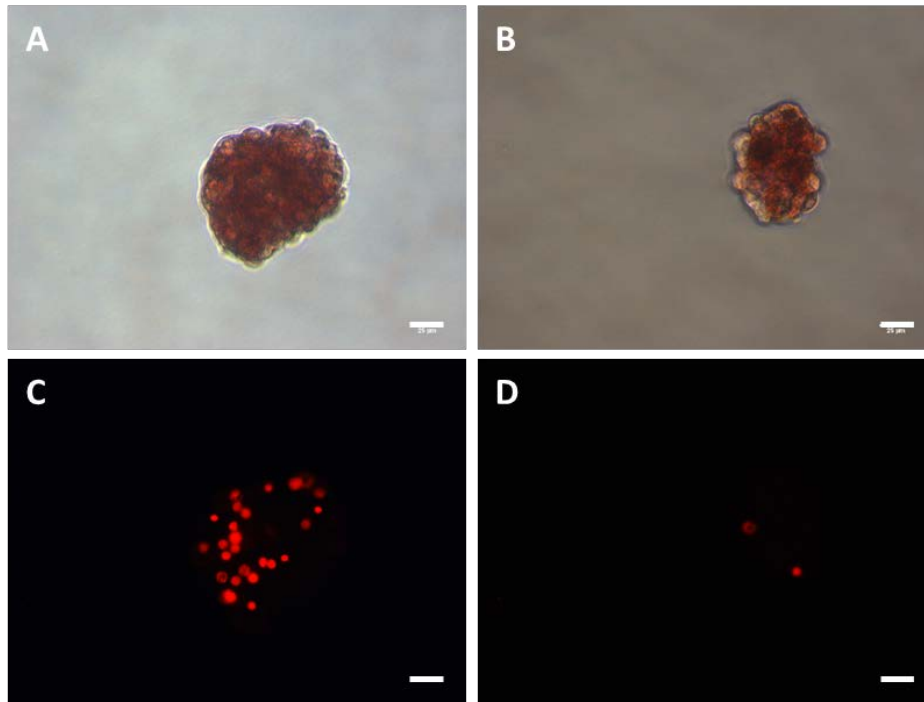


Figure 4.21: Viability assessment of human isolated islets cultured on control wells (A+C) and CAF-coated wells (B+D). Bright field images (A+B) showed size and integrity of islets as well as positivity for insulin with red dithizone stain. Red immunofluorescent PI staining (C+D) showed number of dead cells. Scale bars 25 μ m.

Viability of islets from HI-6 and HI-8 was assessed after 72 h of culture and summarised in Figure 4.22. Viability of human islets after culture on control tissue culture plastic was estimated as $63 \pm 1\%$ with 34 and 50 islets assessed per experiment. After culture on CAF-coated wells viability was estimated at $79 \pm 10\%$ with 12 and 25 islets assessed per experiment.

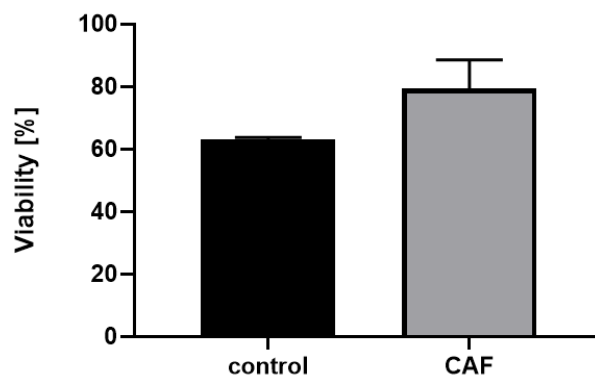


Figure 4.22: Viability of human isolated islets (HI-6 and HI-8) after 72 h culture on tissue culture plastic or CAF-coating. Average value with standard deviation of $n=2$ with 12-50 islets assessed per experiment and condition.

4.3.4.2 Protein expression of human isolated islets after CAF presence

Examples of IF staining are pictured in Figure 4.23 with no primary antibody controls in Figure 4.24 of two batches of human isolated islets (HI-5 and HI-6) after culture in control (Figure 4.23 A1-A5, C1-C5) and CAF-coated wells (Figure 4.23 B1-B5, D1-D5). All islets showed maintained insulin expression in green (Figure 4.23 A2, B2, C2, D2) and glucagon expression in purple (Figure 4.23 A3, B3, C3, D3). Collagen IV expression was visualized in red (Figure 4.23 A4, B4, C4, D4) and was observed in all pictured islets with lower expression in HI-6 after culture in control wells.

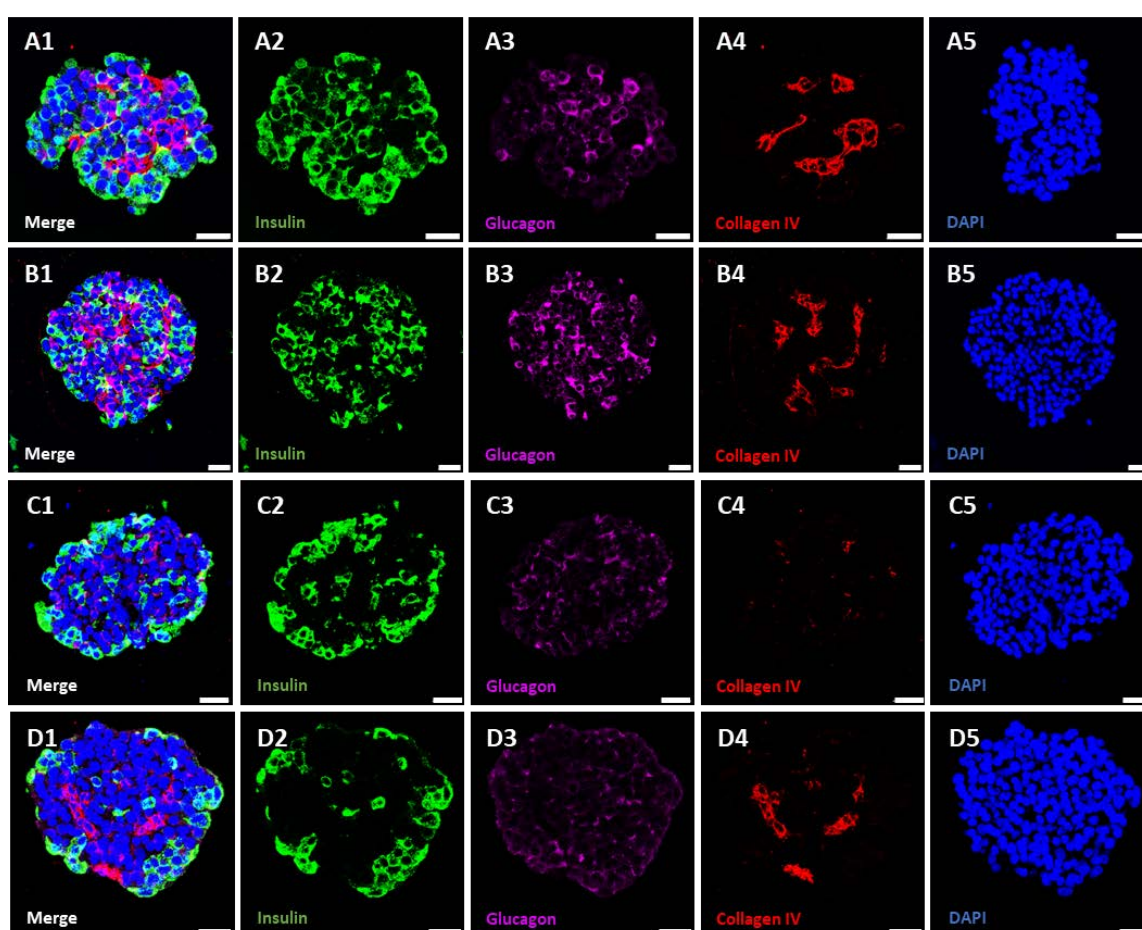


Figure 4.23: IF staining of human isolated islets after 72 h of culture in control or CAF-coated wells. Column 1 showing merge of all four channels, column 2 showing insulin in green, column 3 showing glucagon in purple, column 4 showing collagen IV in red and column 5 showing DAPI in blue. A1-A5: islet of HI-5 after culture in control wells, B1-B5: islet of HI-5 after culture on CAF-coated wells, C1-C5: islet of HI-6 after culture in control wells, and D1-D5: Islet of HI-6 after culture on CAF-coated wells. Scale bars 25 μ m.

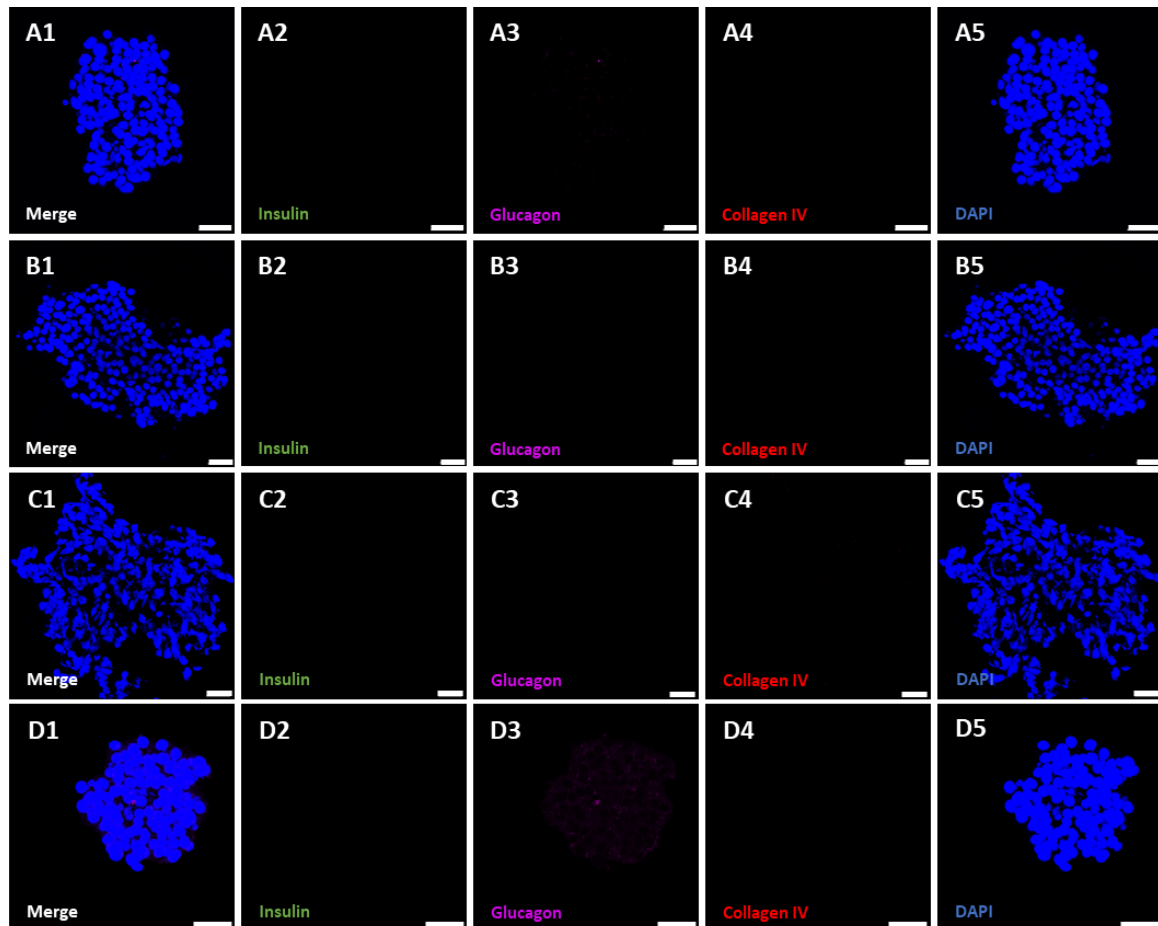


Figure 4.24. No primary antibody control of Figure 4.23.

IF staining of human isolated islets after 72 h of culture in control or CAF-coated wells. Column 1 showing merge of all four channels, column 2 showing insulin in green, column 3 showing glucagon in purple, column 4 showing collagen IV in red and column 5 is showing DAPI in blue. A1-A5: islet of HI-5 after culture in control wells, B1-B5: islet of HI-5 after culture on CAF-coated wells, C1-C5: islet of HI-6 after culture in control wells, and D1-D5: Islet of HI-6 after culture on CAF-coated wells. Scale bars 25 μm.

4.3.4.3 Metabolic analysis of human isolated islets in the presence of CAF

After culture of islets in control and CAF-coated wells ATP production was analysed in glucose stimulated conditions with Seahorse flux analysis indicating ATP production of islets with no observed significant impact of CAF-coating (Figure 4.25 C). In more detail, total ATP production for HI-6 after culture in CAF-coated wells seemed lower, especially without consideration of one outlier of ATP produced via glycolysis. For HI-7 ATP production was lower in both conditions compared to HI-6. ATP production via glycolysis after culture in CAF-coated wells was higher in one well leading to a higher total ATP production in this condition compared to control.

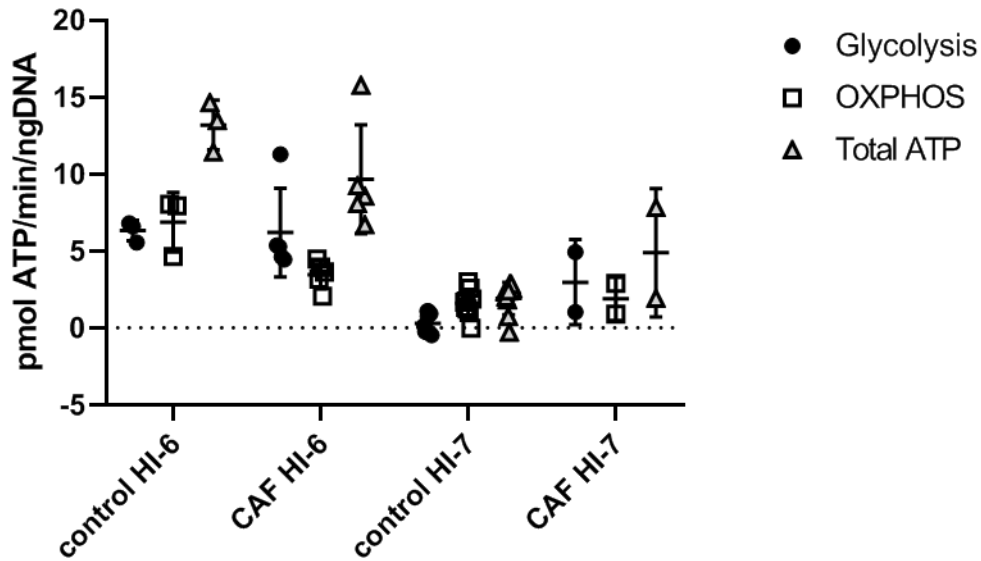


Figure 4.25: ATP production per well of human isolated islets (IL-6 and IL-7) after 72 h of culture on control or CAF-coated wells (on Day 6 after isolation). ATP production via glycolysis displayed with black dots, ATP production via OXPHOS displayed with white squares and total ATP production displayed with grey triangles. ATP is displayed per ng DNA.

4.4 Discussion

In this chapter it was analysed how a provision of a three-component hydrogel impacts on islet health. It was hypothesised that the culture of islets in proximity or in contact with the CAF hydrogel improves islet integrity, viability and function.

4.4.1 Pseudoislet model

In a first step a readily available pseudoislet model was established out of a MIN6 β -cell-line to eliminate high variable results through differences in isolated islet preparations. Pseudoislets have been widely used as a model for islet research and are established from rodent or human cell lines including MIN6, INS1E, α TC1.6, β TC3 or EndoC- β H1 (Hauge-Evans et al., 1999, Kojima et al., 2014, Merglen et al., 2004, Persaud et al., 2010, Spelios et al., 2018, Spelios et al., 2013). Through culture of MIN6 cells in a Petri dish, different sized cell clusters (pseudoislets) were generated mimicking primary isolated islets. Viability of pseudoislets five days after generation (~75%) (Figure 4.4) was comparable with viability of human isolated islets over up to 72 h of culture (~77-74%) (Figure 4.19). IF analysis of pseudoislets (Figure 4.5) showed comparable morphology and insulin distribution to human isolated islets (Chapter 3 Figure 17). Additionally, TEM analysis

revealed characteristic similarities of pseudoislets (Figure 4.6) with human isolated islets (Chapter 3 Figure 19) including presence of mitochondria, ER and insulin vesicles (Persaud et al., 2010, Riopel et al., 2014). However, due to their tumour origin MIN6 cells have a higher proliferation rate compared to primary β -cells leading to continuous growth and therefore hypoxia in the islet core (Reers et al., 2011, Komatsu et al., 2017). Additionally, less insulin vesicles were observed in pseudoislets compared to primary islets *in situ* and after isolation confirming previously observed differences in insulin content (Persaud et al., 2010). Presence of E-cadherin evidenced strong cell-to-cell connection between MIN6 cells similar to primary islets (Figure 4.5). This has previously been reported in association with improved function compared to monolayers (Hauge-Evans et al., 1999). Presence of insulin (Figure 4.5+Figure 4.6) as well as ability to generate ATP in response to a glucose challenge (Figure 4.7) indicated glucose-responsivity.

The mitochondria stress test with Seahorse flux analysis for pseudoislets was optimised in cooperation with Deborah Cornell and Dr Satomi Miwa who optimised seeding density to 200-300 IEQ/well and observed better response if islets were seeded into the plates on the day before the experiment. Contrary to this 50-80 islets per well were seeded on the day of the experiment in the literature (Wikstrom et al., 2012, Taddeo et al., 2018). Figure 4.7 A showed pseudoislets are present in the well of the islet capture plate and their shape is still intact after plating and fitting of the capture screen, visible under the microscope. Even after the Seahorse experiment, pseudoislets remain in the cell cluster (Figure 4.7B) showing the obtained data can be assumed to originate from pseudoislets rather than single MIN6 cells. Cell-to-cell contacts influenced function of MIN6 cells with insulin expression more similar to isolated islets if assembled in a three-dimensional culture (Hauge-Evans et al., 1999). For pseudoislets the concentration of oligomycin was increased to 50 mM and time after oligomycin injection was increased to 51-71 min which led to decrease of OCR till a plateau was observed (Figure 4.7 C). During the mitochondria stress test, OCR of pseudoislets (Figure 4.7) changed through injection of the drugs oligomycin, FCCP and antimycin A, similar to human isolated islets and mouse islets in the literature with decrease after oligomycin, increase after FCCP and decrease after antimycin (Taddeo et al., 2018, Wikstrom et al., 2012). Total ATP production was increasing with glucose stimulation with rising of ATP production via glycolysis whereas

ATP production via OXPHOS was similar in both conditions for the example wells (Figure 4.7 F+G). This trend could be observed in all experiments with pseudoislets as well as human isolated islets with and without glucose stimulation indicating utilization of increased available glucose via glycolysis. This may indicate that increased levels of pyruvate, produced by glycolysis, are not completely passing through the Krebs cycle, but may accumulate as malate and citrate (Schuit et al., 1997).

Similarities of pseudoislet model with human isolated islets regarding morphology, cell-to-cell connections, viability, protein expression and metabolic function led to the conclusion that MIN6 pseudoislets provide a reproducible and readily available model for islet research.

4.4.2 Cytocompatibility of CAF with pseudoislet model

Cytocompatibility was assessed with the impact of CAF on viability, integrity, protein expression and function. Single components of CAF hydrogel dissolved in medium did not negatively impact on viability of pseudoislets (Figure 4.8). Furthermore, a hydrogel composed of all components in a ratio of 2:1:2 was compatible with pseudoislets with maintained overall viability (Figure 4.13) as well as maintained viability in the different size groups (Figure 4.14). In addition to that, cell-to-cell connections are strongly expressed after both culture conditions with pan-cadherin staining (Figure 4.15 A3+C3). Despite a variability between wells and experiments, metabolic activity seemed maintained through presence of CAF compared to pseudoislets cultured in control wells (Figure 4.16) and insulin was expressed after culture on CAF-coated wells (Figure 4.15 A2+C2). However, no improvement of viability, key protein marker expression or function was observed. This may indicate that the presence of ECM components is not sufficient for improving islet viability and function, but that contact to ECM components via integrin receptors is necessary (Kaido et al., 2006). Isolated canine islets lost integrin expression over time in culture, with decreasing insulin expression and increasing apoptosis (Wang and Rosenberg, 1999). Rat insulinoma cells possessed a higher expression of integrin beta-1 subunit during pseudoislets formation compared to monolayers, but this expression was decreased during prolonged culture without ECM components present (Maillard et al., 2009). However, an improvement was observed with integrity of pseudoislets assessed through scoring. This confirmed previous observations with bright field microscopy

(Figure 4.12 A+B), with a general trend of pseudoislets appearing to possess a better integrity, pseudocapsule and shape after culture on CAF-coating compared to tissue culture wells. Often an attachment of pseudoislets after prolonged culture on non-adherent tissue culture plastic was observed which was reduced through the CAF-coating. One explanation may be that cells including pseudoislets lack receptors for alginate, which is typically circumvented by adding RGD sequences to the alginate for better recognition (Andersen et al., 2015). Through the application of untreated alginate, the adherence of the CAF hydrogel may have decreased maybe through masking of the present RGD sequences of collagen I and fibrinogen by alginate (Daoud et al., 2010a, Janmey Paul et al., 2009). But in the case of the CAF hydrogel the decreased possibility to attach may be an advantage for improved integrity of islets.

4.4.3 Cytocompatibility of CAF with human isolated islets

Prolonged culture decreased viability of human isolated islets (Figure 4.21) previously associated with reduction in function (MacGregor et al., 2006). Presence of ECM components through CAF hydrogel improved viability with culture over 72 h (Figure 4.22), together with maintained protein expression of insulin and glucagon (Figure 4.23) demonstrating basic biocompatibility of the CAF hydrogel with human isolated islets. Assessment of metabolic function revealed variability in between-donors (HI-6 and HI-7) with no significant differences observed with and without CAF-coating (Figure 4.25). These two examples confirmed previous observations of variability in between preparations of human isolated islets (Persaud et al., 2010, Taddeo et al., 2018). The high variability between wells and experiments was also observed closer to the isolation before prolonged culture and exposure to CAF (Figure 4.20) with analysis on the first (HI-6), second (HI-7) and third (HI-5) day after isolation. In all three experiments glucose stimulation did increase ATP production via increase of ATP production via glycolysis confirming observed results with pseudoislets (Figure 4.7), whereas ATP production via OXPHOS remained on the same level with exception of one outlier I low glucose conditions of HI-6. HI-7 had a relatively low ATP production via OXPHOS in both culture conditions indicating stressed islets, which could be due to age or circulatory death of the donor (Leemkuil et al., 2019). Additionally, the variability fluctuated between donors and stimulated/unstimulated conditions. ATP values of HI-5 were less variable in unstimulated

wells, ATP values of HI-6 were less variable in stimulated wells, and ATP values of HI-7 were less variable in unstimulated wells. As high variability between OCR measurements with Seahorse flux analysis of different human islet batches has not been reported in the literature (Wikstrom et al., 2012, Taddeo et al., 2018). However cell clusters and especially islets can be very heterogeneous in their function which may explain varying ATP generation rates (Taddeo et al., 2018).

In summary, it has been shown that MIN6 pseudoislets show comparable viability, integrity and ATP production to human isolated islets. The seahorse flux analysis was optimised for the analysis of ATP production in pseudoislets and isolated islets, but further optimisation seems necessary to reduce variability between wells and experiments. The CAF hydrogel was cytocompatible with pseudoislets and human isolated islets whereby integrity of pseudoislets and viability of human isolated islets were improved after culture on CAF-coated wells. However, a higher benefit was hypothesised through presence of ECM components which may indirectly influence intracellular signalling cascades, but the direct contact to ECM components seems necessary (Jung et al., 2011). Additionally, the CAF hydrogel could be improved by adding pancreas specific proteins like collagen IV, laminin or fibronectin (Daoud et al., 2010a). Furthermore, pseudoislets and human isolated islets may develop increasing hypoxia especially in the core, impacting on viability and function and therefore diminishing any advantageous effects of ECM exposure (MacGregor et al., 2006, Dionne et al., 1993). Additionally, a different delivery of ECM components towards islets enabling cell-to-matrix contact may improve outcomes of short-term culture. The combination of providing ECM components in a more refined system as well as reducing hypoxia was thus proposed to further investigate the impact of CAF on pseudoislets and human isolated islets.

Chapter 5. Development of bioengineering approaches to reduce hypoxia in β -cell/hydrogel products

5.1 Introduction

Through the isolation process islets are cut off from their blood supply leading to increasing hypoxia over culture time especially in the core (Komatsu et al., 2017). Insufficient supply of oxygen and nutrients impacts on cellular processes leading to changes in glucose uptake and ATP generation (Cantley et al., 2010). Hypoxia also affects islet morphology through loss of integrity and increasing fragmentation (Giuliani et al., 2005). Additionally, reduced oxygen is associated with increased cell death through both apoptosis and necrosis (Giuliani et al., 2005, Olsson et al., 2011). Islet size impacts on the degree of hypoxia in islets which can be reduced through increased oxygen tension in the medium, whereas potential toxicity of oxygen must also be considered (Komatsu et al., 2017, Olsson et al., 2011). Typical marker which show an increased mRNA expression in hypoxic β -cells are *Ldha*, *Glut-1* and *Mct-4* (Cantley et al., 2010). These genes encode proteins leading to a shift in ATP production from aerobic OXPHOS to anaerobic glycolysis (Cantley et al., 2013, Cantley et al., 2010). Increase in lactate dehydrogenase (LDHA) converts pyruvate to lactate and monocarboxylate transporter 4 (Mct4) transports lactate out of the cell to prevent acidification (Cantley et al., 2013, Mookerjee et al., 2017). Glut1 is a glucose transporter used to transfer glucose into the cell through the cell membrane for intracellular energy generation (Cantley et al., 2013, Cantley et al., 2010). Interest in analysing impact of oxygen deprivation is driven by the relationship between hypoxia and transplant outcomes with impaired insulin release and glucose homeostasis as well as glucose sensing (Cantley et al., 2013). Hypoxia is not only a problem after isolation and during culture, but also after transplantation with the revascularisation taking up to ten days during which time islets are dependent on oxygen supply via diffusion (Menger et al., 1989). Furthermore it was shown by a study of Olsson et al., that revascularisation is still increasing up to at least three months after transplantation (Olsson et al., 2011). It was shown that the oxygen tension in transplanted islets was dramatically reduced at 5-10 mmHg even 9-12 weeks after transplantation, compared to islets *in situ* with 40 mmHg (Carlsson et al., 2001). In addition to the loss of oxygen supply, decreased supply of nutrients due to loss of connection to the capillary network may lead to increasing cell

death in the islet core (Giuliani et al., 2005). Various approaches have been studied to date to reduce hypoxia in islets during culture as well as after transplantation towards improved transplant outcomes. For improvement of oxygenation during islet preservation, different culture systems including a rotating platform or a microgravity bioreactor have been used (Murray et al., 2005, Rutzky et al., 2002, Daoud et al., 2010b). The rotating system improved morphology and insulin secretion over a prolonged preservation time (Murray et al., 2005). Culture in a microgravity system introduced hollow channels into isolated mouse islets potentially improving oxygenation leading to maintained ultrastructure of endocrine cells (Rutzky et al., 2002). These techniques improved islets *in vitro*, but as soon as islets were transplanted, they were exposed to low oxygen conditions again. One strategy to improve islets even after transplantation is to provide oxygen through encapsulation in oxygen generating materials or external through bioartificial devices including β -Air (Pedraza et al., 2012, Barkai et al., 2013). With oxygen generating CaO_2 islet cell death *ex vivo* could be decreased in addition to improved *in vivo* function of islets in an encapsulated mouse model (Pedraza et al., 2012, Coronel et al., 2019). Bioartificial pancreata have shown a beneficial effect of oxygen supply on islets in a mouse model, but could not improve metabolic control in a phase I study (Barkai et al., 2013, Carlsson et al., 2018).

5.2 Aims

Islets lose their specific microenvironment through the isolation process increasing stress and hypoxia leading to impaired function and loss of mass. ECM replacement therapies provide islets with crucial cell matrix contacts but can increase existent hypoxia even further. This chapter examined different strategies to provide islets with ECM components simultaneously with reducing hypoxia for improved islet viability and function. The specific aims and objectives were:

Overall aim: To develop bioengineering approaches to reduce hypoxic impact on β -cells and restore lost ECM in the islet microenvironment.

Objective 1: To develop a bioengineered construct with CAF hydrogel.

Objective 2: To characterise impact of dynamic culture on pseudoislet viability and gene expression with and without the presence of CAF hydrogel.

Objective 3: To characterise the impact of an electrospun nanofiber membrane on viability and morphology in mouse islets.

Objective 4: To develop a proof of concept system for hydrogel perfusion.

Objective 5: To characterise CAF hydrogel in a perfusion system.

5.3 Results

5.3.1 *Microwells in hydrogel as ECM replacement*

To overcome the problem of increasing hypoxia with ECM replacement during prolonged islet culture a model with microwells was developed similar to that by (Skrzypek et al., 2017). This model allows contact to ECM components while through an open top access to nutrients and oxygen. Therefore, a synthetic polymer stamp, generated by a 3D laser bioprinting method, was provided by the mechanical engineering group with 200 μm barrels at an interval of 500 μm (Figure 5.1 A). In a first step the stamp was used to generate a hydrogel composed of 2% agarose with microwells (Figure 5.1 B), which was chosen due to its stiffness, making the generated microwell hydrogel easy to handle. Microwells appeared with even shape and distribution correlating with the stamp. After freeze drying of the hydrogel (Figure 5.1 C), some of the microwells were visible (arrows), but it was more difficult to spot them compared to the hydrated hydrogel under the microscope. Pseudoislets were able to fit within microwells (Figure 5.1 D) with 1-3 pseudoislets in a single microwell. Some microwells were observed to be empty and pseudoislets were visible on top of the hydrogel between microwells.

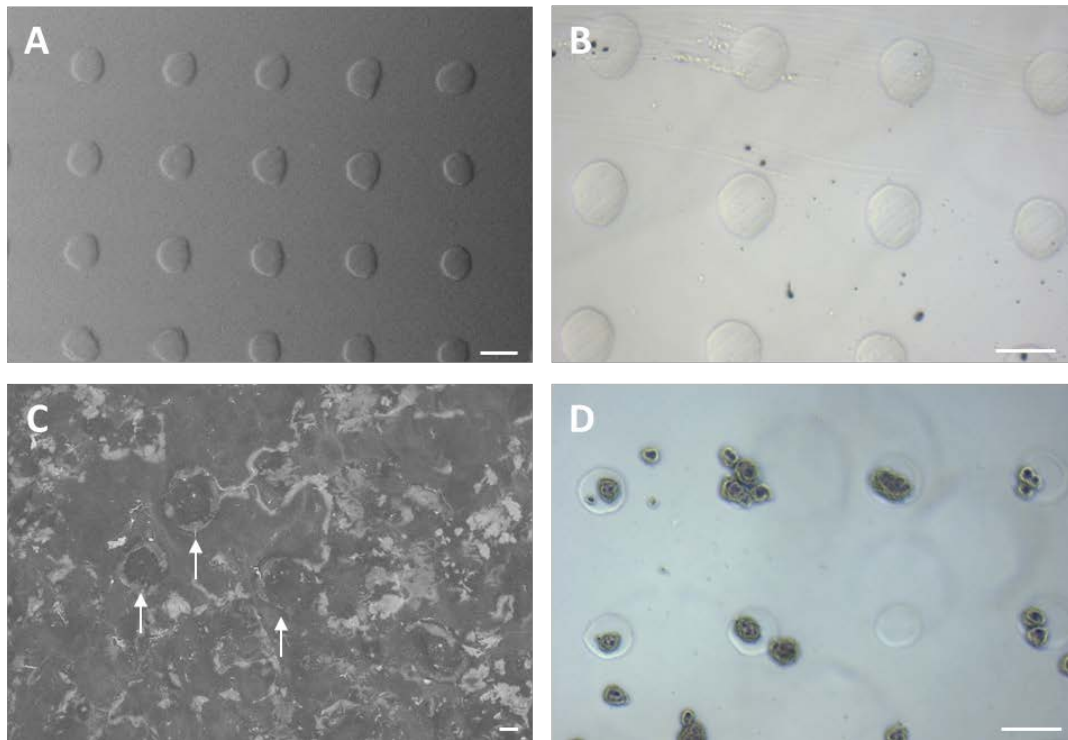


Figure 5.1: Microwells in 2% agarose hydrogel.

A: SEM analysis of stamp with 200 μm diameter barrels at an interval of 500 μm . B: Agarose hydrogel with microwells visible. C: Freeze dried agarose hydrogel with microwells (arrow) visible. D: Agarose hydrogel with microwells and pseudoislets. Scale bars 200 μm .

Exchanging agarose with the CAF hydrogel led to difficulties in removing the hydrogel from the stamp, due to the different mechanical properties and resulting softness of the CAF hydrogel leading to breaks in the gel. The photograph in Figure 5.2 shows fragments of CAF hydrogel after removal from the stamp in PBS in a 12-well plate.



Figure 5.2: CAF hydrogels after removal from the stamp in PBS in a 12-well plate.

5.3.2 Coated wells in dynamic culture for reduction of hypoxia

5.3.2.1 Morphology and integrity assessment

Another approach to reduce hypoxia during islet culture and provide ECM components at the same time was to add a dynamic platform to the coated well system. Pseudoislets were either added onto wells with or without CAF and were then incubated in static culture or on a rotating platform (63 rpm). Figure 5.3 showed pseudoislets after 72 h of static culture in control (A) and CAF-coated (B) wells and rotation culture in control (C) and CAF-coated wells (D). Pseudoislets possessed smaller diameter after static compared to rotation culture with loss of pseudocapsule being observed after static culture in control wells. Integrity and shape of pseudoislets was improved through CAF-coating in static culture and through rotation culture in control wells. Rotation culture in CAF-coated wells often led to clumping of pseudoislets.

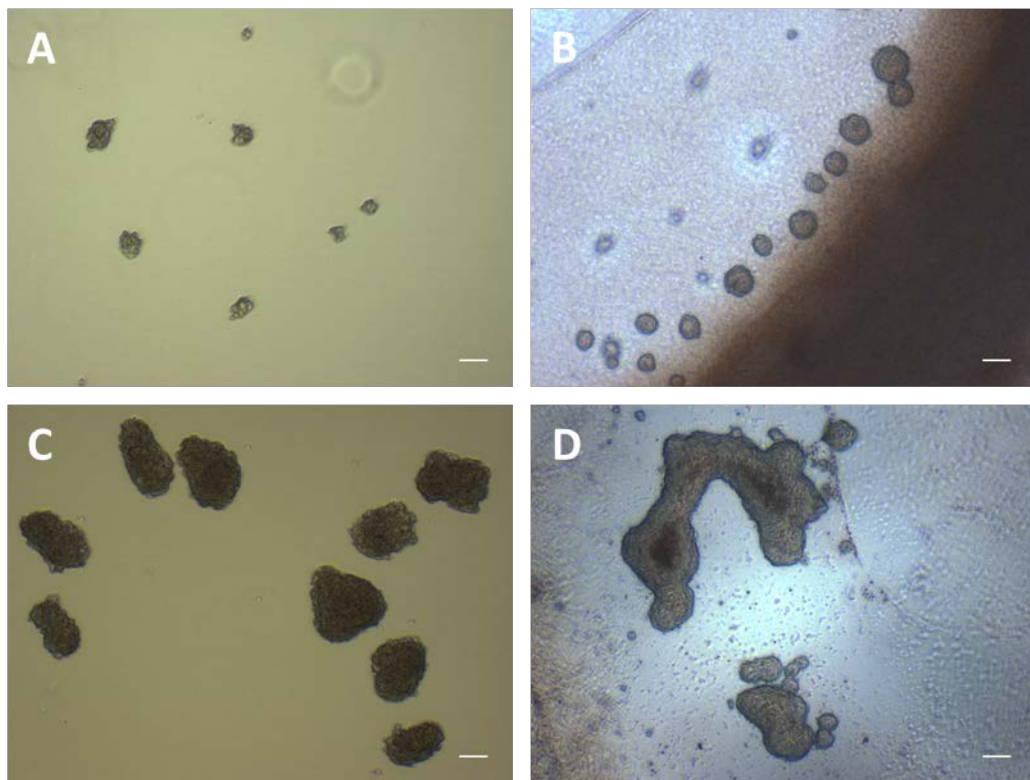


Figure 5.3: Pseudoislets after 72 h of static (A+B) or rotation (C+D) culture in control wells (A+C) or CAF-coated wells (D). Scale bars 100 μ m.

These observations could be confirmed with a qualitative scoring described in 4.3.2.6 (Matsumoto et al., 2004). Integrity was scored the lowest after static culture in control wells at 2.5 ± 0.6 (n=4) and was increased after static culture on CAF-coated wells 5.6 ± 0.6 (n=3), as well as rotation culture in control 5.1 ± 1.0 (n=2) and CAF-coated wells 5.2 ± 1.3 (n=3) (Figure 5.4). Statistical analysis with an unpaired t-test showed significant improvement of integrity score after static culture in CAF-coated wells ($p < 0.001$), rotation culture in control wells ($p < 0.05$), and rotation culture in CAF-coated wells ($p < 0.05$) compared to static culture in control wells.

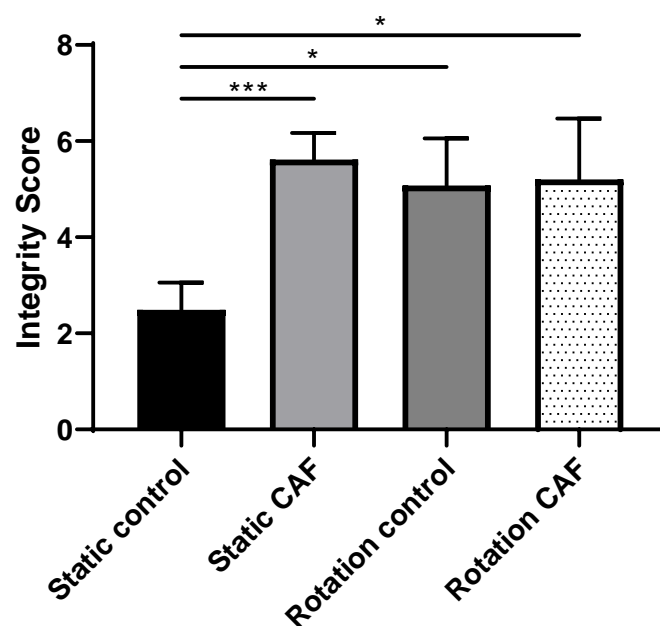


Figure 5.4: Integrity score of pseudoislets after static and rotation culture in control and CAF-coated wells (n≥2). Unpaired Student's t-tests revealed significant differences between static culture in control wells with static culture in CAF-coated wells ($p < 0.001$), rotation culture in control wells ($p < 0.05$), and rotation culture in CAF-coated wells ($p < 0.05$).

5.3.2.2 Viability assessment

Viability was assessed by PI staining after 72 h culture in the different culture systems (Figure 5.5). With viability of $76 \pm 6\%$ (n=7) after static culture in control wells, $78 \pm 6\%$ (n=6) after static culture in CAF-coated wells, $69 \pm 5\%$ (n=3) after rotation culture in control wells, $73 \pm 4\%$ (n=3) after rotation culture in CAF-coated wells. The minor decrease of viability after rotation culture in control wells can be explained with the higher diameter in these islets (Figure 5.3). However, overall viability appeared to be maintained in all conditions with no significant differences.

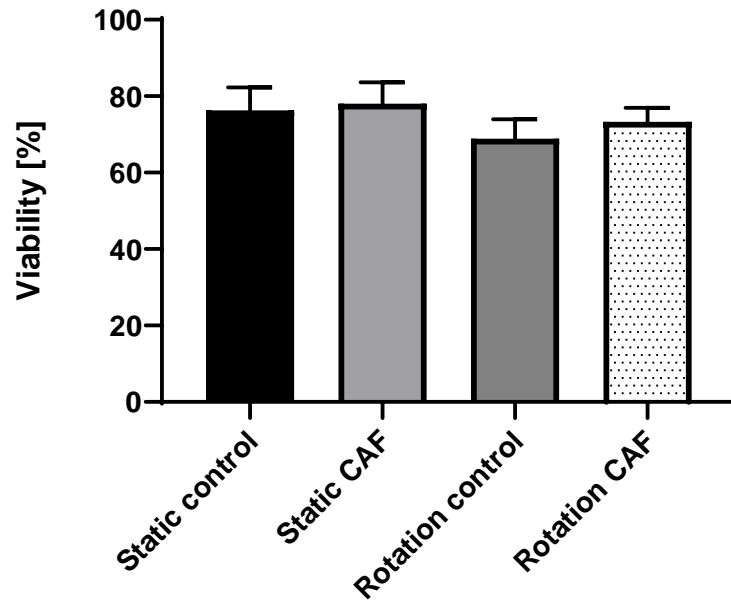


Figure 5.5: Viability assessment of pseudoislets (p27-p29) in different culture systems including static control, static CAF, rotation control and rotation CAF.

For control conditions pseudoislets were cultured in tissue culture suspension wells and for CAF conditions wells were coated with CAF hydrogel and pseudoislets were cultured on top of the hydrogel. Static culture was implemented by incubation at 37°C with 20% O₂ and 5% CO₂. For rotation culture the plates were incubated on a rotating platform with a speed of 63 rpm. N≥3 independent experiments.

5.3.2.3 Hypoxia assessment with pimonidazole staining and gene expression

Staining with pimonidazole (PIM) revealed the presence of hypoxia in pseudoislet cores after static culture in control wells (Figure 5.6 A1-A3) as well as CAF-coated wells (Figure 5.6 C1-C3), whereas islets with comparable size did not show PIM present inside the islet core after rotation culture (Figure 5.6 B1-B3, D1-D3).

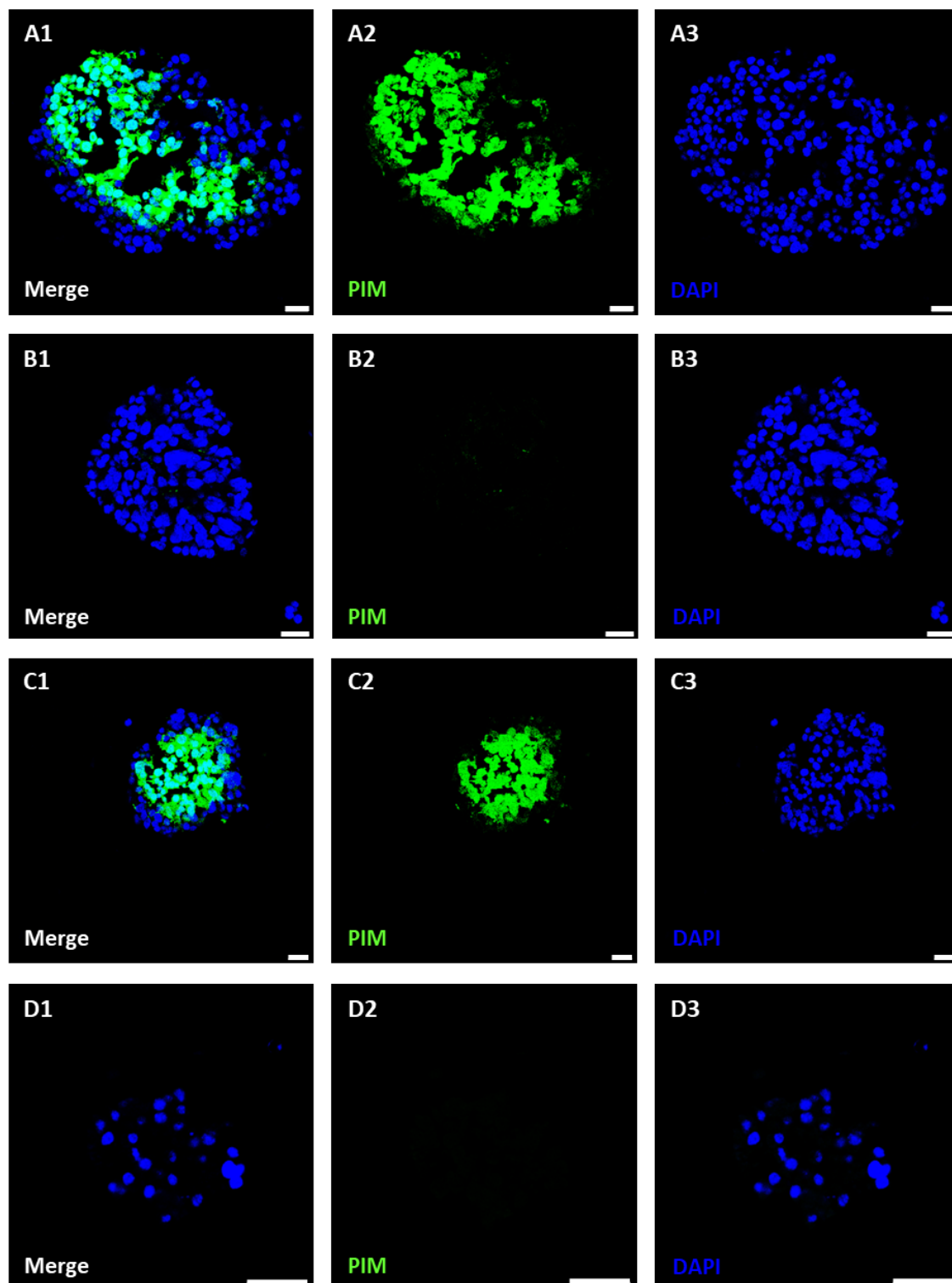


Figure 5.6: Immunofluorescence staining of pseudoislets after different culture conditions with pimonidazole (PIM) in green (A2, B2, C2, D2) and DAPI in blue (A3, B3, C3, D3).

Merge of both channels in A1, B1, C1, D1. Pseudoislets after static (A1-A3) and rotation (B1-B3) culture in control wells, after static (C1-C3) and rotation (D1-D3) culture in CAF-coated wells. Scale bars: 25 μm .

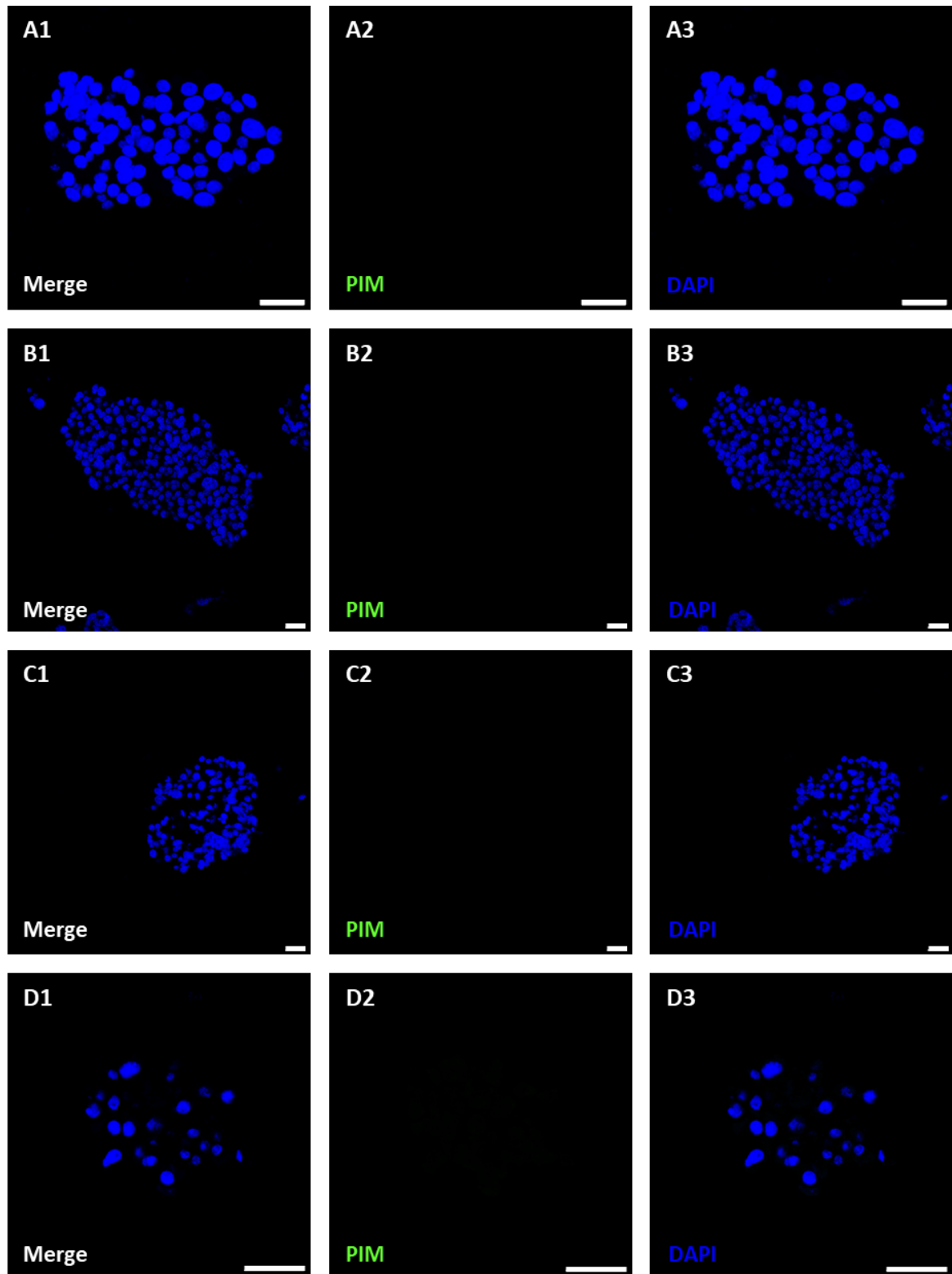


Figure 5.7: No primary antibody control of pseudoislets after different culture conditions with pimonidazole (PIM) in green (A2, B2, C2, D2) and DAPI in blue (A3, B3, C3, D3). Merge of both channels in A1, B1, C1, and D1. Pseudoislets after static (A1-A3) and rotation (B1-B3) culture in control wells, after static (C1-C3) and rotation (D1-D3) culture in CAF-coated wells. Scale bars: 25 μ m.

Gene expression was analysed with qRT-PCR for insulin (*Ins 1* and *Ins 2*), hypoxia induced genes *LDHA*, *Mct4* and *Glut1*, and the β -cell dedifferentiation marker *urocortin 3* (*U3*) (Figure 5.8). After static culture in CAF-coated wells insulin gene expression was similar to control culture, whereas hypoxia induced genes showed a slight reduction, and *U3* an increased expression. After rotation culture in control wells *Ins 1* was expressed at a similar level compared to static control conditions whereas *Ins 2* showed an increased expression. Hypoxia induced gene expression was reduced, and *U3* expression increased. Rotation culture on CAF-coated wells led to a small reduction in *Ins 1* expression, whereas *Ins 2* was expressed at a similar level to static control conditions. Hypoxia induced genes showed further reduced expression compared rotation control conditions. Expression of *U3* was at a similar level compared to static control conditions.

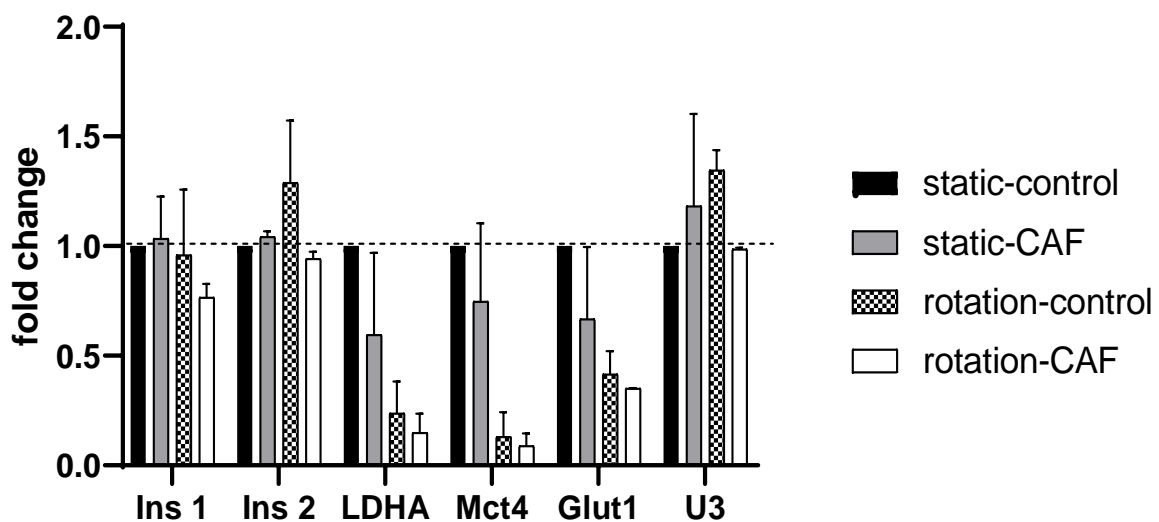


Figure 5.8: Expression of insulin genes (*Ins 1* and *Ins 2*), hypoxia induced genes (*LDHA*, *Mct4*, *Glut1*) and *urocortin 3* (*U3*) in pseudoislets (p26 and p27) after 72 h of culture in static control, static CAF, rotation control, and rotation CAF conditions.

Displayed are averages with SD from two independent experiments composed of three wells. Expression was normalised to static control culture conditions.

5.3.2.4 Metabolic assessment of static and rotation culture in CAF-coated wells

Seahorse flux analysis revealed ATP production rate of pseudoislets after culture on CAF-coated wells in static and rotation conditions (Figure 5.9). Due to the limited number of wells on the islet capture plate, just two different conditions could be analysed per one experiment. Pseudoislets in CAF-coated wells and static culture (S1+S2) showed a higher

ATP production rate via OXPHOS leading to a higher total ATP production rate compared to rotation culture (R1+R2). ATP production via glycolysis was similar in CAF S1 and CAF R1 excluding one higher value in CAF S1. ATP production via glycolysis in CAF S2 and CAF R2 was very low compared to CAF S1 and CAF R1. ATP production via OXPHOS in CAF S2 and CAF R2 was very low compared to CAF S1 and CAF R1. ATP production via OXPHOS seemed more variable after static culture compared to rotation culture excluding one very high value in CAF R2.

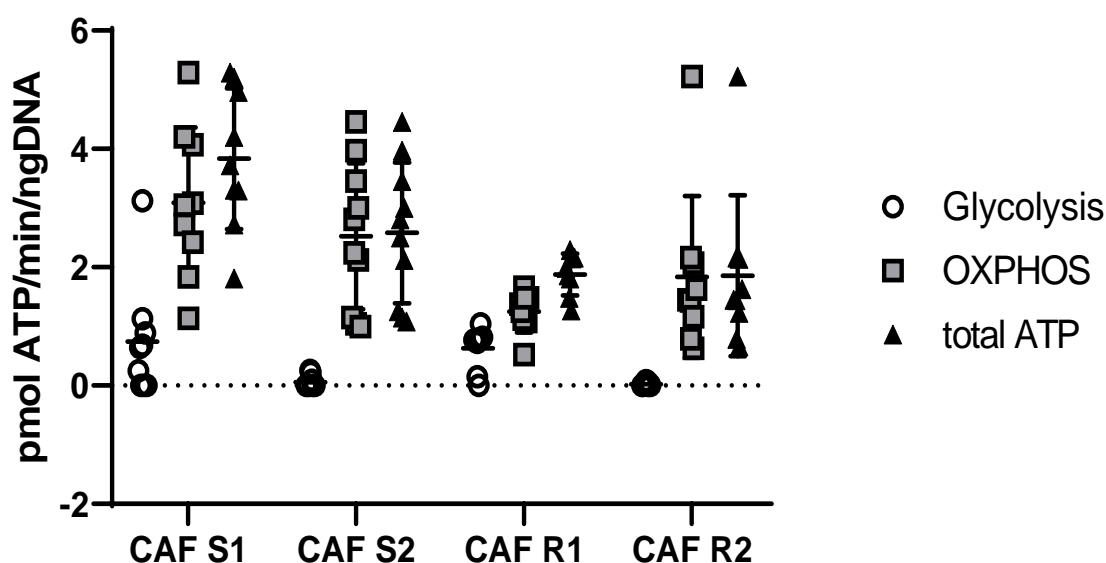


Figure 5.9: Analysis of metabolic activity of pseudoislets (p27 and p28) cultured on CAF-coated wells in static (S1+S2) or rotation (R1+R2) condition. ATP production rate via glycolysis (white circles), OXPHOS (grey squares) and total (black triangles) is shown for each well for two independent experiments.

5.3.3 Electrospun nanofiber membrane for improved revascularisation of isolated islets

5.3.3.1 Fibre analysis and mouse islet seeding

An additional idea to reduce hypoxia during islet culture was to use electrospun nanofiber membranes for the possible delivery of angiogenesis markers including VEGF-A. Electrospun PCL nanofibers were kindly provided by Dr Piergiorgio Gentile from the School of Engineering at Newcastle University. Mouse islets were isolated and seeded on top of the membrane and interaction of islets and membrane was analysed after 1-4 days of culture. Obtained fibre membranes were analysed with SEM showing fibre mesh/network at low (Figure 5.10 A) and higher magnification (Figure 5.10 B). Analysis with Image J

revealed a fibre diameter between $\sim 0.17\ \mu\text{m}$ and $\sim 1.39\ \mu\text{m}$. Mouse islets were visible after three days of culture in control wells (Figure 5.10 C) and seeded on top of the membrane (Figure 5.10 D) with a round shape, distinct border and high integrity in both culture conditions.

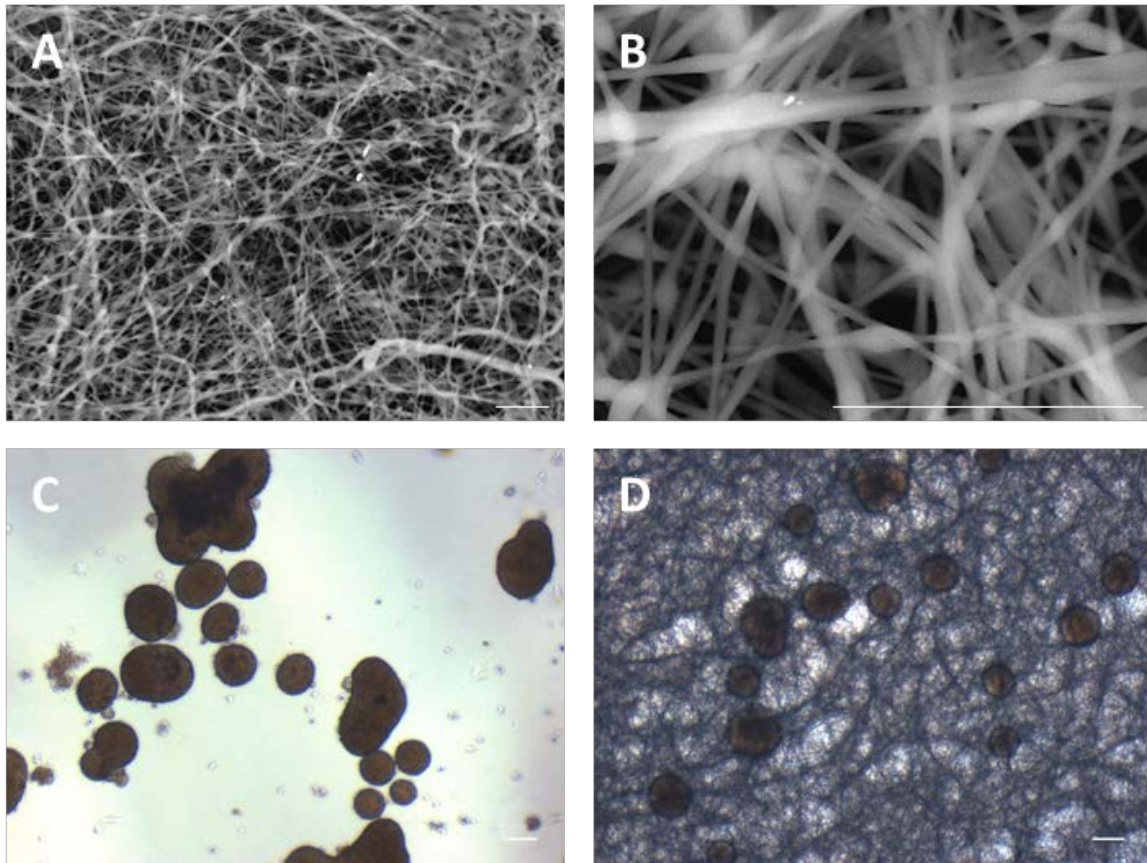


Figure 5.10: Electrospun nanofibers with mouse islets. Nanofibers were analysed with the SEM in low (A) and higher (B) magnification. Mouse islets were analysed after culture in control wells (C) and on top of the membrane (D) after 72 h of culture. Scale bars $10\ \mu\text{m}$ (A+B) and $100\ \mu\text{m}$ (C+D).

5.3.3.2 Viability assessment of mouse islets over culture time

Viability of mouse islets was assessed with PI staining after culture in control wells. Due to low numbers of isolated islets per isolation different batches were analysed at different time points of culture in control conditions, but not of islets cultured on the membrane (Figure 5.11). Viability was assessed as followed: On Day 1 of culture it was $89\pm 14\%$ (10 mouse islets), on Day 2 of culture it was $89\pm 10\%$ (58 mouse islets), on Day 3 of culture it was $85\pm 18\%$ (18 mouse islets), and on Day 4 of culture it was $87\pm 10\%$ (13 mouse islets).

This shows maintenance of viability of mouse islets over at least four days of culture in control wells.

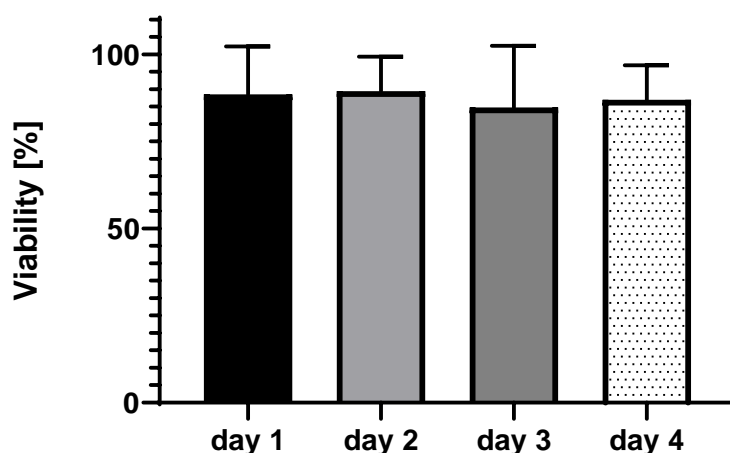


Figure 5.11: Viability of different batches of mouse islets at Day 1-4 of culture in control wells. Average viability displayed with SD of 10-58 islets assessed.

5.3.3.3 Immunofluorescent staining of mouse islets after culture on membrane

Mouse islets cultured on top of the membrane were fixed and stained for insulin, collagen IV and DAPI (Figure 5.12). Due to low mouse islet numbers no control without primary antibody was used. Insulin staining in green (Figure 5.12 A2+B2) as well as DAPI staining in blue (Figure 5.12 A4+B4) showed islet location in addition to indicating viability and function. Analysis of an islet at lower magnification (Figure 5.12 A1-A4) suggested out-growth of single cells from the islet, which could be confirmed with the analysis of an islet at higher magnification (Figure 5.12 B1-B4). Collagen IV staining in red (Figure 5.12 A3+B3) seemed to non-specific.

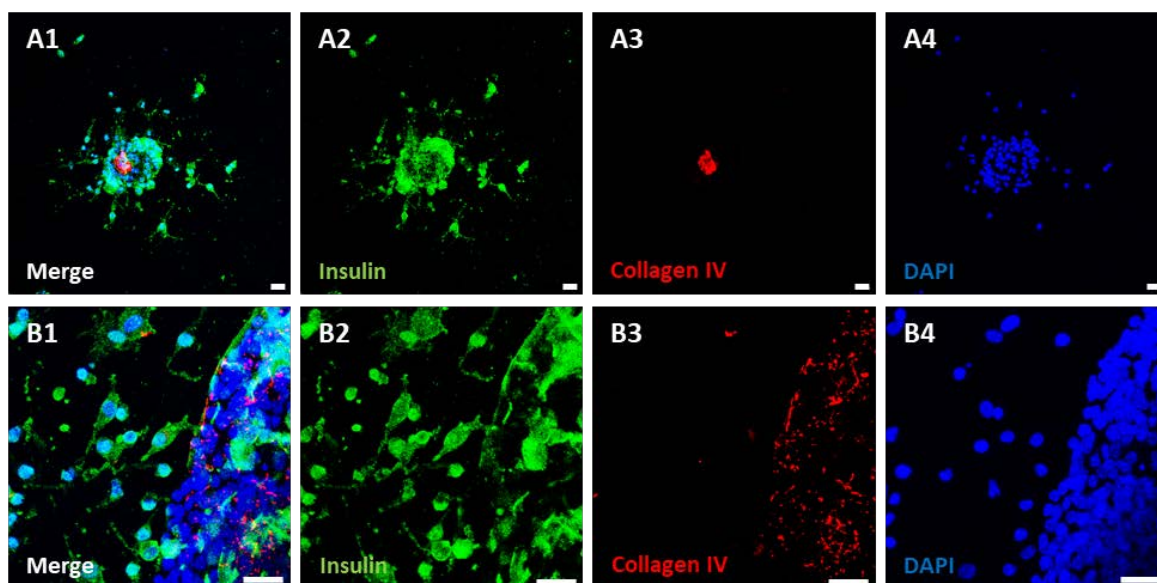


Figure 5.12: Immunofluorescence staining of mouse islets after culture on electrospun nanofiber membrane for three days.

A whole islet (A1-A4) as well as an islet boarder (B1-B4) were stained for insulin in green (A2+B2), collagen IV in red (A3+B3) and DAPI in blue (A4+B4). Merge were shown in A1 and B1. Scale bars: 25 μ m.

5.3.4 Hydrogel perfusion for reduction of hypoxia in encapsulated pseudoislets

5.3.4.1 Morphology of encapsulated pseudoislets in static culture

Pseudoislets were encapsulated in CAF hydrogel and cultured for 72 h in static conditions. Most pseudoislets in control wells were attached to the plastic after 72 h of culture, showing loss of integrity and shape with single cells growing out of the cell cluster (Figure 5.13 A). Encapsulated pseudoislets on the other hand contained their pseudocapsule and integrity with no single cell out-growth from the cell cluster observed (Figure 5.13 B+C). It was possible to observe encapsulated pseudoislets if the CAF hydrogel was thin enough for the light to penetrate the gel whereas this was increasingly challenging with thickening of gel where the light could no longer penetrate, seen in the bottom right corner of Figure 5.13 C.

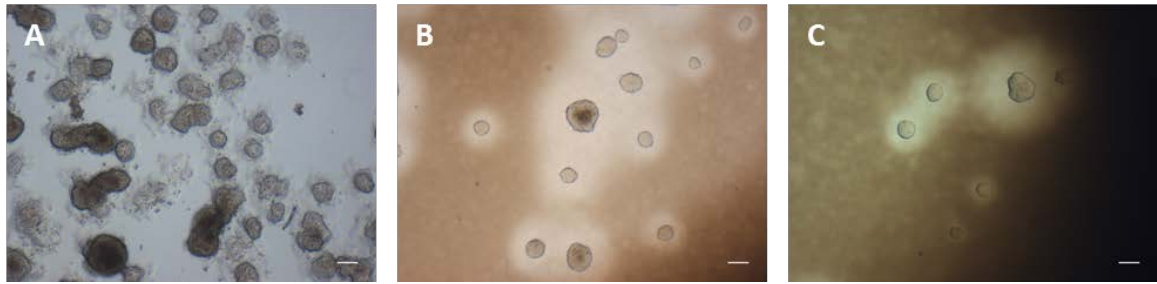


Figure 5.13: Pseudoislets after culture of 72 h in control wells (A) and encapsulated (B+C). Scale bars 100 μ m.

Integrity was assessed with the previously employed scoring method (4.3.2.6) and compared to static culture in control wells (Figure 5.14). Integrity of encapsulated pseudoislets after 72 h of static culture was assessed with mean score 6.0 ± 0.5 ($n=5$) compared to static culture in control wells with a score of 2.5 ± 0.6 ($n=4$) (Figure 5.1). A significant positive impact of encapsulation on the integrity score was evaluated with the statistical assessment through an unpaired Student's t-test, compared to static culture in control wells with $p < 0.0001$.

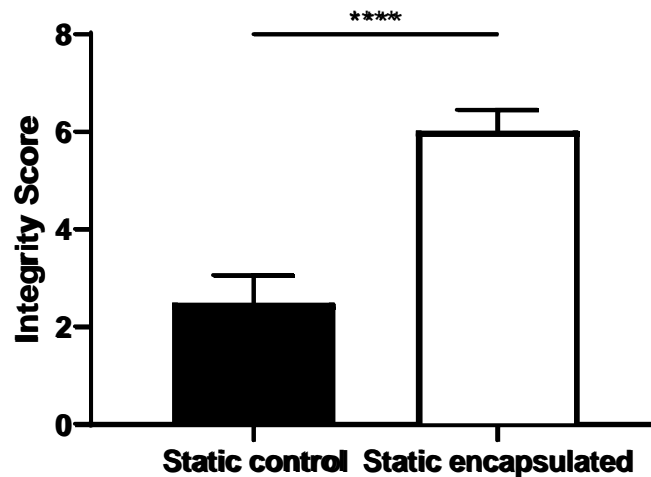


Figure 5.14: Integrity score of pseudoislets after static culture encapsulated in CAF hydrogel compared to islets in static control conditions. Average score displayed of $n \geq 4$ experiments with SD. Unpaired t-test showed significant impact of encapsulation on integrity score ($p < 0.0001$).

5.3.4.2 Viability of encapsulated islets

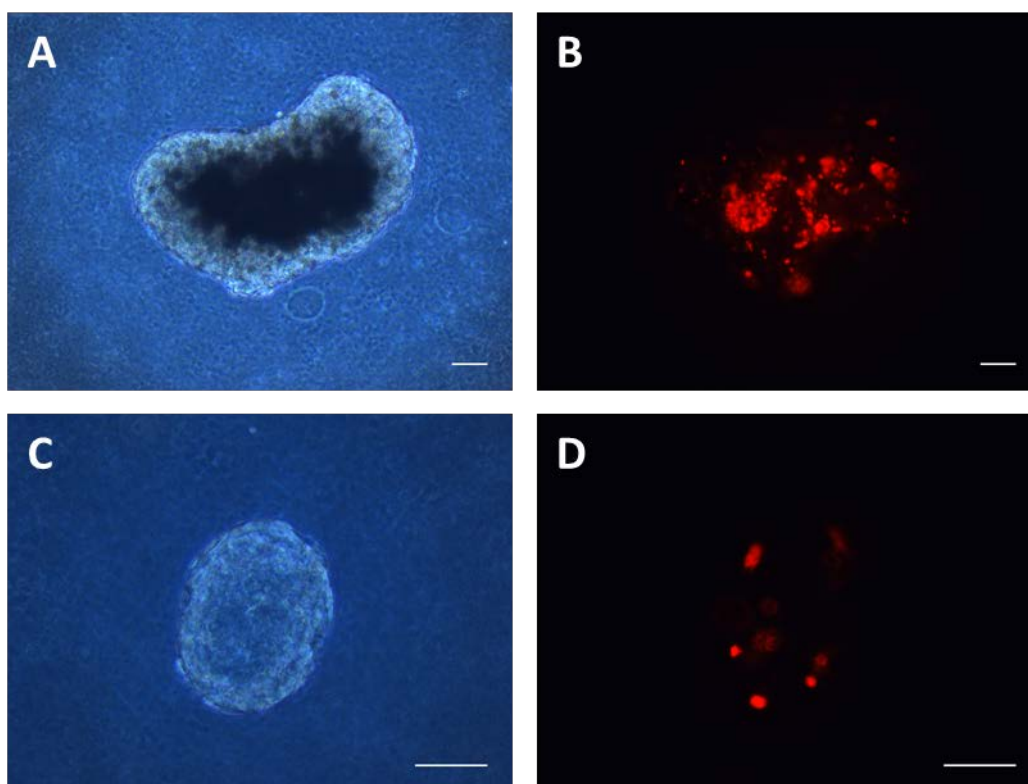


Figure 5.15: Viability assessment with PI staining with two examples of encapsulated pseudoislets shown after 72 h of static culture.

A bigger islet (A+B) and a smaller islet (C+D) were assessed with phase contrast (A+C) and with red fluorescent PI staining (B+D). Scale bars 50 μ m.

Viability of pseudoislets was assessed using PI staining after 72 h of culture (Figure 5.15+Figure 5.16). PI staining was possible if hydrogel was thin enough for assessment of pseudoislets under the microscope (Figure 5.15 A+C). PI stain was able to penetrate the hydrogel and differences between bigger and smaller sized islets could be assessed in the red fluorescent channel (Figure 5.15 B+D). After static culture in control wells pseudoislets had an average viability of 76 ± 6 (n=7) and after encapsulation $83 \pm 5\%$ (n=4), showing a slight, but non-significant improvement.

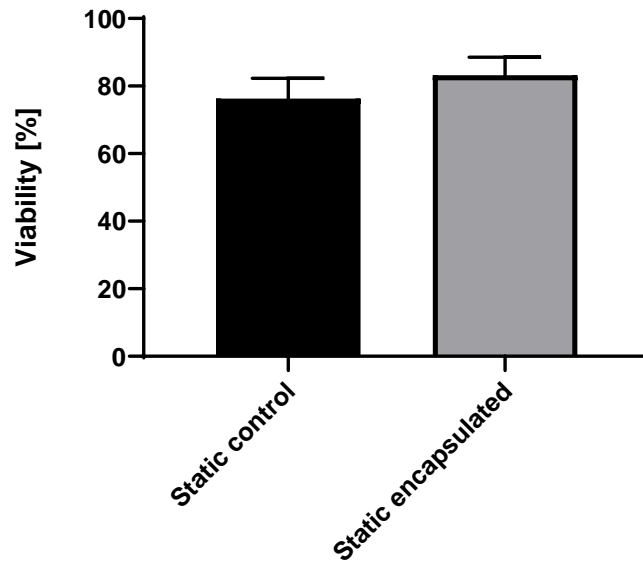


Figure 5.16: Viability of pseudoislets after 72 h of static culture in control wells and encapsulated in hydrogel. Average of $n \geq 4$ displayed with SD.

5.3.4.3 Gene expression of encapsulated pseudoislets

Expression of insulin genes *Ins 1* and *Ins 2*, hypoxia-induced genes *LDHA*, *Mct-4* and *Glut-1* and the end-differentiated β -cell marker *U3* was assessed. Static culture of pseudoislets encapsulated in CAF hydrogel was associated with increased hypoxia-induced gene expression whereas expression of insulin genes and *U3* was comparable to control culture. The addition of dynamic culture to encapsulated pseudoislets decreased the expression of hypoxia induced genes whereas *Ins1*, *Ins2* and *U3* expression were similar to static culture in control wells.

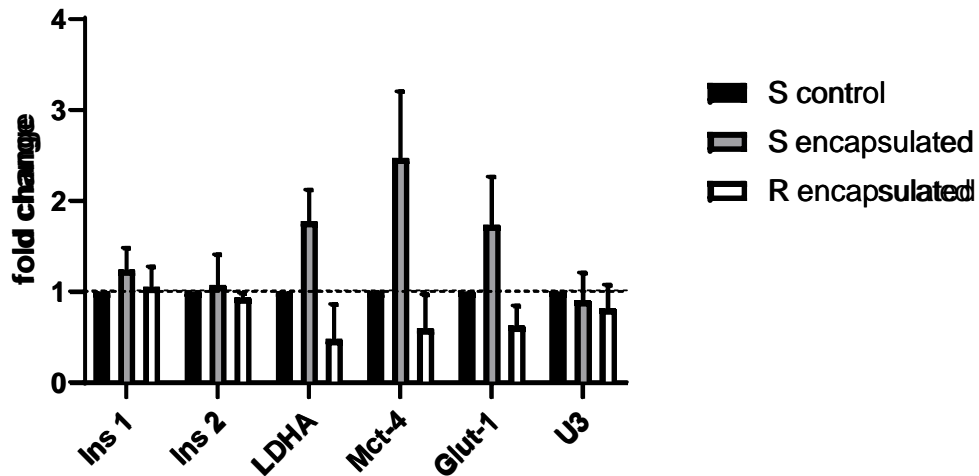


Figure 5.17: Hypoxia induced gene expression of encapsulated pseudoislets after 72 h of static versus rotation culture. Average of two independent experiments displayed with SD.

5.3.4.4 Protein expression of encapsulated islets with and without hypoxia reduction

Encapsulated pseudoislets still express insulin after static (Figure 5.18 1B) as well as rotation culture (Figure 5.18 2B). Additionally, MIN6 cells showed cell-to-cell contacts via E-cadherin protein expression after both culture conditions (Figure 5.18 1C+2C). This indicated that the encapsulated pseudoislets are still functional cell clusters.

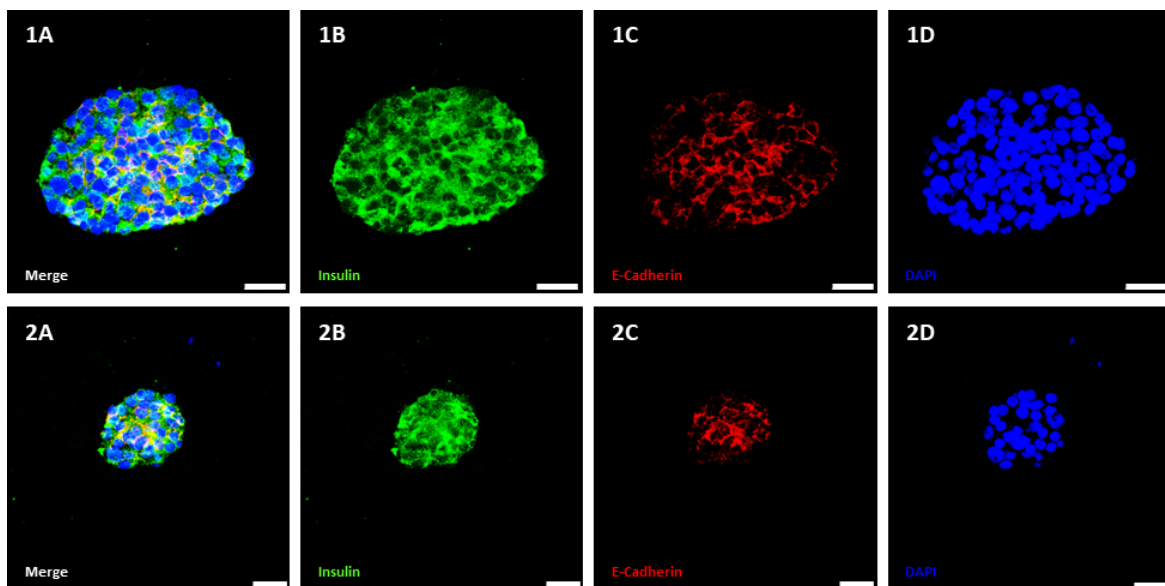


Figure 5.18: Immunofluorescence staining of encapsulated islets after static (1A-1D) and rotation culture (2A-2D). Insulin stained in green (1B, 2B), E-cadherin stained in red (1C, 2C) and DAPI stained in blue (1D, 2D). Merge showed combination of all channels (1A, 2A). Scale bars: 25 μ m.

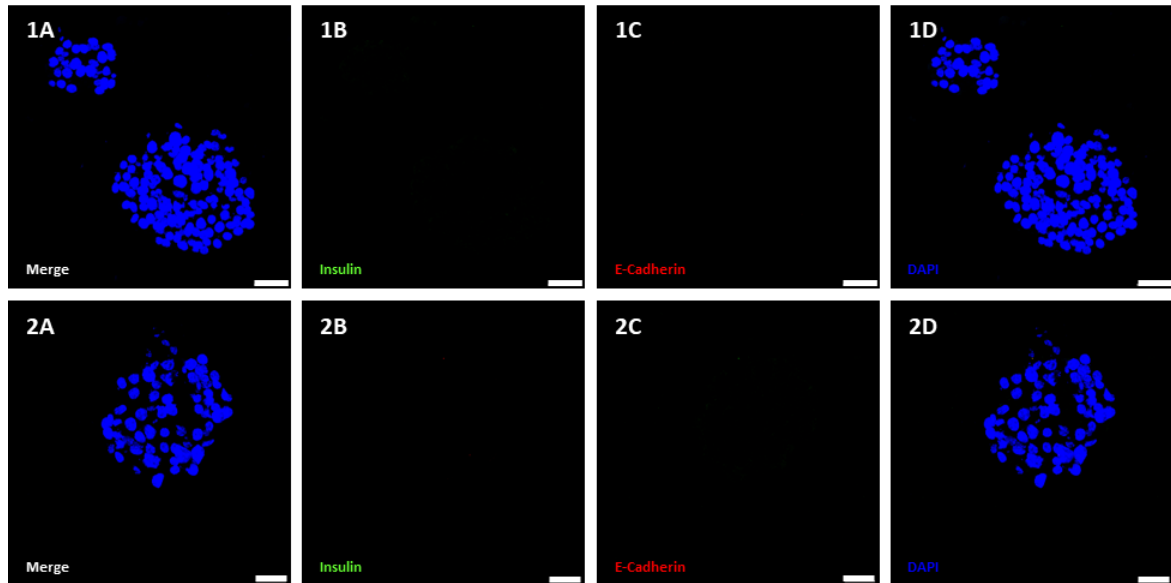


Figure 5.19: No primary antibody control of immunofluorescence staining of encapsulated islets after static (1A-AD) and rotation culture (2A-2D). Insulin stained in green (1B, 2B), E-cadherin stained in red (1C, 2C) and DAPI stained in blue (1D, 2D). Merge showed combination of all channels (1A, 2A). Scale bars: 25 μ m.

5.3.4.5 Perfusion of CAF hydrogel

For primary investigations of the perfusion system, 20 μ l CAF hydrogel without pseudoislets was cross-linked on top of a nylon membrane to enable transfer of the gel in and out of the chambers (Figure 5.20 A). The system was filled with PBS and was adjusted to the lowest possible flow rate of 6.5 ml/min and was allowed to run for \sim 7 h with no observed leaks especially at the chambers (Figure 5.20 B). The CAF hydrogel was still present after the perfusion period (Figure 5.21) which was encouraging for future experiments of perfusion with encapsulated pseudoislets.

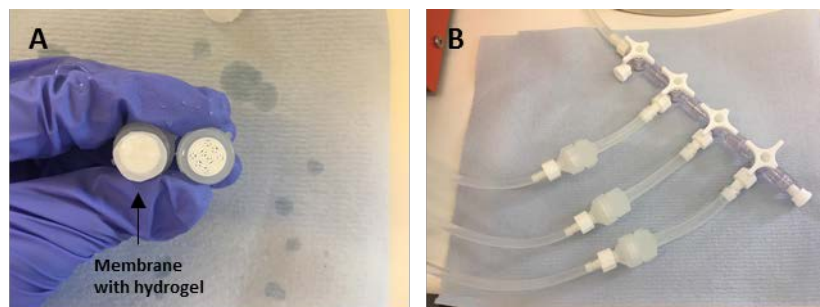


Figure 5.20: Photographs of the perfusion set up with hydrogel. A: Membrane with hydrogel crosslinked on top was placed inside the chamber. B: Three chambers after \sim 7 h of perfusion showing no leak.

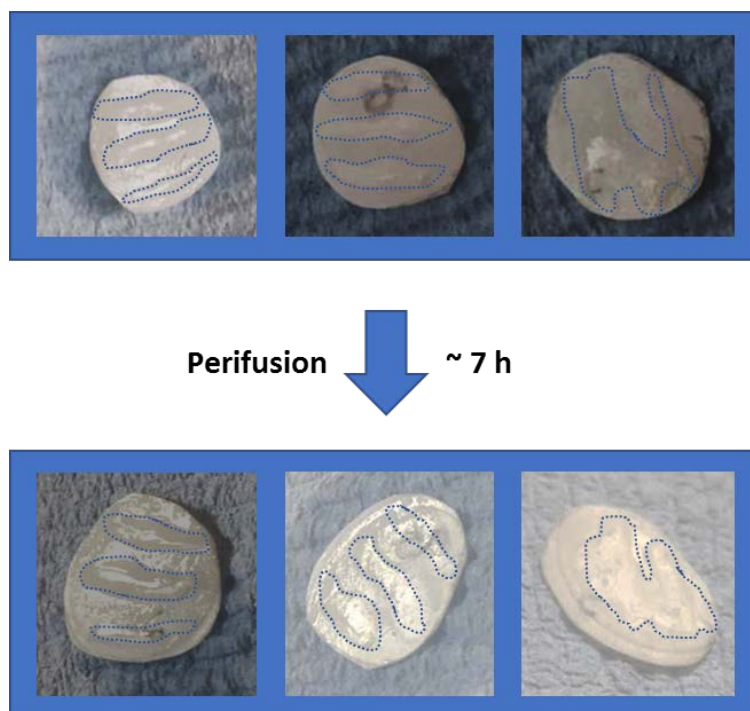


Figure 5.21: Three membranes with CAF hydrogel before and after ~7 h of perfusion.

5.4 Discussion

The present chapter investigated different strategies to provide ECM components to islets while decreasing hypoxia to analyse how a nanofiber-membrane, different hydrogel designs or dynamic culture systems impact on islet health through reduction of hypoxia in combination with ECM presence. It was hypothesised that the reduction of hypoxic stress improves islet integrity, viability and function.

5.4.1 Microwells

Microwells were fabricated to provide ECM contact, but enable oxygen and nutrient supply through an open top. 200 μm was chosen as optimal well, based on an average islet diameter of 100-150 μm to enable as much contact between islet and hydrogel (Longnecker, 2014). However, it has to be noted that microwells in the literature have often had a diameter of 500 μm and therefore larger compared to the microwells in the current experiments, but in previous publications the wells were primarily used to prevent agglutination of islets (Skrzypek et al., 2017, Darling et al., 2018). Microwells in the current study were present in agarose gels generated via a stamp and they were large enough to fit pseudoislets (Figure 5.1). Nevertheless, distribution of pseudoislets inside the wells remained challenging with a lot of them located in between the holes, which has been

observed previously (Darling et al., 2018). One potential for improvement would be to change the design of the gel leaving less space in between single wells similar to designs in the literature with inter-well spaces of 100-200 μm (Darling et al., 2018, Skrzypek et al., 2017). Closer proximity may be beneficial for paracrine effects and communication between islets, which has been shown to be important between single islet cells and therefore could be critical for inter-islet communication (Cabrera et al., 2006, Benninger et al., 2011). Furthermore, the high vascularisation of islets is in keeping with signalling via the vascular network to attain inter-islet communication (Bonner-Weir and Orci, 1982, Cabrera et al., 2006).

Another way of improvement of the hydrogel construct could be a more precise distribution of islets with a bioprinter positioning one islet per well preventing them from sticking together and providing them with a higher gel surface inside the microwells. Previous studies showed that islet cell lines as well as primary islets are still viable after a bioplotting process (Marchioli et al., 2015). Different printing techniques are available for manufacturing of cell containing hydrogels with different resolution, cost and compatible viscosities (Blaeser et al., 2017, Mandrycky et al., 2016).

Preparation of a microwell construct out of CAF hydrogel was not successful due to the mechanical properties leading to a very soft gel which fragmented when the mould was removed (Figure 5.2). Changing gel components could improve mechanical properties towards a stiffer gel, however it must be taken into consideration that the pancreas is a soft tissue and change of mechanical properties may negatively impact islets. It was shown previously that stiffness of cell substrates can impact proliferation, migration, spreading and adhesion of cells (Yang et al., 2017). Analysis of 22 pancreata with magnetic resonance elastography revealed a mean pancreatic stiffness of 1.42 kPa which is comparable to a formulation of the CAF hydrogel with quantities of 2:1:1 and 0.5% collagen (Kolipaka et al., 2017, Montalbano et al., 2018). Furthermore, the preparation of the microwell CAF construct with a stamp may not be the ideal method. The construct could be printed for example with a reactive jet impingement bioprinter which was able to print a CAF hydrogel with the composition of 1:2:8 (da Conceicao Ribeiro et al., 2018). Within an improved microwell construct hypoxia of islets could be assessed after the culture period with PIM staining or analysis of gene expression.

5.4.2 CAF-coating in combination with dynamic culture

An additional approach of providing ECM replacement with simultaneous hypoxia reduction was introduction of dynamic culture for CAF-coated wells. It was shown previously that constant movement in culture systems with rotating vessels or microgravity cultures can be beneficial towards islet viability, integrity and function (Rutzky et al., 2002, Murray et al., 2005, Daoud et al., 2010b).

This combination of CAF-coating and rotating culture in the current project showed improvement of pseudoislet integrity (Figure 5.4), maintenance of viability (Figure 5.5) and reduction of hypoxia-induced gene expression (Figure 5.8). Improvement in integrity and morphology may be due to the lowered adherence properties through alginate containing coating or the continuous movement or a combination of both (Kaido et al., 2006).

Rotation culture of pseudoislets in CAF-coated wells led to clumping (Figure 5.3 D). The seeding density in the current project ranged from 104-208 IEQ/cm² and was therefore in a range where viability and function has been presumed (Brandhorst et al., 2016). However, Papas proposed that at a seeding density of 110-150 IE/cm² anoxia will already impact on islets (Papas et al., 2005). Clumping of islets was also observed by Smink after culture on hydrophilic compared to hydrophobic biomaterials and, with the hydrogel being hydrophilic, aggregation of pseudoislets may be enhanced (Smink et al., 2017). Additionally, the hydrogel may change the dynamics of the medium during the rotation culture due to changes in the liquid volume or the rougher surface (Figure 4.10) compared to the tissue culture plastic. Therefore, a lower rotation speed or seeding density may decrease formation of aggregates. Yet the beneficial effects of the CAF-coating and the rotation culture still positively impacted on pseudoislet viability (Figure 5.5) and morphology (Figure 5.4) compared to static culture in control wells. The decrease in metabolic function after rotation culture in CAF-coated wells (Figure 5.9) in addition to lack of improvement of insulin gene expression with reduced hypoxia (Figure 5.8) may indicate ongoing β -cell stress. This stress could either be due to the hydrophilic properties or components of the hydrogel, but also the increased handling of pseudoislets during the preparation of the Seahorse experiment (Smink et al., 2016, Lim et al., 2011). Changes to the protocols to reduce transfer and washing steps as well as adjustment of hydrogel

components to better match native islet ECM may reduce stress and therefore improve islet function.

5.4.3 Nanofiber membrane

Hypoxia is not only a problem during islet preservation, but also after transplantation until full revascularisation has taken place (Olsson et al., 2011). To approach this problem, it was hoped that islets may incorporate electrospun nanofibers which could have been used to deliver angiogenetic factors into the centre of the islet to attract endothelial cells. Nanofibers built up porous scaffolds with a high surface-to-volume area due the high amount of nanofibers building up the membrane (Ramakrishna et al., 2006). The idea for reducing hypoxia was to improve revascularisation by providing angiogenetic factors including VEGF-A inside of the islets which may stimulate blood vessel formation through attraction of endothelial cells towards the islet core where hypoxia is highest (Komatsu et al., 2017). Delivery of VEGF-A linked to PCL scaffolds was shown to increase revascularisation in a chicken chorioallantoic membrane assay and human islets embedded inside the construct showed maintained response to glucose challenge after seven days' culture (Marchioli et al., 2016). Phase contrast microscopy as well as confocal microscopy confirmed that mouse islets attached to the membrane with single cells growing out of the islets (Figure 5.10 and Figure 5.12) impacting on integrity and possible differentiation status (Weinberg et al., 2007). Minimal outgrowth of single cells was observed with rat islets cultured on laminin coated nanofibers after seven days' culture, but not to as high degree as observed in the current experiments (Sojoodi et al., 2013). Suitable coating of the nanofibers may prevent the attachment of islets and therefore outgrowth of single cells with maintained islet integrity. However, due to the undesired impact on islet integrity the electrospun nanofiber membrane was not further investigated.

5.4.4 Perifusion of encapsulated pseudoislets

A widely used method to provide ECM components is encapsulation of islets, where various techniques have been developed including macro-, micro-, or nano-encapsulation (Desai and Shea, 2017, Song and Roy, 2015, Vaithilingam et al., 2017). ECM contacts have been shown to be beneficial for islets in different models with improved viability, morphology and function (Chun et al., 2008, Blomeier et al., 2006, Daoud et al., 2011).

Encapsulation of pseudoislets in CAF hydrogel improved morphology (Figure 5.14) and maintained viability (Figure 5.16). Furthermore, it was confirmed that viability assessment with PI staining was possible for encapsulated pseudoislets if the CAF hydrogel was thin enough for microscopic assessment (Figure 5.15). However, with the encapsulation process existing hypoxia in islets was increased through decreased nutrient and oxygen transfer (Figure 5.17). It has been shown previously that increasing hypoxia impacts negatively on islet viability and function whereas increased oxygen supply can improve islets (Pedraza et al., 2012, Komatsu et al., 2017). To take advantage of improved morphology and maintained viability of encapsulated pseudoislets, but address the challenge of increasing hypoxia, movement of medium was introduced through a rotating platform. It was shown that through dynamic culture, via a rotating platform, hypoxia in encapsulated pseudoislets could be decreased (Figure 5.17). However, expression of insulin genes was not increased suggesting that the construct needed further improvement. Therefore, a perfusion system was developed to accommodate the hydrogel/ β -cell construct and provide improved oxygen and nutrient supply to the encapsulated islets (2.8.4). Perfusion of islets has been used previously for analysis of function, but not to provide oxygenated media for encapsulated islets. Existing examples of perfusion systems for islet analysis include microfluidic devices, where 1-100 islets are trapped locally in chambers and dynamically perfused for up to 1 h (Shackman et al., 2005, Mohammed et al., 2009). The concept of medium flow around the islets was used in combination with encapsulation to develop the perfusion set up. Preliminary experiments with the perfusion system of the CAF-hydrogel without islets for ~7 h showed promising results for future experiments with encapsulated pseudoislets and human islets.

In summary this thesis showed that the fabrication of microwells in a CAF hydrogel as well as the electrospun nanofiber membrane need further optimisation for their application with β -cells. It was shown that a contact of β -cells to ECM components is necessary for improved islet health with no improved function through dynamic culture on CAF-coated wells. However, encapsulation is increasing hypoxia inside islets and needs to be addressed in future studies, possibly through perfusion methods.

Chapter 6. General discussion and future experiments

6.1 General discussion

Continuous refinements including in organ procurement, isolation processes, islet culture or immunosuppression protocols successfully enhanced outcomes of clinical islet transplantation with improved glycaemic control and insulin independence in 44% of recipients three years after transplantation (Shapiro et al., 2000, Barton et al., 2012). However, insulin independence still requires up to three islet transplants indicating that islet mass and function is compromised through the isolation and transplantation process (Figure 6.1) (Shapiro et al., 2006). Through the isolation process ~50% of the original islet mass can be lost (Ichii et al., 2005). The following culture can further decrease this mass depending on the duration by up to 35% (Noguchi et al., 2012). Approximately 70% can be lost through transplantation and engraftment coupled with stressors including IBMIR or low oxygen tension (Emamaullee and Shapiro, 2007).



Figure 6.1: Loss of islet mass through the isolation and transplantation process.

Maintenance of islet mass, viability and function during the steps of islet transplantation may lead to better transplant outcomes. Therefore, further investigation regarding organ preservation, islet isolation, islet preservation and islet transplantation are needed. The first part of this thesis set out to achieve a better understanding of the impact of pancreas preservation time and the isolation process on exocrine and endocrine cells at the cellular level. In the second part, approaches to replace the lost ECM with a novel hydrogel composed of the three different components collagen I, alginate and fibrinogen were explored (Montalbano et al., 2018, da Conceicao Ribeiro et al., 2018). In the course of the project the three different islet models, MIN6 pseudoislets, mouse isolated islets and human isolated islets, were used to investigate the impact of biomaterials on β -cells. All of these have their advantages and disadvantages (Table 6.1). MIN6 pseudoislets are generated of an insulinoma cell line, which leads to unchecked proliferation of monolayers, in contrast to the low proliferation rate of primary β -cells (Miyazaki et al., 1990, Hauge-Evans et al., 1999). However, they are readily available and can circumvent

ethical concerns of use of animal tissue (Kaur and Dufour, 2012, Persaud et al., 2010). Additionally, they should provide higher repeatability due to their uniform nature and background (Persaud et al., 2010). However, in the current studies, some variability was observed in between different batches of MIN6 cells which may be due to different passage number as well as freezing/thawing techniques. The second used model utilised was isolated mouse islets. These are primary islets which are composed of the different endocrine cell types enabling full *in vitro* evaluation of islet function (Bosco et al., 2010). However, it has to be taken into consideration that the architecture of mouse islets differs to human islets (Cabrera et al., 2006). During this project mouse islets were successfully isolated, but the numbers of isolated islets was too low for the planned experiments which is why MIN6 pseudoislets were mainly used for preliminary biomaterial/cell experiments. Third, human isolated islets were available for a number of experiments. The advantage is that they are composed of all islet cell types and the goal is clearly to improve human isolated islets for transplantation (Bosco et al., 2010, Cabrera et al., 2006). The disadvantage is the availability of islets in addition to a considerable variability in between isolations, but also donor centres *et cetera*. (Persaud et al., 2010, Bonner-Weir et al., 2015). Together, these models provided complementary source of β -cells for the different experiments investigating the impact of the microenvironment on islets.

Table 6.1: Advantages and disadvantages of different islet models used in this thesis.

	Advantages	Disadvantages
MIN6 pseudoislets	<ul style="list-style-type: none"> • Readily available • Higher repeatability 	<ul style="list-style-type: none"> • Tumour origin • Solely β-cells
Isolated mouse islets	<ul style="list-style-type: none"> • Composed of different islet cell types • Readily available 	<ul style="list-style-type: none"> • Different islet architecture to human • Low islet numbers for inexperienced isolator
Isolated human islets	<ul style="list-style-type: none"> • Composed of different islet cell types 	<ul style="list-style-type: none"> • Availability • Variations in donor criteria • Variations in isolation centres

6.1.1 Microenvironment of islets

Islets are highly specialised micro-organs composed of different cell types and tight cell-to-cell connections surrounded by a highly specified niche including an ECM scaffold, a vascular network and acinar tissue (Benninger et al., 2011, Cross et al., 2017, Bosco et al., 2010, Longnecker, 2014). The present study investigated the islet microenvironment at a histological and ultrastructural level and confirmed presence of BM proteins collagen IV and laminin, vasculature and cell-to-cell connections (Figure 3.2, Figure 3.3, Figure 3.6, Figure 3.8, Figure 3.9). All these components are important for optimal function of β -cells. The connection of islet cells to ECM components is important for intracellular signalling pathways via integrin receptors also impacting (Bosco et al., 2000). The vasculature does not solely provide oxygen, but also contact to ECM components through peri-vascular capsule, itself impacting on islet function (Nikolova et al., 2006). Cell-to-cell connection are also important for communication between islet cells. Knock down experiments of connexin 36 led to decreased function revealing a role in insulin secretion (Calabrese et al., 2003). Additionally, E-cadherin has been shown to impact insulin response in a knock out mouse model as well as in human β -cells adhered to cadherin proteins (Wakae-Takada et al., 2013, Parnaud et al., 2015).

Stress during organ preservation and islet isolation impacts on the microenvironment of islets potentially impairing function post-transplant. DBD as well as DCD pancreata with a range of CIT were analysed in this thesis revealing that a histopathological analysis does not reliably show impact of acute stress on pancreas tissue, but TEM analysis with NEMIS revealed impact on some cell organelles (3.3.2). Variation in scores revealed complexity of cellular stress due to hypoxia (Figure 3.13). Previous studies revealed that increasing hypoxia can have a negative affect pancreas transplant outcomes (Rudolph et al., 2017). Extended CIT of 18 h decreased islet yield and *in vivo* function in a mouse model, but K hltreiber was able to show that islet yields from pancreata with CIT ~13 h were acceptable in addition to *in vitro* assessment of function (Pileggi et al., 2009, K hltreiber et al., 2010). However, it was shown that ischaemia affected metabolic pathways of cells leading to accumulation of succinate which generating increased reactive oxygen species after reperfusion of the organ (Chouchani et al., 2014). Furthermore, the lack of oxygen and nutrients leads to damage of cells through apoptosis and necrosis (Giuliani et al.,

2005). In this thesis, the NEMIS score was developed as a new tool to investigate the status of donor pancreata in order to better understand impact of ischaemia on cell morphology. Cell death, especially via necrosis, may have a higher impact on the pancreas due to the digestive enzymes within the acinar cells causing inflammation in the surrounding tissue (Logsdon and Ji, 2013). Pancreatic islets may be more sensitive to ischaemia due to their naturally high oxygen demand (Lifson et al., 1989, Jansson et al., 2016). Improved preservation methods including perfusion or persufflation may decrease organ damage and therefore improve transplant outcomes (Scott et al., 2010, Iwanaga et al., 2008).

Through islet isolation, a large proportion of damaged acinar cells are removed, but the process puts further stress on islets through the mechanical and enzymatic separation of endocrine and exocrine tissue (Rosenberg et al., 1999). Through the ultrastructural analysis of isolated islets, the impact of CIT of the pancreas in addition to the isolation process may be more meaningfully assessed. The severity of the damage may indicate the level of potential reversibility to restore function of islets after transplantation. NEMIS analysis showed differences in degradation of some organelles, but further tissue samples should be analysed for a statistic analysis.

Overall acute stress at a cellular level could be observed through ischaemia as well as islet isolation. NEMIS provides a reliable tool for quantification, but further studies are needed with a standardised imaging and cell number to verify these preliminary findings.

6.1.2 ECM replacement

Islet isolation is leading to loss of the peri-islet capsule impacting on islet health and mass and therefore transplant outcomes. Replacement of this ECM appears to be critical to improve islet viability, morphology and function as shown by previous publications (Chun et al., 2008, Blomeier et al., 2006, Salvay et al., 2008, Daoud et al., 2011). The novel CAF hydrogel has been proposed for use as ECM replacement for isolated islets (Montalbano et al., 2018, da Conceicao Ribeiro et al., 2018). Analysis of the individual components showed no impact on the viability of pseudoislets, demonstrating their biocompatibility (Figure 4.9). The current work showed that presence of ECM components through CAF-coating of tissue culture wells did not impair viability and expression of key protein markers in the pseudoislet model or human isolated islets (Figure 4.13-Figure 4.15). This confirmed basic biocompatibility of CAF hydrogel with both MIN6 pseudoislets and

isolated human islets over 72 h in culture. However, *in vivo* biocompatibility testing remains outstanding to reveal adverse or beneficial effects. Biocompatibility of collagen I, alginate and fibrinogen *in vivo* has been demonstrated previously in rodent and primate models for cartilage, islet and bone research (Dufrane et al., 2006, Liao et al., 2007, Kneser et al., 2005). Nevertheless, the possibility for alginate to cause fibrous capsule formation must be fully investigated as it has been shown previously that alginate encapsulated islets can be surrounded by fibrotic tissue in human trials (Tuch et al., 2009, Jacobs-Tulleneers-Thevissen et al., 2013). In the present study, metabolic activity was maintained in the pseudoislet model after culture on CAF-coated wells compared to control wells, but mixed results were observed for human islets (Figure 4.16). This may indicate better reproducibility of the Seahorse experiment with the pseudoislet model compared to primary islets (Persaud et al., 2010, Hart and Powers, 2019). However, the numbers of experiments was relatively low (as methodology for Seahorse studies in islets had not previously been established in our group) and more repeats may better demonstrate any underlying trend. Providing ECM components via a coating may not be sufficient for β -cell improvement, indicating that a direct contact is required. It was shown previously that rat islets had improved morphology, viability and function if they were in direct contact to ECM producing mesenchymal stem cells compared to co-culture through separated by a semi-permeable insert (Jung et al., 2011). Nevertheless, the integrity score was improved through CAF-coating in the pseudoislet model showing a beneficial effect of the presence of ECM components on morphology. Metabolic analysis revealed increased glycolysis with glucose stimulation potentially as an adaptation to the hypoxic status of the pseudoislets and the isolated human islets with a shift from oxidative phosphorylation to anaerobic glycolysis (Giuliani et al., 2005). Overall, cytocompatibility of CAF with MIN6 pseudoislets as well as human isolated islets could be demonstrated, but hypoxia may decrease positive impact of ECM presence. Approaches to reduce hypoxic exposure were further analysed in the last part of the thesis.

6.1.3 Hypoxia reduction

Presence of ECM components was able to maintain certain aspects of islet health, but did not improve it indicating that hypoxia in the islets may decrease any benefits of the hydrogel (Figure 4.13, Figure 4.16, Figure 4.17). To date, the common method for ECM

replacement has been encapsulation of islets which increases the problem of hypoxia (Pedraza et al., 2012, Smink and de Vos, 2018). Hence, different strategies to reduce hypoxia, but provide ECM components at the same time were assessed.

One approach was the culture of islets in microwells (5.3.1). Therefore, microwells were fabricated with a stamp into a hydrogel, which worked with a stiff gel such as agarose, but remained challenging with the CAF hydrogel (Figure 5.1, Figure 5.2). For better generation of microwells in CAF hydrogel the properties of the hydrogel could be changed towards a stiffer gel, but that may negatively impact on islets. It was shown previously that rat islets as well as MIN6 pseudoislets had a lower insulin gene expression on stiffer scaffolds (Nyitray et al., 2014). Another approach would be to generate microwells without a stamp for example through printing. A previous study showed the potential for bioprinting CAF with a reactive jet impingement, but the different proportion of CAF components to this study needs to be noted (da Conceicao Ribeiro et al., 2018). Additionally, the distribution of islets into the wells remained difficult showing the need for an improvement. Positioning of one islet per well could be achieved with a bioprinter, but the additional stress of handling or printing may impact on islet health (Sankar et al., 2011, Lim et al., 2011). If these challenges could be solved the microwells may be a promising tool to provide ECM components with improved oxygen and nutrient supply compared to fully encapsulated islets.

To reduce hypoxia in islets a dynamic culture was combined with CAF-coating in tissue culture wells to detect if hypoxia was minimizing the beneficial effects of ECM presence (5.3.2). With the rotation platform hypoxia was reduced in pseudoislets, but expression of insulin genes *Ins 1* and *Ins 2* as well as metabolic function was not positively impacted (Figure 5.8, Figure 5.9). This might be caused by the higher passages (p24-p29) of pseudoislets which can impact on their function (Persaud et al., 2010). Furthermore, the rotation speed for CAF-coated wells needs optimisation which was indicated by the clumping of some of the pseudoislets (Figure 5.3). The clumping may impact negatively on the function due to increasing hypoxia (O'Sullivan et al., 2011). Another possibility might be that the presence of ECM components is not sufficient, but that islets need the contact via integrins to trigger intracellular pathways (Krishnamurthy et al., 2011, Stendahl et al., 2009).

To improve revascularisation of islets the interaction of electrospun nanofibers was investigated (5.3.3). Due to the attachment of islets and outgrowth of single insulin positive cells the integrity and possibly the differentiation status were impacted (Russ et al., 2008). The possibility that islets can incorporate nanofibers seems unlikely as Buitinga could not observe that after seven days' culture on electrospun scaffolds (Buitinga et al., 2013).

To improve oxygen and nutrient supply in culture a perfusion system for encapsulated islets was developed (5.3.4). Encapsulation of pseudoislets further improved the integrity score compared to other culture conditions (Figure 5.4). Jung showed that the contact with ECM-producing mesenchymal stem cells leads to significant improvement of rat islet morphology compared to co-culture through an insert (Jung et al., 2011). However, hypoxia in encapsulated islets in static culture was increased (Figure 5.17) which might explain why the beneficial effect of the gel was not evident through improved viability (Figure 5.16) or insulin protein expression (Figure 5.18). Insulin gene expression was not highly impacted through hypoxia or reduction of hypoxia in dynamic culture of encapsulated islets. But the reduction of hypoxia exposure might not have been sufficient for a beneficial effect. Towards a better oxygen supply for the islets the perfusion system was developed with the goal of combining the positive effects of ECM contact with hypoxia minimisation for improved islet health. This may also provide a tool for continuous long term monitoring of encapsulated islets and impact of changes in glucose levels on islet function, similar to existing perfusion systems (Lacy et al., 1976, Bentsi-Barnes et al., 2011). Preliminary tests with CAF hydrogel showed promising stability for around 7 h.

Overall it was shown that presence of ECM components even with reduced hypoxia through dynamic culture is not sufficient for improving islet viability, morphology and function during culture (5.3.2). This leads to the assumption that direct contact of β -cells with ECM components is necessary. However, increasing hypoxia in encapsulated systems needs to be addressed. In this thesis it was hypothesised that a media flow alongside the hydrogel may decrease hypoxia and at the same time provide necessary ECM contact. Therefore, a perfusion system was developed and preliminary experiments with CAF hydrogel alone showed promising stability for future experiments.

6.2 Future experiments

For a better understanding of impact of CIT on acinar and endocrine cells, the NEMIS could be applied to higher quality images for additional pancreata. In addition, pancreata with low CIT will be sampled over various time points of increasing CIT to investigate whether the score increases with extended storage time. It would also be interesting to combine these findings with the analysis of stress markers such cytokines or cell death with protein analysis or IF staining of the corresponding pancreata for greater mechanistic understanding. The impact of islet isolation should be investigated further with the extended NEMIS on more isolated islet preparations. If a biopsy sample prior to the isolation process is available, impact of the isolation process on endocrine cells could be analysed through comparison of islet *in situ* and following isolation. In addition, fresh islet samples and tissue sections could be interrogated for stress markers.

For a better understanding of islet function glucose stimulated insulin secretion could be measured in parallel to Seahorse flux analysis. It would also be interesting to investigate islet function *in situ* which may be possible through precision cut tissue slicing. Expression of proteins participating in glycolysis and oxidative phosphorylation could be analysed via western blot or staining in pancreas sections, isolated islets and islets after different culture conditions to investigate changes in metabolic pathways.

As a next step in the ECM replacement strategy, the combination of encapsulation and perfusion will be investigated. Therefore, the perfusion system requires further optimisation to reduce the flow rate as well as provide sterile conditions for cell experiments. After an extended culture, encapsulated pseudoislets will be analysed for viability, morphology, protein expression and function. If possible, human isolated islets will be used to investigate impact of encapsulation and decreased hypoxia in primary cells. In a final step the CAF hydrogel should be tested in an *in vivo* model for biocompatibility, but predominantly to assess potential for improve function of transplanted islets compared to a conventional transplantation method.

References

- ABDUL-RASOUL, M., HABIB, H. & AL-KHOULY, M. 2006. 'The honeymoon phase' in children with type 1 diabetes mellitus: frequency, duration, and influential factors. *Pediatric Diabetes*, 7, 101-107.
- AKINLADE, A. T., OGBERA, A. O., FASANMADE, O. A. & OLAMOYEGUN, M. A. 2014. Serum C-peptide assay of patients with hyperglycemic emergencies at the Lagos State University Teaching Hospital (LASUTH), Ikeja. *International archives of medicine*, 7, 50.
- AMERICAN DIABETES ASSOCIATION 2004. Diagnosis and Classification of Diabetes Mellitus. *Diabetes Care*, 27, s5-s10.
- AMERICAN DIABETES ASSOCIATION 2010. Diagnosis and classification of diabetes mellitus. *Diabetes Care*, 33 Suppl 1, S62-9.
- ANDERSEN, T., AUK-EMBLEM, P. & DORNISH, M. 2015. 3D Cell Culture in Alginate Hydrogels. *Microarrays (Basel, Switzerland)*, 4, 133-161.
- ANDRALI, SREENATH S., SAMPLEY, MEGAN L., VANDERFORD, NATHAN L. & ÖZCAN, S. 2008. Glucose regulation of insulin gene expression in pancreatic β -cells. *Biochemical Journal*, 415, 1-10.
- ASHCROFT, FRANCES M. & RORSMAN, P. 2012. Diabetes Mellitus and the β Cell: The Last Ten Years. *Cell*, 148, 1160-1171.
- ATKINSON, M. A., EISENBARTH, G. S. & MICHELS, A. W. 2014. Type 1 diabetes. *The Lancet*, 383, 69-82.
- BAILEY, C. 2005. Treating insulin resistance in type 2 diabetes with metformin and thiazolidinediones. *Diabetes, Obesity and Metabolism*, 7, 675-691.
- BANTING, F. G., BEST, C., COLLIP, J., CAMPBELL, W., FLETCHER, A., MACLEOD, J. & NOBLE, E. 1922. The effect produced on diabetes by extracts of pancreas. *Transactions Association of American Physicians*, 37, 337-347.
- BARDEESY, N. & DEPINHO, R. A. 2002. Pancreatic cancer biology and genetics. *Nature Reviews Cancer*, 2, 897-909.
- BARKAI, U., WEIR, G. C., COLTON, C. K., LUDWIG, B., BORNSTEIN, S. R., BRENDDEL, M. D., NEUFELD, T., BREMER, C., LEON, A., EVRON, Y., YAVRIYANTS, K., AZAROV, D., ZIMERMANN, B., MAIMON, S., SHABTAY, N., BALLYURA, M., ROZENSHTAIN, T., VARDI, P., BLOCH, K., DE VOS, P. & ROTEM, A. 2013. Enhanced Oxygen Supply Improves Islet Viability in a New Bioartificial Pancreas. *Cell Transplantation*, 22, 1463-1476.
- BARRETT, J. C., CLAYTON, D. G., CONCANNON, P., AKOLKAR, B., COOPER, J. D., ERLICH, H. A., JULIER, C., MORAHAN, G., NERUP, J., NIERRAS, C., PLAGNOL, V., POCIOT, F., SCHUILENBURG, H., SMYTH, D. J., STEVENS, H., TODD, J. A., WALKER, N. M. & RICH, S. S. 2009. Genome-wide association study and meta-analysis find that over 40 loci affect risk of type 1 diabetes. *Nature Genetics*, 41, 703-707.
- BARTON, F. B., RICKELS, M. R., ALEJANDRO, R., HERING, B. J., WEASE, S., NAZIRUDDIN, B., OBERHOLZER, J., ODORICO, J. S., GARFINKEL, M. R., LEVY, M., PATTOU, F., BERNEY, T., SECCHI, A., MESSINGER, S., SENIOR, P. A., MAFFI, P., POSSELT, A., STOCK, P. G., KAUFMAN, D. B., LUO, X., KANDEEL, F., CAGLIERO, E., TURGEON, N. A., WITKOWSKI, P., NAJI, A., O'CONNELL, P. J., GREENBAUM, C., KUDVA, Y. C., BRAYMAN, K. L., AULL, M. J., LARSEN, C., KAY, T. W., FERNANDEZ, L. A., VANTYGHM, M. C., BELLIN, M. & SHAPIRO, A. M. 2012. Improvement in outcomes of clinical islet transplantation: 1999-2010. *Diabetes Care*, 35, 1436-45.
- BENNET, W., GROTH, C.-G., LARSSON, R., NILSSON, B. & KORSGREN, O. 2011. Isolated Human Islets Trigger an Instant Blood Mediated Inflammatory Reaction: Implications for Intraportal Islet Transplantation as a Treatment for Patients with Type 1 Diabetes. *Uppsala Journal of Medical Sciences*, 105, 125-133.

- BENNINGER, R. K. P., HEAD, W. S., ZHANG, M., SATIN, L. S. & PISTON, D. W. 2011. Gap junctions and other mechanisms of cell-cell communication regulate basal insulin secretion in the pancreatic islet. *The Journal of Physiology*, 589, 5453-5466.
- BENTSI-BARNES, K., DOYLE, M. E., ABAD, D., KANDEEL, F. & AL-ABDULLAH, I. 2011. Detailed protocol for evaluation of dynamic perfusion of human islets to assess beta-cell function. *Islets*, 3, 284-90.
- BERMAN, D. M., MOLANO, R. D., FOTINO, C., ULISSI, U., GIMENO, J., MENDEZ, A. J., KENYON, N. M., KENYON, N. S., ANDREWS, D. M. & RICORDI, C. 2016. Bioengineering the endocrine pancreas: intraomental islet transplantation within a biologic resorbable scaffold. *Diabetes*, 65, 1350-1361.
- BIARNES, M., MONTOLIO, M., NACHER, V., RAURELL, M., SOLER, J. & MONTANYA, E. 2002. b-Cell Death and Mass in Synergeically Transplanted Islets Exposed to Short- and Long-Term Hyperglycemia. *Diabetes*, 51, 66-72.
- BLAESER, A., DUARTE CAMPOS, D. F. & FISCHER, H. 2017. 3D bioprinting of cell-laden hydrogels for advanced tissue engineering. *Current Opinion in Biomedical Engineering*, 2, 58-66.
- BLOMEIER, H., ZHANG, X., RIVES, C., BRISSOVA, M., HUGHES, E., BAKER, M., POWERS, A. C., KAUFMAN, D. B., SHEA, L. D. & LOWE, W. L. 2006. Polymer Scaffolds as Synthetic Microenvironments for Extrahepatic Islet Transplantation. *Transplantation*, 82, 452-459.
- BOGDANI, M., BLACKMAN, S. M., RIDAURA, C., BELLOCQ, J.-P., POWERS, A. C. & AGUILAR-BRYAN, L. 2017. Structural abnormalities in islets from very young children with cystic fibrosis may contribute to cystic fibrosis-related diabetes. *Scientific reports*, 7, 17231.
- BONNER-WEIR, S. & ORCI, L. 1982. New Perspectives on the Microvasculature of the Islets of Langerhans in the Rat. *Diabetes*, 31, 883-889.
- BONNER-WEIR, S., SULLIVAN, B. A. & WEIR, G. C. 2015. Human Islet Morphology Revisited: Human and Rodent Islets Are Not So Different After All. *Journal of Histochemistry & Cytochemistry*, 63, 604-12.
- BOSCO, D., ARMANET, M., MOREL, P., NICLAUSS, N., SGROI, A., MULLER, Y. D., GIOVANNONI, L., PARNAUD, G. & BERNEY, T. 2010. Unique Arrangement of α - and β -Cells in Human Islets of Langerhans. *Diabetes*, 59, 1202-1210.
- BOSCO, D., MEDA, P., HALBAN, P. A. & ROUILLER, D. G. 2000. Importance of cell-matrix interactions in rat islet beta-cell secretion in vitro: role of α 6 β 1 integrin. *Diabetes*, 49, 233-243.
- BOTTALICO, J. N. 2007. Recurrent Gestational Diabetes: Risk Factors, Diagnosis, Management, and Implications. *Seminars in Perinatology*, 31, 176-184.
- BRANDHORST, D., BRANDHORST, H., MULLOOLY, N., ACREMAN, S. & JOHNSON, P. R. 2016. High Seeding Density Induces Local Hypoxia and Triggers a Proinflammatory Response in Isolated Human Islets. *Cell Transplant*, 25, 1539-46.
- BRANDHORST, H., BRANDHORST, D., BRENDL, M. D., HERING, B. J. & BRETZEL, R. G. 1998. Assessment of intracellular insulin content during all steps of human islet isolation procedure. *Cell Transplantation*, 7, 489-495.
- BRITISH TRANSPLANTATION SOCIETY. 2019. *UK Guidelines on Pancreas and Islet Transplantation* [Online]. Available: <https://bts.org.uk/wp-content/uploads/2019/07/Pancreas-guidelines-FINAL-FOR-WEB-CONSULTATION-July-2019.pdf> [Accessed 24/09 2019].
- BROOKS, A., WALKER, N., ALDIBBIAT, A., HUGHES, S., JONES, G., DE HAVILLAND, J., CHOUDHARY, P., HUANG, G., PARROTT, N. & MCGOWAN, N. 2013. Attainment of metabolic goals in the integrated UK islet transplant program with locally isolated and transported preparations. *American Journal of Transplantation*, 13, 3236-3243.
- BUITINGA, M., TRUCKENMÜLLER, R., ENGELSE, M. A., MORONI, L., TEN HOOPEN, H. W. M., VAN BLITTERSWIJK, C. A., DE KONING, E. J. P., VAN APELDOORN, A. A. & KARPERIEN, M. 2013. Microwell Scaffolds for the Extrahepatic Transplantation of Islets of Langerhans. *PLOS ONE*, 8, e64772.

- CABRERA, O., BERMAN, D. M., KENYON, N. S., RICORDI, C., BERGGREN, P. O. & CAICEDO, A. 2006. The unique cytoarchitecture of human pancreatic islets has implications for islet cell function. *Proceedings of the National Academy of Sciences of the United States of America*, 103, 2334-9.
- CALABRESE, A., ZHANG, M., SERRE-BEINIER, V., CATON, D., MAS, C., SATIN, L. S. & MEDA, P. 2003. Connexin 36 Controls Synchronization of Ca²⁺ Oscillations and Insulin Secretion in MIN6 Cells. *Diabetes*, 52, 417-424.
- CANTLEY, J., GREY, S. T., MAXWELL, P. H. & WITHERS, D. J. 2010. The hypoxia response pathway and β -cell function. *Diabetes, Obesity and Metabolism*, 12, 159-167.
- CANTLEY, J., WALTERS, S. N., JUNG, M.-H., WEINBERG, A., COWLEY, M. J., WHITWORTH, P. T., KAPLAN, W., HAWTHORNE, W. J., O'CONNELL, P. J. & WEIR, G. 2013. A preexistent hypoxic gene signature predicts impaired islet graft function and glucose homeostasis. *Cell Transplantation*, 22, 2147-2159.
- CARLSSON, P.-O., PALM, F., ANDERSSON, A. & LISS, P. 2001. Markedly Decreased Oxygen Tension in Transplanted Rat Pancreatic Islets Irrespective of the Implantation Site. *Diabetes*, 50, 489-495.
- CARLSSON, P. O., ESPES, D., SEDIGH, A., ROTEM, A., ZIMMERMAN, B., GRINBERG, H., GOLDMAN, T., BARKAI, U., AVNI, Y. & WESTERMARK, G. T. 2018. Transplantation of macroencapsulated human islets within the bioartificial pancreas β Air to patients with type 1 diabetes mellitus. *American Journal of Transplantation*, 18, 1735-1744.
- CHAN, B. P. & LEONG, K. W. 2008. Scaffolding in tissue engineering: general approaches and tissue-specific considerations. *European spine journal : official publication of the European Spine Society, the European Spinal Deformity Society, and the European Section of the Cervical Spine Research Society*, 17 Suppl 4, 467-479.
- CHERNYSH, I. N., NAGASWAMI, C., PUROHIT, P. K. & WEISEL, J. W. 2012. Fibrin Clots Are Equilibrium Polymers That Can Be Remodeled Without Proteolytic Digestion. *Scientific Reports*, 2, 879.
- CHOUCHANI, E. T., PELL, V. R., GAUDE, E., AKSENTIJEVIĆ, D., SUNDIER, S. Y., ROBB, E. L., LOGAN, A., NADTOCHIY, S. M., ORD, E. N. J., SMITH, A. C., EYASSU, F., SHIRLEY, R., HU, C.-H., DARE, A. J., JAMES, A. M., ROGATTI, S., HARTLEY, R. C., EATON, S., COSTA, A. S. H., BROOKES, P. S., DAVIDSON, S. M., DUCHEN, M. R., SAEB-PARSY, K., SHATTOCK, M. J., ROBINSON, A. J., WORK, L. M., FREZZA, C., KRIEG, T. & MURPHY, M. P. 2014. Ischaemic accumulation of succinate controls reperfusion injury through mitochondrial ROS. *Nature*, 515, 431.
- CHOW, L. W., WANG, L.-J., KAUFMAN, D. B. & STUPP, S. I. 2010. Self-assembling nanostructures to deliver angiogenic factors to pancreatic islets. *Biomaterials*, 31, 6154-6161.
- CHUN, S., HUANG, Y., XIE, W. J., HOU, Y., HUANG, R. P., SONG, Y. M., LIU, X. M., ZHENG, W., SHI, Y. & SONG, C. F. 2008. Adhesive Growth of Pancreatic Islet Cells on a Polyglycolic Acid Fibrous Scaffold. *Transplantation Proceedings*, 40, 1658-1663.
- CNOP, M., HUGHES, S. J., IGOILLO-ESTEVE, M., HOPPA, M. B., SAYYED, F., VAN DE LAAR, L., GUNTER, J. H., DE KONING, E. J. P., WALLS, G. V. & GRAY, D. W. G. 2010. The long lifespan and low turnover of human islet beta cells estimated by mathematical modelling of lipofuscin accumulation. *Diabetologia*, 53, 321.
- CORONEL, M. M., LIANG, J. P., LI, Y. & STABLER, C. L. 2019. Oxygen generating biomaterial improves the function and efficacy of beta cells within a macroencapsulation device. *Biomaterials*, 210, 1-11.
- CROSS, S. E., VAUGHAN, R. H., WILLCOX, A. J., MCBRIDE, A. J., ABRAHAM, A. A., HAN, B., JOHNSON, J. D., MAILLARD, E., BATEMAN, P. A., RAMRACHEYA, R. D., RORSMAN, P., KADLER, K. E., DUNNE, M. J., HUGHES, S. J. & JOHNSON, P. R. V. 2017. Key Matrix Proteins Within the Pancreatic Islet Basement Membrane Are Differentially Digested During Human Islet Isolation. *American Journal of Transplantation*, 17, 451-461.

- DA CONCEICAO RIBEIRO, R., PAL, D., FERREIRA, A. M., GENTILE, P., BENNING, M. & DALGARNO, K. 2018. Reactive jet impingement bioprinting of high cell density gels for bone microtissue fabrication. *Biofabrication*, 11, 015014.
- DAI, Z.-J., GAO, J., MA, X.-B., YAN, K., LIU, X.-X., KANG, H.-F., JI, Z.-Z., GUAN, H.-T. & WANG, X.-J. 2012. Up-regulation of hypoxia inducible factor-1 α by cobalt chloride correlates with proliferation and apoptosis in PC-2 cells. *Journal of Experimental & Clinical Cancer Research* 31, 28-28.
- DANEMAN, D. 2006. Type 1 diabetes. *The Lancet*, 367, 847-858.
- DAOUD, J., PETROPAVLOVSKAIA, M., ROSENBERG, L. & TABRIZIAN, M. 2010a. The effect of extracellular matrix components on the preservation of human islet function in vitro. *Biomaterials*, 31, 1676-82.
- DAOUD, J., ROSENBERG, L. & TABRIZIAN, M. 2010b. Pancreatic islet culture and preservation strategies: advances, challenges, and future outlook. *Cell Transplant*, 19, 1523-35.
- DAOUD, J. T., PETROPAVLOVSKAIA, M. S., PATAPAS, J. M., DEGRANDPRÉ, C. E., DIRADDO, R. W., ROSENBERG, L. & TABRIZIAN, M. 2011. Long-term in vitro human pancreatic islet culture using three-dimensional microfabricated scaffolds. *Biomaterials*, 32, 1536-1542.
- DARLING, M. R.-C., MICHAELA, W., AURELIEN, F., DANIELLA, P., JODIE, N., FRAN, J. H., BAHMAN, D., ANTON, B., THOMAS, L., SHANE, T. G., HELEN, E. T., THOMAS, W. H. K., CHRIS, J. D., NICOLAS, H. V. & PATRICK, T. C. 2018. Oxygen-permeable microwell device maintains islet mass and integrity during shipping. *Endocrine Connections*, 7, 490.
- DENG, S., VATAMANIUK, M., HUANG, X., DOLIBA, N., LIAN, M.-M., FRANK, A., VELIDEDEOGLU, E., DESAI, N. M., KOEBERLEIN, B., WOLF, B., BARKER, C. F., NAJI, A., MATSCHINSKY, F. M. & MARKMANN, J. F. 2004. Structural and Functional Abnormalities in the Islets Isolated From Type 2 Diabetic Subjects. *Diabetes*, 53, 624-632.
- DESAI, T. & SHEA, L. D. 2017. Advances in islet encapsulation technologies. *Nature Reviews Drug Discovery*, 16, 338-350.
- DIONNE, K. E., COLTON, C. K. & LYARMUSH, M. 1993. Effect of hypoxia on insulin secretion by isolated rat and canine islets of Langerhans. *Diabetes*, 42, 12-21.
- DO AMARAL, A. S. R., PAWLICK, R. L., RODRIGUES, E., COSTAL, F., PEPPER, A., GALVÃO, F. H. F., CORREA-GIANNELLA, M. L. & SHAPIRO, A. M. J. 2013. Glutathione ethyl ester supplementation during pancreatic islet isolation improves viability and transplant outcomes in a murine marginal islet mass model. *PLoS One*, 8, e55288.
- DUFRANE, D., GOEBBELS, R.-M., SALIEZ, A., GUIOT, Y. & GIANELLO, P. 2006. Six-month survival of microencapsulated pig islets and alginate biocompatibility in primates: proof of concept. *Transplantation*, 81, 1345-1353.
- EMAMAULLEE, J. A. & SHAPIRO, A. M. 2007. Factors influencing the loss of beta-cell mass in islet transplantation. *Cell Transplant*, 16, 1-8.
- ESPES, D., LAU, J., QUACH, M., ULLSTEN, S., CHRISTOFFERSSON, G. & CARLSSON, P. O. 2016. Rapid Restoration of Vascularity and Oxygenation in Mouse and Human Islets Transplanted to Omentum May Contribute to Their Superior Function Compared to Intraportally Transplanted Islets. *American Journal of Transplantation*, 16, 3246-3254.
- EUROTRANSPLANT INTERNATIONAL FOUNDATION. 2018. *Annual Report 2018* [Online]. Available: https://www.eurotransplant.org/cms/mediaobject.php?file=ET_Jaarverslag_20186.pdf [Accessed 18.07.2019 2019].
- FLATT, A. J. S., BENNETT, D., COUNTER, C., BROWN, A. L., WHITE, S. A. & SHAW, J. A. M. 2019. Beta-cell and renal transplantation options for diabetes. *Diabetic Medicine*.
- FORBES, J. M. & COOPER, M. E. 2013. Mechanisms of diabetic complications. *Physiological Reviews*, 93, 137-88.
- FRANTZ, C., STEWART, K. M. & WEAVER, V. M. 2010. The extracellular matrix at a glance. *Journal of Cell Science*, 123, 4195-4200.

- FUCHS, E. & RAGHAVAN, S. 2002. Getting under the skin of epidermal morphogenesis. *Nature Reviews Genetics*, 3, 199-209.
- GAN, W. J., DO, O. H., COTTLE, L., MA, W., KOSOBRODOVA, E., COOPER-WHITE, J., BILEK, M. & THORN, P. 2018. Local integrin activation in pancreatic β cells targets insulin secretion to the vasculature. *Cell Reports*, 24, 2819-2826. e3.
- GILLESPIE, K. M., BAIN, S. C., BARNETT, A. H., BINGLEY, P. J., CHRISTIE, M. R., GILL, G. V. & GALE, E. A. M. 2004. The rising incidence of childhood type 1 diabetes and reduced contribution of high-risk HLA haplotypes. *The Lancet*, 364, 1699-1700.
- GIULIANI, M., MORITZ, W., BODMER, E., DINDO, D., KUGELMEIER, P., LEHMANN, R., GASSMANN, M., GROSCURTH, P. & WEBER, M. 2005. Central Necrosis in Isolated Hypoxic Human Pancreatic Islets: Evidence for Postisolation Ischemia. *Cell Transplantation*, 14, 67-76.
- GRAYSON, B. E., SEELEY, R. J. & SANDOVAL, D. A. 2013. Wired on sugar: the role of the CNS in the regulation of glucose homeostasis. *Nature Reviews Neuroscience*, 14, 24-37.
- GRUESSNER, A. C. & GRUESSNER, R. W. 2016. Long-term outcome after pancreas transplantation: a registry analysis. *Current Opinion in Organ Transplantation*, 21, 377-85.
- GRUESSNER, R. W. G. & GRUESSNER, A. C. 2013. The current state of pancreas transplantation. *Nature Reviews Endocrinology*, 9, 555.
- HALLER, M. J., ATKINSON, M. A. & SCHATZ, D. 2005. Type 1 diabetes mellitus: etiology, presentation, and management. *Pediatric Clinics of North America*, 52, 1553-78.
- HANLEY, S. C., PARASKEVAS, S. & ROSENBERG, L. 2008. Donor and Isolation Variables Predicting Human Islet Isolation Success. *Transplantation*, 85, 950-955.
- HANSON, M. S., PARK, E. E., SEARS, M. L., GREENWOOD, K. K., DANOBEITIA, J. S., HULLETT, D. A. & FERNANDEZ, L. A. 2010. A simplified approach to human islet quality assessment. *Transplantation*, 89, 1178-1188.
- HARJUTSALO, V., SJÖBERG, L. & TUOMILEHTO, J. 2008. Time trends in the incidence of type 1 diabetes in Finnish children: a cohort study. *The Lancet*, 371, 1777-1782.
- HART, N. J. & POWERS, A. C. 2019. Use of human islets to understand islet biology and diabetes: progress, challenges and suggestions. *Diabetologia*, 62, 212-222.
- HART, P. A., BELLIN, M. D., ANDERSEN, D. K., BRADLEY, D., CRUZ-MONSERRATE, Z., FORSMARK, C. E., GOODARZI, M. O., HABTEZION, A., KORC, M. & KUDVA, Y. C. 2016. Type 3c (pancreatogenic) diabetes mellitus secondary to chronic pancreatitis and pancreatic cancer. *The Lancet Gastroenterology & Hepatology*, 1, 226-237.
- HAUGE-EVANS, A. C., SQUIRES, P. E., PERSAUD, S. J. & JONES, P. M. 1999. Pancreatic beta-cell-to-beta-cell interactions are required for integrated responses to nutrient stimuli: enhanced Ca^{2+} and insulin secretory responses of MIN6 pseudoislets. *Diabetes*, 48, 1402-1408.
- HEILEMAN, K. L., DAOUD, J. & TABRIZIAN, M. 2016. Elaboration of a finite element model of pancreatic islet dielectric response to gap junction expression and insulin release. *Colloids and Surfaces B: Biointerfaces*, 148, 474-480.
- HOLT, R. I. G., COCKRAM, C., FLYVBJERG, A. & GOLDSTEIN, B. J. 2010. *Textbook of diabetes*. , Chichester, West Sussex; Hoboken, NJ: Wiley-Blackwell.
- HSU, D. C. & KATELARI, C. H. 2009. Long-term management of patients taking immunosuppressive drugs. *Australian Prescriber*, 32, 68-71.
- HUDSON, A., BRADBURY, L., JOHNSON, R., FUGGLE, S. V., SHAW, J. A., CASEY, J. J., FRIEND, P. J. & WATSON, C. J. 2015. The UK Pancreas Allocation Scheme for Whole Organ and Islet Transplantation. *American Journal of Transplantation*, 15, 2443-55.
- HUMAR, A., RAMCHARAN, T., KANDASWAMY, R., GRUESSNER, R. W., GRUESSNER, A. G. & SUTHERLAND, D. E. 2004. The impact of donor obesity on outcomes after cadaver pancreas transplants. *American Journal of Transplantation*, 4, 605-10.
- HUNG, T. H., SKEPPER, J. N., CHARNOCK-JONES, D. S. & BURTON, G. J. 2002. Hypoxia-reoxygenation: a potent inducer of apoptotic changes in the human placenta and possible etiological factor in preeclampsia. *Circulation Research*, 90, 1274-81.

- HYNES, R. O. & NABA, A. 2012. Overview of the matrisome—an inventory of extracellular matrix constituents and functions. *Cold Spring Harbor perspectives in biology*, 4, a004903.
- ICHII, H., PILEGGI, A., MOLANO, R. D., BAIDAL, D. A., KHAN, A., KURODA, Y., INVERARDI, L., GOSS, J. A., ALEJANDRO, R. & RICORDI, C. 2005. Rescue purification maximizes the use of human islet preparations for transplantation. *American Journal of Transplantation*, 5, 21-30.
- IRVING-RODGERS, H. F., CHOONG, F. J., HUMMITZSCH, K., PARISH, C. R., RODGERS, R. J. & SIMEONOVIC, C. J. 2014. Pancreatic Islet Basement Membrane Loss and Remodeling After Mouse Islet Isolation and Transplantation: Impact for Allograft Rejection. *Cell Transplantation*, 23, 59-72.
- ISHIHARA, H., ASANO, T., TSUKUDA, K., KATAGIRI, H., INUKAI, K., ANAI, M., KIKUCHI, M., YAZAKI, Y., MIYAZAKI, J. I. & OKA, Y. 1993. Pancreatic beta cell line MIN6 exhibits characteristics of glucose metabolism and glucose-stimulated insulin secretion similar to those of normal islets. *Diabetologia*, 36, 1139-1145.
- IWANAGA, Y., SUTHERLAND, D. E., HARMON, J. V. & PAPAS, K. K. 2008. Pancreas preservation for pancreas and islet transplantation. *Current opinion in organ transplantation*, 13, 445-451.
- JACOBS-TULLENEERS-THEVISSEN, D., CHINTINNE, M., LING, Z., GILLARD, P., SCHOONJANS, L., DELVAUX, G., STRAND, B. L., GORUS, F., KEYMEULEN, B., PIPELEERS, D. & ON BEHALF OF THE BETA CELL THERAPY CONSORTIUM, E.-F. 2013. Sustained function of alginate-encapsulated human islet cell implants in the peritoneal cavity of mice leading to a pilot study in a type 1 diabetic patient. *Diabetologia*, 56, 1605-1614.
- JANMEY PAUL, A., WINER JESSAMINE, P. & WEISEL JOHN, W. 2009. Fibrin gels and their clinical and bioengineering applications. *Journal of The Royal Society Interface*, 6, 1-10.
- JANSSON, L., BARBU, A., BODIN, B., DROTT, C. J., ESPES, D., GAO, X., GRAPENSPARR, L., KÄLLSKOG, Ö., LAU, J., LILJEBÄCK, H., PALM, F., QUACH, M., SANDBERG, M., STRÖMBERG, V., ULLSTEN, S. & CARLSSON, P.-O. 2016. Pancreatic islet blood flow and its measurement. *Uppsala journal of medical sciences*, 121, 81-95.
- JAYADEV, R. & SHERWOOD, D. R. 2017. Basement membranes. *Current Biology*, 27, R207-R211.
- JOHNSON, R. J., BRADBURY, L. L., MARTIN, K. & NEUBERGER, J. 2014. Organ donation and transplantation in the UK—the last decade: a report from the UK national transplant registry. *Transplantation*, 97, S1-S27.
- JUNG, E.-J., KIM, S.-C., WEE, Y.-M., KIM, Y.-H., CHOI, M. Y., JEONG, S.-H., LEE, J., LIM, D.-G. & HAN, D.-J. 2011. Bone marrow-derived mesenchymal stromal cells support rat pancreatic islet survival and insulin secretory function in vitro. *Cytotherapy*, 13, 19-29.
- KAHN, S. E., HULL, R. L. & UTZSCHNEIDER, K. M. 2006. Mechanisms linking obesity to insulin resistance and type 2 diabetes. *Nature*, 444, 840-846.
- KAIDO, T., YEBRA, M., CIRULLI, V., RHODES, C., DIAFERIA, G. & MONTGOMERY, A. M. 2006. Impact of Defined Matrix Interactions on Insulin Production by Cultured Human β -Cells - Effect on Insulin Content, Secretion, and Gene Transcription. *Diabetes*, 55, 2723-2729.
- KANG, P. M., HAUNSTETTER, A., AOKI, H., USHEVA, A. & IZUMO, S. 2000. Morphological and molecular characterization of adult cardiomyocyte apoptosis during hypoxia and reoxygenation. *Circulation Research*, 87, 118-25.
- KATSAROU, A., GUDBJORNSDOTTIR, S., RAWSHANI, A., DABELEA, D., BONIFACIO, E., ANDERSON, B. J., JACOBSEN, L. M., SCHATZ, D. A. & LERNMARK, A. 2017. Type 1 diabetes mellitus. *Nature Reviews Disease Primers*, 3, 17016.
- KAUFMAN, B. A., LI, C. & SOLEIMANPOUR, S. A. 2015. Mitochondrial regulation of β -cell function: maintaining the momentum for insulin release. *Molecular aspects of medicine*, 42, 91-104.
- KAUR, G. & DUFOUR, J. M. 2012. Cell lines: Valuable tools or useless artifacts. *Spermatogenesis*, 2, 1-5.
- KAVIANI, M. & AZARPIRA, N. 2016. Insight into microenvironment remodeling in pancreatic endocrine tissue engineering: Biological and biomaterial approaches. *Tissue engineering and regenerative medicine*, 13, 475-484.

- KAWAI, T., TAKEI, I., TOKUI, M., FUNAE, O., MIYAMOTO, K., TABATA, M., HIRATA, T., SARUTA, T., SHIMADA, A. & ITOH, H. 2010. Effects of epalrestat, an aldose reductase inhibitor, on diabetic peripheral neuropathy in patients with type 2 diabetes, in relation to suppression of N ϵ -carboxymethyl lysine. *Journal of Diabetes and its Complications*, 24, 424-432.
- KIEFFER, T. J., WOLTJEN, K., OSAFUNE, K., YABE, D. & INAGAKI, N. 2017. Beta-cell replacement strategies for diabetes. *Journal of diabetes investigation*, 9, 457-463.
- KIM, A., MILLER, K., JO, J., KILIMNIK, G., WOJCIK, P. & HARA, M. 2009. Islet architecture: A comparative study. *Islets*, 1, 129-136.
- KIN, T., SENIOR, P., O'GORMAN, D., RICHER, B., SALAM, A. & SHAPIRO, A. M. J. 2008. Risk factors for islet loss during culture prior to transplantation. *Transplant International*, 21, 1029-1035.
- KITZMANN, J. P., O'GORMAN, D., KIN, T., GRUESSNER, A. C., SENIOR, P., IMES, S., GRUESSNER, R. W., SHAPIRO, A. M. J. & PAPAS, K. K. 2014. Islet oxygen consumption rate dose predicts insulin independence for first clinical islet allotransplants. *Transplantation proceedings*, 46, 1985-1988.
- KNESER, U., VOOGD, A., OHNOLZ, J., BUETTNER, O., STANGENBERG, L., ZHANG, Y., STARK, G. & SCHAEFER, D. 2005. Fibrin gel-immobilized primary osteoblasts in calcium phosphate bone cement: in vivo evaluation with regard to application as injectable biological bone substitute. *Cells Tissues Organs*, 179, 158-169.
- KNIP, M., VEIJOLA, R., VIRTANEN, S. M., HYÖTY, H., VAARALA, O. & ÅKERBLOM, H. K. 2005. Environmental Triggers and Determinants of Type 1 Diabetes. *Diabetes*, 54, S125-S136.
- KNOP, F. K. & TAYLOR, R. 2013. Mechanism of Metabolic Advantages After Bariatric Surgery: It's all gastrointestinal factors versus it's all food restriction. *Diabetes Care*, 36, S287-S291.
- KOJIMA, N., TAKEUCHI, S. & SAKAI, Y. Engineering of pseudoislets: effect on insulin secretion activity by cell number, cell population, and microchannel networks. *Transplantation proceedings*, 2014. Elsevier, 1161-1165.
- KOLIPAKA, A., SCHROEDER, S., MO, X., SHAH, Z., HART, P. A. & CONWELL, D. L. 2017. Magnetic resonance elastography of the pancreas: Measurement reproducibility and relationship with age. *Magnetic Resonance Imaging*, 42, 1-7.
- KOMATSU, H., COOK, C., WANG, C.-H., MEDRANO, L., LIN, H., KANDEEL, F., TAI, Y.-C. & MULLEN, Y. 2017. Oxygen environment and islet size are the primary limiting factors of isolated pancreatic islet survival. *PloS one*, 12, e0183780.
- KOPP, W. H., LAM, H.-D., SCHAAPHERDER, A. F. M., HUURMAN, V. A. L., VAN DER BOOG, P. J. M., DE KONING, E. J. P., DE FIJTER, J. W., BARANSKI, A. G. & BRAAT, A. E. 2018. Pancreas Transplantation With Grafts From Donors Deceased After Circulatory Death: 5 Years Single-Center Experience. *Transplantation*, 102, 333-339.
- KRIEGER, N. R., ODORICO, J. S., HEISEY, D. M., D'ALESSANDRO, A. M., KNECHTLE, S. J., PIRSCH, J. D. & SOLLINGER, H. W. 2003. Underutilization of pancreas donors. *Transplantation*, 75, 1271-1276.
- KRISHNAMURTHY, M., LI, J., FELLOWS, G. F., ROSENBERG, L., GOODYER, C. G. & WANG, R. 2011. Integrin α 3, But Not β 1, Regulates Islet Cell Survival and Function via PI3K/Akt Signaling Pathways. *Endocrinology*, 152, 424-435.
- KUEHN, C., LAKEY, J. R. T., LAMB, M. W. & VERMETTE, P. 2013. Young porcine endocrine pancreatic islets cultured in fibrin show improved resistance toward hydrogen peroxide. *Islets*, 5, 207-215.
- KÜHTREIBER, W. M., HO, L. T., KAMIREDDY, A., YACOUB, J. A. W. & SCHARP, D. W. 2010. Islet Isolation From Human Pancreas With Extended Cold Ischemia Time. *Transplantation Proceedings*, 42, 2027-2031.
- KUMAR, N., JOISHER, H. & GANGULY, A. 2018. Polymeric Scaffolds for Pancreatic Tissue Engineering: A Review. *The Review of Diabetic Studies : RDS*, 14, 334-353.

- KURIAN, S. M., FERRERI, K., WANG, C.-H., TODOROV, I., AL-ABDULLAH, I. H., RAWSON, J., MULLEN, Y., SALOMON, D. R. & KANDEEL, F. 2017. Gene expression signature predicts human islet integrity and transplant functionality in diabetic mice. *PLoS one*, 12, e0185331-e0185331.
- LACY, P. E., FINKE, E. H., CONANT, S. & NABER, S. 1976. Long-term perfusion of isolated rat islets in vitro. *Diabetes*, 25, 484-93.
- LANKISCH, P. G. & BANKS, P. A. 1998. *Pancreatitis*, Springer Berlin Heidelberg.
- LEBLEU, V. S., MACDONALD, B. & KALLURI, R. 2007. Structure and Function of Basement Membranes. *Experimental Biology and Medicine*, 232, 1121-1129.
- LEE, B. R., HWANG, J. W., CHOI, Y. Y., WONG, S. F., HWANG, Y. H., LEE, D. Y. & LEE, S.-H. 2012. In situ formation and collagen-alginate composite encapsulation of pancreatic islet spheroids. *Biomaterials*, 33, 837-845.
- LEEMKUIL, M., LEUVENINK, H. G. D. & POL, R. A. 2019. Pancreas Transplantation from Donors after Circulatory Death: an Irrational Reluctance? *Current Diabetes Reports*, 19, 129.
- LEMAIRE, K. & SCHUIT, F. 2012. Integrating insulin secretion and ER stress in pancreatic [beta]-cells. *Nature Cell Biology*, 14, 979-981.
- LEMELMAN, M. B., LETOURNEAU, L. & GREELEY, S. A. W. 2018. Neonatal Diabetes Mellitus: An Update on Diagnosis and Management. *Clinics in perinatology*, 45, 41-59.
- LIAO, E., YASZEMSKI, M., KREBSBACH, P. & HOLLISTER, S. 2007. Tissue-engineered cartilage constructs using composite hyaluronic acid/collagen I hydrogels and designed poly (propylene fumarate) scaffolds. *Tissue engineering*, 13, 537-550.
- LIFSON, N., KRAMLINGER, K. G., ROBERT, R. & LENDER, J. 1989. Blood Flow to the Rabbit Pancreas with Special Reference to the Islets of Langerhans. *Gastroenterology*, 79, 408-473.
- LIM, D.-J., ANTIPENKO, S. V., ANDERSON, J. M., JAIMES, K. F., VIERA, L., STEPHEN, B. R., BRYANT, S. M. J., YANCEY, B. D., HUGHES, K. J., CUI, W., THOMPSON, J. A., CORBETT, J. A. & JUN, H.-W. 2011. Enhanced Rat Islet Function and Survival In Vitro Using a Biomimetic Self-Assembled Nanomatrix Gel. *Tissue Engineering. Part A*, 17, 399-406.
- LIM, F. & SUN, A. M. 1980. Microencapsulated islets as bioartificial endocrine pancreas. *Science*, 210, 908-910.
- LINSLEY, C. S., WU, B. M. & TAWIL, B. 2016. Mesenchymal stem cell growth on and mechanical properties of fibrin-based biomimetic bone scaffolds. *Journal of Biomedical Materials Research Part A*, 104, 2945-2953.
- LIU, J., WU, P., WANG, Y., DU, Y., A, N., LIU, S., ZHANG, Y., ZHOU, N., XU, Z. & YANG, Z. 2016. Ad-HGF improves the cardiac remodeling of rat following myocardial infarction by upregulating autophagy and necroptosis and inhibiting apoptosis. *American Journal of Translational Research*, 8, 4605-4627.
- LOGSDON, C. D. & JI, B. 2013. The role of protein synthesis and digestive enzymes in acinar cell injury. *Nature reviews. Gastroenterology & hepatology*, 10, 362-370.
- LONGNECKER, D. 2014. Anatomy and Histology of the Pancreas. *Pancreapedia: Exocrine Pancreas Knowledge Base*.
- MA, K., TITAN, A. L., STAFFORD, M., ZHENG, C. H. & LEVENSTON, M. E. 2012. Variations in chondrogenesis of human bone marrow-derived mesenchymal stem cells in fibrin/alginate blended hydrogels. *Acta Biomaterialia*, 8, 3754-3764.
- MACGREGOR, R. R., WILLIAMS, S. J., TONG, P. Y., KOVER, K., MOORE, W. V. & STEHNO-BITTEL, L. 2006. Small rat islets are superior to large islets in in vitro function and in transplantation outcomes. *American Journal of Physiology-Endocrinology and Metabolism*, 290, E771-E779.
- MAILLARD, E., SENCIER, M.-C., LANGLOIS, A., BIETIGER, W., KRAFFT, M., PINGET, M. & SIGRIST, S. 2009. Extracellular matrix proteins involved in pseudoislets formation. *Islets*, 1, 232-241.
- MALLETT, A. G. & KORBUTT, G. S. 2008. Alginate modification improves long-term survival and function of transplanted encapsulated islets. *Tissue engineering Part A*, 15, 1301-1309.

- MANDRYCKY, C., WANG, Z., KIM, K. & KIM, D. H. 2016. 3D bioprinting for engineering complex tissues. *Biotechnology Advances*, 34, 422-34.
- MARCHIOLI, G., LUCA, A. D., DE KONING, E., ENGELSE, M., VAN BLITTERSWIJK, C. A., KARPERIEN, M., VAN APELDOORN, A. A. & MORONI, L. 2016. Hybrid Polycaprolactone/Alginate Scaffolds Functionalized with VEGF to Promote de Novo Vessel Formation for the Transplantation of Islets of Langerhans. *Advanced Healthcare Materials*, 5, 1606-1616.
- MARCHIOLI, G., VAN GURP, L., VAN KRIEKEN, P. P., STAMATIALIS, D., ENGELSE, M., VAN BLITTERSWIJK, C. A., KARPERIEN, M. B. J., DE KONING, E., ALBLAS, J., MORONI, L. & VAN APELDOORN, A. A. 2015. Fabrication of three-dimensional bioplotting hydrogel scaffolds for islets of Langerhans transplantation. *Biofabrication*, 7, 025009.
- MARSELLI, L., TRINCAVELLI, L., SANTANGELO, C., LUPI, R., DEL GUERRA, S., BOGGI, U., FALLENI, A., GREMIGNI, V., MOSCA, F., MARTINI, C., DOTTA, F., DI MARIO, U., DEL PRATO, S. & MARCHETTI, P. 2004. The role of peripheral benzodiazepine receptors on the function and survival of isolated human pancreatic islets. *European Journal of Endocrinology*, 151, 207-14.
- MARTÍN-TIMÓN, I. & DEL CAÑIZO-GÓMEZ, F. J. 2015. Mechanisms of hypoglycemia unawareness and implications in diabetic patients. *World journal of diabetes*, 6, 912-926.
- MATSUMOTO, S., TANAKA, K., STRONG, D. M. & REEMS, J. A. 2004. Efficacy of human islet isolation from the tail section of the pancreas for the possibility of living donor islet transplantation. *Transplantation*, 78, 839-843.
- MATSUSHIMA, H., KUROKI, T., ADACHI, T., KITASATO, A., ONO, S., TANAKA, T., HIRABARU, M., KUROSHIMA, N., HIRAYAMA, T., SAKAI, Y., SOYAMA, A., HIDAKA, M., TAKATSUKI, M., KIN, T., SHAPIRO, J. & EGUCHI, S. 2016. Human Fibroblast Sheet Promotes Human Pancreatic Islet Survival and Function In Vitro. *Cell Transplantation*, 25, 1525-1537.
- MATTSSON, G., JANSSON, L. & CARLSSON, P.-O. 2002. Decreased vascular density in mouse pancreatic islets after transplantation. *Diabetes*, 51, 1362-1366.
- MCCALL, M. & SHAPIRO, A. M. 2012. Update on islet transplantation. *Cold Spring Harbor Perspectives in Medicine*, 2, a007823.
- MCDONALD, T. J. & ELLARD, S. 2013. Maturity onset diabetes of the young: identification and diagnosis. *Annals of Clinical Biochemistry*, 50, 403-415.
- MENGER, M. D., JAEGER, S., WALTER, P., FEIFEL, G., HAMMERSEN, F. & MESSMER, K. 1989. Angiogenesis and hemodynamics of microvasculature of transplanted islets of Langerhans. *Diabetes*, 38, 199-201.
- MERGLIN, A., THEANDER, S., RUBI, B., CHAFFARD, G., WOLLHEIM, C. B. & MAECHLER, P. 2004. Glucose Sensitivity and Metabolism-Secretion Coupling Studied during Two-Year Continuous Culture in INS-1E Insulinoma Cells. *Endocrinology*, 145, 667-678.
- MILLER, R. G., SECREST, A. M., SHARMA, R. K., SONGER, T. J. & ORCHARD, T. J. 2012. Improvements in the life expectancy of type 1 diabetes: the Pittsburgh Epidemiology of Diabetes Complications study cohort. *Diabetes*, 61, 2987-92.
- MILLMAN, J. R., XIE, C., VAN DERVORT, A., GÜRTLER, M., PAGLIUCA, F. W. & MELTON, D. A. 2016. Generation of stem cell-derived β -cells from patients with type 1 diabetes. *Nature Communications*, 7, 11463.
- MITTAL, S. & GOUGH, S. C. L. 2014. Pancreas transplantation: a treatment option for people with diabetes. *Diabetic Medicine*, 31, 512-521.
- MIYAZAKI, J., ARAKI, K., YAMATO, E., IKEGAMI, H., ASANO, T., SHIBASAKI, Y., OKA, Y. & YAMAMURA, K. 1990. Establishment of a pancreatic beta cell line that retains glucose-inducible insulin secretion: special reference to expression of glucose transporter isoforms. *Endocrinology*, 127, 126-32.
- MOHAMMED, J. S., WANG, Y., HARVAT, T. A., OBERHOLZER, J. & EDDINGTON, D. T. 2009. Microfluidic device for multimodal characterization of pancreatic islets. *Lab on a Chip*, 9, 97-106.

- MONTALBANO, G., TOUMPANIARI, S., POPOV, A., DUAN, P., CHEN, J., DALGARNO, K., SCOTT, W. E. & FERREIRA, A. M. 2018. Synthesis of bioinspired collagen/alginate/fibrin based hydrogels for soft tissue engineering. *Materials Science and Engineering: C*, 91, 236-246.
- MOOKERJEE, S. A., GERENCSE, A. A., NICHOLLS, D. G. & BRAND, M. D. 2017. Quantifying intracellular rates of glycolytic and oxidative ATP production and consumption using extracellular flux measurements. *Journal of Biological Chemistry*, jbc. M116. 774471.
- MOOKERJEE, S. A., GONCALVES, R. L. S., GERENCSE, A. A., NICHOLLS, D. G. & BRAND, M. D. 2015. The contributions of respiration and glycolysis to extracellular acid production. *Biochimica et Biophysica Acta (BBA) - Bioenergetics*, 1847, 171-181.
- MOORE, S. J., GALA-LOPEZ, B. L., PEPPER, A. R., PAWLICK, R. L. & SHAPIRO, A. J. 2015. Bioengineered stem cells as an alternative for islet cell transplantation. *World journal of transplantation*, 5, 1-10.
- MURPHY, S. V. & ATALA, A. 2014. 3D bioprinting of tissues and organs. *Nature Biotechnology*, 32, 773-785.
- MURRAY, H. E., PAGET, M. B. & DOWNING, R. 2005. Preservation of glucose responsiveness in human islets maintained in a rotational cell culture system. *Molecular and Cellular Endocrinology*, 238, 39-49.
- MUTHUSAMY, A., MUMFORD, L., HUDSON, A., FUGGLE, S. & FRIEND, P. 2012. Pancreas transplantation from donors after circulatory death from the United Kingdom. *American Journal of Transplantation*, 12, 2150-2156.
- NAFTANEL, M. A. & HARLAN, D. M. 2005. Pancreatic Islet Transplantation. *PLOS Medicine*, 1, e58.
- NAGY, N., DE LA ZERDA, A., KABER, G., JOHNSON, P. Y., HU, K. H., KRATOCHVIL, M. J., YADAVA, K., ZHAO, W., CUI, Y. & NAVARRO, G. 2018. Hyaluronan content governs tissue stiffness in pancreatic islet inflammation. *Journal of Biological Chemistry*, 293, 567-578.
- NAJJAR, M., MANZOLI, V., ABREU, M., VILLA, C., MARTINO, M. M., MOLANO, R. D., TORRENTE, Y., PILEGGI, A., INVERARDI, L., RICORDI, C., HUBBELL, J. A. & TOMEI, A. A. 2015. Fibrin gels engineered with pro-angiogenic growth factors promote engraftment of pancreatic islets in extrahepatic sites in mice. *Biotechnology and Bioengineering*, 112, 1916-1926.
- NAM, K.-H., YONG, W., HARVAT, T., ADEWOLA, A., WANG, S., OBERHOLZER, J. & EDDINGTON, D. T. 2010. Size-based separation and collection of mouse pancreatic islets for functional analysis. *Biomedical Microdevices*, 12, 865-874.
- NATHAN, D. M. 2009. International Expert Committee Report on the Role of the A1C Assay in the Diagnosis of Diabetes. *Diabetes Care*, 32, 1327-1334.
- NATHAN, D. M. 2014. The Diabetes Control and Complications Trial/Epidemiology of Diabetes Interventions and Complications Study at 30 Years: Overview. *Diabetes Care*, 37, 9-16.
- NEVALAINEN, T. J. & ANTTINEN, J. 1977. Ultrastructural and functional changes in pancreatic acinar cells during autolysis. *Virchows Archiv B*, 24, 197-207.
- NHSBT. 2018a. *Annual Report on Pancreas and Islet Transplantation 2017/2018* [Online]. Available: <https://nhsbtdbe.blob.core.windows.net/umbraco-assets-corp/12251/nhsbt-pancreas-and-islet-transplantation-annual-report-2017-2018.pdf> [Accessed 18.07.2019 2019].
- NHSBT. 2018b. *National Standards for Organ Retrieval from Deceased Donors* [Online]. Available: <https://nhsbtdbe.blob.core.windows.net/umbraco-assets-corp/12548/mpd1043-nors-standard.pdf> [Accessed 24/09 2019].
- NIKOLOVA, G., JABS, N., KONSTANTINOVA, I., DOMOGATSKAYA, A., TRYGGVASON, K., SOROKIN, L., FÄSSLER, R., GU, G., GERBER, H.-P., FERRARA, N., MELTON, D. A. & LAMMERT, E. 2006. The Vascular Basement Membrane: A Niche for Insulin Gene Expression and β Cell Proliferation. *Developmental Cell*, 10, 397-405.
- NOGUCHI, H., NAZIRUDDIN, B., JACKSON, A., SHIMODA, M., IKEMOTO, T., FUJITA, Y., CHUJO, D., TAKITA, M., PENG, H. & SUGIMOTO, K. 2012. Fresh islets are more effective for islet transplantation than cultured islets. *Cell transplantation*, 21, 517-523.

- NYITRAY, C. E., CHAVEZ, M. G. & DESAI, T. A. 2014. Compliant 3D microenvironment improves β -cell cluster insulin expression through mechanosensing and β -catenin signaling. *Tissue engineering. Part A*, 20, 1888-1895.
- NYQVIST, D., SPEIER, S., RODRIGUEZ-DIAZ, R., MOLANO, R. D., LIPOVSEK, S., RUPNIK, M., DICKER, A., ILEGEMS, E., ZAHR-AKRAWI, E., MOLINA, J., LOPEZ-CABEZA, M., VILLATE, S., ABDULREDA, M. H., RICORDI, C., CAICEDO, A., PILEGGI, A. & BERGGREN, P.-O. 2011. Donor islet endothelial cells in pancreatic islet revascularization. *Diabetes*, 60, 2571-2577.
- O'BRIEN, F. J. 2011. Biomaterials & scaffolds for tissue engineering. *Materials Today*, 14, 88-95.
- O'SULLIVAN, E. S., VEGAS, A., ANDERSON, D. G. & WEIR, G. C. 2011. Islets transplanted in immunoisolation devices: a review of the progress and the challenges that remain. *Endocrine reviews*, 32, 827-844.
- OKERE, B., LUCACCIONI, L., DOMINICI, M. & IUGHETTI, L. 2016. Cell therapies for pancreatic beta-cell replenishment. *Italian Journal of Pediatrics*, 42, 62.
- OLSSON, R. & CARLSSON, P.-O. 2011. A low-oxygenated subpopulation of pancreatic islets constitutes a functional reserve of endocrine cells. *Diabetes*, 60, 2068-2075.
- OLSSON, R., OLERUD, J., PETTERSSON, U. & CARLSSON, P.-O. 2011. Increased Numbers of Low-Oxygenated Pancreatic Islets After Intraportal Islet Transplantation. *Diabetes*, 60, 2350-2353.
- OTONKOSKI, T., BANERJEE, M., KORSGREN, O., THORNELL, L. E. & VIRTANEN, I. 2008. Unique basement membrane structure of human pancreatic islets: implications for β -cell growth and differentiation. *Diabetes, Obesity and Metabolism*, 10, 119-127.
- PAPAS, K. K., AVGOUSTINIATOS, E. S., TEMPELMAN, L. A., WEIR, G. C., COLTON, C. K., PISANIA, A., RAPPEL, M. J., FRIBERG, A. S., BAUER, A. C. & HERING, B. J. 2005. High-Density Culture of Human Islets on Top of Silicone Rubber Membranes. *Transplantation Proceedings*, 37, 3412-3414.
- PAPAS, K. K., BELLIN, M. D., SUTHERLAND, D. E. R., SUSZYNSKI, T. M., KITZMANN, J. P., AVGOUSTINIATOS, E. S., GRUESSNER, A. C., MUELLER, K. R., BEILMAN, G. J., BALAMURUGAN, A. N., LOGANATHAN, G., COLTON, C. K., KOULMANDA, M., WEIR, G. C., WILHELM, J. J., QIAN, D., NILAND, J. C. & HERING, B. J. 2015. Islet Oxygen Consumption Rate (OCR) Dose Predicts Insulin Independence in Clinical Islet Autotransplantation. *PLOS ONE*, 10, e0134428.
- PAPAS, K. K., COLTON, C. K., NELSON, R. A., ROZAK, P. R., AVGOUSTINIATOS, E. S., SCOTT, W. E., 3RD, WILDEY, G. M., PISANIA, A., WEIR, G. C. & HERING, B. J. 2007. Human islet oxygen consumption rate and DNA measurements predict diabetes reversal in nude mice. *American Journal of Transplantation*, 7, 707-13.
- PARK, C.-G., BOTTINO, R. & HAWTHORNE, W. J. 2015. Current status of islet xenotransplantation. *International Journal of Surgery*, 23, 261-266.
- PARNAUD, G., LAVALLARD, V., BEDAT, B., MATTHEY-DORET, D., MOREL, P., BERNEY, T. & BOSCO, D. 2015. Cadherin Engagement Improves Insulin Secretion of Single Human β -Cells. *Diabetes*, 64, 887-896.
- PEDRAZA, E., CORONEL, M. M., FRAKER, C. A., RICORDI, C. & STABLER, C. L. 2012. Preventing hypoxia-induced cell death in beta cells and islets via hydrolytically activated, oxygen-generating biomaterials. *Proceedings of the National Academy of Sciences*, 109, 4245-4250.
- PEIRIS, H., BONDER, C. S., COATES, P. T. H., KEATING, D. J. & JESSUP, C. F. 2014. The β -Cell/EC Axis: How Do Islet Cells Talk to Each Other? *Diabetes*, 63, 3-11.
- PEREZ-BASTERRECHEA, M., ESTEBAN, M. M., VEGA, J. A. & OBAYA, A. J. 2018. Tissue-engineering approaches in pancreatic islet transplantation. *Biotechnology and Bioengineering*, 115, 3009-3029.
- PERSAUD, S. J., ARDEN, C., BERGSTEN, P., BONE, A. J., BROWN, J., DUNMORE, S., HARRISON, M., HAUGE-EVANS, A. C., KELLY, C. & KING, A. 2010. Pseudoislets as primary islet

- replacements for research: report on a symposium at King's College London, London UK. *Islets*, 2, 236-239.
- PICKARTZ, T., MAYERLE, J. & LERCH, M. M. 2007. Autoimmune pancreatitis. *Nature Reviews Gastroenterology & Hepatology*, 4, 314.
- PILEGGI, A., RIBEIRO, M. M., HOGAN, A. R., MOLANO, R. D., EMBURY, J. E., ICHII, H., COBIANCHI, L., FORNONI, A., RICORDI, C. & PASTORI, R. L. 2009. Effects of pancreas cold ischemia on islet function and quality. *Transplant Proceedings*, 41, 1808-9.
- PLOWS, J. F., STANLEY, J. L., BAKER, P. N., REYNOLDS, C. M. & VICKERS, M. H. 2018. The Pathophysiology of Gestational Diabetes Mellitus. *International journal of molecular sciences*, 19, 3342.
- POLONSKY, K. S., GIVEN, B. D. & VAN CAUTER, E. 1988. Twenty-four-hour profiles and pulsatile patterns of insulin secretion in normal and obese subjects. *Journal of Clinical Investigation*, 81, 442-448.
- POZZI, A., YURCHENCO, P. D. & IOZZO, R. V. 2017. The nature and biology of basement membranes. *Matrix Biology*, 57-58, 1-11.
- QI, M., BARBARO, B., WANG, S., WANG, Y., HANSEN, M. & OBERHOLZER, J. 2009a. Human pancreatic islet isolation: Part I: digestion and collection of pancreatic tissue. *Journal of visualized experiments : JoVE*, 1125.
- QI, M., BARBARO, B., WANG, S., WANG, Y., HANSEN, M. & OBERHOLZER, J. 2009b. Human pancreatic islet isolation: Part II: purification and culture of human islets. *Journal of visualized experiments : JoVE*, 1343.
- RAMAKRISHNA, S., FUJIIHARA, K., TEO, W.-E., YONG, T., MA, Z. & RAMASESHAN, R. 2006. Electrospun nanofibers: solving global issues. *Materials Today*, 9, 40-50.
- RAYMOND, N. T., JONES, J. R., SWIFT, P. G. F., DAVIES, M. J., LAWRENCE, I. G., MCNALLY, P. G., BURDEN, M. L., GREGORY, R., BOTHA, J. L. & BURDEN, A. C. 2001. Comparative incidence of Type I diabetes in children aged under 15 years from South Asian and White or Other ethnic backgrounds in Leicestershire, UK, 1989 to 1998. *Diabetologia*, 44, B32-B36.
- RECH, T. H., CRISPIM, D., RHEINHEIMER, J., BARKAN, S. S., OSVALDT, A. B., GREZZANA FILHO, T. J., KRUEL, C. R., MARTINI, J., GROSS, J. L. & LEITAO, C. B. 2014. Brain death-induced inflammatory activity in human pancreatic tissue: a case-control study. *Transplantation*, 97, 212-9.
- REERS, C., HAUGE-EVANS, A. C., MORGAN, N. G., WILCOX, A., PERSAUD, S. J. & JONES, P. M. 2011. Down-regulation of proliferation does not affect the secretory function of transformed β -cell lines regardless of their anatomical configuration. *Islets*, 3, 80-88.
- REZANIA, A., BRUIN, J. E., ARORA, P., RUBIN, A., BATUSHANSKY, I., ASADI, A., O'DWYER, S., QUISKAMP, N., MOJIBIAN, M., ALBRECHT, T., YANG, Y. H. C., JOHNSON, J. D. & KIEFFER, T. J. 2014. Reversal of diabetes with insulin-producing cells derived in vitro from human pluripotent stem cells. *Nature Biotechnology*, 32, 1121.
- RICORDI, C., GRAY, D. W. R., HERING, B. J., KAUFMAN, D. B., WARNOCK, G. L., KNETEMAN, N. M., LAKE, S. P., LONDON, N. J. M., SOCCI, C. & ALEJANDRO, R. 1990. Islet isolation assessment in man and large animals. *Acta diabetologia latina*, 27, 185-195.
- RICORDI, C., LACY, P. E., FINKE, E. H., OLACK, B. J. & SCHARP, D. W. 1988. Automated method for isolation of human pancreatic islets. *Diabetes*, 37, 413-420.
- RIOPEL, M., LI, J., FELLOWS, G. F., GOODYER, C. G. & WANG, R. 2014. Ultrastructural and immunohistochemical analysis of the 8-20 week human fetal pancreas. *Islets*, 6, e982949.
- RORSMAN, P., ELIASSON, L., RENSTRÖM, E., GROMADA, J., BARG, S. & GÖPEL, S. 2000. The Cell Physiology of Biphasic Insulin Secretion. *Physiology*, 15, 72-77.
- ROSE, S., FRYE, R., SLATTERY, J., WYNNE, R., TIPPETT, M., PAVLIV, O., MELNYK, S. & JAMES, S. 2014. Oxidative Stress Induces Mitochondrial Dysfunction in a Subset of Autism Lymphoblastoid Cell Lines in a Well-Matched Case Control Cohort. *PloS one*, 9, e85436.

- ROSENBERG, L., WANG, R., PARASKEVAS, S. & MAYSINGER, D. 1999. Structural and functional changes resulting from islet isolation lead to islet cell death. *Surgery*, 126, 393-398.
- ROSENGREN, A. H., BRAUN, M., MAHDI, T., ANDERSSON, S. A., TRAVERS, M. E., SHIGETO, M., ZHANG, E., ALMGREN, P., LADENVALL, C., AXELSSON, A. S., EDLUND, A., PEDERSEN, M. G., JONSSON, A., RAMRACHEYA, R., TANG, Y., WALKER, J. N., BARRETT, A., JOHNSON, P. R. V., LYSENKO, V., MCCARTHY, M. I., GROOP, L., SALEHI, A., GLOYN, A. L., RENSTRÖM, E., RORSMAN, P. & ELIASSON, L. 2012. Reduced Insulin Exocytosis in Human Pancreatic β -Cells With Gene Variants Linked to Type 2 Diabetes. *Diabetes*, 61, 1726-1733.
- RUDOLPH, E. N., DUNN, T. B., SUTHERLAND, D. E. R., KANDASWAMY, R. & FINGER, E. B. 2017. Optimizing outcomes in pancreas transplantation: Impact of organ preservation time. *Clinical Transplantation*, 31.
- RUSS, H. A., BAR, Y., RAVASSARD, P. & EFRAT, S. 2008. In vitro proliferation of cells derived from adult human β -cells revealed by cell-lineage tracing. *Diabetes*, 57, 1575-1583.
- RUTZKY, L. P., BILINSKI, S., KLOC, M., PHAN, T., ZHANG, H., KATZ, S. M. & STEPKOWSKI, S. M. 2002. Microgravity culture condition reduces immunogenicity and improves function of pancreatic islets. *Transplantation*, 74, 13-21.
- SACKETT, S. D., TREMMEL, D. M., MA, F., FEENEY, A. K., MAGUIRE, R. M., BROWN, M. E., ZHOU, Y., LI, X., O'BRIEN, C., LI, L., BURLINGHAM, W. J. & ODORICO, J. S. 2018. Extracellular matrix scaffold and hydrogel derived from decellularized and delipidized human pancreas. *Scientific Reports*, 8, 10452.
- SAH, R. P., NAGPAL, S. J. S., MUKHOPADHYAY, D. & CHARI, S. T. 2013. New insights into pancreatic cancer-induced paraneoplastic diabetes. *Nature Reviews Gastroenterology & Hepatology*, 10, 423.
- SALVAY, D. M., RIVES, C. B., ZHANG, X., CHEN, F., KAUFMAN, D. B., LOWE, W. L., JR. & SHEA, L. D. 2008. Extracellular matrix protein-coated scaffolds promote the reversal of diabetes after extrahepatic islet transplantation. *Transplantation*, 85, 1456-64.
- SANKAR, K. S., GREEN, B. J., CROCKER, A. R., VERITY, J. E., ALTAMENOV, S. M. & ROCHELEAU, J. V. 2011. Culturing Pancreatic Islets in Microfluidic Flow Enhances Morphology of the Associated Endothelial Cells. *PLOS ONE*, 6, e24904.
- SCHARP, D. W., LACY, P. E., SANTIAGO, J. V., MCCULLOUGH, C. S., WEIDE, L. G., FALQUI, L., MARCHETTI, P., GINGERICH, R. L., JAFFE, A. S., CRYER, P. E., ANDERSON, C. B. & FLYE, M. W. 1990. Insulin Independence After Islet Transplantation Into Type I Diabetic Patient. *Diabetes*, 39, 515-518.
- SCHUIT, F., DE VOS, A., FARFARI, S., MOENS, K., PIPELEERS, D., BRUN, T. & PRENTKI, M. 1997. Metabolic Fate of Glucose in Purified Islet Cells; Glucose-regulated anaplerosis in β cells. *Journal of Biological Chemistry*, 272, 18572-18579.
- SCHWARZ, P., CUSTÓDIO, G., RHEINHEIMER, J., CRISPIM, D., LEITÃO, C. B. & RECH, T. H. 2018. Brain Death-Induced Inflammatory Activity is Similar to Sepsis-Induced Cytokine Release. *Cell Transplantation*, 27, 1417-1424.
- SCOTT, W. E., 3RD, O'BRIEN, T. D., FERRER-FABREGA, J., AVGOUSTINIATOS, E. S., WEEGMAN, B. P., ANAZAWA, T., MATSUMOTO, S., KIRCHNER, V. A., RIZZARI, M. D., MURTAUGH, M. P., SUSZYNSKI, T. M., AASHEIM, T., KIDDER, L. S., HAMMER, B. E., STONE, S. G., TEMPELMAN, L. A., SUTHERLAND, D. E., HERING, B. J. & PAPAS, K. K. 2010. Persufflation improves pancreas preservation when compared with the two-layer method. *Transplantation Proceedings*, 42, 2016-9.
- SHACKMAN, J. G., DAHLGREN, G. M., PETERS, J. L. & KENNEDY, R. T. 2005. Perfusion and chemical monitoring of living cells on a microfluidic chip. *Lab on a Chip*, 5, 56-63.
- SHAPIRO, A. M. J. 2011. State of the Art of Clinical Islet Transplantation and Novel Protocols of Immunosuppression. *Current Diabetes Reports*, 11, 345.
- SHAPIRO, A. M. J. 2012. Islet transplantation in type 1 diabetes: ongoing challenges, refined procedures, and long-term outcome. *The review of diabetic studies : RDS*, 9, 385-406.

- SHAPIRO, A. M. J., LAKEY, J. R. T., RYAN, E. A., KORBUTT, G. S., TOTH, E., WARNOCK, G. L., KNETEMAN, N. M. & RAHOTTE, R. V. 2000. Islet Transplantation In Seven Patients With Type 1 Diabetes Mellitus Using A Glucocorticoid-Free Immunosuppressive Regimen. *The New England Journal of Medicine*, 343, 230-238.
- SHAPIRO, A. M. J., RICORDI, C., HERING, B. J., AUCHINCLOSS, H., LINDBLAD, R., ROBERTSON, R. P., SECCHI, A., BRENDEN, M. D., BERNEY, T., BRENNAN, D. C., CAGLIERO, E., ALEJANDRO, R., RYAN, E. A., DIMERCURIO, B., MOREL, P., POLONSKY, K. S., REEMS, J.-A., BRETZEL, R. G., BERTUZZI, F., FROUD, T., KANDASWAMY, R., SUTHERLAND, D. E. R., EISENBARTH, G., SEGAL, M., PREIKSAITIS, J., KORBUTT, G. S., BARTON, F. B., VIVIANO, L., SEYFERT-MARGOLIS, V., BLUESTONE, J. & LAKEY, J. R. T. 2006. International Trial of the Edmonton Protocol for Islet Transplantation. *New England Journal of Medicine*, 355, 1318-1330.
- SHEPPARD, M. N. & NICHOLSON, A. G. 2002. The pathology of cystic fibrosis. *Current diagnostic pathology*, 8, 50-59.
- SINGH, R., BARDEN, A., MORI, T. & BEILIN, L. 2001. Advanced glycation end-products: a review. *Diabetologia*, 44, 129-146.
- SINGH, V. P., BALI, A., SINGH, N. & JAGGI, A. S. 2014. Advanced glycation end products and diabetic complications. *The Korean journal of physiology & pharmacology : official journal of the Korean Physiological Society and the Korean Society of Pharmacology*, 18, 1-14.
- SKRZYPEK, K., NIBBELINK, M. G., LENTE, J., BUITINGA, M., ENGELSE, M. A., KONING, E. J. P., KAPERIEN, M., APELDOORN, A. & STAMATIALIS, D. 2017. Pancreatic islet macroencapsulation using microwell porous membranes. *Scientific reports*, 7, 9186.
- SMINK, A. M., DE HAAN, B. J., PAREDES-JUAREZ, G. A., WOLTERS, A. H., KUIPERS, J., GIEPMANS, B. N., SCHWAB, L., ENGELSE, M. A., VAN APELDOORN, A. A., DE KONING, E., FAAS, M. M. & DE VOS, P. 2016. Selection of polymers for application in scaffolds applicable for human pancreatic islet transplantation. *Biomedical Materials*, 11, 035006.
- SMINK, A. M. & DE VOS, P. 2018. Therapeutic Strategies for Modulating the Extracellular Matrix to Improve Pancreatic Islet Function and Survival After Transplantation. *Current diabetes reports*, 18, 39-39.
- SMINK, A. M., HERTSIG, D. T., SCHWAB, L., VAN APELDOORN, A. A., DE KONING, E., FAAS, M. M., DE HAAN, B. J. & DE VOS, P. 2017. A Retrievable, Efficacious Polymeric Scaffold for Subcutaneous Transplantation of Rat Pancreatic Islets. *Annals of Surgery*, 266, 149-157.
- SNEDDON, J. B., TANG, Q., STOCK, P., BLUESTONE, J. A., ROY, S., DESAI, T. & HEBROK, M. 2018. Stem cell therapies for treating diabetes: progress and remaining challenges. *Cell Stem Cell*, 22, 810-823.
- SOJODI, M., FARROKHI, A., MORADMAND, A. & BAHARVAND, H. 2013. Enhanced maintenance of rat islets of Langerhans on laminin-coated electrospun nanofibrillar matrix in vitro. *Cell Biology International*, 37, 370-9.
- SONG, S. & ROY, S. 2015. Progress and Challenges in Macroencapsulation Approaches for Type 1 Diabetes (T1D) Treatment: Cells, Biomaterials, and Devices. *Biotechnology and Bioengineering*, 113, 1381-1402.
- SPELIOS, M. G., AFINOWICZ, L. A., TIPON, R. C. & AKIRAV, E. M. 2018. Human EndoC- β H1 β -cells form pseudoislets with improved glucose sensitivity and enhanced GLP-1 signaling in the presence of islet-derived endothelial cells. *American Journal of Physiology-Endocrinology and Metabolism*, 314, E512-E521.
- SPELIOS, M. G., KENNA, L. A., WALL, B. & AKIRAV, E. M. 2013. In Vitro Formation of β Cell Pseudoislets Using Islet-Derived Endothelial Cells. *PLOS ONE*, 8, e72260.
- SPIERS, R. M., CROSS, S. E., BROWN, H. L., BATEMAN, P. A., VAUGHAN, R. H., HUGHES, S. J. & JOHNSON, P. R. V. 2018. Development of a Simple In Vitro Assay to Assess Digestion of the Extracellular Matrix of the Human Pancreas by Collagenase Enzyme Blends. *Cell Transplantation*, 27, 1039-1046.

- SRIDHARAN, G. & SHANKAR, A. A. 2012. Toluidine blue: A review of its chemistry and clinical utility. *Journal of oral and maxillofacial pathology: JOMFP*, 16, 251.
- STEINER, D., PARK, S. Y., STØY, J., PHILIPSON, L. & BELL, G. 2009. A brief perspective on insulin production. *Diabetes, Obesity and Metabolism*, 11, 189-196.
- STEINER, D. J., KIM, A., MILLER, K. & HARA, M. 2010. Pancreatic islet plasticity: Interspecies comparison of islet architecture and composition. *Islets*, 2, 135-145.
- STENDAHL, J. C., KAUFMAN, D. B. & STUPP, S. I. 2009. Extracellular Matrix in Pancreatic Islets: Relevance to Scaffold Design and Transplantation. *Cell Transplantation*, 18, 1-12.
- STEPHENS, C. H., ORR, K. S., ACTON, A. J., TERSEY, S. A., MIRMIRA, R. G., CONSIDINE, R. V. & VOYTIK-HARBIN, S. L. 2018. In situ type I oligomeric collagen macroencapsulation promotes islet longevity and function in vitro and in vivo. *American Journal of Physiology-Endocrinology and Metabolism*, 315, E650-E661.
- STØY, J., EDGHILL, E. L., FLANAGAN, S. E., YE, H., PAZ, V. P., PLUZHNIKOV, A., BELOW, J. E., HAYES, M. G., COX, N. J., LIPKIND, G. M., LIPTON, R. B., GREELEY, S. A. W., PATCH, A.-M., ELLARD, S., STEINER, D. F., HATTERSLEY, A. T., PHILIPSON, L. H. & BELL, G. I. 2007. Insulin gene mutations as a cause of permanent neonatal diabetes. *Proceedings of the National Academy of Sciences*, 104, 15040-15044.
- STRIEDER-BARBOZA, C., BAKER, N. A., FLESHER, C. G., KARMAKAR, M., NEELEY, C. K., POLSINELLI, D., DIMICK, J. B., FINKS, J. F., GHAFERI, A. A., VARBAN, O. A., LUMENG, C. N. & O'ROURKE, R. W. 2019. Advanced glycation end-products regulate extracellular matrix-adipocyte metabolic crosstalk in diabetes. *Scientific Reports*, 9, 19748.
- SWEET, I. R., GILBERT, M., SCOTT, S., TODOROV, I., JENSEN, R., NAIR, I., AL-ABDULLAH, I., RAWSON, J., KANDEEL, F. & FERRERI, K. 2008. Glucose-Stimulated Increment in Oxygen Consumption Rate as a Standardized Test of Human Islet Quality. *American Journal of Transplantation*, 8, 183-192.
- TADDEO, E. P., STILES, L., SEREDA, S., RITOU, E., WOLF, D. M., ABDULLAH, M., SWANSON, Z., WILHELM, J., BELLIN, M. & MCDONALD, P. 2018. Individual islet respirometry reveals functional diversity within the islet population of mice and human donors. *Molecular metabolism*, 16, 150-159.
- TAYLOR, R. 2013. Type 2 Diabetes: Etiology and reversibility. *Diabetes Care*, 36, 1047-1055.
- TEMNEANU, O. R., TRANDAFIR, L. M. & PURCAREA, M. R. 2016. Type 2 diabetes mellitus in children and adolescents: a relatively new clinical problem within pediatric practice. *Journal of medicine and life*, 9, 235-239.
- THE DIABETES CONTROL & COMPLICATIONS TRIAL RESEARCH GROUP 1993. The Effect of Intensive Treatment of Diabetes on the Development and Progression of Long-Term Complications in Insulin-Dependent Diabetes Mellitus. *New England Journal of Medicine*, 329, 977-986.
- THEOCHARIS, A. D., SKANDALIS, S. S., GIALELI, C. & KARAMANOS, N. K. 2016. Extracellular matrix structure. *Advanced Drug Delivery Reviews*, 97, 4-27.
- THOMAS, F. T., CONTRERAS, J. L., BILBAO, G., RICORDI, C., CURIEL, D. & THOMAS, J. M. 1999. Anoikis, extracellular matrix, and apoptosis factors in isolated cell transplantation. *Surgery*, 126, 299-304.
- THUNANDER, M., PETERSSON, C., JONZON, K., FORNANDER, J., OSSIANSSON, B., TORN, C., EDVARDSSON, S. & LANDIN-OLSSON, M. 2008. Incidence of type 1 and type 2 diabetes in adults and children in Kronoberg, Sweden. *Diabetes Research and Clinical Practice*, 82, 247-255.
- TOWNSEND, S. E. & GANNON, M. 2019. Extracellular Matrix-Associated Factors Play Critical Roles in Regulating Pancreatic β -Cell Proliferation and Survival. *Endocrinology*, 160, 1885-1894.
- TSUKITA, S., FURUSE, M. & ITOH, M. 2001. Multifunctional strands in tight junctions. *Nature Reviews Molecular Cell Biology*, 2, 285-293.

- TUCH, B. E., KEOGH, G. W., WILLIAMS, L. J., WU, W., FOSTER, J. L., VAITHILINGAM, V. & PHILIPS, R. 2009. Safety and Viability of Microencapsulated Human Islets Transplanted Into Diabetic Humans. *Diabetes Care*, 32, 1887-1889.
- UK PROSPECTIVE DIABETES STUDY GROUP 1998. Intensive blood-glucose control with sulphonylureas or insulin compared with conventional treatment and risk of complications in patients with type 2 diabetes (UKPDS 33). *The Lancet*, 352, 837-853.
- VAARALA, O., KLEMETTI, P., JUHELA, S., SIMELL, O., HYÖTY, H. & ILONEN, J. 2002. Effect of coincident enterovirus infection and cows' milk exposure on immunisation to insulin in early infancy. *Diabetologia*, 45, 531-534.
- VACANTI, J. P. & LANGER, R. 1999. Tissue engineering: the design and fabrication of living replacement devices for surgical reconstruction and transplantation. *The Lancet*, 354, S32-S34.
- VAITHILINGAM, V., BAL, S. & TUCH, B. E. 2017. Encapsulated Islet Transplantation: Where Do We Stand? *The review of diabetic studies : RDS*, 14, 51-78.
- VAN DEIJNEN, J. H. M., HULSTAERT, C. E., WOLTERS, G. H. J. & VAN SCHILFGAARDE, R. 1992. Significance of the peri-insular extracellular matrix for islet isolation from the pancreas of rat, dog, pig, and man. *Cell & Tissue Research*, 267, 139-146.
- VAN DER WINDT, D. J., BOTTINO, R., KUMAR, G., WIJKSTROM, M., HARA, H., EZZELARAB, M., EKSER, B., PHELPS, C., MURASE, N., CASU, A., AYARES, D., LAKKIS, F. G., TRUCCO, M. & COOPER, D. K. C. 2012. Clinical islet xenotransplantation: how close are we? *Diabetes*, 61, 3046-3055.
- VIRTANEN, I., BANERJEE, M., PALGI, J., KORSGREN, O., LUKINIUS, A., THORNELL, L. E., KIKKAWA, Y., SEKIGUCHI, K., HUKKANEN, M., KONTTINEN, Y. T. & OTONKOSKI, T. 2008. Blood vessels of human islets of Langerhans are surrounded by a double basement membrane. *Diabetologia*, 51, 1181-1191.
- WAHBA, N. S., SHABAN, S. F., KATTAIA, A. A. & KANDEEL, S. A. 2016. Efficacy of zinc oxide nanoparticles in attenuating pancreatic damage in a rat model of streptozotocin-induced diabetes. *Ultrastructural Pathology*, 40, 358-373.
- WAKAE-TAKADA, N., XUAN, S., WATANABE, K., MEDA, P. & LEIBEL, R. L. 2013. Molecular basis for the regulation of islet beta cell mass in mice: the role of E-cadherin. *Diabetologia*, 56, 856-866.
- WANG, R. & ROSENBERG, L. 1999. Maintenance of beta-cell function and survival following islet isolation requires re-establishment of the islet-matrix relationship. 163, 181.
- WANG, R. N., PARASKEVAS, S. & ROSENBERG, L. 1999. Characterization of Integrin Expression in Islets Isolated from Hamster, Canine, Porcine, and Human Pancreas. *The Journal of Histochemistry & Cytochemistry*, 47, 499-506.
- WEINBERG, N., OUZIEL-YAHALOM, L., KNOLLER, S., EFRAT, S. & DOR, Y. 2007. Lineage tracing evidence for in vitro dedifferentiation but rare proliferation of mouse pancreatic β -cells. *Diabetes*, 56, 1299-1304.
- WHITE, S. A., SHAW, J. A. & SUTHERLAND, D. E. R. 2009. Pancreas transplantation. *The Lancet*, 373, 1808-1817.
- WIEDERKEHR, A. & WOLLHEIM, C. B. 2006. Minireview: implication of mitochondria in insulin secretion and action. *Endocrinology*, 147, 2643-2649.
- WIKSTROM, J. D., SEREDA, S. B., STILES, L., ELORZA, A., ALLISTER, E. M., NEILSON, A., FERRICK, D. A., WHEELER, M. B. & SHIRIHAI, O. S. 2012. A novel high-throughput assay for islet respiration reveals uncoupling of rodent and human islets. *PLoS one*, 7, e33023.
- WILHELM, V., FISCHER, U., WEIGHARDT, H., SCHULZE-OSTHOFF, K., NICKEL, C., STAHLMECKE, B., KUHNBUSCH, T. A., SCHERBART, A. M., ESSER, C., SCHINS, R. P. & ALBRECHT, C. 2013. Zinc oxide nanoparticles induce necrosis and apoptosis in macrophages in a p47phox- and Nrf2-independent manner. *PLoS One*, 8, e65704.

- WITTINGEN, J. & FREY, C. F. 1974. Islet concentration in the head, body, tail and uncinat process of the pancreas. *Annals of Surgery*, 179, 412-414.
- WOJTUSCISZYN, A., ARMANET, M., MOREL, P., BERNEY, T. & BOSCO, D. 2008. Insulin secretion from human beta cells is heterogeneous and dependent on cell-to-cell contacts. *Diabetologia*, 51, 1843.
- WORLD HEALTH ORGANISATION 1999. Report of a WHO Consultation. Definition, diagnosis and classification of diabetes mellitus and its complications. 1. Diagnosis and classification of diabetes mellitus. *WHO/NCD/NCS/99.2Geneva: WHO*.
- XU, L., GUO, Y., HUANG, Y., XU, Y., LU, Y. & WANG, Z. 2019. Hydrogel materials for the application of islet transplantation. *Journal of biomaterials applications*, 33, 1252-1264.
- YAN, L.-J. 2018. Redox imbalance stress in diabetes mellitus: Role of the polyol pathway. *Animal models and experimental medicine*, 1, 7-13.
- YANG, Y., WANG, K., GU, X. & LEONG, K. W. 2017. Biophysical Regulation of Cell Behavior—Cross Talk between Substrate Stiffness and Nanotopography. *Engineering*, 3, 36-54.
- ZHANG, D., LIU, Y., TANG, Y., WANG, X., LI, Z., LI, R., TI, Z., GAO, W., BAI, J. & LV, Y. 2018. Increased mitochondrial fission is critical for hypoxia-induced pancreatic beta cell death. *PLoS One*, 13, e0197266.